Sari Agricultural & natural Resources University

JPMB

GABIT
Genetics and Agricultural Biotechnology Institute of Tabarestan

Journal of Plant Molecular Breeding

December 2023, Volume 11, Issue 2

ISSN: 2322-3332

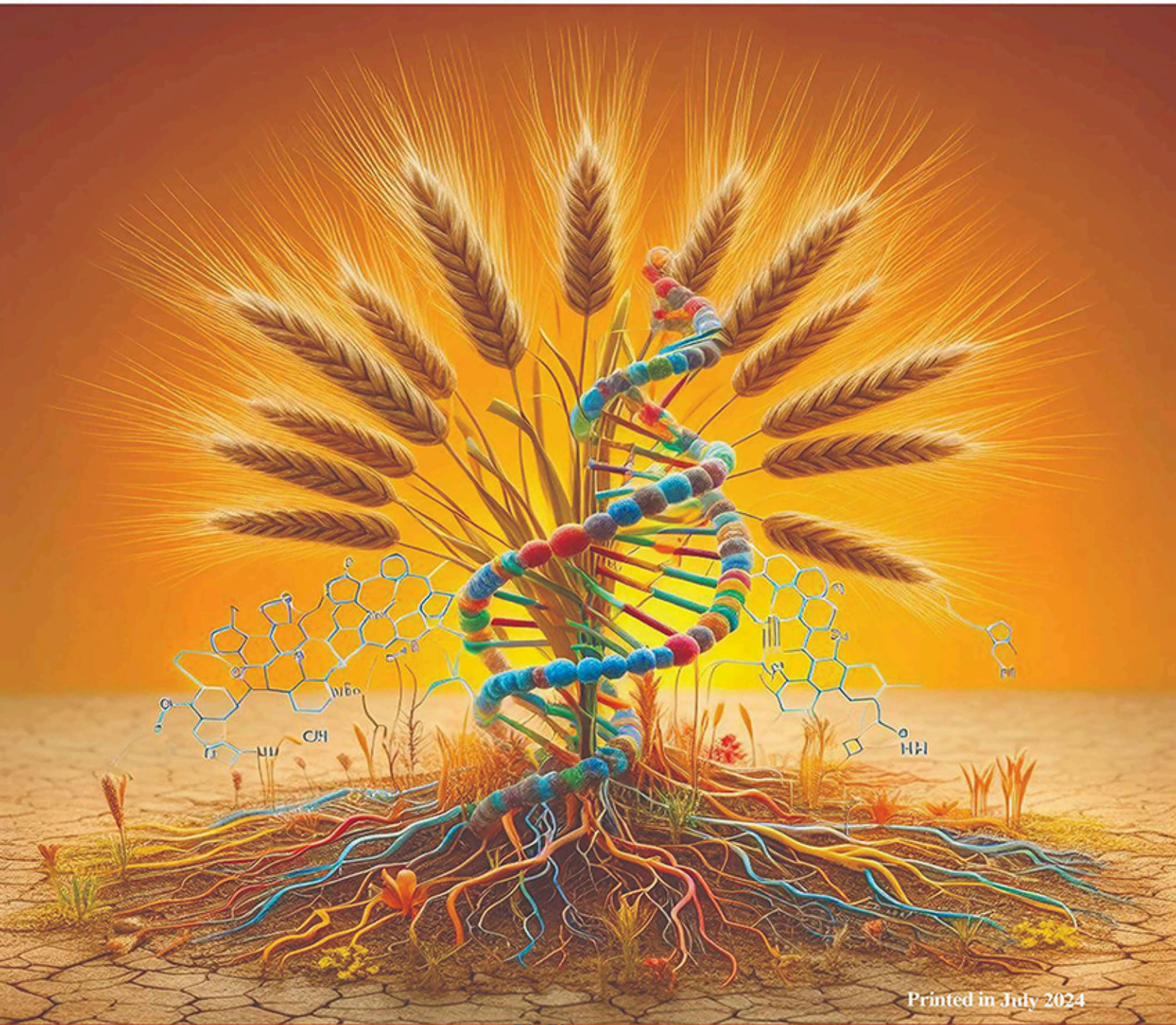

Printed in July 2024

JPMB

Contact

Sari Agricultural Sciences and Natural Resources University, Genetics and Agricultural Biotechnology Institute of Tabarestan, Sari, P.O. Box: 578, Iran.
Tel: +98-11-33687577
Email: jpmbjournal@sanru.ac.ir
www.jpmb-gabit.ir

Message from the Editor-in-Chief

JPMB is an open-access journal that serves as an advanced forum for research findings in plant molecular genetics and breeding along with other related areas such as plant biology, physiology, taxonomy, stresses, and interactions with other organisms. The journal publishes original research articles, reviews, reports, conference proceedings (peer-reviewed full articles), and short communications. In original research papers, full experimental details must be provided. We also encourage the submission of lab protocols, data management protocols, and analytical procedures in sufficient detail on topics of interest to the plant research community.

Editorial Board

Aims and Scope

Journal of Plant Molecular Breeding | JPMB is an international, open-access, peer-reviewed, biannual scholarly publication that aims to offer comprehensive coverage of progress in the field of plant molecular breeding. It seeks to present findings to researchers, academics, and students, addressing the growing demand for applied plant improvement technologies, tools, and methodologies.

- **Biotic and abiotic stress in plants**
- **Plant biodiversity and genetic resources**
- **Plant genetics and breeding**
- **Plant genomics (structural, functional, and applied)**
- **Plant genetic engineering**
- **Plant biochemical and regulatory networks**
- **Plant bioinformatics**

Visit our main website https://www.jpmb-gabit.ir/ for more information including contact details.

Contents

2023 |
Volume 11 |
Issue 2

JPMB | Journal of Plant Molecular Breeding
Published by Genetics and Agricultural Biotechnology Institute of Tabarestan
2023 | Volume 11 | Issue 2

Epigenetic adaptation to drought and salinity in crop plants

Mohsen Hoseini and Ahmad Arzani *

Department of Agronomy and Plant Breeding, College of Agriculture, Isfahan University of Technology, Isfahan, Iran

Review paper

OPEN ACCESS

Edited by

Prof. Suresh Kumar,
Indian Agricultural Research Institute, India

Date

Received: 26 January 2024
Accepted: 31 January 2024
Published: 12 February 2024

Correspondence

Prof. Ahmad Arzani
a_arzania@iut.ac.ir

Citation

Hoseini, M. and Arzani, A. (2023). Epigenetic adaptation to drought and salinity in crop plants. *J Plant Mol Breed 11* (2): 1-16.
doi: 10.22058/JPMB.2024.2021261.1292.

Abstract: The severe impact of drought and salinity on plant productivity presents a significant threat to worldwide food security. Plants exhibit the capacity to sense stimuli in their environment and adjust defense mechanisms through diverse regulatory networks to cope with abiotic stress. The complexities of drought and salinity tolerances can be deconstructed into contributing factors and mechanisms, classified under two categories: genetics and epigenetics. Epigenetic mechanisms play a role in partially attributing crop adaptation to the most formidable drought and salinity stresses. Plants respond to stress in part by undergoing stable alterations in gene expression, a process that involves the physical "marking" of DNA or its associated proteins, commonly called epigenetics. Plants utilize various epigenetic mechanisms to refine gene expression, vital for adaptation and phenotypic plasticity. These include DNA methylation, histone modifications, chromatin remodeling, epitranscriptomics, and gene silencing mediated by small RNAs. Notably, epigenetic modifications can be inherited or erased. Enhanced knowledge of epigenetics complements genetics and will aid in developing strategies to integrate them into crop improvement programs aimed at addressing adaptation to abiotic stress. This review highlights the latest and noteworthy findings regarding crop epigenetic responses to abiotic stress signals, particularly those pertinent to drought and salinity tolerance.

Keywords: Drought tolerance, CpG island, epigenomics, osmotic stress, salt tolerance, water stress.

Introduction

The productivity of plants is directly reliant on their growth and development, with their ability to adapt to drought and salinity serving as crucial factors, given these are among the most impactful environmental stresses. Drought stress induces numerous adverse effects on plants, subjecting them to common stressors like osmotic and oxidative stresses, similar to those associated with salinity. Drought and salinity stress cause osmotic stress, leading to subsequent dehydration in plant cells. Plant response to osmotic stress involves modifications to constitutively expressed TFs, triggered by both ABA-independent and -dependent mechanisms (Zhu, 2002; Li et al., 2014). With escalating salt concentration, plants experience two primary impairments: osmotic stress and specific ion toxicity, leading to secondary stresses like nutritional disorders and oxidative stress. These effects contribute to a reduction in plant growth, disrupting physiological and metabolic functions, including reduced water and nutrient absorption, membrane dysfunction, and critical process impairments like protein synthesis, respiration, and photosynthesis (Arzani et al., 2023). Various research studies indicate that plants are unable to ignore the onset of challenging environmental conditions, and they demonstrate a form of "stress memory" (Bruce et al., 2007; Lämke and Bäurle, 2017; Gallusci et al., 2023). They guide or supervise their adaptation to recurring, chronic, and combined abiotic stresses by reorganizing their genomic and biochemical architecture (Walter et al., 2013). Cellular response and adaptation to environmental stress depend on a diverse array of tightly controlled regulatory mechanisms, operating at the transcriptional and post-transcriptional tiers. Generally, drought and salinity stimuli can induce different epigenetic mechanisms for regulating the key gene expressions such as inward rectifying K+ channel (*AKT1*), pyrroline-5-carboxylate synthetase (*P5CS*), high-affinity potassium transporters (*HKTs*), and ABA biosynthesis genes (*i.e.*, *NCED1*, *NCED3*, *ABA1*, *ABA2*, *ABA3*, *ABF2*, *ABF4*, *ABI3*, *ABI4*, and *ABI5*) (Arzani and Ashraf, 2016).

Epigenetics is a term with various definitions currently employed across the literature. Nevertheless, a more frequently employed definition, pertinent to the role of epigenetics in plant defense responses, asserts that epigenetics is the mechanism responsible for the persistent changes in the expression of genes. There are two fundamental epigenetic modifications: the covalent alteration of DNA through methylation and modifications of histones at the post-translational for the modulation of chromatin structure. Broadly speaking, these dynamic mechanisms control the capacity of DNA and chromatin to undertake transcription of the gene. These processes entail marking DNA or its related histones physically, allowing cells that are genotypically identical to manifest distinct phenotypes (Felsenfeld, 2014). In addition, several noncoding RNAs, such as micro RNAs, and long noncoding RNAs are also altered, influencing many biochemical pathways. In recent years, notable progress has been made in our comprehension of the role played by epigenetic mechanisms in plant responses to environmental stimuli, particularly in the context of stress (Mladenov et al., 2021). Hence, these heritable chemical changes in covalent DNA and histones, which control the expression of genes without modifying the underlying nucleotide sequence, constitute a group of regulators influencing plant response and resilience to stress (Li et al., 2021b; Singroha et al., 2022).

DNA methylation

Methylation of DNA is a vital process in gene expression regulation and the plant's responsiveness to abiotic stress (Kumar and Mohapatra, 2021). In plants, DNA methylation primarily involves a methyl group addition at the 5′ position of cytosine resulting in 5-methylcytosine (5mC), or at the N6 position of adenine resulting in N6-methyladenine (6mA) (Li et al., 2020). DNA methylation more frequently happens on cytosines adjacent to guanine nucleobases (CpG) and is commonly regarded as a transcriptional repression marker for genes. It interferes with the transcriptional machinery binding to regulatory sites and recruits transcriptional repressors to facilitate the establishment of a heterochromatin state. DNA methyltransferases (DNMTs) are specific enzymes that transfer methyl groups to the 5-position of the pyrimidine ring of DNA cytosine

nucleotides (Quadrana and Colot, 2016; Li et al., 2020) (Quadrana and Colot, 2016).

Besides the sequence and quantity of methylation, the genomic locations of DNA methylation, such as gene bodies, regulatory elements, transcriptional start sites, transposable elements, and repeat sequences have varying functional consequences. In plants, gene body methylation (GBM) pertains to genes where, in contrast to the absence of methylated cytosine at the start and termination of transcriptional sites, CG methylation of DNA occurs inside the coding regions (Bewick and Schmitz, 2017). DNA methylation within gene bodies may influence diverse processes, including differential promoter usage, transcription elongation, and alternative splicing (Jones, 2012). GBM-associated genes, unlike other epigenetic modifications leading to transcriptional repression, are essentially expressed and are linked to constitutive genes exhibiting moderate to high expression levels (Bewick and Schmitz, 2017; Muyle and Gaut, 2019).

Thus, in addition to contributing to phenotypic diversity (Quadrana and Colot, 2016; Noshay and Springer, 2021), changes in methylation patterns can prompt significant plastic responses to abiotic stress. Disruptions in the enzymes responsible for DNA methylation result in varied survival outcomes in the plant's stress response, emphasizing the crucial function of DNA methylation in responses to stress (Wibowo et al., 2016; Kumar et al., 2024). Consequently, methylation of DNA, going beyond a binary on-off switch, imparts a diverse and nuanced spectrum of "different meanings of gene expression," contingent on the underlying sequence and its genomic position (Niederhuth and Schmitz, 2017). Unlike highly variable gene expression, the plasticity of DNA methylation in genic regions appears to be minimally affected by environmental changes. Its associations with differential gene expression vary across tissues, species, and environmental conditions (Okitsu and Hsieh, 2007; Colak and Karadayi, 2022; Hämälä et al., 2022). For instance, in pigeonpea (*Cajanus cajan* L. Huth), genes with high gene body methylation (GBM) had the lowest expression, while those with moderate GBM showed the highest expression (Junaid et al., 2022). In *Eutrema salsugineum* (Muyle and Gaut, 2019), rice (Rajkumar et al., 2020), and *Populus euphratica* (Su et al., 2018), the loss of GBM was linked to decreased gene expression levels. However, in maize, drought stress-induced gene body DNA methylation was negatively correlated with gene expression (Wang et al., 2021).

Plant studies have demonstrated the significant role of GBM in the regulation of AS (Hu et al., 2014). Alternative splicing (AS) is a mechanism conserved throughout evolution that enhances the complexity of transcriptome and proteome. Consequently, a single gene generates multiple mRNA isoforms, thereby increasing phenotypic diversity (Reddy et al., 2013). Genes encoding AS factors are typically down-regulated at the transcription stage but often undergo alternative splicing themselves (Reddy et al., 2013), a process influenced by changes in DNA methylation (Wang et al., 2016). Analysis of RNA-seq and BS-seq data from identical tissue (seedling) in rice isogenic lines reveal the impact of cytosine methylation loss in regions of the gene body through AS changes in plants (Hu et al., 2014). In maize, DNA methylation in the gene body positively correlates with exon splicing events under drought stress (Wang et al., 2021).

The various reports that adenine nucleotides in DNA are also methylated by adding a CH_3 group at the N1 or N6 position although at very lower rates than cytosine, introduce an additional complexity layer to the epigenetic phenomena influencing genomic DNA in the plant cell (Kumar et al., 2018; Liang et al., 2018). The first position (N1) and the sixth position (C6) of the purine ring of adenine are methylated to form N1-methyladenine and N6-methyladenine (6-mA), respectively (Sedgwick et al., 2007). The effects of 6-mA vary depending on the location in the genome, encompassing transcriptional silencing and activation, transgenerational chromatin regulation, as well as the source and severity of stress. 6mA in the gene body is related to actively expressed genes in *Arabidopsis thaliana* (Liang et al., 2018) and rice (Zhou et al., 2018). In general, DNA N6-methyladenine, unlike 5-methylcytosine in the gene promoter, does not play a definitive role in repression but leads to divergent modulation of gene expression. In rice, an increase in density of 6 mA is associated with an increase in salt and heat

resistance and a decrease in cold resistance (Zhang et al., 2018).

The regulation of gene expression during a plant's response to abiotic stress is significantly influenced by DNA methylation (Kumar and Mohapatra, 2021). The association between DNA methylation and drought stress tolerance has been established in rice cultivars, particularly in IR20, a drought-sensitive cultivar. When exposed to drought stress, IR20 exhibits hypomethylation, while tolerant cultivars display hypermethylation (Gayacharan and Joel, 2013). DNA methylation under drought stress is expected to be genotypic and growth stage-dependent, and it also appears to be organ/tissue-dependent. Drought induces 12.1% methylation alteration in Indica rice (*Oryza sativa* L.), spanning various genotypes, tissues, and growth stages. Notably, the DNA methylation in leaves was higher than that in roots during similar developmental stages, suggesting a pivotal role for roots in responding to water deficiency (Suji and Joel, 2010). Salinity stress induces opposing effects on methylation or demethylation of 5mC in the regulation of transcription in various species of plants, thereby differentially modulating the downstream expression of salinity-related genes. Salinity stress triggers 5mC demethylation at the promoter of certain transporters, leading to improved salinity tolerance through higher expression of the transporter genes in soybean (Zhang et al., 2020) and rice (Zhu et al., 2015). Conversely, salinity stress causes higher turnover rates of 5mC, potentially influencing the ion transporter gene expressions (such as HKT2;1 and HKT2;3) or miRNA and thereby enhancing tolerance to salinity (Ganie et al., 2016; Kumar et al., 2017).

The alterations in methylation/demethylation are largely durable even after recovery of the plant, suggesting the potential to establish stress memory. Numerous studies have sought to elucidate the mechanism of establishing memory for stress in crops, spanning biochemical and physiological perspectives, as well as epigenome modification, to enhance stress tolerance in crops. Evidence suggests that induced stress memory in Arabidopsis, after salt stress treatment, is accomplished by modulating the transcription level of the light-induced *P5CS1* gene involved in proline synthetase (Feng et al., 2016).

Histone modifications and histone post-transcriptional modifications

The organization and modification of chromatin have pivotal roles in shaping how plants respond to environmental shifts, such as salinity (Nguyen et al., 2019) and drought (Peirats-Llobet et al., 2016), by regulating the accessibility of genes to TFs. In certain instances, the memory of stress exposure can be transmitted to successive generations through mechanisms of epigenetic inheritance (Sun et al., 2021). The fundamental functional unit of chromatin, known as the nucleosome, comprises an octamer of histones consisting of H2A, H2B, H3, and H4 histones two copies each. This octamer is wrapped around 147 base pairs of DNA. In response to abiotic stress, such as drought and salinity stress, plants exhibit transcriptional induction in target genes. This response is attributed to the rapid and dynamic removal of the H2A.Z variant from stress-related genes. In contrast, under non-stress conditions, the existence of H2A.Z nucleosomes within gene bodies safeguards the repression of drought and salinity stress-responsive genes (Nguyen and Cheong, 2018).

Moreover, post-translational covalent alterations of histones have the potential to modify chromatin structure, thereby influencing the cis-regulatory element accessibility to TFs (Zhang et al., 2020). Out of numerous histone post-translational modifications (HPTMs) documented (Zhu et al., 2015), methylation, acetylation, phosphorylation, and ubiquitination have garnered more attention in the context of plant stress response. These marks on the histone are produced by complexes of histone "writer" including histone methyltransferases (HMT), acetyltransferases (HAT), ubiquitinases, and kinases, and excluded by "erasers" such as demethylases (HDM), deacetylases (HDA), de-ubiquitinases, and phosphatases, (Maeji and Nishimura, 2018).

Histone acetylation: Histone lysine acetylation and deacetylation serve as widespread epigenetic regulators in nearly all eukaryotes, influencing multiple cellular processes by modifying chromatin structure and function (Ma et al., 2013). The

acetylation of lysine residues (K) on histones H3 and H4, notably at K9, K14, K18, K23, K27, and K36 positions for H3, and K5, K8, K12, K16, and K20 positions for H4, diminishes the binding strength between histones and DNA. This occurs through the neutralization of the positive charge of histones, ultimately resulting in a looser structure of chromatin. Conversely, deacetylation has the opposite effect, causing chromatin compaction and restricting the access of TFs to DNA (Berger, 2007). The antagonism between HATs and HDACs (histone deacetylases), that write and erase the histone acetylation mark respectively, results in dynamic regulation of the structure of chromatin (Boycheva et al., 2014). In addition to altering the chromatin structure, histone acetylation modifies the surface of nucleosomes, influencing their configuration for binding proteins essential in gene transcription (Berger, 2007). Consequently, histone acetylation serves as a pivotal factor in regulating the extent of chromatin folding, thereby modulating the homeostatic gene program and gene expression in plants responding to stress. This regulation occurs through alterations in the quantity and/or arrangement of acetylated histones (Hu et al., 2019). The gene activations in response to drought and salinity are mainly governed by alterations in histones and nucleosome density within the promoters, with less frequent occurrences in the open reading frames (ORFs) of these genes. Under drought stress, alterations in histones, such as H3K9ac and H3K4me3, were observed within the regions of Rd20 and Rd29A in comparison to conditions optimal for growth (Kim et al., 2008). Research indicates that moisture stress triggers heightened expression of HAT genes in rice (Hou et al., 2021), Chinese cabbage (Eom and Hyun, 2018), and *Brachypodium distachyon* (Tan et al., 2019). HAT genes (*TaHAC2*, *TaHAG2*, and *TaHAG3*) exhibited up-regulation under drought stress in a wheat cultivar with higher drought tolerance, but not in other drought-sensitive cultivars (Li et al., 2021a). The acetylation of H3K9/14 contributes to salinity tolerance in Arabidopsis by modulating the expression of *MYB54*, *PGX3*, and *CTL1* (Wang et al., 2019). In maize, the expression of cell wall-associated genes, *ZmXET1* and *ZmEXPB2*, increases during salt stress due to H3K9 hyperacetylation in the promoter region (Li et al., 2014). Another instance involves the upregulation of ABA-responsive genes and salt stress, including *OsLEA3*, *OsbZIP72*, *OsABI5*, and *OsNHX1* in rice. This upregulation correlates with the promoter regions, which exhibit increased acetylation of histone H4 under salt stress and ABA treatment (Ullah et al., 2021). The overexpression of gene 9-cis-epoxy carotenoid dioxygenase, producing the enzyme involved in the biosynthesis of ABA, was notably enhanced by HMT (Ding et al., 2011).

Histone methylation: The modification of histone is a dynamic process that involves addition, removal, recognition, and interpretation by distinct writer enzymes, eraser enzymes, and reader proteins, respectively. Methylation occurring at single, double, or triple sites on histone tails, specifically at lysine (K) or arginine (R), modifies the hydrophobicity properties of side chains of histone, thus influencing their binding with the transcriptional machinery and reader proteins. K and R methylation affects the organization of chromatin and gene expression, exhibiting variations based on the specific amino acid position of the modification (Lämke and Bäurle, 2017).

Research studies suggest that DNA methylation, whether hyper or hypo, holds a pivotal significance in modifying gene functions under adverse environments. In the context of salinity stress, methylation of gene bodies and promoters is instrumental in modulating gene expression genotypically in a manner specific to the organ. Numerous investigations into histone methylation dynamics and the response to effective mutations in HMT/HDMT activities emphasize the significance of histone methylation in development and stress responses (Ueda and Seki, 2020).

Importantly, findings indicate that under certain stressful environments, active expression of stress-related genes necessitates eliminating repressive methylation marks and the addition of active methylation marks (Sun et al., 2019). For instance, salinity stress results in the reduction of suppressive histone marks including H3K27me and 3H3K9me2, coupled with the accrual of functional methylation marks such as H3K4me3 on salt-tolerance genes (Song et al., 2012; Paul et al., 2017). In soybean, the deactivation of genes in salt-exposed plants firmly correlates with the H3K27me3 establishment under *de novo* conditions in the coding regions or

promoters not present in control plants (Sun et al., 2019).

A diminished quantity of H3K27me3 within the drought-responsive TF loci is associated with increased tolerance to stress in Arabidopsis (Ramirez‐Prado et al., 2019). In rice, H3K4me3 modification of 4837 genes was observed under moisture stress, with the status of methylation affecting the activation of a limited set of drought-responsive genes (Zong et al., 2013). Additionally, during salinity stress in Arabidopsis, the reduced amount of H4R3sme2 (histone4 arginine3 symmetric dimethylation) induces the expression of the flowering gene FLC and stress-responsive genes (Zhang et al., 2011). Under drought stress, H4R3sme2-type histone methylation in the ANAC055 region of promoter results in increased expression of *P5CS1* and elevated proline levels in wild-type Arabidopsis ((Fu et al., 2017).

Histones ubiquitylation: Ubiquitination is a form of post-translational alteration of proteins, wherein the selective degradation of proteins in the cell through the post-translational addition of ubiquitin for their breakdown by proteases (March and Farrona, 2018). This process not only influences protein stability but also has the potential to alter protein localization, transcriptional activity, or functional activity within a cell (March and Farrona, 2018; Chen et al., 2020). Multi-ubiquitination on target proteins often leads to degradation by 26S proteasome, while mono-ubiquitination regulates the function and localization of protein independently of proteolysis (Chen et al., 2020). Mono-ubiquitination of histones is a significant type of HPTM occurring at lysine 121 (K121) for histone H2A and lysine 143 (K143) for histone H2B (March and Farrona, 2018).

The mono-ubiquitination of histone lysine H2B (H2Bub1) is viewed as an active transcriptional mark participating in defense response, flowering timing, seed dormancy, and regulation of salinity and drought stress (Chen et al., 2019; Chen et al., 2020). The downregulation of MPK4 and MYB42 under salinity stress was accompanied by lower levels of H3K4me3 and H2Bub1 in hypersensitive mutants of *A. thaliana* (Sun et al., 2020). It has been indicated that ubiquitination changes of H2A.Z contribute to the regulation of the stress-responsive genes in Arabidopsis under drought stress (Sura et al., 2017).

Histone phosphorylation: Histone H3 can undergo phosphorylation at arginine and threonine. While the putative role of this epigenetic change has been extensively investigated within the framework of the cell cycle (Houben et al., 2007), its response to environmental stress in plants remains not well-understood. In addition to the rapid response to stresses, histone post-translational modifications (HPTMs), such as histone methylation, also function as an environmental memory, aiding plant adaptation to environmental changes. This memory mechanism enables previously stressed plants to better cope with the same stress in subsequent exposures (Lämke and Bäurle, 2017).

Chromatin remodeling complexes

The contribution of chromatin remodeling complexes to epigenetic regulation of the expression of genes, especially in the context of plant stress responses is vital (Eichten and Springer, 2015; Pandey et al., 2016; Tonosaki et al., 2022). These complexes are responsible for altering chromatin structure, influencing the accessibility of DNA to regulatory proteins and transcriptional apparatus (Pandey et al., 2016). Amid biotic and abiotic stress, chromatin remodeling complexes contribute to altering the expression of stress-related genes, shaping the plant's ability to withstand and thrive in challenging environments (Kim, 2019). Chromatin remodeling complexes reprogram gene expression patterns in plants responding to stress. These complexes facilitate structural alterations to either repress or activate the responsive genes, securing precise regulation of gene expression and ensuring survival (Wang and Qiao, 2020).

In the context of plant stress responses, chromatin remodeling complexes modify gene expression through the ATP hydrolysis-derived energy, sliding, evicting, or changing nucleosome composition (He et al., 2023). Enzymes that modify histones catalyze posttranslational changes in histone proteins, either inhibiting or stimulating gene transcription. Highly condensed chromatin hinders the access of polymerases, TFs, and other nuclear proteins to DNA. Chromatin undergoes structural alterations in response to stress signals,

enabling DNA to be rendered accessible (Bhadouriya et al., 2021).

Noncoding RNAs

Noncoding RNAs, which lack an open reading frame, critical for translation, are abundantly present and contribute to various cellular processes. This category encompasses short non-coding RNAs shorter than 200 nucleotides (e.g., siRNAs and miRNAs), long non-coding RNAs (lncRNAs) comprising over 200 nucleotides, and circular RNAs. Research indicates that a substantial fraction of noncoding RNAs, including lncRNAs and miRNAs, have diverse biological functions in cellular processes including the modulation of replication of DNA, transcription, translation, and stability (Ma et al., 2022). While noncoding RNAs are not traditionally regarded as epigenetic factors, they actively participate in epigenetic modifications. The miRNAs and siRNAs, a group of single-stranded RNAs with a length ranging from 21 to 24 nucleotides, represent one of the more prevalent categories of molecules involved in gene regulation. Also known as small RNAs (sRNA) or RNA interference (RNAi), this group of RNAs is prevalent in both plant and animal genomes, influencing growth, cellular behavior, gene expression regulation, genome protection against endogenous and extrinsic threats, and conveying adaptation to biotic and abiotic stress. The varied category of small RNAs demonstrates variability in their specific functions, including adaptation to abiotic stress, like drought in plants (Ferdous et al., 2015). These small non-coding RNAs have appeared as crucial regulators of essential genomic activations, like modifications in chromatin structure, transcription, and translation (Borges and Martienssen, 2015). Double-stranded RNAs are synthesized during their processing as intermediates by RNA-dependent RNA polymerases (RDRs) to originate the small interfering RNAs (siRNAs) (Song et al., 2019). The activities of small RNAs, like miRNA, induced by abiotic stress, such as drought, cold, salinity, and oxidative stress are documented (Sunkar and Zhu, 2004), underscoring the function of intrinsic endogenic pathways of small RNAs in combating these stresses. Transgenic approaches contribute to improvements at various degrees in modern crop-improvement schemes, ensuring plasticity and increased yield under environmental stress conditions. RNAi has been instrumental in addressing abiotic stresses in various crops. For instance, RACK1 genetically modified RNAi rice, (Younis et al., 2014), exhibited an improved tolerance to drought compared to wild types (non-transgenic lines).

Table 1 provides a summary of studies investigating epigenetic modifications in crop plants in response to drought and salinity stress, employing the aforementioned methodologies. Furthermore, Figure 1 depicts the significant contribution of plant epigenetic responses in conferring tolerance to drought and salinity stresses, overcoming environmental challenges, and evolving.

Epitranscriptomics

Post-transcriptional modification is an additional epigenetic alteration, extending beyond those induced by histone modifications and DNA methylation. These modifications occur in diverse RNAs including mRNA, tRNA, rRNA, and lncRNA, introducing a new layer of regulatory mechanisms in plants (Rajkumar et al., 2020). Among these, N5-methylcytidine (m5C) and N6-methyladenosine (m6A) are prevalent, and ample internal modifications are identified in mRNAs. Numerous investigations have observed that covalent RNA modifications contribute to regulating the quantity and quality of eukaryotic transcripts. These modifications influence the secondary structure, stability, translatability, degradation, and functionality of RNA molecules (Yang et al., 2019; Kumar and Mohapatra, 2021).

Studies have demonstrated that these epitranscriptomic signals have broad effects on the plant's response to salinity stress through the regulation of RNA fate (Hu et al., 2021; Zheng et al., 2021; Wang et al., 2022). When the plant was exposed to drought stress, there was an elevation in m6A levels within the 5'UTR region, facilitating the translation of transcripts that exhibit resistance (Shoaib et al., 2022). Consequently, stress induces a reorganization of m6A across the transcriptome, resulting in a heightened presence of mRNAs with 5′ UTR m6A.

Table 1. The epigenetic modifications in response to drought and salinity stress in crop plants.

Species	Stress condition	Epigenetic modification			Reference
		Histone modification	**DNA modification**	**RNA modification**	
Zea mays	Drought	H3K4me3, H3K9ac			(Forestan et al., 2020)
Gossypium hirsutum	Drought	H2Bub, H3K4me3			(Chen et al., 2019)
Oryza sativa	Drought			Non-coding RNA (mir162b)	(Tian et al., 2015)
O. sativa	Drought			Non-coding RNA (mir164)	(Feng et al., 2016)
O. sativa	Drought	H2Bub1			(Ma et al., 2013)
Glycine max	Drought			Non-coding RNA (miR169g)	(Ni et al., 2013)
Nicotiana tabacum	Drought	HDAC			(Ma et al., 2017)
Hordeum vulgare	Drought	H3K9ac, H3K14ac, H3K27ac			(Papaefthimiou et al., 2010)
Z. mays	Drought		Hypermethylation		(Wang et al., 2021)
O. sativa	Drought		Promoter Hypomethylation (CLT1 and PSBP gene)		(Ding et al., 2011)
O. sativa	Drought		Hypermethylation		(Kou et al., 2022)
Triticum aestivum	Drought		Hypermethylation		(Duan et al., 2020)
T. aestivum	Osmotic (PEG)		Hypermethylation		(Li et al., 2020)
Medicago sativa	Salinity	H3K9Ac			(Deng et al., 2018)
G. max	Salinity	HDAC		miR482bd-5	(Cadavid et al., 2020)
G. hirsutum	Salinity			LncRNA973	(Zhang et al., 2019)
G. hirsutum	Salinity			lnc_388, lnc_973, lnc_253	(Deng et al., 2018)
Solanum lycopersicum	Salinity			miR156, miR398	(Çakır et al., 2021)
Ipomoea batatas	Salinity			nta-miR156a_R + 3, farmiR159_L + 2_1ss22T, mes-MIR319ep5_2ss12GC19 GA	(Yang et al., 2020)
O. sativa	Salinity			miR171b, miR167f	(Parmar et al., 2020)
T. aestivum	Salinity			TaemiR408	(Bai et al., 2018)
Z. mays	Salinity			miR164s, mir-36	(Fu et al., 2017)
Z. mays	Salinity		Hypomethylation		(Sun et al., 2018; Shams et al., 2020)
Capsicum annuum	Salinity		Hypermethylation		(Shams et al., 2020)
Beta vulgaris	Salinity		Hypomethylation		(Skorupa et al., 2021)
T. aestivum	Salinity		Coding region hypermethylation (TaHKT2;1 & TaHKT2;3)		(Kumar et al., 2017)
T. aestivum	Salinity		hypomethylation		(Hosseinpour et al., 2022)

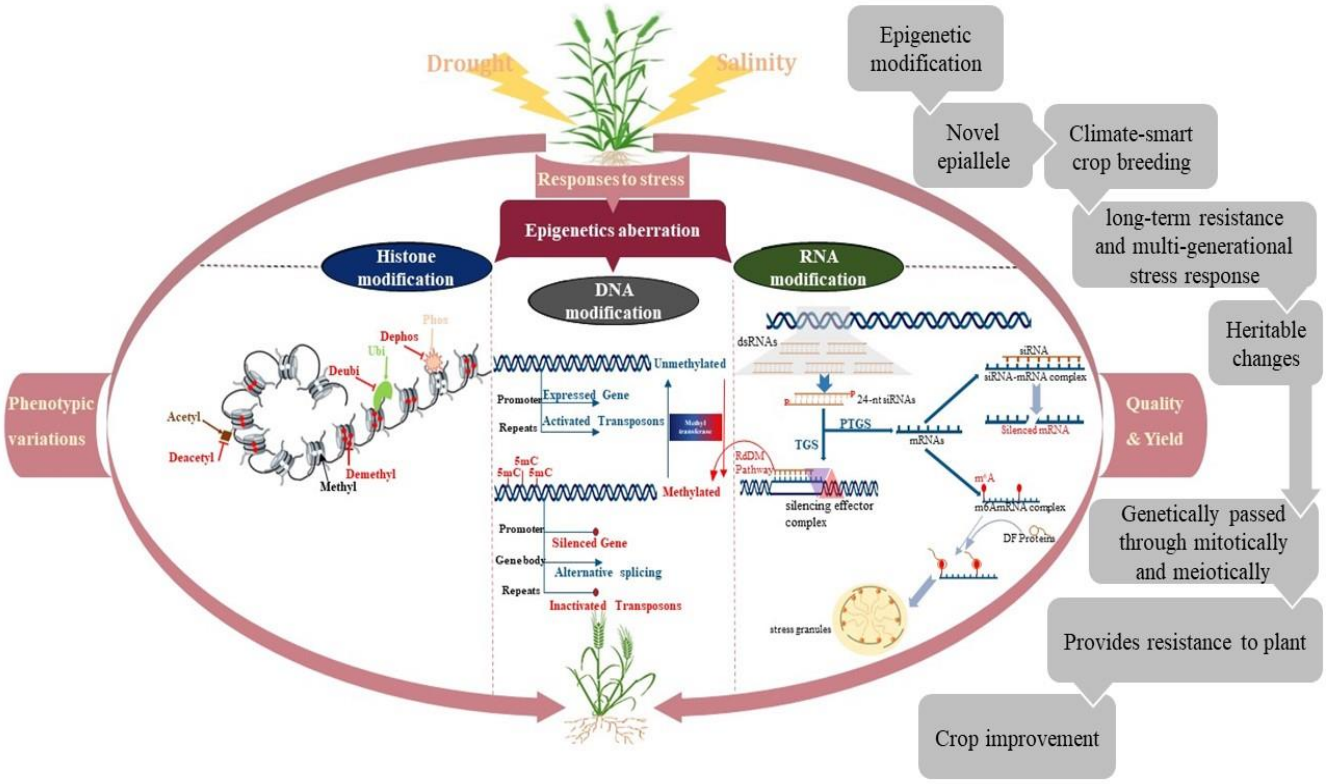

Figure 1. The vital role of plant epigenetic responses for tolerance of drought and salinity stresses, overcoming environmental challenges, and evolution over time. These changes modifications include histone modifications such as methylation (Methyl), acetylation (Acetyl), phosphorylation (Phos), and ubiquitination (Ubi), DNA modifications, and RNA modifications of the two pathways of transcriptional gene silencing (TGS) and post-transcriptional gene silencing (PTGS).

These findings suggest that the redistribution of m6A on mRNAs remains consistent across organisms, both under stress and normal conditions.

The long-distance transport of RNA information molecules, including siRNAs, miRNAs, tRNAs, rRNAs, and mRNAs, which exhibit systemic signaling functions in vascular tissues, contributes to facilitating the adaptation of plants to abiotic stress (Thieme et al., 2015; Zhang et al., 2018)

Conclusion

Losses in crop production due to drought and salinity stresses pose a significant challenge for staple food crops, and the issue is expected to be exacerbated by the global warming scenario in the future. The use of epigenetic technologies bears great potential for developing novel crop cultivars, particularly in enhancing stress tolerance through the generation of new epialleles. Epigenetic alterations can result in modified gene transcription, facilitating better adaptation to abiotic stresses. Additionally, acting as "plant stress memory," these modifications enable plants to respond effectively to challenges in their environment, providing resilience for future generations to withstand environmental stresses. The intricate cross-talk between various epigenetic regulation levels contributes to shaping stress responses, fostering resilience, and enhancing adaptability in plants.

Substantial advancement has been achieved in comprehending the function of epigenetic modulation in plant responses to various stressful environmental conditions. Transitioning from epigenetics to potential breeding applications and shifting from an "experimental" to a "conventional" methodology in plant improvement requires overcoming key challenges. This involves enhancing technology, refining data workflow

systems, advancing information about plant species across all epigenetic levels, and better integrating data of epigenomic studies with other "omics" datasets.

Supplementary Materials

No supplementary material is available for this article.

Author Contributions

Conceptualization; M.H. and A.A., writing original draft, investigation, reviewing and editing; A.A., supervision; A.A. All authors listed have made substantial, direct, and intellectual contributions to the work and have approved it for publication. All data were generated in-house, and no paper mill was used. All authors agree to be accountable for all aspects of work ensuring integrity and accuracy.

Funding

This research has received no external funding.

Conflict of Interest Statement

The authors declare no conflict of interest.

References

Arzani, A., and Ashraf, M. (2016). Smart engineering of genetic resources for enhanced salinity tolerance in crop plants. *Crit Rev Plant Sci* 35(3): 146-189.

Arzani, A., Kumar, S., and Mansour, M.M.F. (2023). Salt tolerance in plants: molecular and functional adaptations. *Front Plant Sci* 14: 1280788.

Bai, Q., Wang, X., Chen, X., Shi, G., Liu, Z., Guo, C., and Xiao, K. (2018). Wheat miRNA TaemiR408 acts as an essential mediator in plant tolerance to Pi deprivation and salt stress via modulating stress-associated physiological processes. *Front Plant Sci* 9: 499.

Berger, S.L. (2007). The complex language of chromatin regulation during transcription. *Nature* 447(7143): 407-412.

Bewick, A.J., and Schmitz, R.J. (2017). Gene body DNA methylation in plants. *Front Plant Sci* 36: 103-110.

Bhadouriya, S.L., Mehrotra, S., Basantani, M.K., Loake, G.J., and Mehrotra, R. (2021). Role of chromatin architecture in plant stress responses: an update. *Front Plant Sci* 11: 603380.

Borges, F., and Martienssen, R.A. (2015). The expanding world of small RNAs in plants. *Nat Rev Mol Cell Biol* 16(12): 727-741.

Boycheva, I., Vassileva, V., and Iantcheva, A. (2014). Histone acetyltransferases in plant development and plasticity. *Curr Genomics* 15(1): 28.

Bruce, T.J., Matthes, M.C., Napier, J.A., and Pickett, J.A. (2007). Stressful "memories" of plants: evidence and possible mechanisms. *Plant Sci* 173(6): 603-608.

Cadavid, I.C., da Fonseca, G.C., and Margis, R. (2020). HDAC inhibitor affects soybean miRNA482bd expression under salt and osmotic stress. *J Plant Physiol* 253: 153261.

Cakır, O., Arıkan, B., Karpuz, B., and Turgut-Kara, N. (2021). Expression analysis of miRNAs and their targets related to salt stress in *Solanum lycopersicum* H-2274. *Biotechnol Biotechnol Equip* 35(1): 275-282.

Chen, H., Feng, H., Zhang, X., Zhang, C., Wang, T., and Dong, J. (2019). An Arabidopsis E3 ligase HUB 2 increases histone H2B monoubiquitination and enhances drought tolerance in transgenic cotton. *Plant Biotechnol J* 17(3): 556-568.

Chen, K., Tang, W.-S., Zhou, Y.-B., Xu, Z.-S., Chen, J., Ma, Y.-Z., Chen, M., and Li, H.-Y. (2020). Overexpression of GmUBC9 gene enhances plant drought resistance and affects flowering time via histone H2B monoubiquitination. *Front Plant Sci* 11: 555794.

Colak, İ., and Karadayi, G. (2022). Comparison of the DNA methylation and expression changes on some cadmium-induced genes in bread wheat exposed to cadmium (Cd) accumulation in the soil. *Preprint available at Research Square*. doi: [https://doi.org/10.21203/rs.3.rs-1718779/v1].

Deng, F., Zhang, X., Wang, W., Yuan, R., and Shen, F. (2018). Identification of *Gossypium hirsutum* long non-coding RNAs (lncRNAs) under salt stress. *BMC Plant Biol* 18: 1-14.

Ding, Y., Avramova, Z., and Fromm, M. (2011). The Arabidopsis trithorax‐like factor ATX1 functions in dehydration stress responses via ABA‐dependent and ABA‐independent pathways. *Plant J* 66(5): 735-744.

Duan, H., Li, J., Zhu, Y., Jia, W., Wang, H., Jiang, L., and Zhou, Y. (2020). Responsive changes of DNA methylation in wheat (*Triticum aestivum*) under water deficit. *Sci Rep* 10(1): 7938.

Eichten, S.R., and Springer, N.M. (2015). Minimal evidence for consistent changes in maize DNA methylation patterns following environmental stress. *Front Plant Sci* 6: 308.

Eom, S.H., and Hyun, T.K. (2018). Histone acetyltransferases (HATs) in Chinese cabbage: insights from histone H3 acetylation and expression profiling of HATs in response to abiotic stresses. *J Am Soc Hort Sci* 143(4): 296-303.

Felsenfeld, G. (2014). A brief history of epigenetics. *Cold Spring Harb Perspect Biol* 6(1): a018200.

Feng, X.J., Li, J.R., Qi, S.L., Lin, Q.F., Jin, J.B., and Hua, X.J. (2016). Light affects salt stress-induced transcriptional memory of P5CS1 in Arabidopsis. *Proc Natl Acad Sci USA* 113(51): E8335-E8343.

Ferdous, J., Hussain, S.S., and Shi, B.J. (2015). Role of micro RNA s in plant drought tolerance. *Plant Biotechnol J* 13(3): 293-305.

Forestan, C., Farinati, S., Zambelli, F., Pavesi, G., Rossi, V., and Varotto, S. (2020). Epigenetic signatures of stress adaptation and flowering regulation in response to extended drought and recovery in *Zea mays*. *Plant Cell Environ* 43(1): 55-75.

Fu, R., Zhang, M., Zhao, Y., He, X., Ding, C., Wang, S., Feng, Y., Song, X., Li, P., and Wang, B. (2017). Identification of salt tolerance-related microRNAs and their targets in maize (*Zea mays* L.) using high-throughput sequencing and degradome analysis. *Front Plant Sci* 8: 864.

Gallusci, P., Agius, D.R., Moschou, P.N., Dobránszki, J., Kaiserli, E., and Martinelli, F. (2023). Deep inside the epigenetic memories of stressed plants. *Trend Plant Sci* 28(2): 142-153.

Ganie, S.A., Dey, N., and Mondal, T.K. (2016). Promoter methylation regulates the abundance of osa-miR393a in contrasting rice genotypes under salinity stress. *Funct Integr Genomics* 16: 1-11.

Gayacharan, and Joel, A.J. (2013). Epigenetic responses to drought stress in rice (*Oryza sativa* L.). *Physiol Molecular Biol Plant* 19: 379-387.

Hamala, T., Ning, W., Kuittinen, H., Aryamanesh, N., and Savolainen, O. (2022). Environmental response in gene expression and DNA methylation reveals factors influencing the adaptive potential of *Arabidopsis lyrata*. *eLife* 11: e83115.

He, M.-Y., Ren, T.X., Jin, Z.D., Deng, L., Liu, H.J., Cheng, Y.Y., Li, Z.Y., Liu, X.X., Yang, Y., and Chang, H. (2023). Precise analysis of potassium isotopic composition in plant materials by multi-collector inductively coupled plasma mass spectrometry. *Spectrochim Acta Part B At Spectrosc* 209: 106781.

Hosseinpour, A., Ilhan, E., Özkan, G., Öztürk, H.İ., Haliloglu, K., and Cinisli, K.T. (2022). Plant growth-promoting bacteria (PGPBs) and copper (II) oxide (CuO) nanoparticle ameliorates DNA damage and DNA Methylation in wheat (*Triticum aestivum* L.) exposed to NaCl stress. *J Plant Biochem. Biotechnol* 31(4): 751-764.

Hou, J., Ren, R., Xiao, H., Chen, Z., Yu, J., Zhang, H., Shi, Q., Hou, H., He, S., and Li, L. (2021). Characteristic and evolution of HAT and HDAC genes in Gramineae genomes and their expression analysis under diverse stress in *Oryza sativa*. *Planta* 253: 1-22.

Houben, A., Demidov, D., Caperta, A.D., Karimi, R., Agueci, F., and Vlasenko, L. (2007). Phosphorylation of histone H3 in plants—a dynamic affair. *Biochim Biophys Acta* 1769(5-6): 308-315.

Hu, J., Cai, J., Park, S.J., Lee, K., Li, Y., Chen, Y., Yun, J.Y., Xu, T., and Kang, H. (2021). N 6‐Methyladenosine mRNA methylation is important for salt stress tolerance in Arabidopsis. *Plant J* 106(6): 1759-1775.

Hu, L., Li, N., Xu, C., Zhong, S., Lin, X., Yang, J., Zhou, T., Yuliang, A., Wu, Y., and Chen, Y.-R. (2014). Mutation of a major CG methylase in rice causes genome-wide hypomethylation, dysregulated genome expression, and seedling lethality. *Proc Natl Acad Sci USA* 111(29): 10642-10647.

Hu, Y., Lu, Y., Zhao, Y., and Zhou, D.-X. (2019). Histone acetylation dynamics integrates metabolic activity to regulate plant response to stress. *Front Plant Sci* 10: 1236.

Jones, P.A. (2012). Functions of DNA methylation: islands, start sites, gene bodies and beyond. *Nat Rev Genet* 13(7): 484-492.

Junaid, A., Singh, N.K., and Gaikwad, K. (2022). Evolutionary fates of gene‐body methylation and its divergent association with gene expression in pigeonpea. *Plant Genome* 15(3): e20207.

Kim, J.-H. (2019). Chromatin remodeling and epigenetic regulation in plant DNA damage repair. *Int J Mol Sci* 20(17): 4093.

Kim, J.-M., To, T.K., Ishida, J., Morosawa, T., Kawashima, M., Matsui, A., Toyoda, T., Kimura, H., Shinozaki, K., and Seki, M. (2008). Alterations of lysine modifications on the histone H3 N-tail under drought stress conditions in *Arabidopsis thaliana*. *Plant Cell Physiol* 49(10): 1580-1588.

Kou, S., Gu, Q., Duan, L., Liu, G., Yuan, P., Li, H., Wu, Z., Liu, W., Huang, P., and Liu, L. (2022). Genome-wide bisulphite sequencing uncovered the contribution of DNA methylation to rice short-term drought memory formation. *J Plant Growth Regul* 41(7): 2903-2917.

Kumar, S., Beena, A.S., Awana, M., and Singh, A. (2017). Salt-induced tissue-specific cytosine methylation downregulates expression of HKT genes in contrasting wheat (*Triticum aestivum* L.) genotypes. *DNA Cel Biol* 36(4): 283-294.

Kumar, S., Chinnusamy, V., and Mohapatra, T. (2018). Epigenetics of modified DNA bases: 5-methylcytosine and beyond. *Front Genet* 9: 640.

Kumar, S., and Mohapatra, T. (2021). Dynamics of DNA methylation and its functions in plant growth and development. *Front Plant Sci* 12: 596236.

Kumar, S., Seem, K., Kumar, S., Singh, A., Krishnan, S.G., and Mohapatra, T. (2024). DNA methylome analysis provides insights into gene regulatory mechanism for better performance of rice under fluctuating environmental conditions: epigenomics of adaptive plasticity. *Planta* 259(1): 4.

Lämke, J., and Bäurle, I. (2017). Epigenetic and chromatin-based mechanisms in environmental stress adaptation and stress memory in plants. *Genome Biol* 18(1): 1-11.

Li, H., Liu, H., Pei, X., Chen, H., Li, X., Wang, J., and Wang, C. (2021a). Comparative genome-wide analysis and expression profiling of histone acetyltransferases and histone deacetylases involved in the response to drought in wheat. *J Plant Growth Regul*: 1-14.

Li, H., Yan, S., Zhao, L., Tan, J., Zhang, Q., Gao, F., Wang, P., Hou, H., and Li, L. (2014). Histone acetylation associated up-regulation of the cell wall related genes is involved in salt stress induced maize root swelling. *BMC Plant Biol* 14: 1-14.

Li, J., Jia, W., Wang, H., Zhu, Y., Duan, Z., Jiang, L., Zhou, Y., and Duan, H. (2020). Morpho-physiological adaptation and DNA methylation of wheat seedlings under osmotic stress. *Crop Pasture Sci* 71(4): 349-355.

Li, S., He, X., Gao, Y., Zhou, C., Chiang, V.L., and Li, W. (2021b). Histone acetylation changes in plant response to drought stress. *Genes* 12(9): 1409.

Liang, Z., Shen, L., Cui, X., Bao, S., Geng, Y., Yu, G., Liang, F., Xie, S., Lu, T., and Gu, X. (2018). DNA N6-adenine methylation in *Arabidopsis thaliana*. *Develop Cell* 45(3): 406-416. e403.

Ma, X., Lv, S., Zhang, C., and Yang, C. (2013). Histone deacetylases and their functions in plants. *Plant Cell Rep* 32: 465-478.

Ma, X., Zhang, B., Liu, C., Tong, B., Guan, T., and Xia, D. (2017). Expression of a populus histone deacetylase gene 84KHDA903 in tobacco enhances drought tolerance. *Plant Sci* 265: 1-11.

Ma, X., Zhao, F., and Zhou, B. (2022). The characters of non-coding RNAs and their biological roles in plant development and abiotic stress response. *Int J Mol Sci* 23(8): 4124.

Maeji, H., and Nishimura, T. (2018). "Epigenetic mechanisms in plants," in *Adv Bot Res*. Elsevier), 21-47.

March, E., and Farrona, S. (2018). Plant deubiquitinases and their role in the control of gene expression through modification of histones. *Front Plant Sci* 8: 2274.

Mladenov, V., Fotopoulos, V., Kaiserli, E., Karalija, E., Maury, S., Baranek, M., Segal, N.a., Testillano, P.S., Vassileva, V., and Pinto, G. (2021). Deciphering the epigenetic alphabet involved in transgenerational stress memory in crops. *Int J Mol Sci* 22(13): 7118.

Muyle, A., and Gaut, B.S. (2019). Loss of gene body methylation in *Eutrema salsugineum* is associated with reduced gene expression. *Mol Biol Evol* 36(1): 155-158.

Nguyen, N.H., and Cheong, J.-J. (2018). H2A. Z-containing nucleosomes are evicted to activate AtMYB44 transcription in response to salt stress. *Biochem Biophys Res Commun* 499(4): 1039-1043.

Nguyen, N.H., Jung, C., and Cheong, J.-J. (2019). Chromatin remodeling for the transcription of type 2C protein phosphatase genes in response to salt stress. *Plant Physiol Biochem* 141: 325-331.

Ni, Z., Hu, Z., Jiang, Q., and Zhang, H. (2013). *GmNFYA3*, a target gene of miR169, is a positive regulator of plant tolerance to drought stress. *Plant Mol Biol* 82: 113-129.

Niederhuth, C.E., and Schmitz, R.J. (2017). Putting DNA methylation in context: from genomes to gene expression in plants. *Biochim Biophys Acta* 1860(1): 149-156.

Noshay, J.M., and Springer, N.M. (2021). Stories that can't be told by SNPs; DNA methylation variation in plant populations. *Curr Opin Plant Biol* 61: 101989.

Okitsu, C.Y., and Hsieh, C.-L. (2007). DNA methylation dictates histone H3K4 methylation. *Mol Cell Biol* 27(7): 2746-2757.

Pandey, G., Sharma, N., Pankaj Sahu, P., and Prasad, M. (2016). Chromatin-based epigenetic regulation of plant abiotic stress response. *Curr Genom* 17(6): 490-498.

Papaefthimiou, D., Likotrafiti, E., Kapazoglou, A., Bladenopoulos, K., and Tsaftaris, A. (2010). Epigenetic chromatin modifiers in barley: III. Isolation and characterization of the barley GNAT-MYST family of histone acetyltransferases and responses to exogenous ABA. *Plant Physiol Biochem* 48(2-3): 98-107.

Parmar, S., Gharat, S.A., Tagirasa, R., Chandra, T., Behera, L., Dash, S.K., and Shaw, B.P. (2020). Identification and expression analysis of miRNAs and elucidation of their role in salt tolerance in rice varieties susceptible and tolerant to salinity. *PLoS One* 15(4): e0230958.

Paul, A., Dasgupta, P., Roy, D., and Chaudhuri, S. (2017). Comparative analysis of Histone modifications and DNA methylation at OsBZ8 locus under salinity stress in IR64 and Nonabokra rice varieties. *Plant Mol Biol* 95: 63-88.

Peirats-Llobet, M., Han, S.-K., Gonzalez-Guzman, M., Jeong, C.W., Rodriguez, L., Belda-Palazon, B., Wagner, D., and Rodriguez, P.L. (2016). A direct link between abscisic acid sensing and the chromatin-remodeling ATPase BRAHMA via core ABA signaling pathway components. *Mol Plant* 9(1): 136-147.

Quadrana, L., and Colot, V. (2016). Plant transgenerational epigenetics. *Annu Rev Genet* 50: 467-491.

Rajkumar, M.S., Shankar, R., Garg, R., and Jain, M. (2020). Bisulphite sequencing reveals dynamic DNA methylation under desiccation and salinity stresses in rice cultivars. *Genomics* 112(5): 3537-3548.

Ramirez‐Prado, J.S., Latrasse, D., Rodriguez‐Granados, N.Y., Huang, Y., Manza‐Mianza, D., Brik‐Chaouche, R., Jaouannet, M., Citerne, S., Bendahmane, A., and Hirt, H. (2019). The Polycomb protein LHP1 regulates *Arabidopsis thaliana* stress responses through the repression of the MYC2‐dependent branch of immunity. *Plant J* 100(6): 1118-1131.

Reddy, A.S., Marquez, Y., Kalyna, M., and Barta, A. (2013). Complexity of the alternative splicing landscape in plants. *Plant Cell* 25(10): 3657-3683.

Sedgwick, B., Bates, P.A., Paik, J., Jacobs, S.C., and Lindahl, T. (2007). Repair of alkylated DNA: recent advances. *DNA Repair* 6(4): 429-442.

Shams, M., Yildirim, E., Arslan, E., and Agar, G. (2020). Salinity induced alteration in DNA methylation pattern, enzyme activity, nutrient uptake and H 2 O 2 content in pepper (*Capsicum annuum* L.) cultivars. *Acta Physiol Plant* 42: 1-12.

Shoaib, Y., Usman, B., Kang, H., and Jung, K.-H. (2022). Epitranscriptomics: An additional regulatory layer in plants' development and stress response. *Plants* 11(8): 1033.

Singroha, G., Kumar, S., Gupta, O.P., Singh, G.P., and Sharma, P. (2022). Uncovering the epigenetic marks involved in mediating salt stress tolerance in plants. *Front Genet* 13: 811732.

Skorupa, M., Szczepanek, J., Mazur, J., Domagalski, K., Tretyn, A., and Tyburski, J. (2021). Salt stress and salt shock differently affect DNA methylation in salt-responsive genes in sugar beet and its wild, halophytic ancestor. *PLoS One* 16(5): e0251675.

Song, X., Li, Y., Cao, X., and Qi, Y. (2019). MicroRNAs and their regulatory roles in plant–environment interactions. *Annu Rev Plant Biol* 70: 489-525.

Song, Y., Ji, D., Li, S., Wang, P., Li, Q., and Xiang, F. (2012). The dynamic changes of DNA methylation and histone modifications of salt responsive transcription factor genes in soybean. *PloS One* 7(7): e41274.

Su, Y., Bai, X., Yang, W., Wang, W., Chen, Z., Ma, J., and Ma, T. (2018). Single-base-resolution methylomes of *Populus euphratica* reveal the association between DNA methylation and salt stress. *Tree Genet Genom* 14: 1-11.

Suji, K., and Joel, A.J. (2010). An epigenetic change in rice cultivars under water stress conditions. *Elec J Plant Breed* 1(4): 1142-1143.

Sun, C., Ali, K., Yan, K., Fiaz, S., Dormatey, R., Bi, Z., and Bai, J. (2021). Exploration of epigenetics for improvement of drought and other stress resistance in crops: A review. *Plants* 10(6): 1226. doi: https://doi.org/10.3390/plants10061226.

Sun, L., Miao, X., Cui, J., Deng, J., Wang, X., Wang, Y., Zhang, Y., Gao, S., and Yang, K. (2018). Genome-wide high-resolution mapping of DNA methylation identifies epigenetic variation across different salt stress in Maize (*Zea mays* L.). *Euphytica* 214: 1-15.

Sun, L., Song, G., Guo, W., Wang, W., Zhao, H., Gao, T., Lv, Q., Yang, X., Xu, F., and Dong, Y. (2019). Dynamic changes in genome-wide histone3 lysine27 trimethylation and gene expression of soybean roots in response to salt stress. *Front Plant Sci* 10: 1031.

Sun, Y., Zhao, J., Li, X., and Li, Y. (2020). E2 conjugases UBC1 and UBC2 regulate MYB42 ‐ mediated SOS pathway in response to salt stress in Arabidopsis. *New Phytol* 227(2): 455-472.

Sunkar, R., and Zhu, J.-K. (2004). Novel and stress-regulated microRNAs and other small RNAs from Arabidopsis. *Plant Cell* 16(8): 2001-2019.

Sura, W., Kabza, M., Karlowski, W.M., Bieluszewski, T., Kus-Slowinska, M., Pawełoszek, Ł., Sadowski, J., and Ziolkowski, P.A. (2017). Dual role of the histone variant H2A. Z in transcriptional regulation of stress-response genes. *Plant Cell* 29(4): 791-807.

Tan, S., Gao, L., Li, T., and Chen, L. (2019). Phylogenetic and expression analysis of histone acetyltransferases in *Brachypodium distachyon*. *Genomics* 111(6): 1966-1976.

Thieme, C.J., Rojas-Triana, M., Stecyk, E., Schudoma, C., Zhang, W., Yang, L., Miñambres, M., Walther, D., Schulze, W.X., and Paz-Ares, J. (2015). Endogenous Arabidopsis messenger RNAs transported to distant tissues. *Nat Plant* 1(4): 1-9.

Tian, C., Zuo, Z., and Qiu, J.-L. (2015). Identification and characterization of ABA-responsive microRNAs in rice. *Genet Genom* 42(7): 393-402.

Tonosaki, K., Fujimoto, R., Dennis, E.S., Raboy, V., and Osabe, K. (2022). Will epigenetics be a key player in crop breeding? *Front Plant Sci* 13: 958350.

Ueda, M., and Seki, M. (2020). Histone modifications form epigenetic regulatory networks to regulate abiotic stress response. *Plant Physiol* 182(1): 15-26.

Ullah, F., Xu, Q., Zhao, Y., and Zhou, D.X. (2021). Histone deacetylase HDA710 controls salt tolerance by regulating ABA signaling in rice. *J Integr Plant Biol* 63(3): 451-467.

Walter, J., Jentsch, A., Beierkuhnlein, C., and Kreyling, J. (2013). Ecological stress memory and cross stress tolerance in plants in the face of climate extremes. *Environ Exp Bot* 94: 3-8.

Wang, L., and Qiao, H. (2020). Chromatin regulation in plant hormone and plant stress responses. *Curr Opin Plant Biol* 57: 164-170.

Wang, Q., Xu, J., Pu, X., Lv, H., Liu, Y., Ma, H., Wu, F., Wang, Q., Feng, X., and Liu, T. (2021). Maize DNA methylation in response to drought stress is involved in target gene expression and alternative splicing. *Int J Mol Sci* 22(15): 8285.

Wang, T., Xing, J., Liu, Z., Zheng, M., Yao, Y., Hu, Z., Peng, H., Xin, M., Zhou, D., and Ni, Z. (2019). Histone acetyltransferase GCN5-mediated regulation of long non-coding RNA At4 contributes to phosphate starvation response in Arabidopsis. *J Exp Bot* 70(21): 6337-6348.

Wang, X., Hu, L., Wang, X., Li, N., Xu, C., Gong, L., and Liu, B. (2016). DNA methylation affects gene alternative splicing in plants: an example from rice. *Mol Plant* 9(2): 305-307.

Wang, Y., Du, F., Li, Y., Wang, J., Zhao, X., Li, Z., Xu, J., Wang, W., and Fu, B. (2022). Global N6-methyladenosine profiling revealed the tissue-specific epitranscriptomic regulation of rice responses to salt stress. *Int J Mol Sci* 23(4): 2091.

Wibowo, A., Becker, C., Marconi, G., Durr, J., Price, J., Hagmann, J., Papareddy, R., Putra, H., Kageyama, J., and Becker, J. (2016). Hyperosmotic stress memory in Arabidopsis is mediated by distinct epigenetically labile sites in the genome and is restricted in the male germline by DNA glycosylase activity. *Elife* 5: e13546.

Yang, L., Perrera, V., Saplaoura, E., Apelt, F., Bahin, M., Kramdi, A., Olas, J., Mueller-Roeber, B., Sokolowska, E., and Zhang, W. (2019). m5C methylation guides systemic transport of messenger RNA over graft junctions in plants. *Current Biol* 29(15): 2465-2476. e2465.

Yang, Z., Zhu, P., Kang, H., Liu, L., Cao, Q., Sun, J., Dong, T., Zhu, M., Li, Z., and Xu, T. (2020). High-throughput deep sequencing reveals the important role that microRNAs play in the salt response in sweet potato (*Ipomoea batatas* L.). *BMC Genom* 21: 1-16.

Younis, A., Siddique, M.I., Kim, C.-K., and Lim, K.-B. (2014). RNA interference (RNAi) induced gene silencing: a promising approach of hi-tech plant breeding. *Int J Biol Sci* 10(10): 1150.

Zhang, Q., Liang, Z., Cui, X., Ji, C., Li, Y., Zhang, P., Liu, J., Riaz, A., Yao, P., and Liu, M. (2018). N6-methyladenine DNA methylation in Japonica and Indica rice genomes and its association with gene expression, plant development, and stress responses. *Mol Plant* 11(12): 1492-1508.

Zhang, W., Wang, N., Yang, J., Guo, H., Liu, Z., Zheng, X., Li, S., and Xiang, F. (2020). The salt-induced transcription factor GmMYB84 confers salinity tolerance in soybean. *Plant Sci* 291: 110326.

Zhang, X., Dong, J., Deng, F., Wang, W., Cheng, Y., Song, L., Hu, M., Shen, J., Xu, Q., and Shen, F. (2019). The long non-coding RNA lncRNA973 is involved in cotton response to salt stress. *BMC Plant Biol* 19: 1-16.

Zhang, Z., Zhang, S., Zhang, Y., Wang, X., Li, D., Li, Q., Yue, M., Li, Q., Zhang, Y.-e., and Xu, Y. (2011). Arabidopsis floral initiator SKB1 confers high salt tolerance by regulating transcription and pre-mRNA splicing through altering histone H4R3 and small nuclear ribonucleoprotein LSM4 methylation. *Plant Cell* 23(1): 396-411.

Zheng, H., Sun, X., Li, J., Song, Y., Song, J., Wang, F., Liu, L., Zhang, X., and Sui, N. (2021). Analysis of N6-methyladenosine reveals a new important mechanism regulating the salt tolerance of sweet sorghum. *Plant Sci* 304: 110801.

Zhou, C., Wang, C., Liu, H., Zhou, Q., Liu, Q., Guo, Y., Peng, T., Song, J., Zhang, J., and Chen, L. (2018). Identification and analysis of adenine N 6-methylation sites in the rice genome. *Nat Plants* 4(8): 554-563.

Zhu, J.-K. (2002). Salt and drought stress signal transduction in plants. *Annu Rev Plant Biol* 53(1): 247-273.

Zhu, N., Cheng, S., Liu, X., Du, H., Dai, M., Zhou, D.-X., Yang, W., and Zhao, Y. (2015). The R2R3-type MYB gene *OsMYB91* has a function in coordinating plant growth and salt stress tolerance in rice. *Plant Sci* 236: 146-156.

Zong, W., Zhong, X., You, J., and Xiong, L. (2013). Genome-wide profiling of histone H3K4-tri-methylation and gene expression in rice under drought stress. *Plant Mol Biol* 81: 175-188.

JPMB
Journal of Plant Molecular Breeding
Published by Genetics and Agricultural Biotechnology Institute of Tabarestan
2023 | Volume 11 | Issue 2

مقاله مروری

سازگاری اپی‌ژنتیکی به خشکی و شوری در گیاهان زراعی

محسن حسینی و احمد ارزانی*

گروه زراعت و اصلاح نباتات، دانشکده کشاورزی، دانشگاه صنعتی اصفهان، اصفهان، ایران

چکیده: تأثیر شدید تنش خشکی و شوری بر عملکرد گیاهان، تهدیدی مهم برای امنیت غذایی در سراسر جهان است. گیاهان دارای توانایی درک محرک‌های محیطی خود هستند و مکانیسم‌های دفاعی مقابله با تنش غیرزنده را از طریق شبکه‌های تنظیمی متنوع تنظیم می‌کنند. پیچیدگی‌های تحمل به خشکی و شوری را می‌توان به مشارکت دو عامل و مکانیسم ژنتیک و اپی‌ژنتیک تفکیک کرد. مکانیسم‌های اپی‌ژنتیکی در سازگاری گیاهان به شدیدترین تنش‌های خشکی و شوری نقش دارند. گیاهان تاحدی با انجام تغییرات پایدار در بیان ژن از طریق فرآیند «علامت‌گذاری» فیزیکی DNA یا پروتئین‌های مرتبط با آن که معمولاً اپی‌ژنتیک نامیده می‌شود به تنش پاسخ می‌دهند. گیاهان از مکانیسم‌های اپی‌ژنتیکی مختلف که برای سازگاری و انعطاف‌پذیری فنوتیپی حیاتی است برای تغییر بیان ژن استفاده می‌کنند. این مکانیسم‌ها شامل متیلاسیون DNA، تغییرات هیستون، بازسازی کروماتین، اپی‌ترانسکریپتومیکس و خاموش کردن ژن به واسطه RNAهای کوچک است. قابل ذکر است که تغییرات اپی‌ژنتیکی می‌توانند وراثتی یا غیر وراثتی و ناپایدار باشند. دانش پیشرفته اپی‌ژنتیک مکمل ژنتیک است و به توسعه استراتژی‌ها برای ادغام آن‌ها در برنامه‌های اصلاح گیاهان در جهت سازگاری با تنش غیر زنده کمک می‌کند. این بررسی جدیدترین یافته‌های قابل‌توجه در مورد پاسخ‌های اپی‌ژنتیکی گیاهان زراعی به سیگنال‌های تنش غیرزنده به‌ویژه تحمل به خشکی و شوری را ارائه می‌کند.

کلمات کلیدی: تحمل به خشکی، نواحی CpG، اپی ژنومیک، تنش اسمزی، تحمل به شوری، تنش آبی.

ویراستار علمی
دکتر سروش کومار،
موسسه تحقیقات کشاورزی هندوسنان، هند

تاریخ
دریافت: ۶ بهمن ۱۴۰۲
پذیرش: ۱۱ بهمن ۱۴۰۲
چاپ: ۲۳ بهمن ۱۴۰۲

نویسنده مسئول
دکتر احمد ارزانی
a_arzania@iut.ac.ir

ارجاع به این مقاله
Hoseini, M. and Arzani, A. (2023). Epigenetic adaptation to drought and salinity in crop plants. *J Plant Mol Breed 11* (2): 1-16.
doi: 10.22058/JPMB.2024.2021261.1292.

JPMB | Journal of Plant Molecular Breeding
Published by Genetics and Agricultural Biotechnology Institute of Tabarestan
2023 | Volume 11 | Issue 2

Effects of polyploidy induction on the performance of anise (*Pimpinella anisum* L.)

Haniyeh Ahmadinia and Parviz Heidari*

Faculty of Agriculture, Shahrood University of Technology, Shahrood 3619995161, Iran.

Original paper

OPEN ACCESS

Edited by

Prof. Ahmad Arzani,
Isfahan University of Technology, Iran

Date

Received: 15 January 2024
Accepted: 03 February 2024
Published: 17 February 2024

Correspondence

Dr. Parviz Heidari
heidarip@shahroodut.ac.ir

Citation

Ahmadinia, H., and Heidari, P. (2024). Effects of polyploidy induction on the performance of anise (*Pimpinella Anisum* L.). *J Plant Mol Breed 11* (2): 17-30.
doi: 10.22058/jpmb.2024.2020503.1289.

Abstract: Plant chromosome manipulation is a powerful tool in plant breeding due to its significant impact on various genetic traits and diversity. To investigate the effect of polyploidy induction in anise (*Pimpinella anisum* L.), three different concentrations (0.01%, 0.5%, and 5%) of colchicine were tested. In this study, the seeds and terminal buds of five-week-old plants were treated with colchicine, and the process was repeated for three consecutive days. Subsequently, molecular, physiological, and morphological traits of both control (diploid) and induced (autotetraploid) plants were investigated. The results revealed that 0.01% colchicine had no significant effect on ploidy induction, while significant effects were observed at 0.5% and 5%. Seedlings treated with concentrations higher than 0.5% colchicine exhibited larger stomatal size, lower stomatal density, and darker leaf color. In addition, the contents of DNA, RNA, and total protein increased in seedlings treated with concentrations of 0.5% and 5%. Karyotype observation confirmed polyploidy induction in plants treated with colchicine concentrations above 0.5%. Overall, this study shows that colchicine can alter anise plants' ploidy by 0.5% and 5% and boost leaf size and pigments associated with photosynthesis, resulting in stronger plants.

Keywords: Medical plants, pigment content, nucleic acid content, ploidy level, plant vigor.

Introduction

Anise (*Pimpinella anisum* L.), 2n = 2x = 18, is a medicinal and aromatic plant belonging to the Apiaceae family that is used in the pharmaceutical, perfume production, and food industries (Gülçın et al., 2003). Additionally, the fruits and essential oils of this plant have antispasmodic, antioxidant, antimicrobial, insecticidal and antifungal effects (Özcan and Chalchat, 2006; Tepe et al., 2006). The seeds of this plant contain 5 to 5.5% essential oil, which is mainly composed of volatile phenylpropanoids such as transanthol (Tabanca et al., 2006). In addition, anise seed essential oil contains a small amount of estragole, anisaldehyde and cis-anthole (Omidbaigi et al., 2003; Tabanca et al., 2006). Anise seed and its essential oil are used both in ancient and modern times in salty foods, baked goods and various drinks. Anise seeds are a good source of many essential B complex vitamins, such as pyridoxine, niacin, riboflavin and thiamine. Considering all the positive features, including anti-diabetes, blood fat reduction, antioxidant activities, anticancer and antimicrobial properties, anise seeds and essential oils are recommended for safe use as dietary supplements (Sun et al., 2019).

Today, various methods, such as metabolite engineering, cell culture and the use of elicitors, are used to increase the production of secondary metabolites in medicinal plants. Increasing the ploidy level (polyploidy) is also known as an effective method for producing new genotypes and increasing the yield of plants (Chung et al., 2017; Liu et al., 2023). Polyploidy can also affect secondary metabolites in terms of quantity and chemical diversity. These changes are due to structural and functional modifications caused by an increase in the allelic level (Zahumenická et al., 2018). Polyploid plants are larger than diploids in terms of morphological characteristics such as leaf, stem, and root size, which can be beneficial for yield and crop production (Dhooghe et al., 2011), especially for fodder, vegetables, and medicinal plants. Polyploidy occurs spontaneously in plants but can be induced in a short period of time by using antimitotic substances such as colchicine, which interferes with spindle formation (Eng and Ho, 2019). Polyploidized plants are more tolerant to adverse environmental conditions due to their relatively stronger foundation (Fang et al., 2019). Additionally, polyploidy affects the increase in photosynthesis by increasing the amount of chlorophyll, and as a result, polyploid plants have a stronger foundation than their ancestors (Zahumenická et al., 2018).

Polyploidization is often associated with morphological and physiological changes that can increase plant growth rate and yield other commercially beneficial traits (Cheng et al., 2015). It was previously reported that polyploid plants have advantages in terms of creating tissues and organs; in general, compared with those of diploid species, the size of vegetative tissues, the shape of large flowers and resistance to environmental stresses are improved (Liu et al., 2011; Meng et al., 2011). For example, autotetraploid lavenders (*Lavandula angustifolia*) had larger flowers and leaves, thicker peduncles and larger shield hairs on their leaves than did their diploid genotypes (Urwin et al., 2007). Treating the terminal bud of watercress plants (*Nasturtium officinale*) with 0.5% colchicine was able to induce tetraploidy. Similarly, compared with diploid plants, tetraploid plants exhibit significant differences in leaf dimensions, stomatal number and chlorophyll content (Aqafarini et al., 2019). Investigation of different methods of polyploidy induction in Ispaghul (*Plantago ovata* Forsk.) showed that the use of 0.3% colchicine treatment for 24 hours or 22.5% trifloralin treatment for 72 hours on seeds results in the most tetraploid plants (Sabzehzari et al., 2020). Induction of polyploidy with different concentrations of colchicine was successfully performed in Salvia species such as *Salvia bowleyana* (Duan et al., 2006) and *S. hains* (Grouh et al., 2011). In both species, compared with diploid plants, chromosomally doubled plants had thicker and wider leaves, darker colors, thicker roots and larger stomata. It has been reported that in some cases, increased resistance to pathogens can be associated with polyploidy. For example, the tetraploid *Trifolium pratense* is more resistant to clover rot than is its diploid ancestor (Vestad, 1960; Vleugels et al., 2013), and the tetraploid *Glycine tabacina* is more resistant to leaf rust disease (*Phakopsora pachyrhizi*) than is its diploid ancestor (Burdon and Marshall, 1981). Recent hypotheses show that ploidy can affect plant defense by increasing genetic adaptation to

pathogens through replacement or through new functions of resistance genes and genes related to plant defense (Innes et al., 2008; King et al., 2012). In the present study, different concentrations of colchicine were applied to induce polyploidy in anise. We found that terminal bud treatment with 0.5% and 5% colchicine could increase the polyploidy rate in anise plants, as evidenced by changes in the morphological and physiological traits along with alterations in nucleic acid content.

Materials and Methods

Plant materials and seed treatment

In the first experiment, anise seeds, landraces prepared from Shahrood region, were transferred to 3% sodium hypochlorite solution for 15 minutes for sterilization, after which the seeds were washed three times with distilled water to remove the residues of the solution. Then, the anise seeds were placed between two layers of filter paper and irrigated with distilled water. After one week, the water in the Petri dishes was removed, and the samples (200 seeds) were treated with different concentrations of colchicine (0.01% and 0.5%) for different periods of time (6, 24 and 48 hours). Ten microlitres of colchicine solution was added to each petri dish. Finally, after seven days, the number of plants was counted, and the results were used to measure the survival rate.

Terminal bud treatment

In the second experiment, sterilized anise seeds were grown in pots. First, perlite and peat moss were prepared at a ratio of 2:1, mixed together and transferred to the pots. Seven seeds were subsequently planted in each pot (finally, four plants remained in each pot for treatment). Pots were maintained under a 17-hour photoperiod (6000 lux) and a 25 ± 3°C temperature. After five weeks, the terminal buds of the plants were treated with different concentrations of colchicine (0 (as a control), 0.01%, 0.5%, or 5%). The selection of colchicine concentrations was determined based on the review of previous studies. Between 10 and 11 am (when the mitotic divisions were most common), the terminal bud was treated with 5 µl of colchicine. This work was repeated for three consecutive days.

Measurement of morphological traits

After applying the terminal bud treatment, new leaves were considered to confirm polyploidy. Determination of ploidy level in treated plants was first based on morphological changes in different stages of growth and development by observing plants suspected of polyploidy in comparison with control plants. Morphological traits such as the length and width of new leaves, length of petioles, distance between nodes, and density and size of stomata were measured. A digital caliper was used to measure seedling length, leaf length, the distance between the second leaflet, the length and width of the terminal leaflet and the diameter of the petiole.

Measurement of plant stomata

To determine the number of stomata on the surface of the new leaves, the upper layer of the leaf was covered with a thin layer of colorless varnish. After drying, the above layer was placed on a clean glass slide using adhesive tape, and the number and size of the stomata were counted with an Olympus CH2 optical microscope.

Leaf pigments

The method outlined by Lichtenthaler and Wellburn (1983) was employed to measure leaf chlorophyll pigments. In brief, the chlorophyll and carotenoid contents were measured without crushing. For this purpose, we mixed 50 mg of leaf tissue with 5 ml of dimethyl sulfoxide and put it in an oven at 65°C for 4 hours. After that, using a spectrophotometer, the absorbance was recorded at 470, 645 and 665 nm. Finally, the contents of chlorophyll a and b and carotenoids were obtained using the following relationships:

Chla = (12.19 A665) - (3.45 A645)

Chlb = (21.99 A645 - 5.32 A645)

Cartenoeid = (1000 A470 - 2.14Chla - 70.16Chlb)/200

Protein content

The Bradford method was used to measure the amount of protein (Bradford, 1976). The Bradford method is a fast, simple, accurate and sensitive colorimetric method used to measure the total protein concentration in biological samples. The basis of this method is the binding of protein molecules to Coomassie dye under acidic conditions, which leads to a change in color from brown to blue, and as a result, a change in light

absorption occurs. In fact, Coomassie blue dye binds to proteins and produces a blue color that can be measured at a wavelength of 595 nm.

DNA and RNA extraction

DNA extraction was performed using the CTAB method (Porebski et al., 1997). To ensure comparability of DNA quantity, 100 mg of young leaves from each treatment was used. RNA extraction was performed using a TRIzol reagent kit (Kiagene Fanavar, Iran) according to the manufacturer's instructions. Likewise, to extract RNA, the same amount of plant tissue was used for all samples. Finally, the quantity of the extracted DNA and RNA samples was measured by a Nano Photometer (Implen N50).

Survival rate and seed germination

The number of surviving plants after terminal bud treatment with colchicine was evaluated as the survival percentage. Additionally, the seedlings that were treated with different concentrations were allowed to produce seeds. The seeds were subsequently distributed in Petri dishes, after which the germination rate was calculated.

Preparation of karyotypes and chromosome counts

Karyotyping is the process of depicting the set of chromosomes in the cells of a living organism to check the chromosomal content. To perform anise karyotyping, first, the plants that were treated with different concentrations of terminal buds were allowed to produce seeds, after which the seeds were germinated. The root tips of the germinated seeds were used to prepare the karyotype. After cutting the young roots, karyotype preparation was performed in five steps, namely, root pretreatment (0.01% colchicine), fixation with Carnoy 1 solution (one part of absolute acetic acid and three parts of absolute ethanol), hydrolysis (normal hydrochloric acid at a temperature of 60°C for 8 minutes), root staining with 0.1% Aceto Carmen for 45 minutes, and squashing the roots with 45% acetic acid. Chromosomes were observed using an OLYMPUS CH2 light microscope.

Data analysis

The data were analyzed via Minitab 17 software (version 17) via ANOVA, and the means were compared using Tukey's test at the 5% probability level. Graphs were drawn based on the mean and standard deviation for each treatment by GraphPad Prism 5.0 software.

Results

Toxic effects of colchicine on embryos

The results showed that seed treatment with colchicine caused nongermination and nongrowth of a large number of seeds (Figure 1). The highest percentage of plant survival was obtained in the control treatment (no use of colchicine).

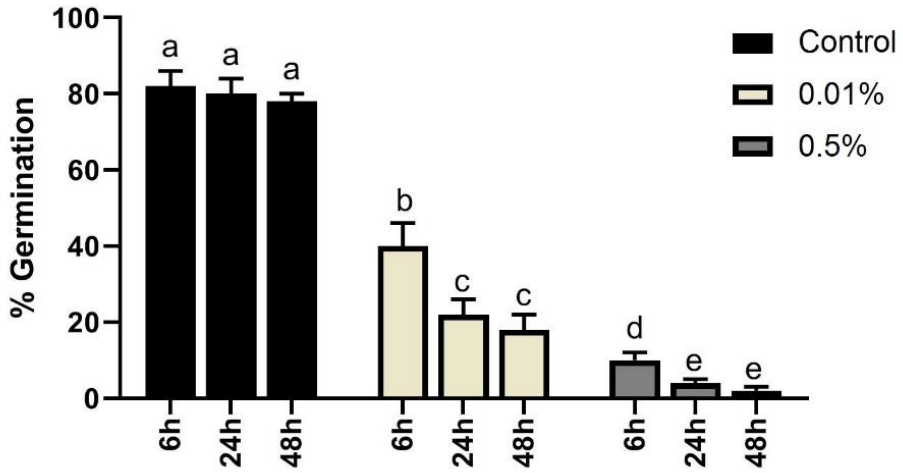

Figure 1. Germination rate of anise seeds treated with colchicine. Different letters indicate significant differences (p value < 0.05) between experimental treatments.

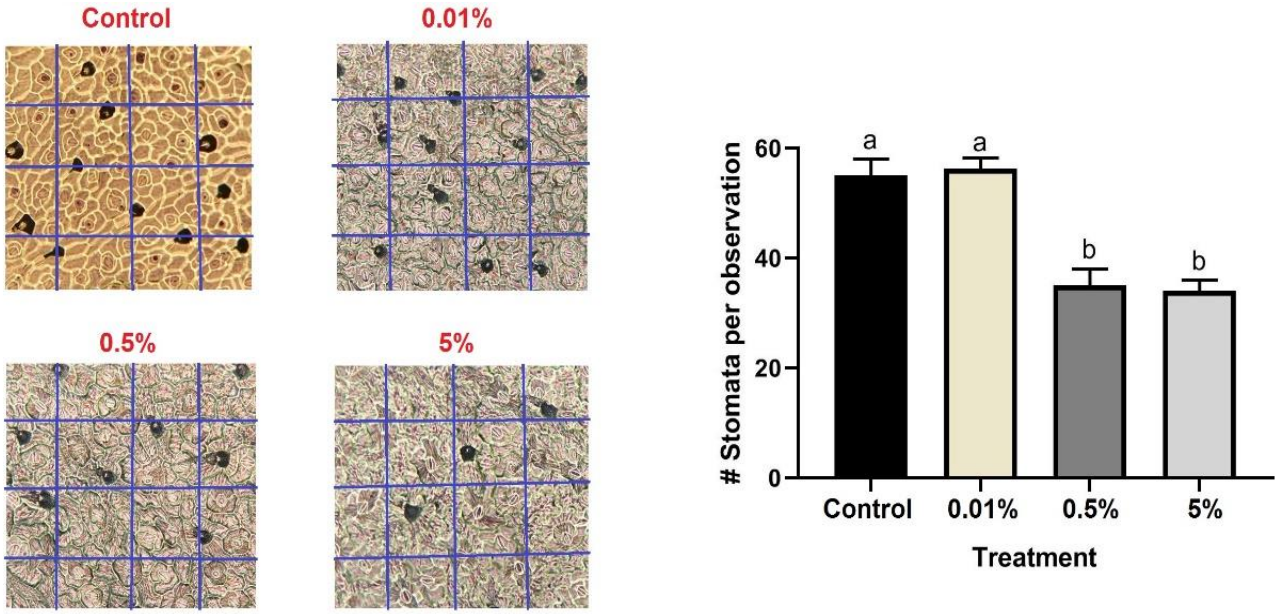

Figure 2. Stomatal density of young leaves after treatment of top buds with different concentrations of colchicine.

The survival percentage of the seedlings (germination) decreased with increasing treatment duration; the highest survival percentage was related to the duration of 6 hours at a concentration of 0.01%, and the lowest survival percentage was related to the duration of 48 hours at a concentration of 0.5%. These results indicate that colchicine has toxic effects on embryos and that seed treatment is not recommended for inducing polyploidy in anise plants.

Stomatal density

Based on microscopic observations of leaf stomatal characteristics in plants treated with colchicine compared to diploids, the density and size of stomata on new leaves were affected by polyploidy induction (Figure 2). A decrease in stomatal density and an increase in stomatal size were observed in seedlings treated with 0.5% and 5% colchicine. The size and density of stomata are among the important traits related to the ploidy level and can be used as biomarkers.

Morphological traits

The effects of polyploidy induction on morphological traits were investigated. A comparison of the means of plants treated with different concentrations of colchicine revealed that the length of the seedlings and leaves and the petiole diameter were not affected by treatment with different concentrations of colchicine (Figure 3). However, treatment with a 5% concentration of colchicine somewhat increased the length of the leaf and petiole diameter. The dimensions (length and width) of the terminal leaflets and the length between the leaflets were significantly greater for the plants treated with high concentrations (0.5% and 5%) of colchicine. In general, the induction of polyploidy did not significantly alter the height of the plant, but it caused changes in the dimensions of the new leaflets and caused compact seedlings with broad leaves (Figure 4a and 4b). In this study, compared with those of the control plants, the shapes of the new leaves on the plants treated with 5% and 0.5% colchicine were wrinkled, uneven, wide and thick (Figure 4b).

Leaf pigment content

A comparison of the mean chlorophyll a content revealed that there was a significant difference between the 5% colchicine treatment and the control treatment. However, the 5% treatment did not significantly differ from the 0.5% treatment (Figure 5).

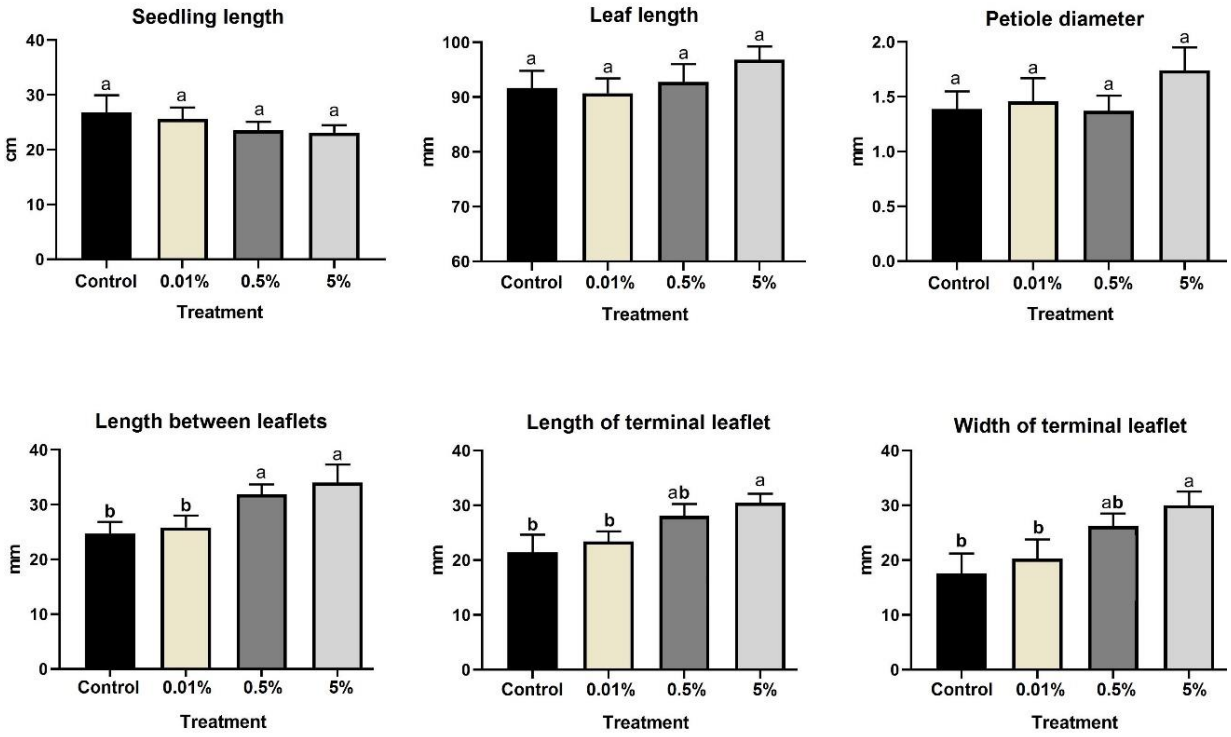

Figure 3. Comparison of the means for morphological traits, including seedling length, leaf length, petiole diameter, length between leaflets, length and width of terminal leaflet, between the control treatment and treatment with different colchicine concentrations. Different letters indicate significant differences ($p < 0.05$) between experimental treatments.

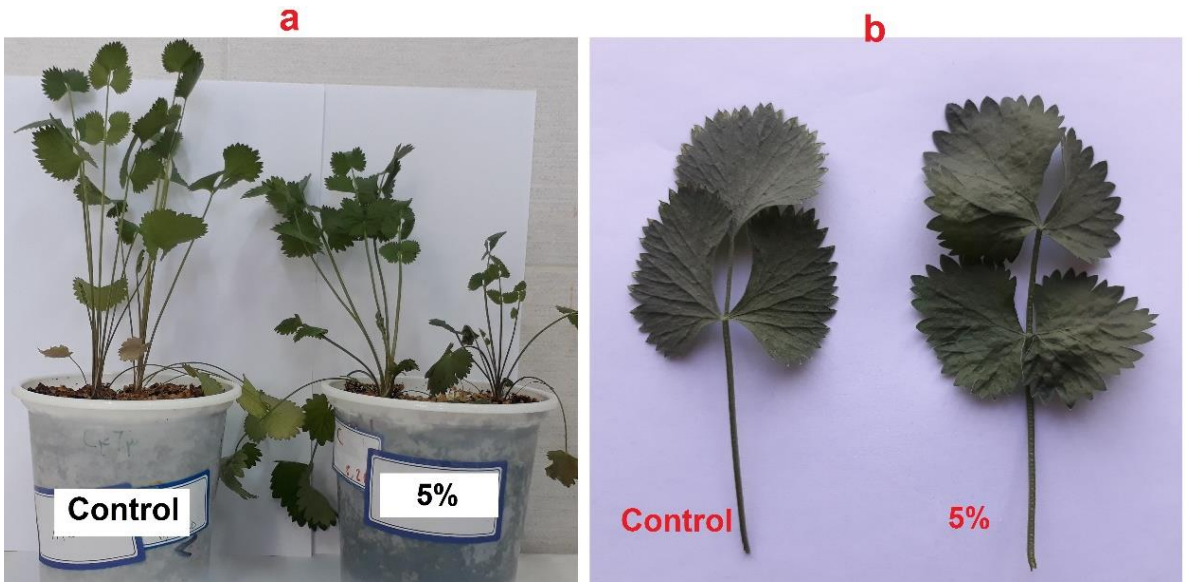

Figure 4. Morphological modifications between the control and 5% colchicine treatment groups in terms of seedling height (a) and leaf length and width (b).

It seems that the content of chlorophyll a increases in induced tetraploid plants. No significant differences were detected in the contents of chlorophyll b and carotenoids between the colchicine treatments and the control, although the amounts of chlorophyll b and carotenoids were somewhat greater in the induced plants and in the 0.5% and 5% treatment groups.

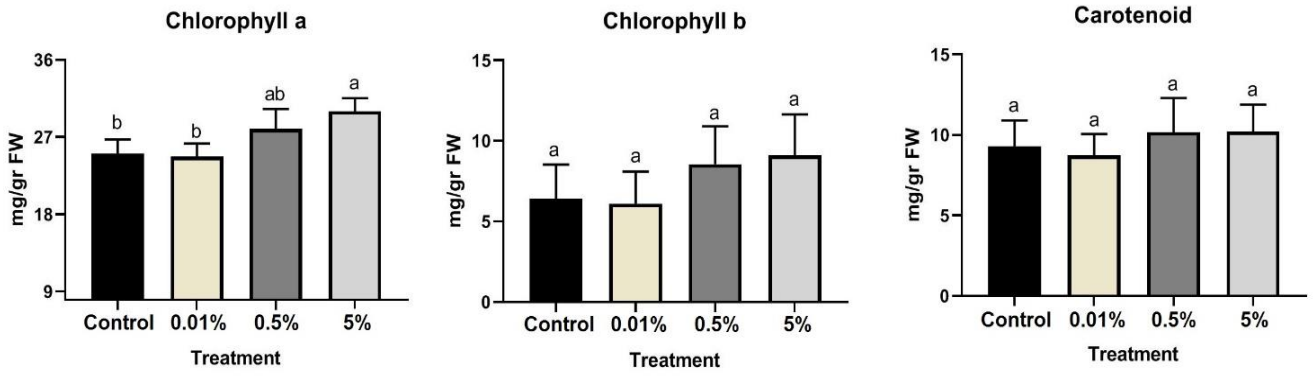

Figure 5. Mean comparison of chlorophyll a and b and carotenoid content under the colchicine treatments. Different letters indicate significant differences (p value < 0.05) between experimental treatments.

Nucleic acids and total protein content

In the present study, the levels of three macromolecules, protein, DNA, and RNA, were measured in seedlings treated with colchicine (Figure 6). Significant increases in the concentrations of protein, DNA, and RNA were observed in the new leaves treated with 0.5% and 5% colchicine. Interestingly, the total RNA content sharply increased in the 5% treatment group compared with the control sample. An increase in the amount of DNA causes an increase in the number of genes and, as a result, the content of RNA and protein is increased. As a result, the effect intensity of each gene increases in related cellular pathways.

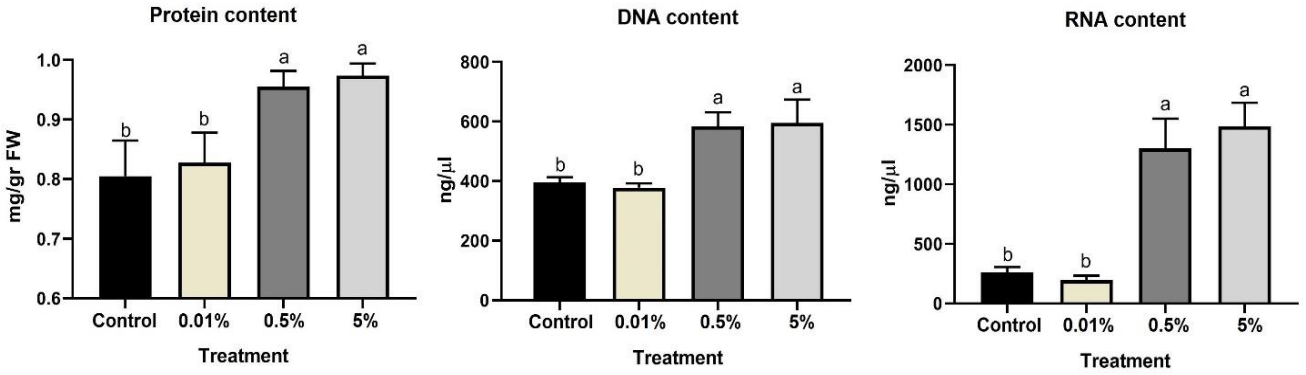

Figure 6. Mean comparison of protein, DNA, and RNA content under the colchicine treatments. Different letters indicate significant differences (p value < 0.05) between experimental treatments.

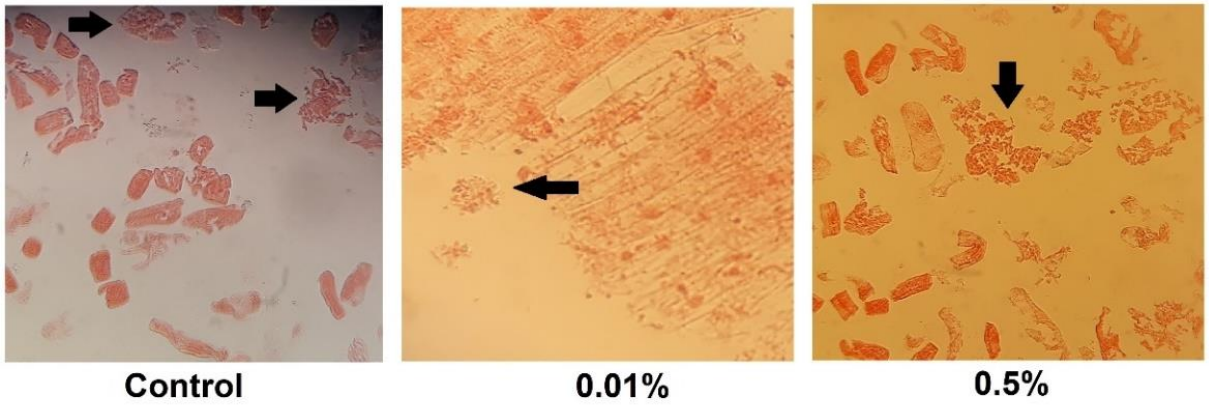

Figure 7. Karyotype analysis of the roots of plants treated with 0.01% or 0.5% colchicine.

Chromosome observation

Chromosome counting is a direct, unambiguous and common way to determine the number of chromosomes in plant cells (Figure 7). This method is vital in plant systematic studies, classification and breeding. To investigate the effects of colchicine treatments on the polyploidy of treated plants, we examined and analyzed the root tip cells. The results revealed that the chromosome number of the plants treated with a concentration of 0.5% colchicine was duplicated comparing to those in the control and 0.01% colchicine samples. The limited seed production in the first generation prevented the preparation of a suitable karyotype for the 5% treatment. However, based on changes at the 0.5% level, the occurrence of polyploidy in this treatment can also be confirmed.

Effects of colchicine on survival and induction rate

The results revealed that tetraploid induction was increased at two high colchicine concentrations, 0.5% and 5%, based on morphological traits and nucleic acid content (Figure 8a). However, fewer than 40% of the seedlings treated with 5% colchicine survived. In addition, the germination rate of seeds from plants treated with 0.5% or 5% colchicine was sharply reduced (Figure 8b). Based on the percentage of tetraploid induction, seedling survival and seed germination, 0.5% colchicine was introduced as an effective dose for inducing tetraploid anise seedlings with high fertility ability.

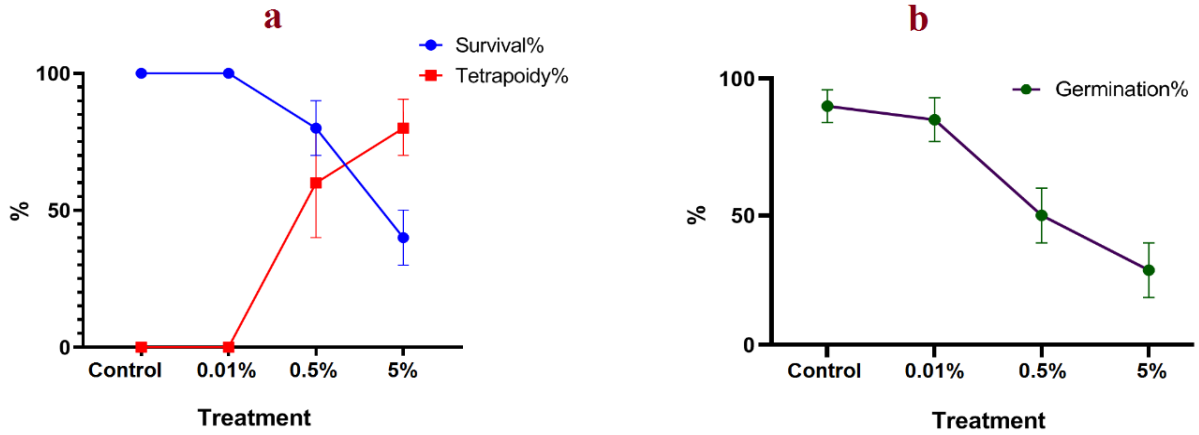

Figure 8. Effects of colchicine on the percentage of surviving plants and tetraploid induction (a) and on the percentage of generated seeds from seedlings (b).

Discussion

Elevating the ploidy level (polyploidy) is recognized as an effective approach for generating novel genotypes with enhancing the biomass, consequently augmenting the bioactive compounds of medicinal plants (Nilanthi et al., 2009; Chung et al., 2017). Polyploidized plants exhibit enhanced tolerance to negative conditions due to their relatively stronger organs (Fang et al., 2019). Additionally, polyploidy affects photosynthesis by increasing the amount of chlorophyll, and as a result, polypoid plants have a stronger foundation than their ancestors (Azoush et al., 2014; Zahumenická et al., 2018). In this research, the induction of polyploidy in anise was investigated. The results showed that applying colchicine to anise seeds is not a suitable method for increasing ploidy. Colchicine likely has toxic effects on embryos and young plants and can cause their death or severe weakening. On the other hand, terminal bud treatment had significant effects on morphological characteristics and other traits related to genome content. In general, according to the results obtained from the morphological studies, it can be said that the treatment of the terminal bud of anise seedlings with concentrations of 5% and 0.5% colchicine has been able to have changes in the distance between the leaflets and the dimensions of the leaves. These results indicate that changes likely occurred at the genomic level, which led to morphological changes in new leaves after treatment. Autopolyploid plants and their organs are often larger than their diploid parents are, which makes them attractive to plant breeders (Dai et al., 2015). Considering that vegetative organs are the main source of active compounds in most medicinal plants, increasing the chromosomal level can be considered a valuable and fast way to increase drug production (Dhawan and Lavania, 1996). However, in many cases, it has been reported that tetraploid plants are smaller than or equal in size to diploid plants (Lavania, 2005).

The usual result of polyploidy in plants is reduced growth due to decreased cell division, which occurs as a result of disturbance of the auxin content in cells. In this regard, the rate of respiration and the activity of a large number of enzymes also decrease (Stebbins, 1971). In our study, a decrease in seedling height and length was observed with increasing colchicine concentration, which was consistent with the results observed for the height of anthurium plants, which showed a decrease in the height of plants treated with colchicine compared to diploids (Chen et al., 2011). Additionally, the induction of polyploidy in chamomile (Saharkhiz, 2007) and *Platanus acerifolia* (Liu et al., 2007) was associated with reduced growth. The decreased growth of induced polypoid plants is due to a decrease in the rate of cell division (Eigsti, 1947), a decrease in growth hormones and decreased activities of metabolites in plants (Larsen and Tung, 1950). The decrease in height of tetraploid plants is probably due to the high toxicity of colchicine and its negative effects on physiological activities, including the production and activity of plant growth hormones. Moreover, differences in leaf margins and leaf shapes were observed between induced plants treated with colchicine (5% and 0.5%) and diploid plants. Some of the observed irregularities in the leaf size, shape, texture and color of the seedlings may be due to initial disturbances caused by colchicine. The leaves of tetraploid plants are significantly thicker than the leaves of diploid plants because of the presence of thick parenchyma, spongy parenchyma and epidermal cells and large intercellular spaces in the spongy parenchyma (Allario et al., 2011).

A decrease in stomatal density and an increase in stomatal size were observed in seedlings treated with 0.5% and 5% colchicine. Increasing the ploidy level of the nucleus often causes structural changes such as stomatal density, increasing the size of stomatal cells and the number of chloroplasts in the cell. Research has shown that the size of stomatal guard cells is more affected by genetic factors than is that of other plant cells and is less influenced by environmental conditions (Watrous and Wimber, 1989). With increasing ploidy level, the length and width of the stomata increase, and as a result, the stomatal density decreases. Increasing ploidy also increases the number of chloroplasts in stomatal guard cells. Studies on chicory and Egyptian bean plants have shown that the number of chloroplasts in the stomatal guard cells of tetraploid plants is greater than that in diploid plants (Ghotbi Ravandi et al., 2013). On the other hand, in tetraploid hop plants, despite the increase in stomatal size, no

significant difference in stomatal density per unit area was observed between diploid and tetraploid plants (Roy et al., 2001). Therefore, the type of species under study plays an important role in determining stomatal indices at different ploidy levels. In most cases, polyploid leaves exhibit a greater volume of mesophyll cells with more chloroplasts and chlorophyll than diploids, resulting in a greater rate of photosynthesis per cell (Coate et al., 2012). Previous research has shown that polyploidization increases the number of chloroplasts and photosynthesis in each cell, which may be due to the increase in genome content and cell size (Warner and Edwards, 1993). The results of the present study showed that colchicine treatment had a significant effect only on the content of chlorophyll a. In the research conducted by Liao et al. (2016)Liao et al. (2016)Liao et al. (2016) on Populus trees, the photosynthetic rate and chlorophyll content were significantly greater in tetraploids than in diploids. In addition, Abdoli et al. (2013)Abdoli et al. (2013)Abdoli et al. (2013) reported that an increase in ploidy causes an increase in the number of chloroplasts in the leaf and thus increases photosynthesis. An increase in the number of gene copies causes an increase in the number of transcripts and the amount of protein, which in turn affects the cell volume and plant stem (Tsukaya, 2008). The results of this research confirmed that the content of genomic material and the amount of total RNA increased in plants treated with 5% colchicine, and as a result, the total protein content also increased in the cells. Additionally, Yan et al. (2014)Yan et al. (2014)Yan et al. (2014) reported an almost twofold increase in total protein in radish plants. Although there is sometimes no direct relationship between RNA and protein levels, different factors affect the translation and stability of proteins. Increasing the genomic level can be considered as a strategy in the breeding of medicinal plants to increase biomass and effective substance

Conclusion

Based on the results obtained from this research, it can be concluded that colchicine, as a disruptor of mitotic spindles, can induce polyploidy in anise plants. Terminal bud treatment was found to be more effective than seed treatment. It seems that colchicine concentrations higher than 0.5% are suitable for increasing ploidy, although the toxicity associated with higher concentrations reduces the survival rates of seedlings and their fertility. Based on four important traits related to polyploidy- namely, DNA content, total RNA content, protein content, and stomatal size and density- it is concluded that it is possible to produce autotetraploid plants using colchicine. An increase in the amount of genomic content caused a change in the appearance of anise plants, as these plants had larger leaves. Additionally, compared with that in the control plants, the amount of chlorophyll in the polyploidized plants increased. An increase in leaf size and chlorophyll content can increase the photosynthesis rate and water consumption efficiency in plants, thereby potentially increasing production rates. In the end, the success of autoploid plant production can be influenced by factors such as the concentration of the inducing substance, the chosen growth stage for treatment and the method of applying the treatment.

Supplementary Materials

No supplementary material is available for this article.

Author Contributions

Conceptualization, P.H.; methodology, P.H. and H.A.; validation, P.H.; formal analysis, P.H. and H.A.; writing—original draft preparation, P.H.; writing—review and editing, P.H.; project administration, P.H.; supervision, P.H. All authors have read and agreed to the published version of the manuscript.

Funding

This research received no external funding.

Acknowledgments

We thank the Shahrood University of Technology for financially supporting and providing the needed facilities.

Conflict of Interest Statement

The authors declare no conflict of interest.

References

Abdoli, M., Moieni, A., and Naghdi Badi, H. (2013). Morphological, physiological, cytological and phytochemical studies in diploid and colchicine-induced tetraploid plants of *Echinacea purpurea* (L.). *Acta Physiol Plant* 35(7): 2075-2083.

Allario, T., Brumos, J., Colmenero-Flores, J.M., Tadeo, F., Froelicher, Y., Talon, M., Navarro, L., Ollitrault, P., and Morillon, R. (2011). Large changes in anatomy and physiology between diploid Rangpur lime (*Citrus limonia*) and its autotetraploid are not associated with large changes in leaf gene expression. *J Exp Bot* 62(8): 2507-2519.

Aqafarini, A., Lotfi, M., Norouzi, M., and Karimzadeh, G. (2019). Induction of tetraploidy in garden cress: morphological and cytological changes. *Plant Cell Tissue Organ Cult* 137: 627-635.

Azoush, S., Kazemitabar, S.K., and Heidari, P. (2014). Polyploidy induction in Iranian Borage (*Echium amoenum* L.) by colchicine treatment. *Biharian Biol* 8(2): 87-89.

Bradford, M.M. (1976). A rapid and sensitive method for the quantitation of microgram quantities of protein utilizing the principle of protein-dye binding. *Anal Biochem* 72(1-2): 248-254.

Burdon, J., and Marshall, D. (1981). Inter-and intra-specific diversity in the disease-response of *Glycine* species to the leaf-rust fungus *Phakopsora pachyrhizi*. *J Ecol*: 381-390.

Chen, C., Hou, X., Zhang, H., Wang, G., and Tian, L. (2011). Induction of *Anthurium andraeanum* "Arizona" tetraploid by colchicine in vitro. *Euphytica* 181: 137-145.

Cheng, S., Zhu, X., Liao, T., Li, Y., Yao, P., Suo, Y., Zhang, P., Wang, J., and Kang, X. (2015). Gene expression differences between high-growth *Populus allotriploids* and their diploid parents. *Forests* 6(3): 839-857.

Chung, H.-H., Shi, S.-K., Huang, B., and Chen, J.-T. (2017). Enhanced agronomic traits and medicinal constituents of autotetraploids in *Anoectochilus formosanus* Hayata, a top-grade medicinal orchid. *Molecules* 22(11): 1907.

Coate, J.E., Luciano, A.K., Seralathan, V., Minchew, K.J., Owens, T.G., and Doyle, J.J. (2012). Anatomical, biochemical, and photosynthetic responses to recent allopolyploidy in *Glycine dolichocarpa* (Fabaceae). *Am J Bot* 99(1): 55-67.

Dai, F., Wang, Z., Luo, G., and Tang, C. (2015). Phenotypic and transcriptomic analyses of autotetraploid and diploid mulberry (*Morus alba* L.). *Int J Mol Sci* 16(9): 22938-22956.

Dhawan, O., and Lavania, U. (1996). Enhancing the productivity of secondary metabolites via induced polyploidy: a review. *Euphytica* 87: 81-89.

Dhooghe, E., Van Laere, K., Eeckhaut, T., Leus, L., and Van Huylenbroeck, J. (2011). Mitotic chromosome doubling of plant tissues in vitro. *Plant Cell Tissue Organ Cult* 104: 359-373.

Duan, Y.-Z., Ke, S.-Y., Cao, J., Niu, Y.-Z., and Peng, C.-Z. (2006). Study on induction of polyploidy in *Salvia bowleyana* by colchicine treatment. *Zhongguo Zhong Yao Za Zhi* 31(6): 445-448.

Eigsti, O. (1947). The pollen tube method for making comparisons of differences in mitotic rates between diploids and tetraploids. *Genetics* 32: 85.

Eng, W.-H., and Ho, W.-S. (2019). Polyploidization using colchicine in horticultural plants: A review. *Sci Hortic* 246: 604-617.

Fang, C., Fernie, A.R., and Luo, J. (2019). Exploring the diversity of plant metabolism. *Trends Plant Sci* 24(1): 83-98.

Ghotbi Ravandi, E., Rezanejad, F., Zolala, J., and Dehghan, E. (2013). The effects of chromosome-doubling on selected morphological and phytochemical characteristics of *Cichorium intybus* L. *J Hortic Sci Biotechnol* 88(6): 701-709.

Grouh, M.S.H., Meftahizade, H., Lotfi, N., Rahimi, V., and Baniasadi, B. (2011). Doubling the chromosome number of *Salvia hains* using colchicine: Evaluation of morphological traits of recovered plants. *J Med Plant Res* 5(19): 4892-4898.

Gulcın, I., Oktay, M., Kırecci, E., and Kufrevıoglu, O.I. (2003). Screening of antioxidant and antimicrobial activities of anise (*Pimpinella anisum* L.) seed extracts. *Food Chem* 83(3): 371-382.

Innes, R.W., Ameline-Torregrosa, C., Ashfield, T., Cannon, E., Cannon, S.B., Chacko, B., Chen, N.W., Couloux, A., Dalwani, A., and Denny, R. (2008). Differential accumulation of retroelements and diversification of NB-LRR disease resistance genes in duplicated regions following polyploidy in the ancestor of soybean. *Plant Physiol* 148(4): 1740-1759.

King, K., Seppälä, O., and Neiman, M. (2012). Is more better? Polyploidy and parasite resistance. *Biol Lett* 8(4): 598-600.

Larsen, P., and Tung, S.M. (1950). Growth-promoting and growth-retarding substances in pollen from diploid and triploid apple varieties. *Botanical Gazette* 111(4): 436-447.

Lavania, U. (2005). Genomic and ploidy manipulation for enhanced production of phyto-pharmaceuticals. *Plant Genet Resour* 3(2): 170-177.

Liao, T., Cheng, S., Zhu, X., Min, Y., and Kang, X. (2016). Effects of triploid status on growth, photosynthesis, and leaf area in *Populus*. *Trees* 30: 1137-1147.

Lichtenthaler, H.K., and Wellburn, A.R. (1983). "Determinations of total carotenoids and chlorophylls a and b of leaf extracts in different solvents", in: *Biochem Soc Trans.* Portland Press Ltd.).

Liu, G., Li, Z., and Bao, M. (2007). Colchicine-induced chromosome doubling in *Platanus acerifolia* and its effect on plant morphology. *Euphytica* 157: 145-154.

Liu, S., Chen, S., Chen, Y., Guan, Z., Yin, D., and Chen, F. (2011). In vitro induced tetraploid of Dendranthema nankingense (Nakai) Tzvel. shows an improved level of abiotic stress tolerance. *Sci Hortic* 127(3): 411-419.

Liu, Y., Duan, S.-D., Jia, Y., Hao, L.-H., Xiang, D.-Y., Chen, D.-F., and Niu, S.-C. (2023). Polyploid induction and karyotype analysis of dendrobium officinale. *Horticulturae* 9(3): 329.

Meng, H.-b., Jiang, S.-s., Hua, S.-j., Lin, X.-y., Li, Y.-l., Guo, W.-l., and Jiang, L.-x. (2011). Comparison between a tetraploid turnip and its diploid progenitor (*Brassica rapa* L.): the adaptation to salinity stress. *Agric Sci China* 10(3): 363-375.

Nilanthi, D., Chen, X.-L., Zhao, F.-C., Yang, Y.-S., and Wu, H. (2009). Induction of tetraploids from petiole explants through colchicine treatments in *Echinacea purpurea* L. *Biomed Res Int* 2009.

Omidbaigi, R., Hadjiakhoondi, A., and Saharkhiz, M. (2003). Changes in content and chemical composition of *Pimpinella anisum* oil at various harvest time. *J Essent Oil Bear Plant* 6(1): 46-50.

Özcan, M.M., and Chalchat, J.C. (2006). Chemical composition and antifungal effect of anise (*Pimpinella anisum* L.) fruit oil at ripening stage. *Ann Microbiol* 56: 353-358.

Porebski, S., Bailey, L.G., and Baum, B.R. (1997). Modification of a CTAB DNA extraction protocol for plants containing high polysaccharide and polyphenol components. *Plant Mol Biol Rep* 15: 8-15.

Roy, A., Leggett, G., and Koutoulis, A. (2001). In vitro tetraploid induction and generation of tetraploids from mixoploids in hop (*Humulus lupulus* L.). *Plant Cell Rep* 20: 489-495.

Sabzehzari, M., Hoveidamanesh, S., Modarresi, M., and Mohammadi, V. (2020). Morphological, anatomical, physiological, and cytological studies in diploid and tetraploid plants of Ispaghul (*Plantago ovata* Forsk.). *Genet Resour Crop Evol* 67: 129-137.

Saharkhiz, M. (2007). The effects of some environmental factors and ploidy level on morphological and physiological characteristics of feverfew (*Tanacetum parthenium* L.) medicinal ornamental plant. *Tarbiat Modares University, Tehran.[In Persian]*.

Stebbins, G.L. (1971). Chromosomal evolution in higher plants. *Q Rev Biol* 48(1).

Sun, W., Shahrajabian, M.H., and Cheng, Q. (2019). Anise (*Pimpinella anisum* L.), a dominant spice and traditional medicinal herb for both food and medicinal purposes. *Cogent Biol* 5(1): 1673688.

Tabanca, N., Demirci, B., Ozek, T., Kirimer, N., Baser, K.H.C., Bedir, E., Khan, I.A., and Wedge, D.E. (2006). Gas chromatographic–mass spectrometric analysis of essential oils from *Pimpinella* species gathered from Central and Northern Turkey. *J Chromatogr A* 1117(2): 194-205.

Tepe, B., Akpulat, H.A., Sokmen, M., Daferera, D., Yumrutas, O., Aydin, E., Polissiou, M., and Sokmen, A. (2006). Screening of the antioxidative and antimicrobial properties of the essential oils of *Pimpinella anisetum* and *Pimpinella flabellifolia* from Turkey. *Food Chem* 97(4): 719-724.

Tsukaya, H. (2008). Controlling size in multicellular organs: focus on the leaf. *PLoS Biol* 6(7): e174.

Urwin, N.A., Horsnell, J., and Moon, T. (2007). Generation and characterisation of colchicine-induced autotetraploid *Lavandula angustifolia*. *Sci Hortic* 156: 257-266.

Vestad, R. (1960). The effect of induced autotetraploidy on resistance to clover rot (*Sclerotinia trifoliorum* Erikss.) in red clover. *Euphytica* 9(1): 35-38.

Vleugels, T., Cnops, G., and Van Bockstaele, E. (2013). Screening for resistance to clover rot (*Sclerotinia* spp.) among a diverse collection of red clover populations (*Trifolium pratense* L.). *Euphytica* 194: 371-382.

Warner, D.A., and Edwards, G.E. (1993). Effects of polyploidy on photosynthesis. *Photosynth Res* 35: 135-147.

Watrous, S.B., and Wimber, D. (1989). Artificial induction of polyploidy in *Paphiopedilum*. *Lindleyana* 3(4): 177-183.

Yan, P., Xu, Y.-y., Zhu, X.-w., Zhe, L., Gong, Y.-q., Liang, X., Gong, M.-y., and Liu, L. w. (2014). Molecular characterization and expression profiles of myrosinase gene (*RsMyr2*) in radish (*Raphanus sativus* L.). *J Integr Agric* 13(9): 1877-1888.

Zahumenicka, P., Fernandez, E., Sediva, J., Ziarovska, J., Ros-Santaella, J.L., Martínez-Fernández, D., Russo, D., and Milella, L. (2018). Morphological, physiological and genomic comparisons between diploids and induced tetraploids in *Anemone sylvestris* L. *Plant Cell Tiss Org Cult* 132: 317-327.

JPMB
Journal of Plant Molecular Breeding
Published by Genetics and Agricultural Biotechnology Institute of Tabarestan
2023 | Volume 11 | Issue 2

مقاله پژوهشی

اثرات القای پلی‌پلوئیدی بر عملکرد انیسون (*Pimpinella Anisum* L.)

هانیه احمدی‌نیا و پرویز حیدری*

دانشکده کشاورزی، دانشگاه صنعتی شاهرود، شاهرود ۳۶۱۹۹۹۵۱۶۱، ایران

چکیده: دستکاری کروموزوم‌های گیاهی به دلیل تأثیر آن بر چندین صفت مهم و تنوع ژنتیکی، روشی قدرتمند برای اصلاح نباتات است. برای بررسی اثر القاء پلی‌پلوئیدی در انیسون (*Pimpinella anisum* L.)، سه غلظت مختلف (۰/۰۱٪، ۰/۵٪ و ۵٪) کلشی‌سین مورد آزمایش قرار گرفت. صفات مولکولی، فیزیولوژیکی و مورفولوژیکی گیاهان شاهد و القاء شده بررسی گردید. نتایج نشان داد که کلشی‌سین در غلظت ۰/۰۱ درصد تأثیر معنی‌داری بر سطح پلوئیدی ندارد، در حالیکه تأثیر معنی‌داری در غلظت‌های ۰/۵ و ۵ درصد کلشی‌سین مشاهده شد. اندازه روزنه بیشتر، تراکم روزنه کمتر و رنگ برگ تیره‌تر در گیاهچه‌های تیمار شده با غلظت‌های بالاتر از ۰.۵ درصد کلشی‌سین مشاهده شد. علاوه بر این، محتوای DNA، RNA و پروتئین کل در گیاهچه‌های تیمار شده با غلظت‌های ۰/۵ و ۵ درصد افزایش یافت. مشاهدات کاریوتیپ همچنین القاء پلی‌پلوئیدی را در گیاهان انیسون تیمار شده با غلظت‌های بالاتر از ۰/۵ درصد کلشی‌سین تایید کرد. یافته‌های این مطالعه نشان داد که کلشی‌سین می‌تواند سطح پلوئیدی گیاهان انیسون را در غلظت ۰/۵ و ۵ درصد تغییر دهد و اندازه برگ و رنگدانه‌ها را افزایش دهد.

کلمات کلیدی: گیاهان دارویی، محتوی رنگدانه، محتوی اسید نوکلئیک، سطح پلوئیدی، بنیه گیاه.

ویراستار علمی
دکتر احمد ارزانی،
دانشگاه صنعتی اصفهان، ایران

تاریخ
دریافت: ۲۵ دی ۱۴۰۲
پذیرش: ۱۴ بهمن ۱۴۰۲
چاپ: ۲۸ بهمن ۱۴۰۲

نویسنده مسئول
دکتر پرویز حیدری
heidarip@shahroodut.ac.ir

ارجاع به این مقاله
Ahmadinia, H., and Heidari, P. (2024). Effects of polyploidy induction on the performance of anise (*Pimpinella Anisum* L.). *J Plant Mol Breed 11* (2): 17-30.
doi: 10.22058/jpmb.2024.2020503.1289.

JPMB | Journal of Plant Molecular Breeding
Published by Genetics and Agricultural Biotechnology Institute of Tabarestan
2023 | Volume 11 | Issue 2

Genetic diversity of *Satureja bachtiarica* Bunge species collected from north-west Iran

Noraddin Hosseinpour Azad*

Plant Science and Medicinal Plants, University of Mohagheghe Ardabili, Ardabili, Iran.

Original paper

Abstract: Sustained availability of genetic resources is essential for successful plant breeding. *Satureja bachtiarica* Bunge is an endemic species to Iran, widely dispersed throughout the country. The rocky mountainous terrain between Asalem and Khalkhal, situated in the Ardabil province, is one of them. The current research focused on the genetic classification of 11 different ecotypes of *S. bachtiarica* collected from northwest Iran using RAPD molecular markers. A significant genetic diversity was observed among the ecotypes, with 64 bands displaying substantial polymorphism. These polymorphic bands served as the foundation for genetic analyses conducted using NTYSYS-pc (2.02e) software. The genetic distance between the ecotypes was determined using the Dice similarity coefficient. Subsequently, a dendrogram was constructed based on the similarity matrix data, employing the unweighted pair-group method with arithmetic averages (UPGMA). Genetic clustering analysis of the molecular marker data from 11 studied ecotypes revealed the lowest genetic similarity among the Khoy and Ardabil ecotypes. In contrast, the Khalkhal and Meshgin Shahr ecotypes exhibited the highest similarity. After examining the dendrogram, it becomes clear that most clusters consist of ecotypes sharing entirely similar or relatively similar climatic conditions. This suggests that the molecular diversity outcomes align with the geographical diversity of the ecotypes.

Keywords: *Satureja bachtiarica*, RAPD molecular marker, classification, genetics distance.

OPEN ACCESS

Edited by

Dr. S. Hamidreza Hashemipetroudi, Genetics and Agricultural Biotechnology Institute of Tabarestan (GABIT), Sari Agricultural Sciences and Natural Resources University (SANRU), Iran

Date

Received: 11 January 2024
Accepted: 31 January 2024
Published: 18 February 2024

Correspondence

Dr. Hosseinpour Azad
gmplant21@gmail.com

Citation

Hosseinpour Azad, N. (2023). Genetic diversity of *Satureja bachtiarica* Bunge species collected from north-west Iran. *J Plant Mol Breed. 11* (2): 31-38.
doi: 10.22058/JPMB.2024.2020152.1288.

Introduction

Rising global demand, fueled by population growth, necessitates increased food production. However, challenges such as genetic resource erosion and climate change loom large. Acknowledging the necessity to preserve botanical diversity signifies an increasing awareness that effective management of natural resources is crucial for sustained utilization (Arzani and Ashraf, 2016). The herbal species *Satureja bachtiarica* Bunge commonly referred to as Bakhtiari savory, exhibits a broad distribution across Iran, with notable prevalence in the western, central, and southwestern provinces. Bakhtiari savory (*S. bachtiarica*), a member of the *Lamiaceae* family, holds significance as a crucial Iranian herb. It is characterized by leaves folded lengthwise and arranged in a rectangular, linear form along the stem. The leaves, flowers, and calyx of *S. bachtiarica* contain secretory glands that hold essential oils. An Iranian accession of *S. bachtiarica*, has essential oil with phenolic compounds such as carvacrol (31.25%), thymol (23.50%), and o-cymene (13.87%) in the aerial parts during the flowering (Fathimoghaddam et al., 2020). Phenolic compounds, such as carvacrol and thymol, abundantly present in the *Lamiaceae* family, exert health-promoting effects on human beings (Soleimani et al., 2022).

Assessing genetic diversity is an effective means of exploiting germplasm resources for a breeding program. Genetic distance, whether determined by the frequency of different genotypes (genotypic distance) or the frequency of different alleles at specific gene locations (genetic distance), is directly linked to the phenomenon of heterosis (El Hafid et al., 2002). An investigation into the molecular analysis of selected *Thymus daenensis* clones revealed significant differences among them, empowering breeders with the ability to select and cultivate clones aligned with breeding objectives. The study also identified several ISSR markers associated with agro-morphological traits and phytochemicals (Heydari et al., 2019). In breeding programs, selecting parents with minimal similarity typically results in increased heterosis. Genetic distance, a multivariate statistical method calculated using various measurable traits, proves valuable in assessing gene or genotypic distance for genetic diversity evaluations.

Many studies have delved into evaluating genetic diversity and its application in breeding different plants (Zhang et al., 2010; Salehi et al., 2018; Baba Nitsa et al., 2023). The RAPD-PCR method, aside from its utility for estimating genetic distance and kinship relationships, can be effectively employed in the identification and classification of plant genotypes (Li et al., 2007). In a study, fifty-seven genotypes from eight populations of *S. bachtiarica* were evaluated using 15 ISSR markers and 11 RAPD markers. DNA profiling using RAPD primers resulted in the amplification of 84 loci, of which 81 were polymorphic, yielding an average of 7.36 polymorphic fragments per locus. Conversely, ISSR primers generated 136 bands, with 134 being polymorphic, and an average of 9.06 pieces per primer (98.52 percent) (Saidi et al., 2013). In a study, the diversity of morphological and phytochemical traits among Iranian and exotic populations of Marzeh (*Satureja hortensis*) grown in field conditions was examined. The research revealed that various Iranian and exotic populations of Marzeh exhibit substantial genetic diversity, presenting valuable potential for utilization in breeding programs. Specifically, cultivars originating from Khuzestan, Greece, and Uzbekistan were recommended based on their notable performance (Fathi et al., 2021). The current study aims to genetically classify various ecotypes of *S. bachtiarica* using RAPD molecular markers

Materials and Methods

Plant materials

Eleven ecotypes of *S. bachtiarica* were used in this study (Table 1). The seeds were cultivated in the plastic pots. At the five-leaf stage, fresh and young leaf tissues were collected and kept at 4°C during transportation to the laboratory. The plant materials were subsequently washed with distilled water to eliminate external contamination and allowed to dry at room temperature before being used for DNA extraction. To check the genetic diversity, DNA extraction was performed using the STE method (Azad and Nematadeh, 2013). The reagents and chemicals used for DNA extraction were Merck products.

Table 1. Eleven *Satureja bachtiarica* accessions used along with their collection area attributes.

No.	Accessions	Province	Code	N Latitude	E Longitude
1	Malekan	East Azerbaijan	M	37.148670	46.094492
2	Marand	East Azerbaijan	R	38.444456	45.749005
3	Ahar	East Azerbaijan	A	38.474632	47.084016
4	Sarab	East Azerbaijan	S	37.943017	47.513255
5	Ardabil	Ardabil	B	38.225497	48.142412
6	Meshgin Shahr	Ardabil	N	38.391922	47.647310
7	Khalkhal	Ardabil	G	37.625130	48.515529
8	Astara	Ardabil	L	38.454065	48.855583
9	Arshag	Ardabil	I	38.729863	48.030296
10	Khoy	West Azerbaijan	X	38.535244	44.968960
11	Mako	West Azerbaijan	K	39.283039	44.444270

The quality and quantity of the extracted genomic DNA were evaluated using two methods, spectrophotometry and electrophoresis on a 0.8% agarose gel. In the electrophoresis of DNA on a 0.8% agarose gel, four microliters of extracted DNA were mixed with two microliters of loading buffer and discharged into the wells of the agarose gel under TBE buffer conditions. The agarose gel was electrophoresed with a constant voltage of 85 for one hour. After staining with ethidium bromide, the DNA was observed under UV light and photographed in the Gel-doc device of the American UVP company. Following the interpretation of the gel, qualitatively and quantitatively suitable samples were selected as template DNA for PCR.

RAPD analysis

The RAPD marker used in this study was based on the method of Monika et al. (2006), which was optimized with some modifications to the PCR reaction. The 14 RAPD primers used in this project were obtained from Sinaclon company. The primers had 5-7 OD at 260 nm wavelength.

Table 2. List of RAPD primers and their sequences.

No.	Primer	Number of nucleotides	Sequences
1	OPD-03	10	5'-GTCGCCGTCA-3'
2	OPD-05	10	5'-TGAGCGGACA-3'
3	OPB-05	10	5'-CAGGCCCTTC-3'
4	OPB-13	10	5'-TTCCCCCGCT-3'
5	OPB-14	10	5'-TCCGCTCTGG-3'
6	OPB-20	10	5'-GGACCCTTAC-3'
7	OPA-01	10	5'-CAGGCCCTTC-3'
8	OPA-10	10	5'-CTGCTGGGAC-3'
9	OPA-04	10	5'-AATCGGGCTG-3'
10	OPH-20	10	5'-GGGAGACATC-3'
11	OPH-04	10	5'-GGAAGTCGCC-3'
12	OPH-15	10	5'-AATGGCGCAG-3'
13	OPH-05	10	5'-AGTCGTCCCC-3'
14	OPH-01	10	5'-GGTCGGAGAA-3'

1

All primers were prepared as lyophilized. The names of the primers along with their ten nucleotide sequences are given in Table 2.

PCR condition and data analysis

All the chemicals mentioned in this section were obtained from Sinaclon company, whose specifications are given in Supplementary Table 1.

To enhance the reproducibility of RAPD markers, all necessary precautionary factors related to PCR reaction conditions were taken into consideration. These factors include DNA quality and quantity, the prevention of biological contamination from *Taq* DNA polymerase, primer and magnesium chloride concentrations, pipetting accuracy, and PCR conditions to perform PCR reactions. The equipment used in the autoclave was sterilized at a temperature of 121 °C and a pressure of 1.5 bar for 15 minutes. The main reaction mixture was prepared as outlined in Supplementary Table 1.

The PCR apparatus used in this project was a T100 model (T100 Thermal Cycler, Bio-Rad) with gradient capabilities. The set program was the same for all primers, except for the annealing temperature, which was determined by the melting temperature of the primers (Supplementary Table 2). The results obtained by molecular markers the GC method were used to estimate the binding temperature of primers to single-stranded DNA. Many companies provide these specifications along with primers to researchers. In this project, the PCR program was adjusted according to the method of Monika et al. (2006).

After the completion of the PCR, a 1.5% agarose gel was used to verify the PCR products. We utilized agarose from Sigma-Aldrich in our experiment. Ten microliters of the mixture of PCR product and loading buffer were dispensed into each of the wells and subsequently loaded onto the gel. We used the weight indicator marker 3 (Lambda DNA / *EcoR* I+*Hind* III from Thermo Fisher Scientific Inc.) to determine the size of the bands in the gel. Electrophoresis conditions were set at 80 V for 1.5 hours. After the electrophoresis and staining of the gel with ethidium bromide, the gel was washed with distilled water, and the DNA was observed and photographed under the light (UV) using UVP gel documentation systems exemplified in Figure 1. The amplification products were assessed for the presence (1) or absence (0) of bands, and a binary matrix for RAPD markers was constructed. The software NTSYS-pc 2.02e was used for genetic analysis. A numerical value for the similarity coefficients was determined, ranging between zero and one, where zero indicates the absence of common bands (genetic dissimilarity) and one indicates identical band patterns (complete genetic similarity). The similarity matrix was entered into the SAHN clustering for dendrogram construction using the UPGMA algorithm.

Results

Fourteen PAPD primers were used in this study to assess the diversity of 11 NW Iranian *S. bachtiarica* ecotypes. Figure 1 represents the electrophoretic profile of agarose gel PCR products, of 11 ecotypes of *S. bachtiarica* using OPD-03 RAPD primer, illustrating the genetic variability among the genotypes analyzed. The Dice similarity coefficient approach was used to calculate the genetic distance between the ecotypes. Among the ecotypes, a notable genetic diversity was identified, marked by 64 bands displaying substantial polymorphism. Genetic clustering analysis of the molecular marker data from 11 studied ecotypes revealed the highest genetic similarity between the Khalkhal and Meshgin ecotypes, whereas Shahr Khoy and Ardabil ecotypes appeared more distantly related.

The dendrogram obtained from cluster analysis using the average distance algorithm (UPGMA) revealed five groups at the level of similarity (0.45) (Figure 2). The first group included the Mako ecotype (K) and the second group was formed separately by the Khoi ecotype (X). The third group had two subgroups of Marand (R) and Malekan (M) ecotypes. The fourth group included five different ecotypes and had three subgroups. The sub-group of the Arshq ecotype (I) was completely separate from the sub-sub-subgroups of the Ahar ecotype (A) and the Sarab ecotype (S). The sub-group Sub-sub-sub-types of Khalkhal (G) and Meshgin Shahr (N) ecotypes were placed. Astara (L) and Ardabil (B) ecotypes were classified in the fifth group (Figure 2). Upon reviewing the resulting dendrogram, it is evident that most groups contain ecotypes with either completely similar or relatively similar climatic conditions.

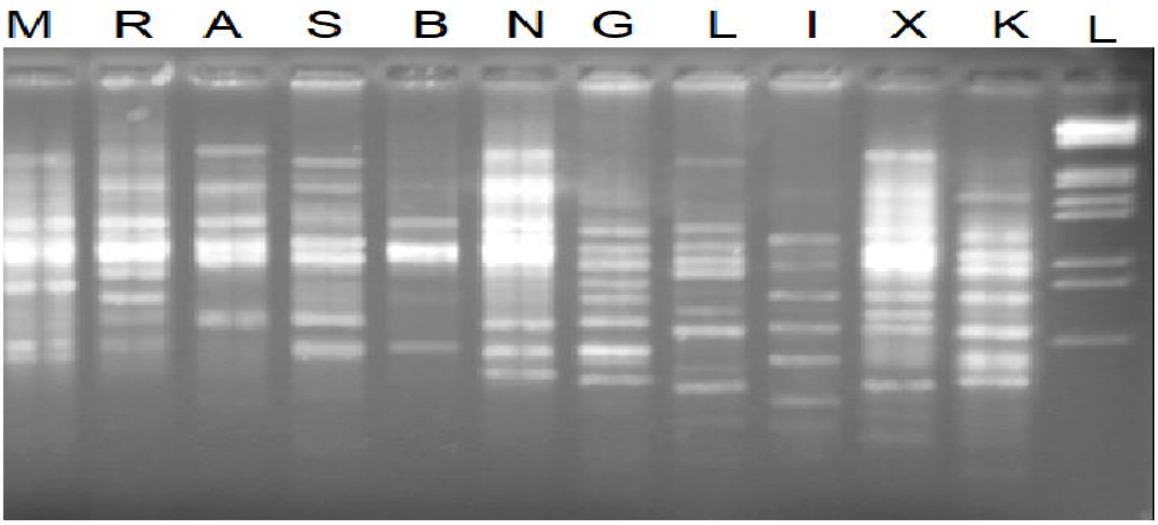

Figure 1. Polymorphic bands within the gel profile generated by the OPD-03 marker in the studied ecotypes. The codes correspond to the initials of the ecotypes as follow: M: Malekan, R: Marand, A: Ahar, S: Sarab, B: Ardabil, N: Meshgin Shahr, G: Khalkhal, L: Astara, I: Arshag, X: Khoy, K: Mako, L: Ladder.

1

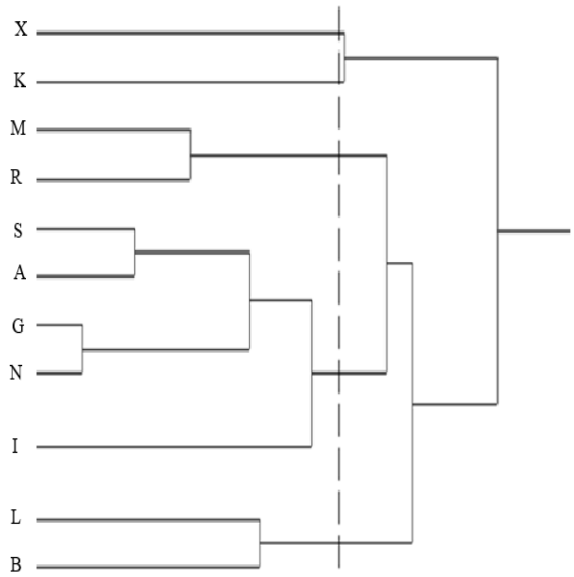

Figure 2. Dendrogram illustrating the clustering of data obtained from RAPD molecular markers using the Dice similarity matrix and UPGMA algorithm**.** The codes correspond to the initials of the ecotypes as follows: M: Malekan, R: Marand, A: Ahar, S: Sarab, B: Ardabil, N: Meshgin Shahr, G: Khalkhal, L: Astara, I: Arshag, X: Khoy, K: Mako.

This indicates that the molecular diversity results of the ecotypes are in harmony with their geographical diversity. However, it is essential to conduct additional studies, such as Bister's research, which is based on specific markers, to enhance the classification of savory plant ecotypes further and complete the overall research. In addition, the EIGEN program was employed to conduct principal component analysis, and a resulting three-dimensional plot was generated as shown in Figure 3. This multivariate method, a grouping method, was chosen to complete the cluster analysis information. The decomposition results into main components were consistent with the results of cluster analysis to a large extent, although there were differences in this field in some clusters.

Discussion

The effectiveness of RAPD molecular markers in genetically classifying a wide range of plants has been demonstrated, aligning well with the data obtained from the present study. Numerous studies have concentrated on exploring the genetic diversity of various plant species, including those classified as savory plants. In a comprehensive study, Kameli et al. (2013) used the ISSR molecular markers to assess the genetic diversity of multiple ecotypes of savory plants.

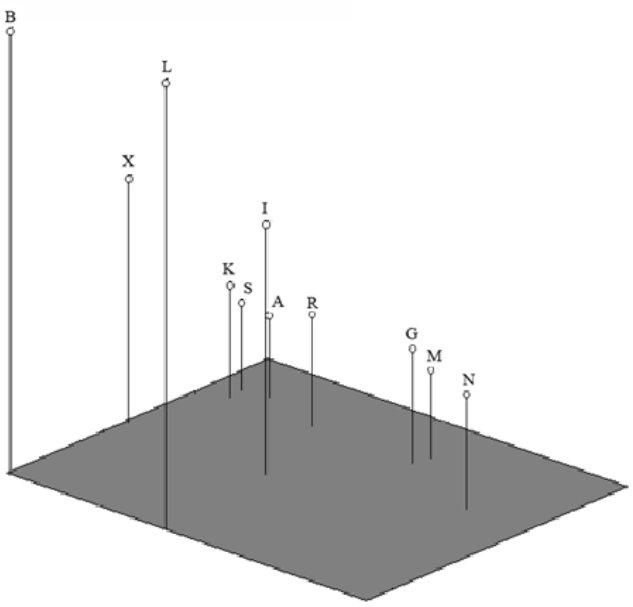

Figure 3. Three-dimensional plot resulting from principal component analysis. (The codes refer to: M: Malekan, R: Marand, A: Ahar, S: Sarab, B: Ardabil, N: Meshgin Shahr, G: Khalkhal, L: Astara, I: Arshag, X: Khoy, K: Mako.

Additionally, Namayandeh et al. (2017) employed RAPD molecular marker primers to estimate the polymorphic information content (PIC) in diverse savory plant ecotypes, yielding an average of 0.34. In a study that accurately identified different ecotypes of savory plant species using the barcode method, genetic materials were extracted and used as templates for amplification with matK, rbcl, and ITS genetic primers. Among these, only the matK primer demonstrated satisfactory amplification. The amplified product was then sequenced to serve as the basis for genetic analysis, and the study's findings indicated that the *matK* gene can be utilized as part of the barcode system for identifying savory species (Peiri and Fazeli, 2022). In another research, the genetic diversity of Iranian stands of *S. hortensis* L. was studied based on horticultural traits and RAPD markers. The results showed that both environmental and genetic factors are influential in the observed changes. Also, their results show that the RAPD approach together with horticultural analysis seems to be more suitable for fingerprinting and evaluating genetic relationships among *S. hortensis* populations with high accuracy (Hadian et al., 2008).

Conclusion

The method employed for isolating high-quality DNA from the *S. bachtiarica* plant was suitable, even in the presence of inhibitory polyphenolic compounds in the cellular contents of the plant. This inference is supported by the generation of distinct and high-resolution band patterns observed during the electrophoresis separation of polymerase chain reaction products. Moreover, the efficiency of RAPD molecular marker-based primers in the genetic classification of the studied ecotypes was evident. Most Bakhtiari savory plant ecotypes in comparable climatic and geographical conditions, were grouped into dendrogram patterns with close genetic distances. Nonetheless, additional investigations employing specific and semi-specific markers are imperative for a more refined classification of ecotypes.

Supplementary Materials:

The Supplementary Material for this article can be found online at: https://www.jpmb-gabit.ir/article_710709.html.

Supplementary Table 1. Specifications of the PCR reaction mixture for a final volume of 18 microliters.

Supplementary Table 2. PCR primer adjusted program for RAPD.

Author Contributions

Not applicable.

Funding

This research received no external funding.

Acknowledgments

The author extend his gratitude to Faculty of Agriculture at the University of Mohaghegh Ardabili for providing the opportunity to pursue studies.

Conflict of Interest Statement

The authors declare no conflict of interest.

References

Arzani, A., and Ashraf, M. (2016). Smart engineering of genetic resources for enhanced salinity tolerance in crop plants. *Crit Rev Plant Sci* 35(3): 146-189.

Azad, H.N., and Nematadeh, G. (2013). Introducing a new method of genomic DNA extraction in dicotyledonous plants. *Sch J Agric Sci* 2: 242-248.

Baba Nitsa, M., Odiyi, A.C., Akinyele, B.O., Aiyelari, O.P., and Fayeun, l.S. (2023). Genetic diversity assessment of thirty nine *Coffea canephora* accessions using EST-SSR markers. *J Plant Mol Breed* 11(1): 17-27. doi: 10.22058/jpmb.2023.2002371.1273.

El Hafid, R., Blade, S., and Hoyano, Y. (2002). Seeding date and nitrogen fertilization effects on the performance of borage (*Borago officinalis* L.). *Ind Crops Prod* 16(3): 193-199.

Fathi, R., Mohebodini, M., and Chamani, E. (2021). Evaluation of genetic diversity of summer savory (*Satureja hortensis* L.) accessions based on morphological and phytochemical characteristics. *Int J Med Aromat Plants Res* 36(6): 1005-1021.

Fathimoghaddam, E., Shakerian, A., Sharafati Chaleshtori, R., and Rahimi, E. (2020). Chemical composition and antioxidant properties and antimicrobial effects of *Satureja bachtiarica* Bunge and *Echinophora platyloba* DC. Essential oils against listeria monocytogenes. *J Medicinal Plants* 9(Special): 47-58.

Hadian, J., Tabatabaei, S., Naghavi, M., Jamzad, Z., and Ramak-Masoumi, T. (2008). Genetic diversity of Iranian accessions of *Satureja hortensis* L. based on horticultural traits and RAPD markers. *Sci Hortic* 115(2): 196-202.

Heydari, A., Hadian, J., Esmaeili, H., Kanani, M.R., Mirjalili, M.H., and Sarkhosh, A. (2019). Introduction of *Thymus daenensis* into cultivation: Analysis of agro-morphological, phytochemical and genetic diversity of cultivated clones. *Ind Crops Prod* 131: 14-24.

Kameli, M., Hesamzadeh Hejazi, S., and Ebadi, M. (2013). Assessment of genetic diversity on populations of three *Satureja* species in Iran using ISSR markers. *Ann Biol Res* 4(3): 64-72.

Li, L., Li, J., Zou, L., Bai, S.-y., Niu, L.-m., and Ma, Y.-k. (2007). RAPD analysis of genetic diversity of nine strains of *Auricularia auricular* cultivated in Heilongjiang Province. *J For Res* 18: 136-138.

Monika, S., Jakub, S., Kornelia, P., Czeslaw, H., and Roman, Z. (2006). Comparison of three *Polygonatum* species from Poland based on DNA markers. *Ann Bot Fenn* 43: 378-388.

Namayandeh, A., Mokhtari, N., Kamelmanesh, M.M., and Bedaf, M.T. (2017). Genetic diversity in *Satureja* species determined by sequence-related amplified polymorphism markers. *J Genet* 96: 5-11.

Peiri, T., and Fazeli, A. (2022). Identification of ecotypes and different species of savory (*Satureja* spp.) using DNA barcoding genes. *J Veg Sci* 6(1): 82-96.

Saidi, M., Movahedi, K., Mehrabi, A.A., and Kahrizi, D. (2013). Molecular genetic diversity of *Satureja bachtiarica*. *Mol Biol Rep* 40: 6501-6508.

Salehi, M., Arzani, A., Talebi, M., and Rokhzadi, A. (2018). Genetic diversity of wheat wild relatives using SSR markers. *Genetika* 50(1): 131-141.

Soleimani, M., Arzani, A., Arzani, V., and Roberts, T.H. (2022). Phenolic compounds and antimicrobial properties of mint and thyme. *J Herb Med* 36: 100604.

Zhang, G.-m., Li, Y.-R., He, W.-Z., He, H., Liu, X.-H., Song, H.-Z., Liu, H.-B., Zhu, R.-C., and Fang, W.-K. (2010). Analysis of the genetic diversity in *Saccharum spontaneum* L. accessions from Guangxi Province of China with RAPD-PCR. *Sugar Tech* 12: 31-35.

JPMB
Journal of Plant Molecular Breeding
Published by Genetics and Agricultural Biotechnology Institute of Tabarestan
2023 | Volume 11 | Issue 2

مقاله پژوهشی

تنوع ژنتیکی گیاه مرزه بختیاری (*Satureja bachtiarica* Bunge) جمع‌آوری شده از شمال غرب ایران

نورالدین حسین‌پورآزاد *

گروه علوم گیاهی و گیاهان دارویی، دانشگاه محقق اردبیلی، اردبیل، ایران.

چکیده: در دسترس بودن پایدار منابع ژنتیکی برای اصلاح گیاهان ضروری است. گیاه مرزه بختیاری *Satureja bachtiarica* یکی از گونه‌های بومی ایران با پراکنش گسترده در کشور بوده و در مناطق کوهستانی صخره‌ای بین اسالم و خلخال در استان اردبیل نیز پراکنده است. پژوهش حاضر بر طبقه‌بندی ژنتیکی ۱۱ اکوتیپ مختلف *S. bachtiarica* جمع‌آوری شده از شمال غرب ایران با استفاده از نشانگرهای مولکولی RAPD متمرکز بود. در این بررسی تعداد ۶۴ باند الکتروفورزی تنوع ژنتیکی قابل توجهی در بین اکوتیپ‌ها نشان دادند که به عنوان مبنای آنالیز ژنتیکی با نرم افزار NTYSYS-pc (2.02 e) مورد استفاده قرار گرفتند. فاصله ژنتیکی بین اکوتیپ‌ها با استفاده از ضریب تشابه دایس تعیین شده و سپس دندروگرام بر اساس داده‌های ماتریس شباهت، با استفاده از الگوریتم (UPGMA) ساخته شد. تجزیه و تحلیل خوشه‌بندی ژنتیکی داده‌های نشانگر مولکولی از ۱۱ اکوتیپ مورد مطالعه کمترین شباهت ژنتیکی را در بین اکوتیپ‌های خوی و اردبیل نشان داد. در مقابل، اکوتیپ‌های خلخال و مشگین‌شهر بیشترین شباهت را داشتند. پس از بررسی دندروگرام، مشخص شد که بیشتر خوشه‌ها در برگیرنده اکوتیپ‌هایی هستند که در شرایط آب و هوایی کاملاً مشابه یا نسبتاً مشابهی رویش دارند. بر این اساس، نتایج از هماهنگی بین تنوع مولکولی با تنوع جغرافیایی اکوتیپ‌ها حکایت داشته است.

کلمات کلیدی: *Satureja bachtiarica* ، نشانگر مولکولی RAPD، دسته‌بندی، فواصل ژنتیکی.

ویراستار علمی
دکتر سیدحمیدرضا هاشمی‌پطرودی،
پژوهشکده ژنتیک و زیست‌فناوری کشاورزی طبرستان،
دانشگاه علوم کشاورزی و منابع طبیعی ساری

تاریخ
دریافت: ۲۱ دی ۱۴۰۲
پذیرش: ۱۱ بهمن ۱۴۰۲
چاپ: ۲۹ بهمن ۱۴۰۲

نویسنده مسئول
دکتر حسین‌پورآزاد
gmplant21@gmail.com

ارجاع به این مقاله
Hosseinpour Azad, N. (2023). Genetic diversity of *Satureja bachtiarica* Bunge species collected from north-west Iran. *J Plant Mol Breed. 11* (2): 31-38.
doi: 10.22058/JPMB.2024.2020152.1288.

JPMB | Journal of Plant Molecular Breeding
Published by Genetics and Agricultural Biotechnology Institute of Tabarestan
2023 | Volume 11 | Issue 2

Response of wheat to drought stress: focus on root and shoot nutrients, as well as leaf chlorophyll and glycine betaine

Original paper

Samaneh Adl, Nahid Masoudian*, Bostan Roodi, Mostafa Ebadi

Department of Biology, Damghan Branch, Islamic Azad University, Damghan, Iran

Abstract: Drought stress is one of the limiting factors for plant growth. To evaluate the effect of drought stress (0, 150, 250 g/L of Polyethylene glycol 6000 (PEG)) on the physiological characteristics of two wheat cultivars ('Gonbad' and 'N8720'), a hydroponic experiment was conducted. A factorial experiment was used and arranged in a completely randomized design with three replications at the Pasteur Institute of Iran (North Research Center). The experimental results showed that the main effect of cultivars was significant for all studied traits except nitrogen and phosphorus in the stems ($p \leq 0.01$). The main effect of drought stress, as well as the interaction effect of drought stress and cultivars were significant for all studied traits ($p \leq 0.01$). The highest content of elements in root and shoot and the chlorophyll content was observed in N8720 cultivar under control treatment. Moreover, in N8720 cultivar, the amount of glycine betaine increased due to drought stress, reaching its maximum at 250 g/L PEG. The results of correlation analysis showed that there is a positive and significant correlation between all traits ($p \leq 0.01$). The result of experiment showed that N8720 cultivar exhibited superior characteristics in terms of all studied traits.

Keywords: Cluster analysis, drought stress, glycine betaine, phosphorus.

OPEN ACCESS

Edited by

Dr. Esmaeil Bakhshandeh,
Genetics and Agricultural Biotechnology Institute of Tabarestan (GABIT), Sari Agricultural Sciences and Natural Resources University (SANRU), Iran

Date

Received: 13 July 2023
Accepted: 06 February 2024
Published: 4 March 2024

Correspondence

Dr. Nahid Masoudian
nahid.masoudian@yahoo.com

Citation

Adl, S., Masoudian, N., Roudi, B., and Ebadi, M. (2023). Response of wheat cultivars to drought stress focusing on chlorophyll and physiological characteristics. *J Plant Mol Breed 11* (2): 39-54. doi: 10.22058/JPMB.2024.2006933.1278.

Introduction

Wheat (*Triticum aestivum* L.) is one of the most important grains, serving as a dominant staple food worldwide (Guo et al., 2018; Webber et al., 2018). Wheat stands as a crucial and invaluable crop on a global scale. Any decline in its production reverberates significantly throughout the human food supply chain. Wheat plays a pivotal role in delivering nutrients and calories to millions of people worldwide (Khalvandi et al., 2023). Therefore, the reduction in wheat yield can have far-reaching consequences on food security and the overall well-being of populations, highlighting the significance of addressing issues related to wheat production and ensuring its sustainable cultivation (Barak et al., 2015; Nuttall et al., 2017; Figueroa et al., 2018).

Drought is an important abiotic stress which is reducing plant growth around the world. This is more evident in arid or semi-arid areas)(Kaur and Asthir, 2017; Khalvandi et al., 2023). The depth of the problem becomes apparent when we consider that over25% of the Earth's surface is arid or semi-arid. Drought is caused by an imbalance between water evaporation, transpiration and rainfall (Salehi et al., 2016). Drought stress leads to different biochemical and physiological reactions in plants and reduces their yield (Kumar et al., 2018). Rehabilitation of crops tolerant of environmental stresses may be a way to meet the nutritional needs of a growing population living in developing countries. Breeding for drought-tolerant crops requires knowledge of the physiological and genetic mechanisms operating at different growth stages (Osmolovskaya et al., 2018).

Cellular responses to abiotic stresses are present in the majority of plant species. One of the most common of these reactions is the overproduction of various types of compatible organic matter in plant cells. These substances have high solutes and are usually non-toxic in high concentrations (Zegaoui et al., 2017; Khalvandi et al., 2019; Keshavarz‐Mirzamohammadi et al., 2021). Organic substances commonly known as osmotic modulators include proline, sucrose, and quaternary ammonium compounds such as glycine betaine and finally proline betaine. Accumulation of glycine betaine in higher plants, which are naturally accumulators of this compound, in response to salinity, drought, and cold stress has been widely reported (Nawaz and Wang, 2020). Glycine betaine is an amphoteric compound and electrically neutral at different pH (You et al., 2019). Some plant species contain small amounts of glycine betaine; However, due to stress exposure, they accumulate larger amounts of glycine betaine (Nawaz and Wang, 2020).

Drought stress, in addition to a negative effect on plant growth, causes or exacerbates other stresses, especially nutrient deficiency stress for the plant. One of the most harmful effects of drought stress is disruption in the process of absorption and accumulation of nutrients, which in addition to fertilizer losses reduces plant growth (Liang et al., 2018; Khalvandi et al., 2021). Mechanisms of uptake and transport of nutrients in plants, such as mass flow, diffusion or uptake by osmosis are all functions of the amount of moisture in the soil and roots. If the moisture content is reduced, the intensity and amount of uptake of nutrients is affected (Bindraban et al., 2015). Although some of these nutrient transfer by shoots, such as diffusion, require less moisture to absorb nutrients, in this regard, with the reduction of moisture to the critical threshold, the process of absorption and transfer of some nutrients by the roots continues (Mitra, 2015; Kazemi et al., 2021). But others, such as mass flow, are highly dependent on the amount of moisture. If the humidity decreases, the elements transferred by this current will have a negative absorption process (Hepworth et al., 2015).

Since the wheat plant has varying needs for nutrients in different phases of growth and development, drought stress greatly affects the absorption and accumulation of nutrients (Nadeem et al., 2019). Seedling stage is one of the most important phases of plant growth and impaired absorption of nutrients can cause irreparable damage to the plant (Li et al., 2015).

The leaf has a special role as a photosynthetic unit in the plant. Photosynthesis is the most vital process that ensures the life of plants and other living organisms (Kazemi et al., 2021). Absorption of light is done by pigments in chloroplast thylakoids such as chlorophyll. Chlorophyll is a pigment whose main responsibility is to receive light energy for use in photosynthesis (Gomes et al., 2016). However, environmental stresses affect the amount of

chlorophyll so drought stress and oxidative stress reduce the amount of chlorophyll and other pigments, this reduction will limit photosynthesis and plant growth (Salehi et al., 2016). Measurement of chlorophyll content is a typical indicator of oxidative stress observed in stressed plants (Cardona et al., 2018). Drought stress has an undeniable effect on plant growth and development by its effect on leaf chlorophyll (Salehi et al., 2016). The purpose of this experiment is to compare the response of two wheat cultivars to drought stress based on physiological and chlorophyll content.

Materials and Methods

Growth conditions

In order to evaluate the effect of drought stress on the physiological and chlorophyll contents of two wheat (*Triticum aestivum* L.) cultivars ('Gonbad' and 'N8720' as a sensitive and resistant cultivar to drought stress, respectively), an experiment was carried out using a factorial arrangement in a completely randomized design with three replications at the Pasteur Institute of Iran (North Research Center) in 2017. Wheat seeds were disinfected in 96% ethanol for 1.5 min followed by 15 min in 15 % Domestos, before being washed 4 times in sterile water. Afterward, grains germinated on wet filter paper for 3 days. Seedlings were put into plastic pots containing water with a half-strength Hoagland solution and maintained in a hydroponics culture in a greenhouse for 21 days. The hydroponic solution was aerated by air pumps. Every day, the hydroponic medium was supplemented with a fresh medium, and every week, it was completely exchanged with a fresh medium. After 21 days of growth in the control treatment (in water), seedlings were exposed to three levels of stress (0, 150, 250 g/L of Polyethylene glycol 6000 (PEG)). For these treatments, osmotic stress was applied with PEG dissolved in half-strength Hoagland. The 20 seedlings of each cultivar for each treatment were harvested 6 weeks after drought stress treatment and the following parameters were separately measured for each cultivar.

Leaf chlorophyll content

The modified Arnon (1949) used to measure chlorophyll content in leaves. According to this method, 0.25 g of 6th extended leaves were freeze-dried with liquid nitrogen, then completely homogenized with 4 ml of 96% ethanol in the dark and stored in a refrigerator at 4 °C for four hours. After centrifugation, supernatants were read at 663 and 645 wavelengths by spectrophotometer (Analytik Jena, Spekol 1300, Germany), and the concentration of chlorophyll was calculated (Equation 1, 2 and 3).

[Equation 1] Chlorophyll a = $(19.3 \times A_{663} - 0.86 \times A_{645})$ V/100W

[Equation 2] Chlorophyll b = $(19.3 \times A_{645} - 3.6 \times A_{663})$ V/100W

[Equation 3] Total chlorophyll = Chlorophyll a + Chlorophyll b

V = the volume of filtered solution (the upper solution from the centrifuge)

A = absorption of light at wavelengths of 663 and 645

W = fresh weight of the sample in gram

Glycine betaine content

Glycine betaine was measured by Grieve and Grattan (1983) method. In this method, 25 mg of leaf dry tissue was homogenized twice with 1 ml of water; the resulting solution was then stored on a shaker for 24 hours at 25 °C. The next day the samples were smooth and diluted 1: 1 with potassium iodide sulfuric acid 2 N and placed on ice for 1 hour; then 0.2 ml of cold potassium iodide reagent was added to the samples and the samples were kept at 0 to 4 °C for 16 hours. The resulting mixture was centrifuged at 10,000 rpm at 4 °C for 15 min. In the next step, the illuminating solution was carefully and gently separated, and the precipitated crystals were slightly washed with distilled water to wash off the color reagent on it; the crystals were then vortexed in one ml of solvent 1 and 2 dichloroethane to dissolve in the solvent and appear red. The resulting dye solution was stored for 2 hours and then the samples were read at 365 nm with the spectrophotometer.

Nutrient content

The content of phosphorus was measured spectrophotometrically (Analytik Jena, Spekol 1300, Germany) at a wavelength of 470 nm using a colorimetric method (molybdate vanadate yellow color) (Chapman and Pratt, 1962). The content of potassium was measured by the method of dry ash

(0.5 g) removal using a Flame photometer (PFP7 model, Jenway, UK) (Hamada and El-Enany, 1994). Moreover, nitrogen was measured by titration after distillation using an automatic Kjeldahl. For this purpose, 0.2 g of the dry matter was used to measure the amount of nitrogen in root and shoot tissue (Chapman and Pratt, 1962). Micro elements included copper, zinc, iron and manganese were measured by atomic absorption device (Cottenie, 1980).

Statistical analysis

All data obtained from the experiment were analyzed by SAS statistical software (version 9.1), and the means comparison test was performed using the least significant difference test (LSD). Mean comparison figures were drawn by Excel software. Also, the UPGMA (unweighted pair group method with arithmetic mean) method was performed using Euclidean distance to create cluster analysis. Varimax rotation was used to optimize principal component analysis.

Results

Based on the results, it was observed that the main effect of cultivars and drought stress, as well astheir interaction were significant for macro nutrients in roots ($p \leq 0.01$) (Table 1).

Table 1. Analysis of variance related to the macro-nutrients in roots under drought stress conditions in two wheat cultivars.

SOV	Df	Mean square		
		Nitrogen	Phosphorus	Potassium
Cultivar (C)	1	0.6498**	0.0072**	0.0007**
Drought stress (Ds)	2	1.4384**	0.0225**	5.7534**
C × Ds	2	0.0341**	0.0012**	1.2365**
Residual	12	0.0170	0.0007	0.0679
Coefficient of variation (%)		4.55	12.09	6.38

* and ** are significant at 0.05 and 0.01 levels of probability, respectively

Table 2. Mean comparison related to the macro nutrients in root under drought stress conditions in two wheat cultivars.

Cultivar	Nitrogen (%)	Phosphorus (%)	Potassium (%)
Gonbad	2.67±0.15 b	0.20±0.02 b	3.93±0.29 b
N8720	3.05±0.15 a	0.24(±0.02 a	4.23±0.29 a
Drought stress (g/L)			
0	3.40±0.09 a	0.28±0.01) a	5.16±0.09 a
150	2.74±0.10 b	0.20±0.01 b	3.83±0.12 b
250	2.45±0.10 c	0.16±0.01 c	3.25±0.14 c
C × Ds			
Gonbad×0	3.21±0.06 b	0.26±0.01 ab	5.01±0.12 a
Gonbad×150	2.55±0.03 d	0.18±0.01 cd	3.68±0.06 bc
Gonbad×250	2.26±0.10 e	0.14±0.02 d	3.10±0.20 d
N8720×0	3.59±0.04 a	0.30±0.01 a	5.31±0.09 a
N8720×150	2.93±0.10 c	0.22±0.02 bc	3.98±0.20 b
N8720×250	2.64±0.09 d	0.18±0.02 cd	3.40±0.17 cd

Results are represented as mean ± standard error. Means in a column followed by the different letters are significantly different at $p \leq 0.05$ using LSD test

Macro and micro nutrients in the roots

The results of the interaction effect of drought stress and cultivar showed that the highest amount of root nitrogen was related to the control condition in the N8720 cultivar (3.59%) (Table 2). In contrast, the lowest amount of root nitrogen related to the application of 250 g/L PEG in the Gonbad cultivar (2.26%). Based on the results, the highest amount of phosphorus and potassium in the root was related to drought stress treatment in the N8720 cultivar by 0.30 and 5.31%, respectively (Table 2).

Based on the results, the content of micro nutrients in roots were significantly affected by cultivars and drought stress levels ($p \leq 0.01$). The interaction (C×Ds) was also statistically significant ($p \leq 0.01$) (Table 3). The highest content of copper, zinc, iron, and manganese in root was related to control treatment in N8720 cultivars by 31.1, 34.1, 83.1, and 55.3 mg/kg DW, respectively. In contrast, the lowest content of elements mentioned in the root was related to the application of 250 g/L PEG in Gonbad cultivar with 22.2, 24.4, 67.6 and 42.8 mg/kg DW, respectively (Table 4).

Table 3. Analysis of variance related to the micro nutrients in roots under drought stress conditions in two wheat cultivars.

SOV	Df	Mean square			
		Copper	Zinc	Iron	Manganese
Cultivar (C)	1	42.9665**	68.0945**	154.0013**	37.3248**
Drought stress (Ds)	2	51.7806**	51.7806**	143.8350**	143.8350**
C × Ds	2	5.0214**	8.0255**	12.6584**	25.3256**
Residual	12	6.7917	6.7917	24.5000	3.0179
Coefficient of variation (%)		9.9	9.01	6.62	3.58

* and ** are significant at 0.05 and 0.01 levels of probability, respectively

Table 4. Mean comparison related to the micro nutrients in roots under drought stress conditions in two wheat cultivars.

Cultivar	Copper (mg/kg DW)	Zinc (mg/kg DW)	Iron (mg/kg DW)	Manganese (mg/kg DW)
Gonbad	24.75±1.09 b	26.97±1.09 b	71.84±1.99 b	47.03±1.49 b
N8720	27.84±1.17 a	30.86±1.17 a	77.69±2.03 a	49.91±1.51 a
Drought stress (g/L)				
0	29.54±0.95 a	32.16±1.08 a	80.17±1.84 a	53.87±0.77 a
150	25.55±1.17 b	28.17±1.28 b	73.52±2.55 b	47.22±0.90 b
250	23.81±1.38 b	26.43±1.47 b	70.62±2.25 b	44.32±1.02 c
C × Ds				
Gonbad×0	27.99±1.15 ab	30.21±1.15 ab	77.24±1.73 ab	52.43±0.77 a
Gonbad×150	24.00±0.58 bc	26.22±0.58 bc	70.59±3.46 bc	45.78±0.39 bc
Gonbad×250	22.26±2.02 c	24.48±2.02 c	67.69±2.89 c	42.88±1.35 c
N8720×0	31.08±0.87 a	34.10±0.87 a	83.09±2.31 a	55.31±0.58 a
N8720×150	27.09±2.02 ab	30.11±2.02 ab	76.44±3.46 a-c	48.66±1.35 b
N8720×250	25.35±1.73 bc	28.37±1.73 bc	73.54±2.89 bc	45.76±1.15 bc

Results are represented as mean ± standard error. Means in a column followed by the different letters are significantly different at $p \leqslant 0.05$ using the LSD test.

Macro and micro nutrients in shoot

Based on the results, it was observed that the main effect of cultivars was significant for potassium in shoot ($p \leq 0.01$) (Table 5). Nitrogen, phosphorous, and potassium of the shoot were affected significantly by the main effect of drought stress ($p \leq 0.01$). Also, the results showed that macro nutrients in shoots were affected by the interaction of cultivars and drought stress ($p \leq 0.01$). The highest content of nitrogen, phosphorus, and potassium in the shoot were related to the control condition in N8720 cultivar with 4.16, 0.23 and 5.03%, respectively (Table 6).

Table 5. Analysis of variance related to the macro nutrients in the shoot under drought stress conditions in two wheat cultivars.

SOV	Df	Mean square		
		Nitrogen	Phosphorus	Potassium
Cultivar (C)	1	0.0761^{NS}	0.0018^{NS}	0.1152**
Drought stress (Ds)	2	5.7534**	0.0225**	5.7534**
C × Ds	2	0.0021**	0.0013**	0.0002**
Residual	12	0.2717	0.0007	0.0170
Coefficient of variation (%)		17.28	16.77	3.37

* and ** are significant at 0.05 and 0.01 levels of probability, respectively

Table 6. Mean comparison related to the macro nutrients in the shoot under drought stress conditions in two wheat cultivars.

Cultivar	Nitrogen (%)	Phosphorus (%)	Potassium (%)
Gonbad	2.95±0.31 ^{a}	0.15±0.02 ^{a}	3.79±0.28 ^{b}
N8720	3.08±0.33 ^{a}	0.17±0.02 ^{a}	3.95±0.29 ^{a}
Drought stress (g/L)			
0	4.10±0.13 ^{a}	0.22±0.01 ^{a}	4.95±0.05 ^{a}
150	2.77±0.19 ^{b}	0.14±0.01 ^{b}	3.62±0.06 ^{b}
250	2.19±0.24 ^{b}	0.10±0.01 ^{c}	3.04±0.07 ^{c}
C × Ds			
Gonbad×0	4.03±0.23 ^{a}	0.21±0.01 ^{a}	4.87±0.06 ^{a}
Gonbad×150	2.70±0.12 ^{b}	0.13±0.01 ^{bc}	3.54±0.03 ^{b}
Gonbad×250	2.12±0.40 ^{b}	0.09±0.02 ^{c}	2.96±0.10 ^{c}
N8720×0	4.16±0.17 ^{a}	0.23±0.01 ^{a}	5.03±0.04 ^{a}
N8720×150	2.83±0.40 ^{b}	0.15±0.02 ^{b}	3.70±0.10 ^{b}
N8720×250	2.25±0.35 ^{b}	0.11±0.02 ^{bc}	3.12±0.09 ^{c}

Results are represented as mean ± standard error. Means in a column followed by the different letters are significantly different at $p \leqslant 0.05$ using LSD test.

The results showed that the main effect of cultivars and drought stress was significant for micro nutrients in shoot ($p \leq 0.01$) (Table 7). Also, the results showed that micro nutrients in shoot were affected by the interaction of cultivars and drought stress ($p \leq 0.01$). The content of copper, zinc, iron and manganese in shoot were affected by cultivar and drought stress interaction (Table 7). The highest content of shoot copper was related to drought stress treatment in N8720 cultivar (22.47 mg/kg DW), while the lowest content of it was observed when 250 g/L PEG was applied in Gonbad cultivar (14.53 mg/kg DW) (Table 8).

Table 7. Analysis of variance related to the micro nutrients in the shoot under drought stress conditions in two wheat cultivars.

SOV	Df	Mean square			
		Copper	Zinc	Iron	Manganese
Cultivar (C)	1	21.9785**	45.2201**	71.2818**	37.4545**
Drought stress (Ds)	2	51.7806**	51.7806**	143.8350**	143.4244**
C × Ds	2	6.8746**	6.8745**	9.5874**	15.3254**
Residual	12	1.3419	6.7917	5.5000	6.7917
Coefficient of variation (%)		6.38	6.74	3.35	3.71

* and ** are significant at 0.05 and 0.01 levels of probability, respectively.

Table 8. Mean comparison related to the micro nutrients in the shoot under drought stress conditions in two wheat cultivars.

Cultivar	Copper (mg/kgDW)	Zinc (mg/kgDW)	Iron (mg/kgDW)	Manganese (mg/kgDW)
Gonbad	17.02±0.90 b	37.06±1.09 b	67.81±1.59 b	68.70±1.57 b
N8720	19.23±0.92 a	40.23±1.17 a	71.79±1.54 a	71.59±1.63 a
Drought stress (g/L)				
0	21.37±0.57 a	41.88±0.96 a	75.20±1.29 a	75.54±0.91 a
150	17.38±0.65 b	37.89±1.18 b	68.55±1.41 b	68.89±1.14 b
250	15.64±0.72 c	36.15±1.39 b	65.65±0.96 b	66.00±1.35 b
C × Ds				
Gonbad×0	20.26±0.51 b	40.30±1.15 ab	73.21±1.73 ab	74.10±1.15 ab
Gonbad×150	16.27±0.26 de	36.31±0.58 bc	66.56±1.73 cd	67.44±0.58 cd
Gonbad×250	14.53±0.90 e	34.57±2.02 c	63.66±0.58 d	64.57±2.02 d
N8720×0	22.47±0.39 a	43.47±0.87 a	77.19±1.15 a	76.98±0.87 a
N8720×150	18.48±0.90 bc	39.48±2.02 ab	70.54±1.73 bc	70.35±2.02 bc
N8720×250	16.74±0.77 cd	37.74±1.73 bc	67.64±0.58 cd	67.44±1.73 cd

Results are represented as mean ± standard error. Means in a column followed by the different letters are significantly different at $p \leqslant 0.05$ using LSD test.

The highest content of zinc, iron and manganese in the shoot were 43.47, 77.19 and 76.98 mg/kg DW, respectively, related to drought stress treatment in N8720 cultivar. In contrast, the lowest content of zinc, iron and manganese in the shoot (34.57, 63.66 and 64.57 mg/kgDW) were related to the 250 g/L PEG treatment in Gonbad cultivar, respectively (Table 8).

Total chlorophyll and glycine betaine

Based on the results, it was observed that the main effect of cultivars and drought stress was significant for total chlorophyll and glycine betaine ($p \leq 0.01$). Also, the results of the analysis of variance showed that total chlorophyll and glycine betaine were affected by the interaction of cultivars and drought stress ($p \leq 0.01$) (Table 9). The highest content of total chlorophyll was observed in the control treatment in both N8720 and Gonbad cultivars (12.9 and 13 µmol/g FW, respectively) (Figure 1A). Based on the results, it was observed that 150 and 250 g/L PEG levels had the lowest content of total chlorophyll.

Table 9. Analysis of variance and mean comparison related to the glycine betaine and total chlorophyll in leaves under drought stress conditions in two wheat cultivars.

S.O.V	Degree of freedom	Glycine betaine	Total chlorophyll
Cultivar (A)	1	0.3362**	0.0456**
Drought stress (B)	2	0.7511**	10.1516**
A × B	2	0.0028**	0.0033**
Residual	12	0.0027	0.6113
Coefficient of variation (%)	-	8.04	6.79

* and ** represent significant levels of probability at 5 and 1%, respectively.

On the other hand, the results of the mean comparison showed that the amount of glycine betaine in both studied cultivars increased significantly with increasing drought stress (Figure 1B). The results showed that the highest content of glycine betaine was observed in the application of 250 g/L PEG in the N8720 cultivar (1.23 µmol / g). In contrast, the lowest content of glycine betaine was related to non-stress treatment in Gonbad and N8720 cultivars.

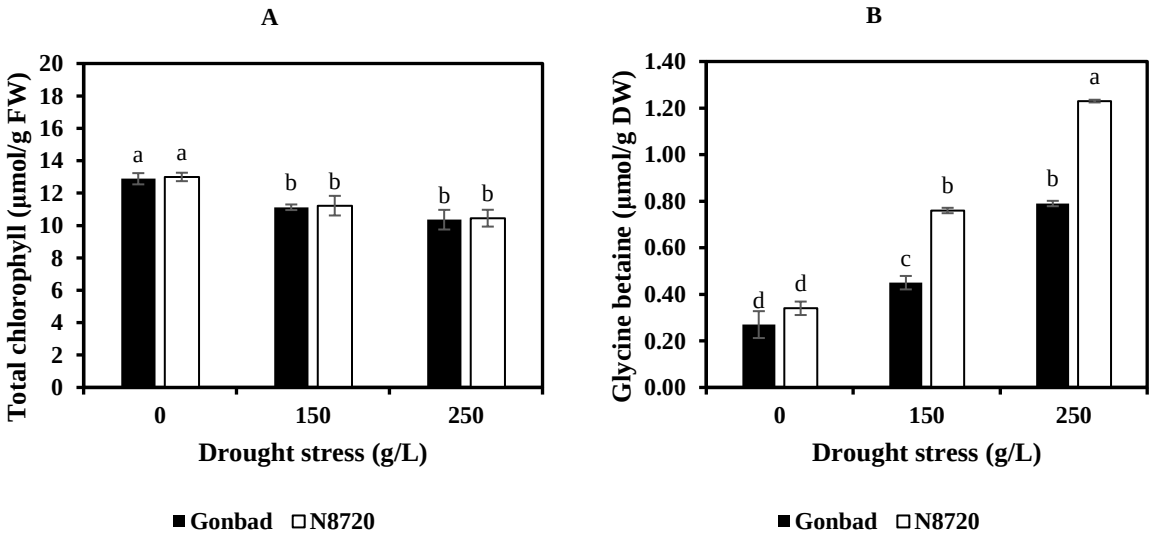

Figure 1. Mean comparison related to the interaction effects of cultivar and drought stress for glycine betaine and total chlorophyll. Results are represented as mean ± standard error.

Principal component analysis results

The results of principal components analysis showed that the first and second components had an eigenvalue higher than one and were selected as the most effective components among all the components (Figure 2A). Based on the results of the principal component analysis, it was shown that the first and second components with 95.93 and 3.67%, respectively, had the highest relative variance and gathered 99.60% of the total variance. Biplot obtained from the first and second components showed that Gonbad+0 g/L PEG, N8720+0 g/L PEG, and N8720+150 g/L PEG treatments had a stronger relationship with all traits.

Cluster analysis

The dendrogram obtained from cluster analysis based on the UPGMA method and Euclidean distance is shown in Figure 2B. Based on the results, cluster analysis divided the different treatments into three separate groups.

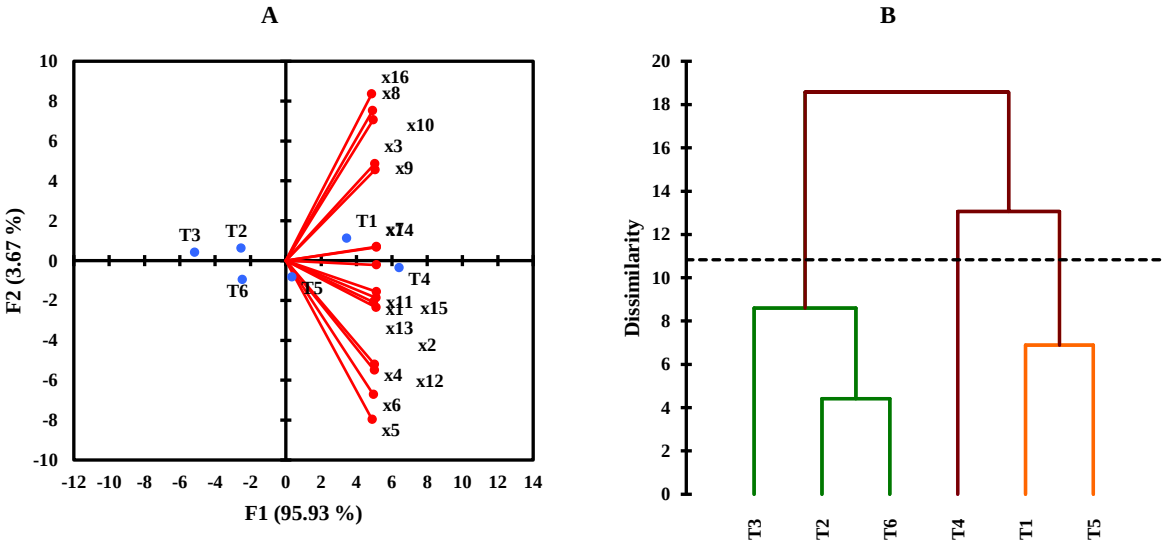

Figure 2. A) Biplot obtained from principal components analysis based on the first and second components related to all studied traits in two wheat cultivars under drought stress. (X1: nitrogen of root; X2: phosphorus of root; X3: potassium of root; X4: copper of root; X5: zinc of root; X6: iron of root; X7: manganese of root; X8: nitrogen of shoot; X9: phosphorus of shoot; X10: potassium of shoot; X11: copper of shoot; X12: zinc of shoot; X13: iron of shoot; X14: manganese of shoot; X15: glycine betaine; X16: total chlorophyll), B) Dendrogram obtained from cluster analysis based on all studied traits in two wheat cultivars under drought stress. (T1: Gonbad+0 (g/L); T2: Gonbad+150(g/L); T3: Gonbad+250(g/L); T4: N8720+0(g/L); T5: N8720+150(g/L); T6: N8720+250(g/L)).

Table 10. Pearson correlation coefficients based on all traits in two wheat cultivars under drought stress conditions.

Traits	x_1	x_2	x_3	x_4	x_5	x_6	x_7	x_8	x_9	x_{10}	x_{11}	x_{12}	x_{13}	x_{14}	x_{15}	x_{16}
x_1	1															
x_2	0.99**	1														
x_3	0.97**	0.98**	1													
x_4	0.91**	0.95**	0.87**	1												
x_5	0.91**	0.94**	0.84**	0.99**	1											
x_6	0.88**	0.91**	0.82**	0.97**	0.97**	1										
x_7	0.99**	0.99**	0.99**	0.93**	0.92**	0.89**	1									
x_8	0.91**	0.96**	0.97**	0.90**	0.87**	0.86**	0.96**	1								
x_9	0.96**	0.99**	0.99**	0.92**	0.89**	0.87**	0.99**	0.99**	1							
x_{10}	0.94**	0.93**	0.99**	0.79**	0.76**	0.74**	0.95**	0.94**	0.96**	1						
x_{11}	0.99**	0.99**	0.97**	0.95**	0.94**	0.91**	0.99**	0.94**	0.97**	0.93**	1					
x_{12}	0.91**	0.95**	0.87**	0.99**	0.99**	0.97**	0.93**	0.90**	0.92**	0.78**	0.95**	1				
x_{13}	0.97**	0.97**	0.93**	0.92**	0.92**	0.93**	0.96**	0.90**	0.94**	0.89**	0.97**	0.92**	1			
x_{14}	0.97**	0.99**	0.97**	0.97**	0.95**	0.93**	0.99**	0.97**	0.99**	0.92**	0.99**	0.97**	0.96**	1		
x_{15}	0.95**	0.92**	0.91**	0.81**	0.81**	0.78**	0.93**	0.83**	0.89**	0.90**	0.93**	0.81**	0.92**	0.89**	1	
x_{16}	0.89**	0.94**	0.95**	0.90**	0.86**	0.85**	0.94**	0.99**	0.98**	0.92**	0.92**	0.90**	0.88**	0.96**	0.80**	1

** is significant at 0.01 levels of probability. (Nitrogen of root (x_1), phosphorus of root (x_2), potassium of root (x_3), copper of root (x_4), zinc of root (x_5), iron of root (x_6), manganese of root (x_7), nitrogen of shoot (x_8), phosphorus of shoot (x_9), potassium of shoot (x_{10}), copper of shoot (x_{11}), zinc of shoot (x_{12}), iron of shoot (x_{13}), manganese of shoot (x_{14}), glycine betaine (x_{15}) and total chlorophyll (x_{16})).

Results showed that Gonbad+250 g/L PEG, Gonbad+150 g/L PEG, and N8720+250 g/L PEG treatments were located in one group. On the other hand, Gonbad+0 g/L PEG and N8720+150 g/L PEG treatments were placed in a similar group and N8720+0 g/L PEG treatment was placed in an independent group alone

Pearson correlation analysis

The results of Pearson correlation coefficients were shown in Table 10. The results showed that there is a positive and significant correlation between all traits ($p \leq 0.01$)

Discussion

Drought stress not only reduces the growth and development of plants but also changes the direction of some metabolic processes (Salehi et al., 2016). These changes can make the plant tolerant to stress. Adaptation to drought depends on reactions through which the initial metabolic processes continue and prepare the plant to deal with it (Sallam et al., 2019). In this experiment, the cultivars reacted similarly to other plants in the face of drought stress and coped with changes in physiological characteristics and changes in the absorption of elements under stress conditions.

Photosynthetic contents

The results of this experiment showed that the total chlorophyll content decreased with increasing drought stress. According to research, drought stress causes the destruction of chloroplasts and the instability of pigment and protein compounds (Gomes et al., 2016; Salehi et al., 2016; Cardona et al., 2018). The researchers indicated that the amount of chlorophyll decreased due to drought stress, it is found that due to higher chlorophyllase activity under drought stress conditions (Siddiqui et al., 2015; Salehi et al., 2016; Guo et al., 2018). In addition, many researchers showed that there is a significant correlation between nutrients absorbed by plants and chlorophyll content (Sohrabi et al., 2012; Rabiei et al., 2020; Khalvandi et al., 2021). However, some growth regulators, such as abscisic acid and ethylene, which increase in drought stress, stimulate the activity of this enzyme (Wang et al., 2019a). According to researchers, the decrease in chlorophyll content may be due to changes in nitrogen metabolism in connection with the production of compounds such as proline, which is used in osmotic regulation (Filstrup and Downing, 2017; Hosseini et al., 2021; Hosseini et al., 2023). Glutamine kinase is one of the key enzymes in proline synthesis, which is the first enzyme in the proline biosynthesis pathway and is found in the cytoplasm and chloroplasts (Bashir et al., 2020). Drought stress has a stimulating effect on the activity of this enzyme. In contrast, glutamate ligase is the first important enzyme in chlorophyll synthesis, which drought stress inhibits its activity. Therefore, under stress conditions, chlorophyll production decreases due to a decreased in glutamate-ligase activity and more glutamate consumption by the activated glutamine kinase enzyme (Ahmad et al., 2016).

Other symptoms presented by the researchers include increased stomatal resistance due to stomatal obstruction, increased mesophilic resistance due to increased cell wall thickness and cell thickness, increased plant respiration, ion toxicity and disruption of plant growth metabolic processes, decreased mineral uptake, reduced RUBP and regeneration efficiency, all of which directly or indirectly reduce photosynthesis (Jangid and Dwivedi, 2016). Drought stress hydrolyzes thylakoid proteins and reduces the content of chlorophyll a and b (Wang et al., 2019b). On the other hand, drought stress disrupts enzymatic activations, reduces the activity of reactive oxygen species, and increases the peroxidation of fats, resulting in damage to cell membranes and the destruction of chlorophyll a and b (Salehi-Lisar and Bakhshayeshan-Agdam, 2016). The researchers reported that increasing drought stress significantly reduced the content of chlorophyll a, b, and total in wheat, which was consistent with the results of this experiment (Abbas et al., 2018; Ahmad et al., 2018).

Uptake of micro and macro elements

Drought stress has a great impact on the absorption of micro and macro elements, so finding the effect of drought stress on the absorption of elements in the seedling stage is very important (Bista et al., 2018). The results of this experiment showed that the adsorption of the micro and macro elements was affected by drought stress and their adsorption decreased with increasing stress. Absorption of nutrients by plant roots and water availability are

closely related. Water availability affects all physiological processes associated with the solubility and availability of nutrients (Bowles et al., 2016). Drought stress reduces active transmission in the shoots, membrane permeability, plant root absorption, and nutrient uptake through transpiration (Nadeem et al., 2019). The responses of nutrient accumulation in plants to drought stress are different. The efficiency of the plant root in order to absorb the nutrients may also be reduced due to lack of moisture (Bista et al., 2018). A number of researchers have shown that the uptake of nitrogen, phosphorus and potassium decreased in the face of drought stress (Delshadi et al., 2017; Tadayyon et al., 2018). Absorption of iron, zinc, copper, and manganese also decreased in the two cultivars, but the amount of uptake in the resistant cultivar was higher than in the sensitive cultivar. Several researchers have suggested that the uptake of iron, copper, zinc and manganese should be reduced under drought stress (Rizwan et al., 2015; Abbas et al., 2018; Liang et al., 2018).

Glycine betaine

The results of the assessment of glycine betaineshowed that drought stress increased the amount of glycine betaine in both cultivars. Also, based on the results, it was observed that more glycine betaine was produced in the resistant cultivar. Depending on the type of stress, plants in their evolutionary path, have found ways to reduce the adverse effects of stress (Seleiman et al., 2021). One of the common reactions that occurs in plant cells as a result of increased accumulation of organic solutions in the cytoplasm is osmotic regulation (Choudhary et al., 2023). Osmotic regulation helps plants to increase the osmotic balance between the cytoplasm and various cell components (Zivcak et al., 2016). Osmotic regulation in plants occurs through the production of various types of compatible organic solutions and some inorganic ions (Aslam et al., 2015). In general, these substances protect plants from stress during different periods by participating in osmotic balance and maintaining membrane fluidity and the stability of proteins or enzymes (Thalmann et al., 2016). Their main role is to insulate plant cells from stress-induced damage by osmotic moderation, to stabilize the structure of key proteins such as Rubisco, and to maintain the photosynthetic apparatus (Singh et al., 2015). Most halophytes increase glycine betaine as an osmotic moderator in their cells when exposed to stress (Pardo-Domènech et al., 2016). Glycine betaine is also increased in response to stress in many other crops, including spinach, barley, wheat, and sorghum (Osman, 2015; Roychoudhury and Banerjee, 2016; Kurepin et al., 2017; Annunziata et al., 2019).

Conclusion

The results of this experiment showed that N8720 cultivar had superior characteristics across all studied traits. Also, severe drought stress had a very negative effect on all characteristics, highlighting the importance of a tolerant cultivar like N8720, which can demonstrate better physiological characteristics in severe stress conditions. Due to the favorable attributes of N8720 cultivar including its efficient nutrient uptake as well as its optimal efficiency of the photosynthetic system, and high content of glycine betaine for combating drought stress, this cultivar holds promise for inclusion in future wheat breeding endeavors.

Supplementary Materials

No supplementary material is available for this article.

Author contributions

Conceptualization, N.M. and S.A.; methodology, N.M.; software, S.A.; validation, B.R., M.E. and S.A.; formal analysis, S.A.; investigation, S.A.; resources, N.M.; data curation, S.A.; writing—original draft preparation, S.A.; writing—review and editing, N.M.; visualization, B.R.; supervision, N.M.; project administration, M.E.; funding acquisition, N.M. All authors have read and agreed to the published version of the manuscript.

Funding

This research received no external funding.

Acknowledgments

We would like to thank our colleagues at the Pasteur Institute of Iran (North Research Center) for cooperating with us on this project.

Conflict of interest statement

The authors declare no conflict of interest.

References

Abbas, T., Rizwan, M., Ali, S., Adrees, M., Mahmood, A., Zia-ur-Rehman, M., Ibrahim, M., Arshad, M., and Qayyum, M.F. (2018). Biochar application increased the growth and yield and reduced cadmium in drought stressed wheat grown in an aged contaminated soil. *Ecotoxicol Environ Saf* 148: 825-833.

Ahmad, N., Malagoli, M., Wirtz, M., and Hell, R. (2016). Drought stress in maize causes differential acclimation responses of glutathione and sulfur metabolism in leaves and roots. *BMC Plant Biol* 16: 1-15.

Ahmad, Z., Waraich, E.A., Akhtar, S., Anjum, S., Ahmad, T., Mahboob, W., Hafeez, O.B.A., Tapera, T., Labuschagne, M., and Rizwan, M. (2018). Physiological responses of wheat to drought stress and its mitigation approaches. *Acta Physiol Plant* 40: 1-13.

Annunziata, M.G., Ciarmiello, L.F., Woodrow, P., Dell'Aversana, E., and Carillo, P. (2019). Spatial and temporal profile of glycine betaine accumulation in plants under abiotic stresses. *Front Plant Sci* 10: 230.

Arnon, D.I. (1949). Copper enzymes in isolated chloroplasts. Polyphenoloxidase in *Beta vulgaris*. *Plant Physiol* 24(1): 1.

Aslam, M., Maqbool, M.A., Cengiz, R., Aslam, M., Maqbool, M.A., and Cengiz, R. (2015). *Drought stress in maize (Zea mays L.) effects, resistance mechanisms, global achievements and biological strategies for improvement.* Springer International Publishing.

Barak, S., Mudgil, D., and Khatkar, B. (2015). Biochemical and functional properties of wheat gliadins: a review. *Crit Rev Food Sci Nutr* 55(3): 357-368.

Bashir, M.A., Silvestri, C., Ahmad, T., Hafiz, I.A., Abbasi, N.A., Manzoor, A., Cristofori, V., and Rugini, E. (2020). Osmotin: a cationic protein leads to improve biotic and abiotic stress tolerance in plants. *Plants* 9(8): 992.

Bindraban, P.S., Dimkpa, C., Nagarajan, L., Roy, A., and Rabbinge, R. (2015). Revisiting fertilisers and fertilisation strategies for improved nutrient uptake by plants. *Biol Fert Soils* 51(8): 897-911.

Bista, D.R., Heckathorn, S.A., Jayawardena, D.M., Mishra, S., and Boldt, J.K. (2018). Effects of drought on nutrient uptake and the levels of nutrient-uptake proteins in roots of drought-sensitive and-tolerant grasses. *Plants* 7(2): 28.

Bowles, T.M., Barrios-Masias, F.H., Carlisle, E.A., Cavagnaro, T.R., and Jackson, L.E. (2016). Effects of arbuscular mycorrhizae on tomato yield, nutrient uptake, water relations, and soil carbon dynamics under deficit irrigation in field conditions. *Sci Total Environ* 566: 1223-1234.

Cardona, T., Shao, S., and Nixon, P.J. (2018). Enhancing photosynthesis in plants: the light reactions. *Essays Biochem* 62(1): 85-94.

Chapman, H.D., and Pratt, P.F. (1962). Methods of analysis for soils, plants and waters. *Soil Sci* 93(1): 68.

Choudhary, S., Wani, K.I., Naeem, M., Khan, M.M.A., and Aftab, T. (2023). Cellular responses, osmotic adjustments, and role of osmolytes in providing salt stress resilience in higher plants: Polyamines and nitric oxide crosstalk. *J Plant Growth Regul* 42(2): 539-553.

Cottenie, A. (1980). Methods of plant analysis. *Soil and Plant Testing. FAO Soils Bulletin* 38(2): 64-100.

Delshadi, S., Ebrahimi, M., and Shirmohammadi, E. (2017). Influence of plant-growth-promoting bacteria on germination, growth and nutrients' uptake of O*nobrychis sativa* L. under drought stress. *J Plant Interact* 12(1): 200-208.

Figueroa, M., Hammond‐Kosack, K.E., and Solomon, P.S. (2018). A review of wheat diseases—a field perspective. *Mol Plant Pathol* 19(6): 1523-1536.

Filstrup, C.T., and Downing, J.A. (2017). Relationship of chlorophyll to phosphorus and nitrogen in nutrient-rich lakes. *Inland Waters* 7(4): 385-400.

Gomes, M.P., Le Manac'h, S.G., Maccario, S., Labrecque, M., Lucotte, M., and Juneau, P. (2016). Differential effects of glyphosate and aminomethylphosphonic acid (AMPA) on photosynthesis and chlorophyll metabolism in willow plants. *Pestic* 130: 65-70.

Grieve, C., and Grattan, S. (1983). Rapid assay for determination of water soluble quaternary ammonium compounds. *Plant Soil* 70: 303-307.

Guo, R., Shi, L., Jiao, Y., Li, M., Zhong, X., Gu, F., Liu, Q., Xia, X., and Li, H. (2018). Metabolic responses to drought stress in the tissues of drought-tolerant and drought-sensitive wheat genotype seedlings. *AoB Plants* 10(2): ply016.

Hamada, A., and El-Enany, A. (1994). Effect of NaCl salinity on growth, pigment and mineral element contents, and gas exchange of broad bean and pea plants. *Biol Plant* 36: 75-81.

Hepworth, C., Doheny‐Adams, T., Hunt, L., Cameron, D.D., and Gray, J.E. (2015). Manipulating stomatal density enhances drought tolerance without deleterious effect on nutrient uptake. *New Phytol* 208(2): 336.

Hosseini, S.J., Tahmasebi-Sarvestani, Z., Mokhtassi-Bidgoli, A., Keshavarz, H., Kazemi, S., Khalvandi, M., Pirdashti, H., Bovand, F., and Abassian, A. (2023). Do various levels of salinity change chlorophyll fluorescence, nutrient uptake, and physiological characteristics of *Mentha ecotypes*? *Ind Crops Prod* 203: 117199.

Hosseini, S.J., Tahmasebi‐Sarvestani, Z., Pirdashti, H., Modarres‐Sanavy, S.A.M., Mokhtassi‐Bidgoli, A., Hazrati, S., and Nicola, S. (2021). Investigation of yield, phytochemical composition, and photosynthetic pigments in different mint ecotypes under salinity stress. *Food Sci Nutr* 9(5): 2620-2643.

Jangid, K.K., and Dwivedi, P. (2016). Physiological responses of drought stress in tomato: a review. *Int J Environ Agric Biotech* 9(1): 53-61.

Kaur, G., and Asthir, B. (2017). Molecular responses to drought stress in plants. *Biologia plantarum* 61: 201-209.

Kazemi, S., Rafati Alashti, M., and Hosseini, S.J. (2021). Response of biochemical and physiological properties of camellia (*Camelina sativa* L.) to foliar application of calcium and silicon nanoparticles. *Silicon*: 1-12.

Keshavarz‐Mirzamohammadi, H., Tohidi‐Moghadam, H.R., and Hosseini, S.J. (2021). Is there any relationship between agronomic traits, soil properties and essential oil profile of peppermint (*Mentha piperita* L.) treated by fertiliser treatments and irrigation regimes? *Ann Appl Biol* 179(3): 331-344.

Khalvandi, M., Amerian, M., Pirdashti, H., and Keramati, S. (2021). Does co-inoculation of mycorrhiza and *Piriformospora indica* fungi enhance the efficiency of chlorophyll fluorescence and essential oil composition in peppermint under irrigation with saline water from the Caspian Sea? *PLoS One* 16(7): e0254076.

Khalvandi, M., Amerian, M., Pirdashti, H., Keramati, S., and Hosseini, J. (2019). Essential oil of peppermint in symbiotic relationship with *Piriformospora indica* and methyl jasmonate application under saline condition. *Ind Crops Prod* 127: 195-202.

Khalvandi, M., Siosemardeh, A., Bahramnejad, B., and Roohi, E. (2023). Protein pattern and physiological responses to drought stress in wheat landraces. *Cereal Res Commun*: 1-13.

Kumar, S., Sachdeva, S., Bhat, K., and Vats, S. (2018). Plant responses to drought stress: physiological, biochemical and molecular basis. In: *Biotic and abiotic stress tolerance in plants*: 1-25.

Kurepin, L.V., Ivanov, A.G., Zaman, M., Pharis, R.P., Hurry, V., and Hüner, N.P. (2017). *Interaction of glycine betaine and plant hormones: Protection of the photosynthetic apparatus during abiotic stress.*

Li, R., Zeng, Y., Xu, J., Wang, Q., Wu, F., Cao, M., Lan, H., Liu, Y., and Lu, Y. (2015). Genetic variation for maize root architecture in response to drought stress at the seedling stage. *Breed Sci* 65(4): 298-307.

Liang, B., Ma, C., Zhang, Z., Wei, Z., Gao, T., Zhao, Q., Ma, F., and Li, C. (2018). Long-term exogenous application of melatonin improves nutrient uptake fluxes in apple plants under moderate drought stress. *Environmental and experimental botany* 155: 650-661.

Mitra, G.N. (2015). *Regulation of nutrient uptake by plants.* Springer, New Delhi.

Nadeem, M., Li, J., Yahya, M., Sher, A., Ma, C., Wang, X., and Qiu, L. (2019). Research progress and perspective on drought stress in legumes: A review. *Int J Mol Sci* 20(10): 2541.

Nawaz, M., and Wang, Z. (2020). Abscisic acid and glycine betaine mediated tolerance mechanisms under drought stress and recovery in *Axonopus compressus*: a new insight. *Sci Rep* 10(1): 6942.

Nuttall, J., O'leary, G., Panozzo, J., Walker, C., Barlow, K., and Fitzgerald, G. (2017). Models of grain quality in wheat—A review. *Field Crops Res* 202: 136-145.

Osman, H.S. (2015). Enhancing antioxidant–yield relationship of pea plant under drought at different growth stages by exogenously applied glycine betaine and proline. *Ann Agric Sci* 60(2): 389-402.

Osmolovskaya, N., Shumilina, J., Kim, A., Didio, A., Grishina, T., Bilova, T., Keltsieva, O.A., Zhukov, V., Tikhonovich, I., and Tarakhovskaya, E. (2018). Methodology of drought stress research: Experimental setup and physiological characterization. *Int J Mol Sci* 19(12): 4089.

Pardo-Domènech, L., Tifrea, A., Grigore, M., Boscaiu, M., and Vicente, O. (2016). Proline and glycine betaine accumulation in two succulent halophytes under natural and experimental conditions. *Plant Biosyst* 150(5): 904-915.

Rabiei, Z., Hosseini, S.J., Pirdashti, H., and Hazrati, S. (2020). Physiological and biochemical traits in coriander affected by plant growth-promoting rhizobacteria under salt stress. *Heliyon* 6(10).

Rizwan, M., Ali, S., Ibrahim, M., Farid, M., Adrees, M., Bharwana, S.A., Zia-ur-Rehman, M., Qayyum, M.F., and Abbas, F. (2015). Mechanisms of silicon-mediated alleviation of drought and salt stress in plants: a review. *Environ Sci Pollut Res* 22: 15416-15431.

Roychoudhury, A., and Banerjee, A. (2016). Endogenous glycine betaine accumulation mediates abiotic stress tolerance in plants. *Trop Plant Res* 3(1): 105-111.

Salehi-Lisar, S.Y., and Bakhshayeshan-Agdam, H. (2016). *Drought stress in plants: causes, consequences, and tolerance.*

Salehi, A., Tasdighi, H., and Gholamhoseini, M. (2016). Evaluation of proline, chlorophyll, soluble sugar content and uptake of nutrients in the German chamomile (M*atricaria chamomilla* L.) under drought stress and organic fertilizer treatments. *Asian Pac J Trop Biomed* 6(10): 886-891.

Sallam, A., Alqudah, A.M., Dawood, M.F., Baenziger, P.S., and Börner, A. (2019). Drought stress tolerance in wheat and barley: advances in physiology, breeding and genetics research. *Int J Mol Sci* 20(13): 3137.

Seleiman, M.F., Al-Suhaibani, N., Ali, N., Akmal, M., Alotaibi, M., Refay, Y., Dindaroglu, T., Abdul-Wajid, H.H., and Battaglia, M.L. (2021). Drought stress impacts on plants and different approaches to alleviate its adverse effects. *Plants* 10(2): 259.

Siddiqui, M.H., Al-Khaishany, M.Y., Al-Qutami, M.A., Al-Whaibi, M.H., Grover, A., Ali, H.M., Al-Wahibi, M.S., and Bukhari, N.A. (2015). Response of different genotypes of faba bean plant to drought stress. *Int J Mol Sci* 16(5): 10214-10227.

Singh, M., Kumar, J., Singh, S., Singh, V.P., and Prasad, S.M. (2015). Roles of osmoprotectants in improving salinity and drought tolerance in plants: a review. *Rev Environ Sci Biotechnol* 14: 407-426.

Sohrabi, Y., Habibi, A., Mohammadi, K., Sohrabi, M., Heidari, G., Khalesro, S., and Khalvandi, M. (2012). Effect of nitrogen (N) fertilizer and foliar-applied iron (Fe) fertilizer at various reproductive stages on yield, yield component and chemical composition of soybean (*Glycine max* L. Merr.) seed. *Afr J Biotechnol* 11(40): 9599-9605.

Tadayyon, A., Nikneshan, P., and Pessarakli, M. (2018). Effects of drought stress on concentration of macro- and micro-nutrients in Castor (*Ricinus communis* L.) plant. *J Plant Nutr* 41(3): 304-310.

Thalmann, M., Pazmino, D., Seung, D., Horrer, D., Nigro, A., Meier, T., Kölling, K., Pfeifhofer, H.W., Zeeman, S.C., and Santelia, D. (2016). Regulation of leaf starch degradation by abscisic acid is important for osmotic stress tolerance in plants. *Plant Cell* 28(8): 1860-1878.

Wang, S., Lin, H., Saito, T., Ohkawa, K., Ohara, H., Jia, H., and Kondo, S. (2019a). Abscisic acid affects ethylene metabolism and carotenoid biosynthesis in Japanese apricot (*Prunus mume* Sieb. et Zucc.). *Agri Gene* 12: 100083.

Wang, Y., Zhang, B., Jiang, D., and Chen, G. (2019b). Silicon improves photosynthetic performance by optimizing thylakoid membrane protein components in rice under drought stress. *Environ Exp Bot* 158: 117-124.

Webber, H., Ewert, F., Olesen, J.E., Müller, C., Fronzek, S., Ruane, A.C., Bourgault, M., Martre, P., Ababaei, B., and Bindi, M. (2018). Diverging importance of drought stress for maize and winter wheat in Europe. *Nat Commun* 9(1): 4249.

You, L., Song, Q., Wu, Y., Li, S., Jiang, C., Chang, L., Yang, X., and Zhang, J. (2019). Accumulation of glycine betaine in transplastomic potato plants expressing choline oxidase confers improved drought tolerance. *Planta* 249: 1963-1975.

Zegaoui, Z., Planchais, S., Cabassa, C., Djebbar, R., Belbachir, O.A., and Carol, P. (2017). Variation in relative water content, proline accumulation and stress gene expression in two cowpea landraces under drought. *J Plant Physiol* 218: 26-34.

Zivcak, M., Brestic, M., and Sytar, O. (2016). *Osmotic adjustment and plant adaptation to drought stress.* In: Drought Stress Tolerance in Plants, Vol 1, Springer. 105-143.

JPMB
Journal of Plant Molecular Breeding
Published by Genetics and Agricultural Biotechnology Institute of Tabarestan
2023 | Volume 11 | Issue 2

مقاله پژوهشی

پاسخ ارقام گندم به تنش خشکی با تمرکز بر عناصر مغذی ریشه و بخش هوائی، کلروفیل و گلاسئین‌بتائین برگ

سمانه عدل، ناهید مسعودیان*، بوستان رودی، مصطفی عبادی

گروه زیست‌شناسی، دانشگاه آزاد اسلامی واحد دامغان، ایران

چکیده: تنش خشکی یکی از عوامل محدودکننده رشد گیاه است. به منظور بررسی اثر تنش خشکی (۰، ۱۵۰، ۲۵۰ گرم در لیتر پلی‌اتیلن گلیکول ۶۰۰۰ (PEG) بر خصوصیات فیزیولوژیکی دو رقم گندم (گنبد و N8720)، آزمایش هیدروپونیک به صورت فاکتوریل در قالب طرح کاملاً تصادفی با سه تکرار در انستیتو پاستور ایران (مرکز تحقیقات شمال) در سال ۱۳۹۶ اجرا شد. نتایج آزمایش نشان داد که اثر ساده ارقام برای تمامی صفات مورد مطالعه به جز نیتروژن و فسفر ساقه معنی‌دار بود. همچنین اثر ساده تنش خشکی و اثر متقابل تنش خشکی و ارقام برای تمامی صفات مورد مطالعه معنی‌دار بود. بیشترین مقدار عناصر در ریشه و اندام هوایی و میزان کلروفیل در رقم N8720 تحت تیمار شاهد مشاهده شد. همچنین در رقم N8720 میزان گلیسین‌بتائین به دلیل تنش خشکی افزایش یافت و در تیمار ۲۵۰ گرم در لیتر PEG به حداکثر خود رسید. نتایج تحلیل همبستگی نشان داد که بین تمامی صفات همبستگی مثبت و معنی‌داری وجود دارد. نتایج آزمایش نشان داد که رقم N8720 از نظر کلیه صفات مورد مطالعه از ویژگی‌های برتر برخوردار بود.

کلمات کلیدی: تجزیه خوشه‌ای، تنش خشکی، فسفر، گلیسین بتائین.

ویراستار علمی
دکتر اسماعیل بخشنده،
پژوهشکده ژنتیک و زیست‌فناوری کشاورزی طبرستان،
دانشگاه علوم کشاورزی و منابع طبیعی ساری، ایران

تاریخ
دریافت: ۲۲ تیر ۱۴۰۲
پذیرش: ۱۷ بهمن ۱۴۰۲
چاپ: ۱۴ اسفند ۱۴۰۲

نویسنده مسئول
دکتر ناهید مسعودیان
nahid.masoudian@yahoo.com

ارجاع به این مقاله
Adl, S., Masoudian, N., Roudi, B., and Ebadi, M. (2023). Response of wheat cultivars to drought stress focusing on chlorophyll and physiological characteristics. *J Plant Mol Breed* *11* (2): 39-54.
doi: 10.22058/JPMB.2024.2006933.1278.

JPMB | Journal of Plant Molecular Breeding
Published by Genetics and Agricultural Biotechnology Institute of Tabarestan
2023 | Volume 11 | Issue 2

Allelopathic effect of *Rapistrum rugosum* L. weed on growth, physiological and biochemical parameters of *Hibiscus sabdariffa* L.

Original paper

Reza Kouhestani, Leila Ahangar *, Mehdi Zarei, Ebrahim Gholamalipour Alamdari, Ziba Avarseji

Faculty of Agriculture and Natural Resources, Gonbad Kavous University

Abstract: To study the allelopathic effect of decomposed fresh aerial parts of *Rapistrum rugosum* on growth, physiological and biochemical traits of *Hibiscus sabdariffa*, a pot experiment was conducted as a completely randomized design with three replications under greenhouse condition at the Gonbad Kavous University. Treatments were different amounts of *R. rugosum* residues (0, 10, 20, 40, 80, and 160 g kg^{-1} soil). The results showed that increasing the amount of *R. rugosum* residues significantly reduced the growth traits of *H. sabdariffa*. The lowest amount of stem and root length, fresh and dry weight of the plant was observed in 160 g kg^{-1} of *R. rugosum* residues. The content of chlorophyll *b* and carotenoids, as well as malondialdehyde, decreased with increasing the amount of *R. rugosum*. However, the trend of changes in the content of catalase enzyme, soluble sugars content, proline, total phenol, and flavonoids increased with increasing the amount of *R. rugosum* residues. Consequently, our findings showed that with the increasing in the amount of *R. rugosum* residues, all the studied traits of *H. sabdariffa* decreased significantly. Therefore, due to the negative allelopathic effect of *R. rugosum* on growth and physiological parameters of *H. sabdariffa*, *R. rugosum* density management should be considered during the cultivation of this plant.

Keywords: allelopathic, physiological traits, *Rapistrum rugosum*, total phenol.

OPEN ACCESS

Edited by

Prof. Hemmatollah Pirdashti,
Genetics and Agricultural Biotechnology Institute of Tabarestan, Sari Agricultural Department Sciences and Natural Resources University, Iran

Date

Received: 06 January 2024
Accepted: 20 February 2024
Published: 05 March 2024

Correspondence

Dr. Leila Ahangar
l.ahangar63@gmail.com

Citation

Kohestani, R., Ahangar, L., Zarei, M., Gholamalipour Alamdari, E. and Avarseji, Z. (2023). Allelopathic effect of *Rapistrum rugosum* L. weed on growth, physiological and biochemical parameters of *Hibiscus sabdariffa* L. *J Plant Mol Breed. 11* (2):55-65.
doi: 10.22058/JPMB.2024.2019717.1286.

Introduction

Allelopathy is defined as any direct or indirect stimulant and inhibitory effect of a plant on other plants and living organisms by releasing chemical compounds (allelochemicals) into the environment (Al-Watban and Salama, 2012; Rahimzadeh et al., 2012). However, most researches has focused on the adverse effects of allelochemicals. Generally, these compounds released by allelopathic plants affect the germination, growth, development, and establishment of receptor plants and play an essential role in the pattern of vegetation and crop production (Gniazdowska and Bogatek, 2005; Elisante et al., 2013). This harmful effect of allelochemicals occurs by altering various metabolic processes in donor plants. Allelochemicals are usually produced as secondary products or in the main pathways of metabolism in plants. These substances are released in the form of solution due to leaching, decomposition, volatilization and root exudation on the surface of the plant parts (Tigre et al., 2012). Allelochemical compounds of plants, especially weeds, can inhibit physiological and biochemical processes such as germination, cell division, reparation, photosynthesis, changes in cell membrane stability, enzyme activity, *etc* (Cruz - Ortega et al., 2002; Al-Watban and Salama, 2012). Cruz - Ortega et al. (2002) reported that allelochemicals released from allelopathic plants increased reactive oxygen species (ROS) in receptor plants and ultimately stimulate the activity of antioxidant enzymes.

One of the proposed methods to reduce the use of synthetic herbicides and decrease weed population in the field is due to exploitation of the toxic plants as herbicides of natural origin (Bhadoria, 2010; Farooq et al., 2011). Chang et al. (2002) found that allelopathic compounds at low concentrations could negative or positive effects on receptor plants, but the inhibition at higher concentrations. Han et al. (2008) reported that inhibition percentage of allelochemicals is directly dependent on the concentration of the extract.

The presence of allelochemicals in the field is a kind of stress, in which plants grow adjacent to allelopathic plants, and might be exposed to some kind of biological stress (Liu et al., 2003). Asgharipour and Armin (2010) reported that both the root and leaf extracts of *Sorghum halepens* in most cases inhibited the seed germination and early seedling growth of *Plantago ovata*, *Plantago psyllium*, *Foeniculum vulgare* and *Ocimum basilicum*, while the seed germination and the early seedling growth of *Nigella sativa* and *Cuminum cyminum* were simulated by both extracts at lower concentrations. Otusanya et al. (2015) showed that the application of the aqueous extract of *Tithonia diversifolia* and *Chromolaena odorata* at a lower and moderate concentration significantly reduced the seed germination and juvenile seedling growth of *Hibiscus sabdariffa*.

Rapistrum rugosum, belongs to the *Brassicaceae* family, an annual, deciduous, and winter plant that is considered the most important weed of rapeseed fields in the world and included Iran (Baghestani et al., 2005). *Brassicaceae* is one of the important plant families due to its allelopathic activity. Glucosinolates and phenolic compounds are the most important allelochemicals synthesized by the plants in the *Brassicaceae* family. The glucosinolates are converted into several isothiocyanates through enzymatic (myrosinase) activity and express an allelopathic activity (Jabran, 2017). Scientific literature reports allelopathic activities of many *Brassicaceae* plants (Jabran et al., 2015; Cipollini, 2016). The study of the allelopathic effects of *R. rugosum* can be critical in the nature because of containing allelopathic compounds like other *Brassicaceae* plants.

H. sabdariffa L. also known as rosella, belongs to the *Malvaceae* family. It is an ideal crop for developing countries as it is relatively easy to grow, can be grown as part of multi-cropping systems and can be used as food and fiber. In many countries, *H. sabdariffa* is used for its medicinal properties (Da-Costa-Rocha et al., 2014). Therefore, studying the growth barriers of *H. sabdariffa*, including the effect of weed residues left from the previous crop on germination, vegetative growth and nutrient uptake of this plant, can be a practical step in improving and developing the cultivation of this plant. Also, there is no sufficient information about the response of *H. sabdariffa* to the residue of *R. rugosum*, therefore, the present study aimed to evaluate the effect of this weed residue on the growth, physiological and biochemical characteristic of *H. sabdariffa*.

Materials and Methods

Plant material

In the present study, *R. rugosum* aerial part was collected at full flowering stage from Azadshar, which is located East of Golestan province (Iran), with a latitude of 37º 14' North and longitude of 55º 16' East, and 89 m above sea level in 2018. The average annual rainfall of the region was 561 mm and the annual average temperature was 15°C.

Identification and preparation of plant samples of R. rugosum

In the beginning, *R. rugosum* weed specimens were accurately identified with the help of Iranian cormophytes (Ghahreman, 1993). Then, to remove the dust, they were washed with distilled water for one min. Subsequently, the samples of weeds were dried in an oven at 60 °C until reaching a constant weight. The samples after 40 days were first ground into small pieces by a mill and then passed through sieve a 8 mesh.

Preparation of R. rugosum residues and planting seeds of H. sabdariffa.

In order to prepare the soil mixture for 5 kg pots, soil from 0-30 cm depth was prepared and sieved. After measuring physico-chemical soil properties (Table 1), different amounts of *R. rugosum* residues such as 0 (control), 10, 20, 40, 80, and 160 g per kg soil were added in each pot. In order to decompose the decayed plant parts by microorganisms, each pot moistened daily with 300 cc of distilled water. At the end of the 40th day, the pots' soil was exposed to the open air for one week to volatile allelochemicals. 20 disinfected seeds (0.1% sodium hypochlorite) of *H. sabdariffa* were cultivated in each pot.

Table 1. Physico-chemical properties of the soil used in this study.

Sand (%)	Silt (%)	Clay (%)	Soil texture	Potassium (ppm)	Phosphorus (ppm)	Total nitrogen (%)	Organic carbon (%)	TNV (%)	pH	EC (dS /m)
13	56	31	Silty clay loam	340	13	0.08	0.78	10.8	7.6	0.96

This experiment was performed under greenhouse condition at the Gonbad Kavous University, with a relative humidity of 65%, light duration of 16 h light and 8 h dark and temperature between 15-25 ºC. After the emergence of seedling, six uniform seedlings were kept in each pot. The study was conducted as a completely randomized design with three replications.

Measurement of morphological traits

All *H. sabdariffa* seedlings were harvested from each pot after 40 days. Then, some morphological traits such as shoot and root length, fresh and dry weight of seedlings, root volume, number of roots, number of leaves and leaf area (using leaf area meter; Delta-t model) were measured.

Measurement of biochemical traits

At the end of the growing stage, leaf samples of *H. sabdariffa* were collected and then stored at -80º C.

Measurement of chlorophyll and carotenoid content

To measure the chlorophyll and carotenoid content, 0.1 g of fresh leaf tissue of *H. sabdariffa* was ground with 10 ml of 80% acetone. The mix was centrifuged at 1000 rpm for 10 minutes. Then the supernatant solution was transferred into a new tube and the volume was adjusted to 25 ml with 80% acetone. Finally, the absorbance was read at 663, 645 and 470 nm for chlorophyll *a*, *b* and carotenoids, respectively using a Biochrom Libera-S22 spectrophotometer. The values were calculated as mg.g^{-1} of fresh weight using the following formula (Arnon, 1949).

1) Chlorophyll *a*= [(19.3×A663- 0.86× A645) V/100W]
2) Chlorophyll *b*= [(19.3× A645- 3.6× A663) V/100W]
3) Carotenoids= [100(A470)- 3.27 (mg chl *a*) - 104 (mg chl *b*)/ 227]

where V, volume of the filtered solution (centrifuge solution); W, wet weight of the sample in grams; A, light absorption at 663, 645 and 470 nm

Measurement of proline content

Proline was extracted from 500 mg of fresh leaf tissue which was grounded in 10 ml of 3% sulfosalicylic acid. The solution was passed through filter paper, then 2 ml of this solution was transferred into the test tube, followed by the immediate addition of 2 ml of ninhydrin acid, and 4 ml of toluene to each tube and shaken for 20 to 30 seconds until the yellow top layer of toluene appeared. This layer was transferred in a new test tube and the proline content was measured at 520 nm using a spectrophotometer (Biochrom Libera-S22). Proline content was determined using the standard proline curve in µmol/g of fresh weight (Bates et al., 1973).

Measurement of soluble sugars content

Soluble sugars content was measured based on (Kochert, 1978) method, 0.1 g of plant dry matter was mixed in 10 ml of 70% ethanol and kept in the refrigerator for one week. Then 1 ml of the upper solution was separated and their volume was set to 2 ml using distilled water. Next, 1 ml of 5% phenol and 5 ml of concentrated sulfuric acid were added. A yellow solution was produced which changed color. The absorbance of the color at 485 nm which was related to soluble carbohydrate concentrations (mg g^{-1} of dry weight) was read by the spectrophotometer (Biochrom Libera-S22).

Measurement of phenolic content

100 mg of dried leaf tissue was dissolved with 10 ml of 80% ethanol and centrifuged at 1000 rpm for 10 min. The supernatant was kept in a boiling water bath for 5 min. Then volume of the concentrated solution was adjusted to 3 ml with distilled water. 0.5 ml of folic acid Siocalto reagent and 2 ml of sodium carbonate were added to this solution. Again, the reaction mixture was kept in a boiling water bath for 10 min. Finally, absorbance was measured at 650 nm using a spectrophotometer (Biochrom Libera-S22). The standard total phenolic content was expressed as mg gallic acid equivalents (GAE) per gram of dry samples (Malik and Singh, 1980).

Measurement of flavonoid content

10 mg of dry leaf tissue was dissolved in 10 ml of acetone and shaken for 24 hours. The solution was passed through a filter paper. For this purpose, 0.5 ml of each plant extract was taken in test tube, and then 1.5 ml of 95% ethanol, 0.1 ml of 10% aluminium chloride ($AlCl_3.6H_2O$), 0.1 ml of potassium acetate, and 2.8 ml of distilled water were added and mixed well. The solution was kept at room temperature for 3 min, after that the absorbance was read at 415 nm in a spectrophotometer (Chang et al., 2002).

Preparation of enzyme extract

At the beginning, 1 g of fine powder sample was ground in 2.5 ml of potassium phosphate buffer (containing 0.1 ml of ethylene dihydramine, amine, tetra acetic acid (EDTA), 1% (W/V) polyvinyl pyrrolidone (PVP), 0.5% triton X-100 and 20 the percentage of glycerol) by pestle and mortar. Then, the obtained solution was centrifuged at 10,000 rpm for 15 min at 4°C. After that, the upper layer was separated and used as enzyme extract (Kala, 2015).

Estimation of catalase enzyme activity

Catalase enzyme activity measurement was performed by Aebi (1984) method. The kinetic activity of the catalase enzyme was determined using 2.5 ml of 0.1 M phosphate buffer (pH = 7), 100 µl of 10 mM H_2O_2 (V/V) as indicator. In the ice bath, the indicator was mixed with 50 µl of the enzyme extract mixture. Absorbance changes at 240 nm were read by spectrophotometer for 2 minutes. Enzyme activity was calculated according to µmol per g of fresh weight.

Estimation of guaiacol peroxidase enzyme activity

To measure guaiacol peroxidase enzyme activity, 780 µl of 50 mM potassium phosphate buffer (pH = 6.6), 90 µl of 1% guaiacol and 90 µl of 0.3% H_2O_2 were placed in a test tube in the ice bath, followed by immediately addition 20 µl of enzyme extract mixture (Hemeda and Klein, 1990). Absorption changes at 470 nm per min were measured by spectrophotometer (Biochrom Libera-S22).

Estimation of Malondialdehyde (MDA) enzyme activity

Heath and Packer (1968) method was used to measure the activity of the malondialdehyde enzyme. 0.2 g of fresh leaf tissue was homogenized in 5 ml of 0.1% trichloroacetic acid (TCA) with

mortar and pestle, and centrifuged at 10,000 rpm for 5 min. Then 1 ml of the upper layer was suspended in 4 ml of 40% TCA solution along with 0.5% thiobarbituric acid (TBA) on ice. The mixture was evaporated at 95°C for 30 min, and immediately centrifuged for the second time at 10,000 rpm for 10 min at 4°C. The absorption of MDA was read at 532 nm by spectrophotometer (Biochrom Libera-S22).

Statistical analyses

The analysis of variance (ANOVA) was performed using the SAS software, version 9.3, and means were compared with the least significant difference test (LSD) at 0.05 probability level.

Results

The effect of R. rugosum residues on the morphological components of H. sabdariffa

The results showed a significant difference in the allelopathic effect of different amounts of *R. rugosum* residues on stem length, root volume, number of roots, number of leaves, fresh and dry weight of plant and leaf area of *H. sabdariffa* (*Pr* <0.01) (Table 2). The mean comparison showed the stem length of *H. sabdariffa* decreased with increasing the amounts of *R. rugosum* residues, so the lowest stem length (7.16 cm) was recorded at 160 g of *R. rugosum* which was 49.5% lower than the control plants (Table 2). The residuals of *R. rugosum* significantly inhibited the number and volume root of *H. sabdariffa* compared to the control. As, seedling of *H. sabdariffa* grown in control and 160 g of residues had the highest and lowest number and volume of roots, respectively. Both 80 and 160 g kg^{-1} of *R. rugosum* residuals showed the greatest inhibitory effects on the number of leaves (36.6 and 39.7%) and leaf area (63.8 and 69.3%) of *H. sabdariffa*, respectively. In contrast, 10 g of *R. rugosum* residues showed the least reduction effect on the above two parameters (Tablel 2).

The effect of different amount of R. rugosum residues on the pigments content of H. sabdariffa

The chlorophyll b and total chlorophyll content of *H. sabdariffa* seedling unlike chlorophyll a, showed a sharp decline with increasing of residues (Table 2). The maximum decreasing level of these two parameters was observed in 160 g of residues, which did not show a significant difference with 80 g. The 10 g kg^{-1} of *R. rugosum* residues has no significant effect on chlorophyll b and total chlorophyll.

Table 2: Analysis of variance (mean square) effect of different amounts of *R. rugosum* residues on morphological and physiological traits and pigments content of *H. sabdariffa.*

S.O.V	df	Stem length	Root volume	Root No.	Leaves No.	Fresh weight of plant	Dry weight of plant	Leaf erea	Cholorophyll *a*	Cholorophyll *b*	Total cholorophyll
Treat	5	18.8 **	0.35 **	4.88 **	4.14 **	2.45 **	0.052 **	62.9 **	0.0002 **	0.012 **	0.017 **
Error	12	0.38	0.014	0.19	0.087	0.057	0.002	0.6	0.0001	0.0004	0.0002
C.V	-	5.8	12.2	6.9	5.17	8.27	14.2	7.5	13.5	4.43	2.8

Continue of Table 2:

S.O.V	df	Carotenoids	Soluble sugars content	Proline activity	Catalase activity	Peroxidase activity	Malondialdehyde activity	Phenol content	Flavonoids content
Treat	5	0.007 **	1705.64 **	673.06 **	75.43 **	2.81 **	0.07 **	47.95 **	0.0005 **
Error	12	0.0002	0.38	0.65	0.15	0.16	0.0007	0.158	0.00001
C.V	-	7.19	0.64	1.1	1.58	4.79	7.81	5.6	5.56

* and **: significant at 5% and 1% levels of probability, respectively.

Table 3: Means comparison of the different amounts of *R. rugosum* residues on morphological and physiological traits and pigments content of *H. sabdariffa*.

Different amounts of *R. rugosum* residues	Stem length (cm)	Root volume (mm^2)	Root No.	Leaves No.	Fresh weight of plant (gr)	Dry weight of plant (gr)	Leaf erea (cm^2)	Cholorophyll a (mg/g fresh weight)	Cholorophyll b (mg/g fresh weight)	Total cholorophyll (mg/g fresh weight)
0	14.16 ^{a}	1.54 ^{a}	8.44 ^{a}	7.55 ^{a}	4.11^{a}	0.57 ^{a}	16.88 ^{a}	0.09 ^{a}	0.55 ^{a}	0.65 ^{a}
10	12.42 ^{b}	1.23 ^{b}	7.11 ^{b}	6.66 ^{b}	3.59 ^{b}	0.45 ^{b}	14.01 ^{b}	0.08 ^{ab}	0.55 ^{a}	0.63 ^{a}
20	11.05 ^{c}	1.05 ^{bc}	6.55 ^{bc}	5.55 ^{c}	3.01 ^{c}	0.32 ^{c}	11.16 ^{c}	0.073 ^{b}	0.51 ^{b}	0.58 ^{b}
40	10.05 ^{c}	0.89 ^{cd}	5.88 ^{cd}	5.11 ^{cd}	2.82 ^{c}	0.29 ^{c}	8.52 ^{c}	0.066 ^{b}	0.45 ^{c}	0.52 ^{c}
80	8.83 ^{d}	0.75 ^{de}	5.66 ^{d}	4.78 ^{de}	2.12 ^{d}	0.26 ^{c}	6.11 ^{e}	0.073 ^{b}	0.42 ^{cd}	0.47 ^{d}
160	7.16 ^{e}	0.57 ^{e}	4.78 ^{e}	4.55 ^{e}	1.67 ^{e}	0.22 ^{c}	5.17 ^{e}	0.07 ^{b}	0.41 ^{d}	0.47 ^{d}
LSD 5%	1.11	0.22	0.8	0.53	0.43	0.09	1.38	0.02	0.04	0.03

Continue of Table 3:

Different amounts of *R. rugosum* residues	Carotenoids (mg/g fresh weight)	Soluble sugars content (mg/g dry weight)	Proline activity (µmol/g fresh weight)	Catalase activity (µmol/g fresh weight)	Peroxidase activity (µmol/g fresh weight)	Malondialdehyde activity (µmol/g fresh weight)	Phenol content (mg/g dry weight)	Flavonoids content (mg/g fresh weight)
0	0.25 ^{a}	63.09 ^{f}	47.47 ^{f}	18.23 ^{f}	9.73 ^{a}	0.53 ^{a}	2.62 ^{c}	0.06 ^{c}
10	0.24 ^{a}	77.82 ^{e}	63.18 ^{e}	20.47 ^{e}	9.12 ^{a}	0.49 ^{a}	4.25 ^{b}	0.07 ^{b}
20	0.18 ^{b}	90.55 ^{d}	76.54 ^{d}	23.05 ^{d}	8.09 ^{b}	0.38 ^{b}	5.77 ^{b}	0.07 ^{b}
40	0.16 ^{cb}	109.45 ^{c}	78.04 ^{c}	25.81 ^{c}	7.87 ^{b}	0.23 ^{c}	6.36 ^{b}	0.07 ^{b}
80	0.15 ^{c}	114.5 ^{b}	82.84 ^{b}	28.19 ^{b}	7.82 ^{b}	0.22 ^{c}	9.78 ^{b}	0.07 ^{b}
160	0.14 ^{c}	125.66 ^{a}	88.47 ^{a}	31.34 ^{a}	7.07 ^{c}	0.17 ^{d}	13.61 ^{a}	0.13 ^{a}
LSD 5%	0.02	1.10	1.44	0.69	0.71	0.05	0.71	0.01

*= The means followed by the different letters in the same column are significantly different from each other based on LSD test at $P < 0.05$ level

The lowest and highest inhibitory effects on the fresh weight of *H. sabdariffa* were observed in 10 and 160 g (12.6 and 59.3%, respectively) (Figure 1). The same results were observed in the dry weight of *H. sabdariffa*, but the differences were not significant among the treatments of 20, 40, 80 and 160 g kg^{-1} of *R. rugosum* residuals.

Effect of R. rugosum residues on the content of adaptive osmolytes, catalase, peroxidase, and malondialdehyde activity in H. sabdariffa

The lowest and highest content of osmolytes were observed in 10g and 160 g of *R. rugosum* residues (which were about 23.3% and 99.17% higher than those in control plants), respectively (Figure 1). Like the soluble sugar trait, the proline content of *H. sabdariffa* was positively correlated with the quantity of residues. The highest content of proline (+86.3% compared to the control) was observed in the 160 g kg^{-1} of *R. rugosum* residuals. The enzyme changes in *H. sabdariffa* showed that of *R. rugosum* residues had an additive effect on the activity of catalase enzyme compared to the control unlike peroxidase and malondialdehyde enzymes. The maximum catalase amount was recorded in 160 g kg^{-1} of *R. rugosum* residuals (72.2 % compared to control). While, the lowest level of peroxidase and malondialdehyde enzymes was observed in 160 g kg^{-1} of *R. rugosum* residuals (Figure 1). The R. rugosum residues significantly stimulate the phenolic content of *H. sabdariffa*. The minimum and maximum values of phenolic content were recorded in 10 and 160 g kg-1 of *R. rugosum* residuals (+62%

and +419% compared to the control, respectively) (Figure 1). Also, the same results were observed in the content flavonoids of *H. sabdariffa*, and Treatment of 160 g of residues caused a 66.6% increase this parameter in compared to control, but the differences were not significant among of 10, 20, 40 and 80 g of residues (about + 16.6% compared to control).

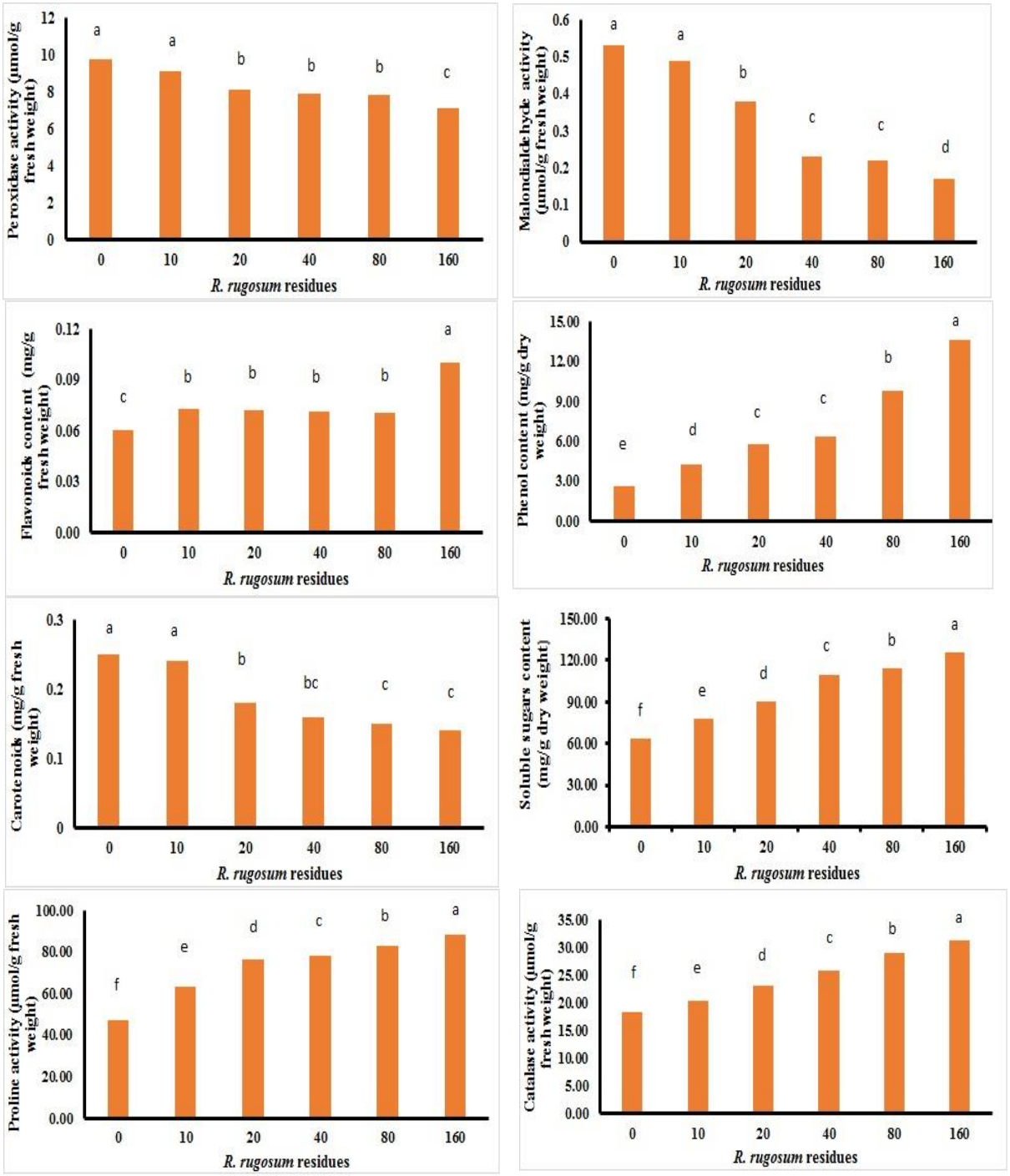

Figure 1. Means comparison of the different amounts of *R. rugosum* residues on physiological traits and pigments content of *H. sabdariffa*.

Discussion

The results of the present study showed that morphological traits of *H. sabdariffa* had a decreasing trend with an increase in *R. rugosum* concentrations. This finding is consistence with the results of Hegab and Ghareib (2010) and Khanh et al. (2008). Poornamazi et al. (2019), who reported that the percentage of inhibition is directly depend on the concentration of the extract. The minimum and maximum number and volume of *H. sabdariffa* roots were recorded at 160 and 10g of residues, respectively. Given that the root is the first organ to be exposed to allelopathic compounds, this is not far-fetched. The negative effect of *R. rugosum* decayed plant parts would be due to the presence of some secondary compounds such as phenolic acid, isothiocyanate, thiocyanate and nitrile Bais et al. (2003). Gulzar et al. (2016) reported that allelopathic compounds target the cell division of growing tissues at the tip of the root and increase the number of abnormal chromosomes. Furthermore, other studies indicated that allelopathic compounds could reduce water uptake and caused stress in plants by affecting root growth and reducing capillary root formation (Feizi et al., 2018). These results showed that the chlorophyll *b*, total chlorophyll and carotenoids in *H. sabdariffa* decreased under different amounts of *R. rugosum* residues. This indicates allelopathic stress due to presence of the harmful compounds (like phenole) in *R. rugosum*. It can also be concluded that chlorophyll *b* and carotenoids, which plays the role of optical protection of chlorophyll *a*, due to its insufficiency in cells, led to the production of chlorophyll triplet and subsequently caused the formation of free radicals and peroxidation of cell membranes, which led to decrease in plant dry weight. The results of Elisante et al. (2013) showed the inhibitory effects of aqueous extract of *Dature stramonium* on chlorophyll content in two wild species of *Cenchrus ciliaris* and *Neonotonia wightii*, which were caused by various factors such as decreased carbon assimilation and increased reactive oxygen species. According to the results, the adaptive osmolytes such as soluble sugars and proline in *H. sabdariffa* leaves were increased under allelopathic stress of various amounts of *R. rugosum*. On the other hand, the activity of peroxidase and malondialdehyde significantly decreased, unlike the content of phenolic compounds and flavonoids. One of the main reasons for the damage of environmental stresses on plants is the production of oxygen free radicals such as singlet oxygen, hydrogen peroxide, superoxide and *etc*, that can target cell organs and cell membrane fats. Studies have shown that flavonoids and phenolic compounds can affect many physiological and biochemical processes, especially plant growth (John and Sarada, 2012). A recent study by (Wang et al., 2018) showed a decreasing trend of CAT, POD and SOD activities on *Amygdalus pedunculata* leaves with an increasing concentration of *Amorpha fruticosa*, *Hedysarum mongolicum*, *Sabina vulgaris*, and *Hippophae rhamnoides* shrubs of aqueous leaf extracts.

Conclusion

Our findings indicated that soluble sugars and proline, the enzymatic antioxidant of catalase and non-enzymatic antioxidants (total phenol and flavonoid) increased under allelopathic stress of *R. rugosum*. While the physiological traits of *H. sabdariffa* such as chlorophyll pigments and malondialdehyde content decreased. This indicates the high stress of *R. rugosum* on *H. sabdariffa* especially at higher concentrations. Due to the fact that *R. rugosum* has a detrimental allelopathic effect on the growth and physiological parameters of *H. sabdariffa*, it is imperative that *R. rugosum* density management be taken into consideration during the cultivation of this plant.

Supplementary Materials

No supplementary material is available for this article.

Author Contributions

Conceptualization, L.A and E.Gh.; methodology, R.K. E. Gh.; software, L.A and E. Gh.; formal analysis, l.A and M.Z.; investigation, L.A, E. Gh and Z.A.; resources, R.K. and L.A.; data curation, L.A.; writing—original draft preparation, R.K., L.A, Z.A and E.Gh.; writing—review and editing, L.A, M.Z and E.Gh.; visualization, E.Gh.; supervision, L.A and M.Z.; project administration, L.A and M.Z.; funding acquisition, L.A.

Funding

This research received no external funding.

Acknowledgments

The authors would like to express their gratitude to all contributors who have played a role in the development of this research.

Conflict of Interest Statement

The authors declare no conflict of interest. The funders had no role in the design of the study; in the collection, analyses, or interpretation of data; in the writing of the manuscript; or in the decision to publish the results.

References

Aebi, H. (1984). "[13] Catalase in vitro," in *Methods in enzymology*. Elsevier, 121-126.

Al-Watban, A., and Salama, H.M. (2012). Physiological effects of allelopathic activity of *Artemisia monosperma* on common bean (*Phaseolus vulgaris* L.). *Int Res J Plant Sci* 3(8): 158-163.

Arnon, D.I. (1949). Copper enzymes in isolated chloroplasts. Polyphenoloxidase in *Beta vulgaris*. *Plant Physiol* 24(1): 1.

Asgharipour, M.R., and Armin, M. (2010). Inhibitory effects of *Sorghum halepens* root and leaf extracts on germination and early seedling growth of widely used medicinal plants. *Adv Environ Biol*: 316-325.

Baghestani, M.A., Najafi, H., and Zand, E. (2005). *Wild mustard biology and management.* Iranian Research Institute of Plant Protection press (In Persian with English summary).

Bais, H.P., Vepachedu, R., Gilroy, S., Callaway, R.M., and Vivanco, J.M. (2003). Allelopathy and exotic plant invasion: from molecules and genes to species interactions. *Science* 301(5638): 1377-1380.

Bates, L.S., Waldren, R.a., and Teare, I. (1973). Rapid determination of free proline for water-stress studies. *Plant Soil* 39: 205-207.

Bhadoria, P. (2010). Allelopathy: a natural way towards weed management. *Am j exp agric* 1(1): 7-20.

Chang, C.-C., Yang, M.-H., Wen, H.-M., and Chern, J.-C. (2002). Estimation of total flavonoid content in propolis by two complementary colorimetric methods. *J Food Drug Anal* 10(3).

Cipollini, D. (2016). A review of garlic mustard (*Alliaria petiolata*, *Brassicaceae*) as an allelopathic plant. *J Torrey Bot Soc* 143(4): 339-348.

Cruz‐Ortega, R., Ayala‐Cordero, G., and Anaya, A.L. (2002). Allelochemical stress produced by the aqueous leachate of *Callicarpa acuminata*: effects on roots of bean, maize, and tomato. *Physiol Plant* 116(1): 20-27.

Da-Costa-Rocha, I., Bonnlaender, B., Sievers, H., Pischel, I., and Heinrich, M. (2014). *Hibiscus sabdariffa* L.–A phytochemical and pharmacological review. *Food Chem* 165: 424-443.

Elisante, F., Tarimo, M.T., and Ndakidemi, P.A. (2013). Allelopathic effect of seed and leaf aqueous extracts of *Datura stramonium* on leaf chlorophyll content, shoot and root elongation of *Cenchrus ciliaris* and *Neonotonia wightii*. *Am J Plant Sci* 2013.

Farooq, M., Jabran, K., Cheema, Z.A., Wahid, A., and Siddique, K.H. (2011). The role of allelopathy in agricultural pest management. *Pest Manag Sci* 67(5): 493-506.

Feizi, H., Salari, A., and Gharar, F. (2018). Study of the allelopathic effect of saffron (*Crocus sativus* L.) organs' aqueous extract on the seed germination and seedling growth of su-gar beet and safflower at different concentrations. *J Herbs Spices Med Plants* 22(4): 156-161.

Ghahreman, A. (1993). Plant systematics: cormophytes of Iran. Iran University Press 720p.

Gniazdowska, A., and Bogatek, R. (2005). Allelopathic interactions between plants. Multi site action of allelochemicals. *Acta Physiol Plant* 27: 395-407.

Gulzar, A., Siddiqui, M., and Bi, S. (2016). Phenolic acid allelochemicals induced morphological, ultrastructural, and cytological modification on *Cassia sophera* L. and *Allium cepa* L. *Protoplasma* 253: 1211-1221.

Han, C.-M., Pan, K.-W., Wu, N., Wang, J.-C., and Li, W. (2008). Allelopathic effect of ginger on seed germination and seedling growth of soybean and chive. *Sci Hortic* 116(3): 330-336.

Heath, R.L., and Packer, L. (1968). Photoperoxidation in isolated chloroplasts: I. Kinetics and stoichiometry of fatty acid peroxidation. *Arch Biochem Biophys* 125(1): 189-198.

Hegab, M.M., and Ghareib, H.R. (2010). Antioxidative effects of acetone fraction and vanillic acid from *Chenopodium murale* L. on tomato plant. *Weed Biol Manag* 10: 64-72.

Hemeda, H., and Klein, B. (1990). Effects of naturally occurring antioxidants on peroxidase activity of vegetable extracts. *J Food Sci* 55(1): 184-185.

Jabran, K. (2017). "Manipulation of allelopathic crops for weed control." Springer, 66-75.

Jabran, K., Mahajan, G., Sardana, V., and Chauhan, B.S. (2015). Allelopathy for weed control in agricultural systems. *Crop Protection* 72: 57-65.

John, J., and Sarada, S. (2012). Role of phenolics in allelopathic interactions. *Allelopathy J* 29(2).

Kala, S. (2015). Effect of Nacl salt stress on antioxidant enzymes of isabgol (*Plantago ovata* Forsk.) genotypes. *Int J Food Sci Tech Res* 4: 40-43.

Khanh, T.D., Cong, L.C., Xuan, T.D., Lee, S.J., Kong, D.S., and Chung, I.M. (2008). Weed-suppressing potential of dodder (*Cuscuta hygrophilae*) and its phytotoxic constituents. *Weed Sci* 56(1): 119-127.

Kochert, G. (1978). Carbohydrate determination by the phenol-sulfuric acid method. In: *Handbook of phycological methods, Physiological and biochemical methods.*: 95.

Liu, D.L., An, M., Johnson, I.R., and Lovett, J.V. (2003). Mathematical modeling of allelopathy. III. A model for curve-fitting allelochemical dose responses. *Nonlinearity in biology, toxicology, medicine* 1(1): 15401420390844456.

Malik, C.P., and Singh, M. (1980). Plant enzymology and histo-enzymology. Kalyani Publishers, New Delhi, p 286.

Otusanya, O., Ogunwole, A., and Tijani, M. (2015). Allelopathic effect of *Tithonia diversifolia* and *Chromolaena odorata* on the germination, growth and chlorophyll accumulation of *Hibiscus sabdariffa* (L.). *Int j botany res* 5(3): 1-14.

Poornamazi, A.R., Gholamalipour, A.E., BIABANI, A., and Taliei, F. (2019). Evaluation of the allelopathic potential of some weeds on germination characteristics and photosynthetic pigments of cress seedlings (*Lepidium sativum*). *Iran J Seed Res* 6(1): 129-143.

Rahimzadeh, F., Tobeh, A., and Jamaati-e-Somarin, S. (2012). Study of allelopathic effects of aqueous extracts of roots and seeds of goosefoot, red-root amaranth and field bindweed on germination and growth of lentil seedlings. *Int J Agron* 3(9): 318-326.

Tigre, R., Silva, N., Santos, M., Honda, N., Falcao, E., and Pereira, E. (2012). Allelopathic and bioherbicidal potential of *Cladonia verticillaris* on the germination and growth of *Lactuca sativa*. *Ecotoxicol Environ Saf* 84: 125-132.

Wang, X., Wang, J., Zhang, R., Huang, Y., Feng, S., Ma, X., Zhang, Y., Sikdar, A., and Roy, R. (2018). Allelopathic effects of aqueous leaf extracts from four shrub species on seed germination and initial growth of *Amygdalus pedunculata* Pall. *Forests* 9(11): 711.

JPMB
Journal of Plant Molecular Breeding
Published by Genetics and Agricultural Biotechnology Institute of Tabarestan
2023 | Volume 11 | Issue

مقاله پژوهشی

تاثیر آللوپاتیک علف هرز شلمی (*Rapistrum rugosum* L.) بر پارامترهای رشدی، فیزیولوژیکی و بیوشیمیایی گیاه دارویی چای ترش (*Hibiscus sabdariffa* L.)

رضا کوهستانی، لیلا آهنگر*، مهدی زارعی، ابراهیم غلامعلی‌پور علمداری، زیبا اورسجی

دانشکده کشاورزی و منابع طبیعی، دانشگاه گنبدکاووس، ایران

چکیده: به منظور بررسی اثر آللوپاتیک اندام‌های هوایی علف هرز شلمی (*Rapistrum rugosum* L.) بر ویژگی‌های رشدی، فیزیولوژیکی و بیوشیمیایی گیاه دارویی چای ترش، آزمایشی گلدانی در قالب طرح کاملاً تصادفی با سه تکرار در شرایط گلخانه در دانشگاه گنبدکاووس اجرا شد. تیمارها شامل مقادیر مختلف بقایای شلمی شامل ۰، ۱۰، ۲۰، ۴۰، ۸۰ و ۱۶۰ گرم بافت شلمی در کیلوگرم خاک بودند. نتایج نشان داد که افزایش میزان بقایای *R. rugosum* به طور معنی‌داری سبب کاهش صفات رشدی چای ترش گردید. کمترین میزان طول ساقه و ریشه، وزن‌تر و خشک گیاه در تیمار ۱۶۰ گرم بقایا *R. rugosum* مشاهده شد. محتوای کلروفیل bو کاروتنوئیدها و همچنین مالون‌دی‌آلدئید با افزایش مقدار *R. rugosum* کاهش یافت. با این حال، روند تغییرات در محتوای آنزیم کاتالاز، محتوای قندهای محلول، پرولین، فنل کل و فلاونوئیدها با افزایش میزان باقیمانده *R. rugosum* افزایش یافت. در کل، یافته‌های حاصل از این آزمایش نشان داد که با افزایش میزان بقایای *R. rugosum*، تمامی صفات مورد مطالعه چای ترش به‌طور معنی‌داری کاهش یافت. بنابراین با توجه به اثر منفی آللوپاتیک علف هرز شلمی بر پارامترهای رشدی و فیزیولوژیکی گیاه چای ترش در زمان کشت این گیاه باید مدیریت تراکم علف هرز مورد توجه قرار گیرد.

کلمات کلیدی: آللوپاتی، صفات فیزیولوژیکی، *Rapistrum rugosum* ، فنل کل.

ویراستار علمی
دکتر همت الله پیردشتی،
پژوهشکده ژنتیک و زیست‌فناوری کشاورزی طبرستان،
دانشگاه علوم کشاورزی و منابع طبیعی ساری

تاریخ
دریافت: ۱۶ دی ۱۴۰۲
پذیرش: ۱ اسفند ۱۴۰۲
چاپ: ۱۵ اسفند ۱۴۰۲

نویسنده مسئول
دکتر لیلا آهنگر
l.ahangar63@gmail.com

ارجاع به این مقاله
Kohestani, R., Ahangar, L., Zarei, M., Gholamalipour Alamdari, E. and Avarseji, Z. (2023). Allelopathic effect of *Rapistrum rugosum* L. weed on growth, physiological and biochemical parameters of *Hibiscus sabdariffa* L. *J Plant Mol Breed. 11* (2): 55-65.
doi: 10.22058/JPMB.2024.2019717.1286.

JPMB | Journal of Plant Molecular Breeding
Published by Genetics and Agricultural Biotechnology Institute of Tabarestan
2023 | Volume 11 | Issue 2

Identification and expression analysis of *HSP100* gene family in *Aeluropus littoralis*

Seyyed Hamidreza Hashemipetroudi[1*], Samira Mohammadi[1], Farzaneh Fatemi[2]

1. Genetics and Agricultural Biotechnology Institute of Tabarestan (GABIT), Agricultural Sciences and Natural Resources University (SANRU), Sari, Iran
2. Department of Agronomy and Plant Breeding, Faculty of Agriculture, Bu-Ali Sina University, Hamedan, Iran

Original paper

OPEN ACCESS

Edited by

Prof. Junhua Peng,
Spring Valley Agriscience Co. Ltd, China

Date

Received: 02 February 2024
Accepted: 13 April 2024
Published: 06 May 2024

Correspondence

Dr. Seyyed H. Hashemipetroudi
shr.hashemi@sanru.ac.ir;
irahamidreza@yahoo.com

Citation

Hashemipetroudi, S.H., Mohammadi, S., Fatemi, F. (2023). Identification and expression analysis of *HSP100* gene family in *Aeluropus littoralis*. *J Plant Mol Breed* 11(2): 66-77.
doi: 10.22058/JPMB.2024.2023541.1294.

Abstract: Heat shock proteins (HSPs), molecular chaperones with many activities, are essential to plant growth, development, and stress responses. To make crops more salt- and drought-resistant, plant breeders have considered halophytic plant. *Aeluropus littoralis*, a halophyte monocot grass, is one potential model species to discover new stress-response genes. Here, exon/intron structure, conserved motifs/ domains, and expression patterns of HSP100 gene family were identified in the genome of *A. littoralis*. This study found six unique AlHSP100 non-repetitive genes, revealing remarkable structural and physicochemical variations between the subfamilies. Phylogenetic and motif analyses revealed that proteins from the same subfamily (AlHSP100.1-4) and proteins from other subfamilies (AlHSP100.5-6) have similar types, ordering, and quantities of motifs. Finally, the expression of *AlHSP100.3* gene was analyzed using RT-qPCR under dehydration, salt, cold, and phytohormone abscisic acid stress treatments, revealed that their expression patterns vary in response to abiotic stresses. The presence of stress-dependent regulation of the *HSP100.3* gene, as evidenced by the early response to osmotic stress and the late response to cold stress, is likely associated with the cis-regulatory elements located upstream of this gene. This study provides more valuable information to deepen our understanding of the abiotic stress responses by *HSP100* genes in *A. littoralis*.

Keywords: Abiotic stress, gene expression, halophyte, heat shock proteins (HSPs), transcriptome analysis.

Introduction

Due to their unique status, plants exhibit heightened sensitivity to a broad spectrum of environmental stressors, encompassing both biotic and abiotic factors. This susceptibility to environmental constraints is particularly pronounced during the reproductive phase, often resulting in diminished crop productivity (Bita and Gerats, 2013; Esmaeili Tazangi et al., 2022). Understanding the gene expression patterns in response to abiotic stresses, as well as the cross-talk among gene family members and gene networks, is the initial step toward identifying and functionally characterizing stress-responsive genes (Hu et al., 2009a). Heat shock proteins (HSPs) are a protein family found in both prokaryotic and eukaryotic organisms that maintain cellular proteostasis and protect cells against stress (Hu et al., 2022). Protein homeostasis in cells and acquired thermotolerance in plants are both regulated by Hsps, which act as molecular chaperones to prevent misfolding and aggregation of proteins (Gong et al., 2021). There are five groups of Hsps, identified by their sequence homologies and estimated molecular weights: sHsps, Hsp60s, Hsp70s, Hsp90s, and Hsp100s (Chen et al., 2018). A subset of the wider AAA+ family of proteins, HSP100/ClpB are chaperones that use the energy of ATP to restore proteins that have aggregated during times of stress. A subset of the wider AAA+ family of proteins, HSP100/ClpB are chaperones that use the energy of ATP to restore proteins that have aggregated during times of stress (Lee et al., 2007). The HSP 100 proteins consist of five distinct domains: (1) The carboxyl-terminus, (2) the middle domain, (3) the nucleotide-binding domain (NBD) 1, (4) the NBD2, and (5) the amine-terminus (Agarwal et al., 2001). There are two classes in this gene family: ClpATPases class I (ClpA, ClpB, ClpC, ClpD, and ClpE) have two ATP binding domains, while ClpATPases class II (ClpM, ClpN, ClpX, and ClpY) have a single ATP binding domain (Panzade et al., 2021).

It is vital to highlight that the HSP100/ClpB subfamily is present in bacteria, protozoa, yeast, and plants, but not in mammals or humans (Kedzierska-Mieszkowska and Arent, 2020). There are three distinct isoforms of HSP100/ClpB found in plants, each of which is localized to a certain cellular compartment: the chloroplast (ClpB-P), the mitochondria (ClpB-M), and the cytoplasm/nucleus (ClpB-C) (Singh et al., 2010).

Thermostotolerance in plants is facilitated by the Hsp100 family members. Arabidopsis, rice, soybean, wheat, and tobacco are among the plant species whose ClpB-C expression is strongly associated with heat tolerance (Mishra and Grover, 2016). Heat stress isn't the only stress that the ClpB-C family members are involved in. Heavy metals and oxidative stress, for example, lead to the overexpression of ClpB-C genes in rice (Singh et al., 2012). Similarly, oilseed rape mosaic virus (ORMV) infection significantly increases the levels of AtClpB-C transcripts (Carr et al., 2006). In addition to stress regulation, *HSP100/ClpB* genes are also involved in other non-stress conditions such as developmental stages. Several plant species have shown constitutive expression of *ClpB-C* genes throughout reproductive phases. *ClpB-C* were highly expressed during flower and seed development in maize, mustard wheat, rice and soybean (Mishra and Grover, 2016; Razzaq et al., 2023).

Aeluropus littoralis (Gouan) Parl., a member of the *Poaceae* family and a monocot halophyte, can withstand salinities of up to 600 mM and flourishes in areas with intermediate to high salinity (Hashemi et al., 2016). The genomic resources of *A. littoralis* give the possibility to discover the abiotic responsive genes and their cis-regulatory elements (Hashemi-Petroudi et al., 2022). This study provides information on the *A. littoralis* HSP100 gene family, including sequence properties, evolutionary relationships, exon/intron structure, motif organization, and expression pattern analysis utilizing genome and transcriptome data. Furthermore, an investigation was performed to identify the differential expression patterns of the *HSP100.3* gene across root and leaf tissues of the *A. littoralis* plant after treatment with ABA, cold, and drought.

Materials and Methods

Identification of the HSP100 gene family members

The protein sequences of the *HSP100* gene family members from *Arabidopsis thaliana* and *Oryza sativa* were downloaded from the TAIR

(http://www.arabidopsis.org/) and RGAP (http://rice.plantbiology.msu.edu/) databases. *Aeluropus* HSP100 gene family was initially identified via local tBLASTN in BioEdit software (Hall, 1999) by defining *A. littoralis* draft genome (Hashemi-Petroudi et al., 2022) as a subject and protein sequences of *Arabidobsis* and rice as a query sequence (E-value < 1E-10). Finally, the coding sequence (CDS), protein, and genomic sequences of *AlHSP100* family were identified. Three protein database including InterProScan (https://www.ebi.ac.uk/interpro/search/sequence-search) (Jones et al., 2014), Pfam (http://pfam.xfam.org/) (Finn et al., 2016) and SMART (http://smart.embl-heidelberg.de/) (Letunic et al., 2015) were used to confirm the specific domains of the HSP100 proteins.

Physiochemical analysis of HSP100 proteins

The subcellular localization of HSP100 proteins was predicted using the WoLF PSORT algorithm (https://wolfpsort.hgc.jp/) (Horton et al., 2007). The sequences of HSP100 were analyzed with ExPASy ProtParam (http://www.expasy.org/tools/protparam.html) to obtain the number of amino acids, theoretical isoelectric point (pI), and molecular weight, GRAVY, instability index, and aliphatic index.

Exon/intron structures and motif organization

The HSP100 genes' exon/intron structures were visualized via Gene Structure Display Server 2.0 (http://gsds.cbi.pku.edu.cn) (Hu et al., 2015). The following parameters were used to find the conserved protein motifs of all HSP100 using the MEME program (http://meme-suite.org/tools/meme/): Twelve is the maximum number of motifs, and the lengths of the motifs range from six to fifty amino acid residues.(Bailey et al., 2009).

Phylogenetic tree construction

HSP100 proteins sequences in soybean, Brachypodium and foxtail millet were obtained from Phytozome database (v12.1) (Goodstein et al., 2012). Multiple sequence alignment of HSP100 proteins in *A. littoralis*, Arabidobsis, rice, soybean, Brachypodium and foxtail millet were performed using MUSCLE and finally the maximum likelihood (ML) phylogenetic tree were constructed using MEGA 11 (Tamura et al., 2013).

Plant material and stress condition

A. littoralis clone samples were used in this investigation. The growth chamber was set up at 25 ± 1 C, with a 16-hour light and 8-hour dark photoperiod and a photon flux density of 100 µmol m-2s-l using cool-white fluorescent light.Transferring the clone samples to a hydroponic culture that contained Hoagland's solution was performed. A stress of 600 mM sodium chloride was applied to plants that were two months old (every three days, 100 mM sodium chloride was received). Polyethylene glycol (PEG) 20% was applied for drought stress. Cold stress was applied at 4 °C. Leaf and root samples were taken at several time-points, including 0 (control), 3, 6, and 48 hours post-stress (hps), as well as one week following treatments. ABA treatment was performed at 100 µM by spraying the hormone solution on the leaves. At 0, 3, 6, 24, and 48 hps, samples of both leaves and roots were taken. The samples that were collected were kept at -80 °C until the next step.

Gene expression analysis of HSP100.3

Based on *A. littoralis* RNA-seq data containing the genes and their expression levels, expression pattern of the *HSP100* gene family was studied in leaves and root tissues, and the results are presented in the Heatmap chart plotted by Clustvis software (https://biit.cs.ut.ee/clustvis/) (Metsalu and Vilo, 2015). In this experiment, *HSP100.3* was selected for RT-qPCR analysis based on down-regulation obtained in RNA-seq data. For the RT-qPCR experiment, the RNA extraction Kit (Threezol, Riragene, Iran) was used to get the total RNA from different samples. The spectrophotometer (Biochrom WPA Biowave II, UK) and 1.2 percent agarose gel electrophoresis were used to check the concentration and integrity of the RNA samples. Subsequently, 1 µg of total DNA-free RNA was reverse transcribed to first-strand cDNA by the RevertAid First Strand cDNA Synthesis Kit (Thermo Scientific) according to the manufacturer's protocol, and the cDNA was diluted 5-fold for RT-qPCR. To avoid binding to other *AlHSP 100* family members, *HSP100.3* (forward: GCCGATTCCAGCCAGTA; reverse: ATATCTTCACAGCGTCTTCCT) *g*ene-specific primer was designed using AlleleID software

(Premiere Biosoft, CA, USA). For normalization of gene expression, *RPS3* and *UBQ* genes were applied as reference genes according to the previous studies. The minimum information for publishing of quantitative real-time PCR experiments (MIQE) guidelines were followed when conducting RT-qPCR studies (Bustin et al., 2009). Using the CFX96 real-time PCR instrument (Bio-Rad, USA) and Maxima SYBR Green Master Mix (Thermo Scientific), RT-qPCR was carried out. To summarize, the following PCR program was used to conduct each reaction in a total volume of 10 µl: 5 µl Maxima Master Mix, 2 µl diluted cDNA, 0.3 µl per primer, and 3.4 µl RNase-free water. 40 cycles of 15 seconds at 95 °C and 1 minute at 60°C. At the annealing/extension stage, data collection was done. To verify the specificity of the amplification, melting curves were generated by progressively heating the amplicon from 60 to 95 °C.There were non-template controls (NTS) added to every primer master mix. Every qPCR test was conducted with three technical replicates. The 2-ΔΔCt method is applied to measure the relative expression based on the quantification cycle (Cq) values (Livak and Schmittgen, 2001).

Results

AllHSP100 gene family identification

A total of 6 *HSP100* non-repetitive genes coding the specific protein domain of HSP100, including Clp N (PF02861) and ClpB_D2- small (PF10431), were detected in *A. littoralis* plant genome (Table 1). AlHSP100.1 and AlHSP100.2 proteins had two Clp_N domains, one AAA (PF00004) domain, one AAA_lid_9 (PF17871) domain, one AAA_2 (PF07724) and one ClpB_D2-small domain. AlHSP100.3 and AlHSP100.4 proteins concluded one AAA domain, one AAA_lid_9 domain, one AAA_2 and one ClpB_D2-small domain. AlHSP100.5 protein had one AAA_2 domain and one ClpB_D2-small. Also, AlHSP100.6 protein had two Clp_N domains (Figure 1).

Physiochemical properties of AlHSP100

Physiochemical characteristics revealed that AlHSP100 proteins had molecular weights ranging from 30.51 kDa (AlHSP70.16) to 102.38 kDa, and lengths ranging from 278 (AlHSP100.5) to 920 (AlHSP100.2) amino acids (AlHSP100.1). The isoelectric point (pI) values of given proteins tend to be acidic except AlHSP100.4 and AlHSP100.6. The gene length and CDS length changed from 914 bp to 5244 bp and from 837 to 2763, respectively. The instability index was highest for AlHSP100.6, whereas the aliphatic index and GRAVY were both highest for AlHSP100.3. The predicted subcellular localization showed that AlHSP100 proteins activated only in chloroplast and cytoplasm (Table 1).

AlHSP100 exon/intron structure

To further investigate the evolutionary relationships of the *AlHSP100* genes, exon/intron schematics of the *AlHSP100s* were generated using their genome and coding sequences. AlHSP100.5 has the fewest introns of all the *AlHSP100* genes—just one—while *AlHSP100.3* had eleven (the highest) (Figure 1).

Table 1. Physiochemical properties of the *HSP100* genes in *A. littoralis*.

Gene name	Gene ID	AC	PL	MW (kDa)	pI	GRAVY	II	AI	SL
AlHSP100.1	Alg12374	MT647608	912	102.38	6.36	-0.460	38.41	90.14	chlo: 9, mito: 3, nucl: 2
AlHSP100.2	Alg6559	MT647609	920	101.86	6.65	-0.303	46.77	94.32	chlo: 14
AlHSP100.3	Alg8703	MT647610	767	84.06	5.81	-0.179	39.07	98.93	cyto: 8, chlo: 3, nucl: 1, plas: 1, golg: 1
AlHSP100.4	Alg7596	MT647611	642	70.20	7.71	-0.193	33.18	93.91	cyto: 6, mito: 4, chlo: 1, plas: 1, pero: 1, cysk_nucl: 1
AlHSP100.5	Alg13672	MT647612	278	30.51	5.84	-0.403	39.50	87.66	chlo: 7, nucl: 4, cyto: 1, mito: 1, cysk: 1
AlHSP100.6	Alg3898	MT647613	832	89.93	7.74	-0.343	54.68	80.71	chlo: 14

A.C.: Accession number; PL: Protein length (aa); MW: Molecular weight; pI: Isoelectric point; II: Instability index; AI: Aliphatic index; SL: Subcellular localization; Chlo: chloroplast; mito: mitochondria; nucl: nucleus; plas: plasma membrane; golg: golgi apparatus; cyto: cytoplasm; pero: peroxide; cysk nucl: cytoskeleton and nucleus; cysk: cytoskeleton.

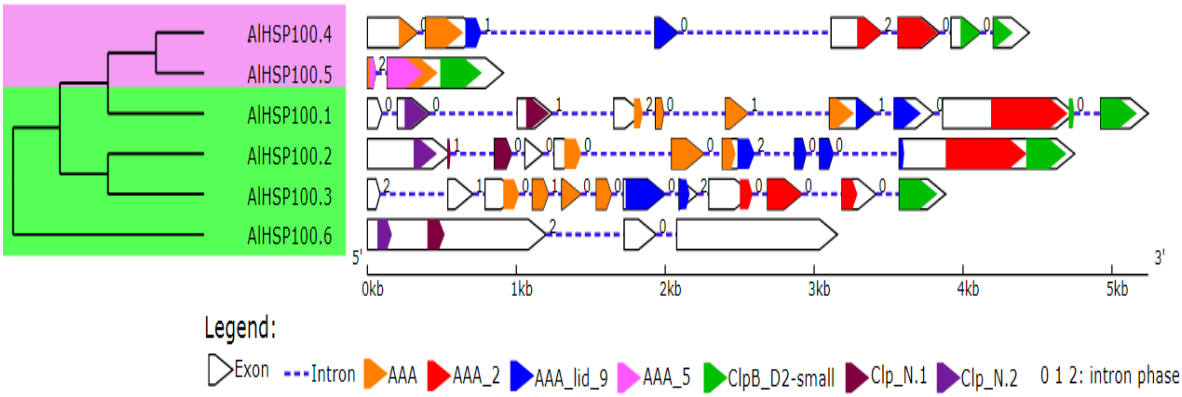

Figure 1. Analysis of *AlHSP100* gene family structures. The orange, red, blue, pink, green, brown, and purple portions denote the AAA, AAA 2, AAA lid 9, AAA 5, ClpB D2-small Clp N.1 and Clp N.2 domains, respectively. The wedges stand for exons, while the blue dashed lines represent introns. The numbers represent the AlHSP100 genes' splicing phases: 0, phase 0; 1, phase 1; and 2, phase 2.

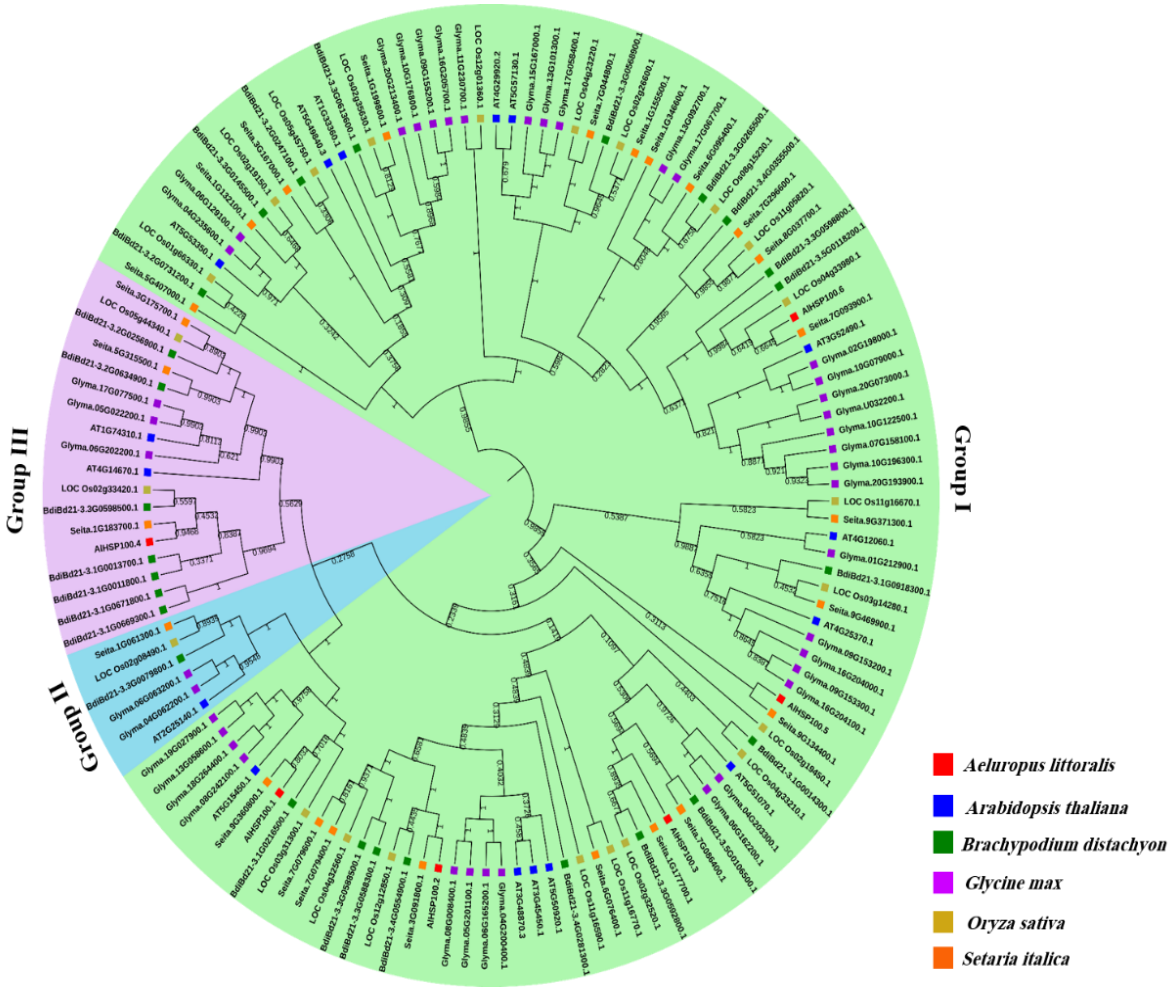

Figure 2. Members of the HSP100 family and their evolutionary relationships across six plant species. MUSCLE method was used to align HSP100 proteins from *A. littoralis*, *A. thaliana*, *Oryza sativa*, *Zea mays*, *Glycine max*, and *B. distachyon*, and MEGA 11 was used to create a phylogenetic tree using the the maximum likelihood.

AlHSP100 motif organization

To study the properties of the AlHSP100 protein sequence, the MEME program predicted 12 motifs independently. All members share a similar motif composition: 1 and 4 (Supplementary Figure 1). Furthermore, protein motifs are highly conserved and dispersed throughout all members, owing to the structural basis for their biological activity. Table 2 lists the sequences and annotations for the motifs.

Phylogenetic Analysis of AlHSP100s

We showed that the 136 HSP100 proteins of the foxtail millet, rice, soybean, *Aeluropus*, *Arabidobsis*, and *Brachypodium* species were divided into three groups by clustering (Figure 2). There were unique patterns and a little difference between *HSP100* distributions in each group. The result showed that each group had similar exon/intron structure and motif composition, while different groups had different exon/intron structure. Moreover, the same pattern was observed inside the species. Subcellular localization analysis indicated that in group I, *HSP100* are active in chloroplast, while in group II, *HSP100* genes were expressed in mitochondria. The third group included activated genes in cytoplasm (Figure 2).

Genes expression analysis

RNA-seq analysis was used to examine the expression patterns of the six *AlHSP100* genes in roots and leaves, providing additional insight into their activities. Figure 3 illustrates that the *AlHSP100.4* gene exhibited no detectable expression. While the other conditions and tissues did not show any noticeable up-regulation, there was a notable increase in expression observed for *AlHSP100.1*. The down-regulation of *AlHSP100.3* transcript level was observed in both stress and recovery conditions.

To gain a clearer understanding of how the *AlHSP100.3* gene responds to different abiotic stimuli and hormone treatments, we opted to investigate its expression in response to cold, salt, PEG, and ABA treatments**.** Although the expression level of AlHSP100.3 reduced modestly at specific time-points in leaf tissue, it remained overexpressed throughout root tissue. The study's findings showed that during salt stress, transcript levels in leaves were noticeably higher than in roots. In leaf, the greatest *AlHSP100.3* transcript level in comparison to the control was detected at the time-point of 6 hours (36.26).

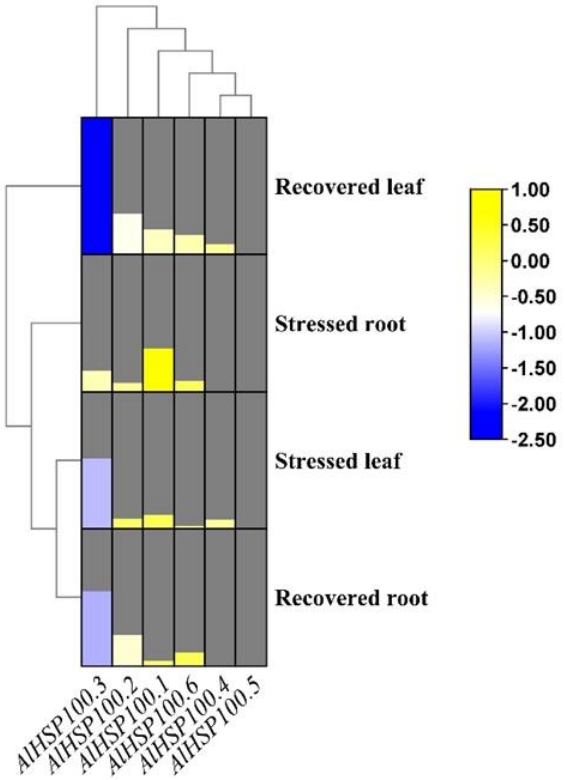

Figure 3. Expression patterns of the *AlHSP100* genes under NaCl treatment and recovery condition. Statistical significance is shown by the color gradient as the log2 fold changes. Significant up-regulation during salt stress is indicated by red, while significant down-regulation is indicated by blue.

The same results were achieved in roots (Figure 4). In drought stress, the lowest *AlHSP100.3* transcript level of leaf was at 1 wps (-3.69) while the highest transcription level was at 48 hps (19.81). The changes of *AlHSP100.3* in roots indicated that the highest transcription level in stressed plant occurred at 48 hps (10.10) compare to the control (Figure 4). The increasing changes of *AlHSP100.3* transcript level was observed in roots in cold stress and the highest amount was at 1 wps (1.60).

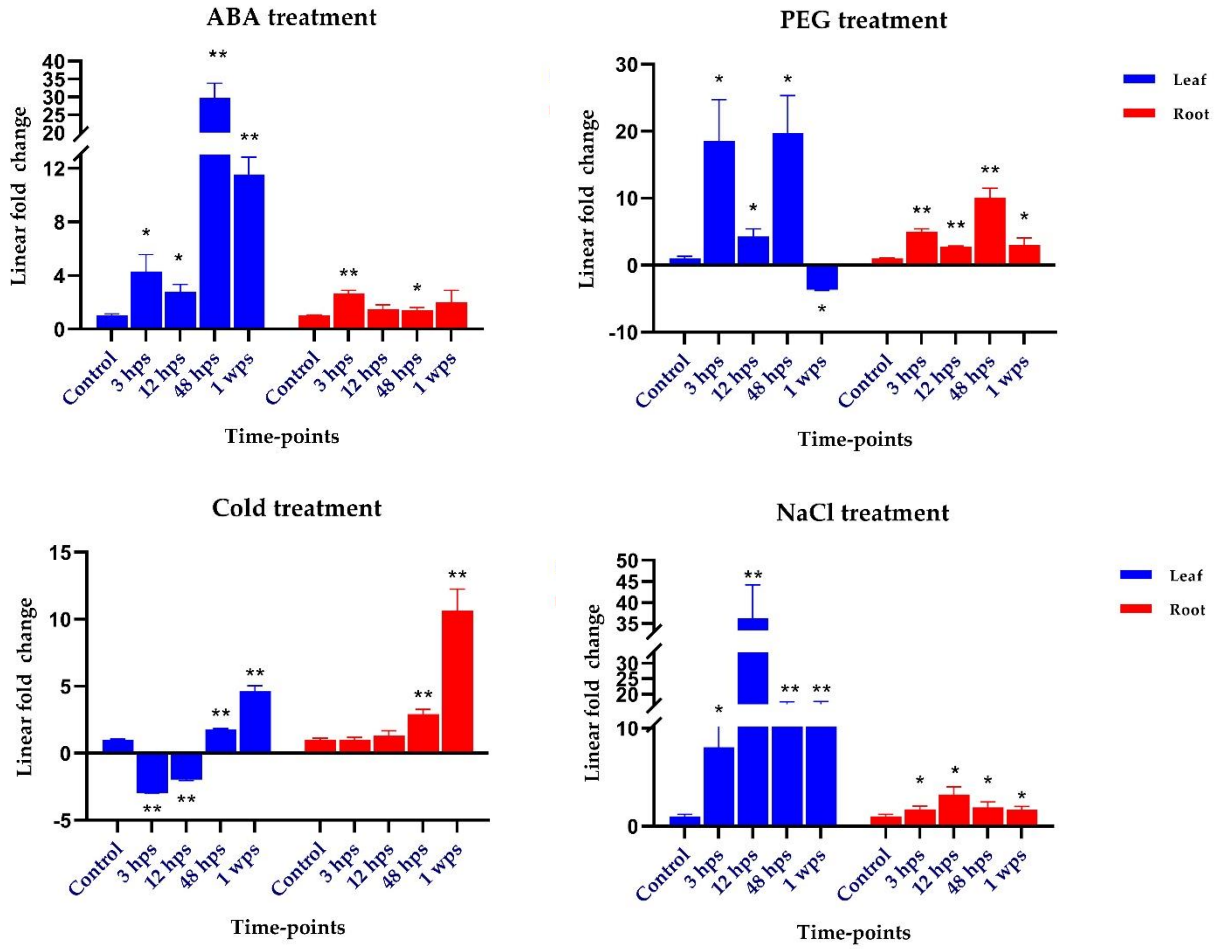

Figure 4. Expression patterns of *AlHSP100.3* gene under abiotic stresses treatments. RT-qPCR was performed to examine the expression profiles of the AlHSP100.3 gene under salt, PEG, ABA, and cold stress. The *RPS3* and *UBQ* genes were applied as reference genes. Error bars were calculated using three technical replicates. Asterisks indicate genes that were significantly up- or down-regulated in response to abiotic stress (* P < 0:05, ** P < 0:01).

At 3 and 6 hps, it was down-regulated in leaf and then increased up to 1 wps (4.62). The transcript level of *AlHSP100.3* in leaf tended to increase from initional point to 24 hps under ABA treatment. The highest and the lowest expression pattern were observed at 3 hps and control, respectively (Figure 4).

Discussion

As molecular chaperones, HSPs play important functions in the growth and development of plants and also provide protection to plant cells when they are under stress (Waters, 2013; Park and Seo, 2015). The HSPs biological function has been studied in wheat (Muthusamy et al., 2017), rice (Ouyang et al., 2009), and Arabidopsis (Lin et al., 2001). This study looked at the *HSP100* gene family in *A. littoralis* on a whole genome level. Six HSP100 genes were identified in the *A. littoralis* plant, which aligns with the findings reported for *Arabidopsis*, which have sixteen HSP100 genes (Goodstein et al., 2012).

The subcellular localizations of HSPs are believed to be tightly linked to their evolutionary relationships.

Isoforms of HSP100 proteins were further classified according to their subcellular localization as chloroplastic, mitochondrial, or cytoplasmic. Subfamilies are commonly designated based on the specific protein localization within each group (Scharf et al., 2001; Sarkar et al., 2009). The same classification was carried out by Singh et al. (Singh et al., 2010). HSP proteins are found in many forms inside plants, each of which is localized in a distinct cellular compartment—the cytoplasm/nucleus, chloroplasts, or mitochondria (Mishra and Grover, 2016). On the other hand, HSP proteins engage in biological processes in numerous subcellular localizations (Razzaq et al., 2023).

Phylogenetic analysis using *Aeluropus* species, *Arabidobsis*, rice, soybean, *Brachypodium* and foxtail millet sequences showed that HSP100 sequences are significantly conserved. The same result of conserved sequences was observed in the reseach of Singh et al (Singh et al., 2010). The tree displayed three main clusters, with each cluster representing a distinct pattern. It is possible that HSP100 proteins play a pivotal role in various cellular contexts due to their distribution to various organelles (Singh et al., 2010).

The importance of genomic organization in the evolutionary interactions of gene families under stress situations has been shown in previous studies (Xu et al., 2012; Chen et al., 2018; Hashemipetroudi et al., 2022). Based on our findings, gene structures shed insight into evolutionary relationships; for example, we found that the structures of the most closely related *HSP100* genes in the same family are quite similar. Additionally, organelle-specific (chloroplast) *HSP100* have more introns, whereas cytoplasmic *HSP100* genes generally have few introns, similar to the *HSP* genes in other plants. The close correlation between intron pattern and protein localization is demonstrated by this finding (Banilas et al., 2012; Guo et al., 2015). In addition, there exist findings that genes, which must be activated in response to stress fast, tend to have decreased intron density during evolution (Guo et al., 2015). The duration of the editing process of primary mRNAs could be affected by intron numbers (Heidari et al., 2023).

Alternative splicing events are possible lead to variations in intron/exon structures within the various AlHSP100 gene families, which may cause an increase in the diversity of gene functions (Panzade et al., 2021).

Within the AlHSP100 family, there was a great deal of variation in the 12 conserved motifs. Proteins belonging to the same subfamily (AlHSP100.1-4) and proteins belonging to distinct subfamilies (AlHSP100.5-6) had similar types, orders, and numbers of motifs. The most conserved protein motifs among HSP100 members are 1 and 4. These motifs may serve as the structural basis for HSP100's biological function (Chen et al., 2018).

We found that the *HSP100.3* genes exhibit distinct responses to different stimuli, indicating a diversity of stress response pathways in *A. littoralis*. Numerous investigations have demonstrated the involvement of the *HSP100/ClpB* genes in the growth, development, and stress response of plants. According to Hu et al. (2009b), heat shock and drought stress stimulate *OsHSP100/ClpB-C* expression in rice, but dehydration and ABA treatment induce *the ClpB-C* ortologous gene expression in wheat (Campbell et al., 2001). In Wu et al. (2009) expriments, the role of HSP100 cis-acting elements to influence desiccation tolerance in rice was disscuased. To detect promoter activity, Singh et al. (Singh et al., 2012) analyzed tissue-specific pattern of rice *ClpB-C* gene by using promoter: GUS reporter system, and shown that *OsClpB-C* gene has higher expression in grain development compare to anther, style and ovary tissues. Despite the complexity and diversity of *HSP100* expression patterns, our data demonstrated that *HSP100.3* was up-regulated in response to salt, drought, cold, and ABA treatment.

Conclusion

Due to climate change and global warming, there is an urgent need to develop transgenic plants with enhanced ability to withstand adverse environmental conditions. In the current study, six members of the *HSP100* gene family were identified in the halophyte Poaceae, *A. littoralis*, using a bioinformatic approach. Subsequently, we investigated the expression of the *AlHSP100.3* gene in response to cold, salt, PEG, and ABA treatments. The induction of the *HSP100.3* gene in response to salt, osmotic, and cold stress suggests its potential contribution to enhanced tolerance to stressful conditions. The presence of stress-dependent

regulation of the *HSP100.3* gene, as evidenced by its early response (3 hps) to PEG treatment and its late response to cold stress, is likely associated with the presence of cis-regulatory elements located upstream of this gene.

Supplementary Materials

The supplementary material for this article can be found online at: https://www.jpmb-gabit.ir/article_712459.html.

Supplementary Figure 1. Distribution of conserved motifs of *HSP100* in *A. littoralis*.

Supplementary Table 1. The motif sequence, length and annotation in *AlHSP100*.

Author Contributions

Conceptualization, S.H.H.; software, S.H.H. and S.M.; formal analysis, S.H.H. and S.M.; investigation, F.F. and S.M.; writing—original draft preparation, S.H.H. and F.F.; writing—review and editing, S.H.H.; All authors have read and agreed to the published version of the manuscript.

Funding

This research received no external funding.

Acknowledgments

This research is supported by the Genetics and Agricultural Biotechnology Institute of Tabarestan (GABIT) and Sari Agricultural Sciences and Natural Resources University (SANRU). The authors also gratefully acknowledge use of the services and facilities of the GABIT during this research.

Conflicts of Interest Statements

The authors declare no conflict of interest.

References

Agarwal, M., Katiyar-Agarwal, S., Sahi, C., Gallie, D.R., and Grover, A. (2001). *Arabidopsis thaliana* Hsp100 proteins: kith and kin. *Cell Stress Chaperon* 6(3): 219-224. doi: 10.1379/1466-1268(2001)006<0219:athpka>2.0.co;2.

Bailey, T.L., Boden, M., Buske, F.A., Frith, M., Grant, C.E., Clementi, L., Ren, J., Li, W.W., and Noble, W.S. (2009). MEME SUITE: tools for motif discovery and searching. *Nucleic Acids Res* 37(Web Server issue): W202-208. doi: 10.1093/nar/gkp335.

Banilas, G., Korkas, E., Englezos, V., Nisiotou, A., and Hatzopoulos, P. (2012). Genome‐wide analysis of the heat shock protein 90 gene family in grapevine (*Vitis vinifera* L.). *Aust J Grape Wine Res* 18(1): 29-38.

Bita, C., and Gerats, T. (2013). Plant tolerance to high temperature in a changing environment: scientific fundamentals and production of heat stress-tolerant crops. *Front Plant Sci* 4: 273.

Bustin, S.A., Benes, V., Garson, J.A., Hellemans, J., Huggett, J., Kubista, M., Mueller, R., Nolan, T., Pfaffl, M.W., Shipley, G.L., Vandesompele, J., and Wittwer, C.T. (2009). The MIQE guidelines: minimum information for publication of quantitative real-time PCR experiments. *Clin Chem* 55(4): 611-622. doi: 10.1373/clinchem.2008.112797.

Campbell, J.L., Klueva, N.Y., Zheng, H.G., Nieto-Sotelo, J., Ho, T.D., and Nguyen, H.T. (2001). Cloning of new members of heat shock protein *HSP101* gene family in wheat (*Triticum aestivum* (L.) Moench) inducible by heat, dehydration, and ABA(1). *Biochim Biophys Acta* 1517(2): 270-277. doi: 10.1016/s0167-4781(00)00292-x.

Carr, T., Wang, Y., Huang, Z., Yeakley, J.M., Fan, J.-B., and Whitham, S.A. (2006). Tobamovirus infection is independent of *HSP101* mRNA induction and protein expression. *Virus Res* 121(1): 33-41.

Chen, J., Gao, T., Wan, S., Zhang, Y., Yang, J., Yu, Y., and Wang, W. (2018). Genome-Wide Identification, Classification and Expression Analysis of the HSP Gene Superfamily in Tea Plant (*Camellia sinensis*). *Int J Mol Sci* 19(9): 2633. doi: 10.3390/ijms19092633.

Esmaeili Tazangi, S., Niazi, A., Ghaffari, M.R., Alemzadeh, A., and Tahmasebi, A. (2022). Identification of drought stress-responsive long non-coding RNAs (lncRNAs) in root tip region of rice (*Oryza sativa*). *J Plant Mol Breed* 10(2): 31-45. doi: 10.22058/jpmb.2023.2007831.1280.

Finn, R.D., Coggill, P., Eberhardt, R.Y., Eddy, S.R., Mistry, J., Mitchell, A.L., Potter, S.C., Punta, M., Qureshi, M., Sangrador-Vegas, A., Salazar, G.A., Tate, J., and Bateman, A. (2016). The Pfam protein families

database: towards a more sustainable future. *Nucleic Acids Res* 44(D1): D279-285. doi: 10.1093/nar/gkv1344.

Gong, C., Pang, Q., Li, Z., Li, Z., Chen, R., Sun, G., and Sun, B. (2021). Genome-wide identification and characterization of *Hsf* and *Hsp* gene families and gene expression analysis under heat stress in eggplant (*Solanum melongema* L.). *Horticulturae* 7(6): 149.

Goodstein, D.M., Shu, S., Howson, R., Neupane, R., Hayes, R.D., Fazo, J., Mitros, T., Dirks, W., Hellsten, U., Putnam, N., and Rokhsar, D.S. (2012). Phytozome: a comparative platform for green plant genomics. *Nucleic Acids Res* 40(Database issue): D1178-1186. doi: 10.1093/nar/gkr944.

Guo, M., Liu, J.H., Lu, J.P., Zhai, Y.F., Wang, H., Gong, Z.H., Wang, S.B., and Lu, M.H. (2015). Genome-wide analysis of the *CaHsp20* gene family in pepper: comprehensive sequence and expression profile analysis under heat stress. *Front Plant Sci* 6: 806. doi: 10.3389/fpls.2015.00806.

Hall, T.A. (1999). BioEdit: a user-friendly biological sequence alignment editor and analysis program for Windows 95/98/NT. *Nucleic Acids Symp Ser* 41: 95-98.

Hashemi-Petroudi, S.H., Arab, M., Dolatabadi, B., Kuo, Y.-T., Baez, M.A., Himmelbach, A., Nematzadeh, G., Maibody, S.A.M.M., Schmutzer, T., and Mälzer, M. (2022). Initial description of the Genome of *Aeluropus littoralis*, a halophile grass. *Front Plant Sci* 13: 906462.

Hashemi, S.H., Nematzadeh, G., Ahmadian, G., Yamchi, A., and Kuhlmann, M. (2016). Identification and validation of *Aeluropus littoralis* reference genes for Quantitative Real-Time PCR Normalization. *J Biol Res (Thessalon)* 23(1): 18. doi: 10.1186/s40709-016-0053-8.

Hashemipetroudi, S., Ghorbani, H., Sohrevardi, F., and Arab, M. (2022). Identification and comprehensive analyses of the *CBL* gene families in sweet orange (*Citrus sinensis* L.). *J Plant Mol Breed* 10(2): 76-91. doi: 10.22058/jpmb.2024.555361.1257.

Heidari, P., Sabari, B., and Seifi, A. (2023). Magnesium transporter family: sequence, evolution and expression analysis in soybean (*Glycine max* L.). *J Plant Mol Breed* 11(1): 62-73. doi: 10.22058/jpmb.2024.2020070.1287.

Horton, P., Park, K.J., Obayashi, T., Fujita, N., Harada, H., Adams-Collier, C.J., and Nakai, K. (2007). WoLF PSORT: protein localization predictor. *Nucleic Acids Res* 35(Web Server issue): W585-587. doi: 10.1093/nar/gkm259.

Hu, B., Jin, J., Guo, A.Y., Zhang, H., Luo, J., and Gao, G. (2015). GSDS 2.0: an upgraded gene feature visualization server. *Bioinformatics* 31(8): 1296-1297. doi: 10.1093/bioinformatics/btu817.

Hu, C., Yang, J., Qi, Z., Wu, H., Wang, B., Zou, F., Mei, H., Liu, J., Wang, W., and Liu, Q. (2022). Heat shock proteins: Biological functions, pathological roles, and therapeutic opportunities. *Med Comm* 3(3): e161.

Hu, W., Hu, G., and Han, B. (2009a). Genome-wide survey and expression profiling of heat shock proteins and heat shock factors revealed overlapped and stress specific response under abiotic stresses in rice. *Plant Sci* 176(4): 583-590.

Hu, W., Hu, G., and Han, B. (2009b). Genome-wide survey and expression profiling of heat shock proteins and heat shock factors revealed overlapped and stress specific response under abiotic stresses in rice. *Plant Sci* 176(4): 583-590. doi: 10.1016/j.plantsci.2009.01.016.

Jones, P., Binns, D., Chang, H.Y., Fraser, M., Li, W., McAnulla, C., McWilliam, H., Maslen, J., Mitchell, A., Nuka, G., Pesseat, S., Quinn, A.F., Sangrador-Vegas, A., Scheremetjew, M., Yong, S.Y., Lopez, R., and Hunter, S. (2014). InterProScan 5: genome-scale protein function classification. *Bioinformatics* 30(9): 1236-1240. doi: 10.1093/bioinformatics/btu031.

Kedzierska-Mieszkowska, S., and Arent, Z. (2020). AAA+ Molecular Chaperone *ClpB* in Leptospira interrogans: Its Role and Significance in Leptospiral Virulence and Pathogenesis of Leptospirosis. *Int J Mol Sci* 21(18): 6645. doi: 10.3390/ijms21186645.

Lee, U., Rioflorido, I., Hong, S.W., Larkindale, J., Waters, E.R., and Vierling, E. (2007). The *Arabidopsis* ClpB/Hsp100 family of proteins: chaperones for stress and chloroplast development. *Plant J* 49(1): 115-127. doi: 10.1111/j.1365-313X.2006.02940.x.

Letunic, I., Doerks, T., and Bork, P. (2015). SMART: recent updates, new developments and status in 2015. *Nucleic Acids Res* 43(Database issue): D257-260. doi: 10.1093/nar/gku949.

Lin, B.L., Wang, J.S., Liu, H.C., Chen, R.W., Meyer, Y., Barakat, A., and Delseny, M. (2001). Genomic analysis of the Hsp70 superfamily in *Arabidopsis thaliana*. *Cell Stress Chaperon* 6(3): 201-208. doi: 10.1379/1466-1268(2001)006<0201:gaoths>2.0.co;2.

Livak, K.J., and Schmittgen, T.D. (2001). Analysis of relative gene expression data using real-time quantitative PCR and the 2− ΔΔCT method. *Methods* 25(4): 402-408.

Metsalu, T., and Vilo, J. (2015). ClustVis: a web tool for visualizing clustering of multivariate data using Principal Component Analysis and heatmap. *Nucleic Acids Res* 43(W1): W566-570. doi: 10.1093/nar/gkv468.

Mishra, R.C., and Grover, A. (2016). ClpB/Hsp100 proteins and heat stress tolerance in plants. *Crit Rev Biotechnol* 36(5): 862-874. doi: 10.3109/07388551.2015.1051942.

Muthusamy, S.K., Dalal, M., Chinnusamy, V., and Bansal, K.C. (2017). Genome-wide identification and analysis of biotic and abiotic stress regulation of small heat shock protein (*HSP20*) family genes in bread wheat. *J Plant Physiol* 211: 100-113. doi: 10.1016/j.jplph.2017.01.004.

Ouyang, Y., Chen, J., Xie, W., Wang, L., and Zhang, Q. (2009). Comprehensive sequence and expression profile analysis of *Hsp20* gene family in rice. *Plant Mol Biol* 70(3): 341-357. doi: 10.1007/s11103-009-9477-y.

Panzade, K.P., Kale, S.S., Chavan, N.R., and Hatzade, B. (2021). Genome-wide analysis of *Hsp70* and *Hsp100* gene families in *Ziziphus jujuba*. *Cell Stress Chaperon* 26(2): 341-353.

Park, C.J., and Seo, Y.S. (2015). Heat Shock Proteins: A Review of the Molecular Chaperones for Plant Immunity. *Plant Pathol J* 31(4): 323-333. doi: 10.5423/PPJ.RW.08.2015.0150.

Razzaq, M.K., Rani, R., Xing, G., Xu, Y., Raza, G., Aleem, M., Iqbal, S., Arif, M., Mukhtar, Z., and Nguyen, H.T. (2023). Genome-Wide Identification and Analysis of the *Hsp40*/J-Protein Family Reveals Its Role in Soybean (*Glycine max*) Growth and Development. *Genes* 14(6): 1254.

Sarkar, N.K., Kim, Y.K., and Grover, A. (2009). Rice sHsp genes: genomic organization and expression profiling under stress and development. *BMC Genomics* 10(1): 393. doi: 10.1186/1471-2164-10-393.

Scharf, K.D., Siddique, M., and Vierling, E. (2001). The expanding family of *Arabidopsis thaliana* small heat stress proteins and a new family of proteins containing alpha-crystallin domains (Acd proteins). *Cell Stress Chaperon* 6(3): 225-237. doi: 10.1379/1466-1268(2001)006<0225:tefoat>2.0.co;2.

Singh, A., Mittal, D., Lavania, D., Agarwal, M., Mishra, R.C., and Grover, A. (2012). OsHsfA2c and OsHsfB4b are involved in the transcriptional regulation of cytoplasmic *OsClpB* (*Hsp100*) gene in rice (*Oryza sativa* L.). *Cell Stress Chaperon* 17(2): 243-254. doi: 10.1007/s12192-011-0303-5.

Singh, A., Singh, U., Mittal, D., and Grover, A. (2010). Genome-wide analysis of rice *ClpB/HSP100*, *ClpC* and *ClpD* genes. *BMC Genomics* 11(1): 95. doi: 10.1186/1471-2164-11-95.

Tamura, K., Stecher, G., Peterson, D., Filipski, A., and Kumar, S. (2013). MEGA6: Molecular Evolutionary Genetics Analysis version 6.0. *Mol Biol Evol* 30(12): 2725-2729. doi: 10.1093/molbev/mst197.

Waters, E.R. (2013). The evolution, function, structure, and expression of the plant sHSPs. *J Exp Bot* 64(2): 391-403. doi: 10.1093/jxb/ers355.

Wu, X., Shiroto, Y., Kishitani, S., Ito, Y., and Toriyama, K. (2009). Enhanced heat and drought tolerance in transgenic rice seedlings overexpressing *OsWRKY11* under the control of HSP101 promoter. *Plant Cell Rep* 28(1): 21-30. doi: 10.1007/s00299-008-0614-x.

Xu, G., Guo, C., Shan, H., and Kong, H. (2012). Divergence of duplicate genes in exon-intron structure. *Proc Natl Acad Sci USA* 109(4): 1187-1192. doi: 10.1073/pnas.1109047109.

JPMB
Journal of Plant Molecular Breeding
Published by Genetics and Agricultural Biotechnology Institute of Tabarestan
2023 | Volume 11 | Issue 2

مقاله پژوهشی

شناسایی و آنالیز بیان خانواده ژنی *HSP100* در *Aeluropus littoralis*

سیدحمیدرضا هاشمی‌پطرودی[1*]، سمیرا محمدی[1]، فرزانه فاطمی[2]

[1] پژوهشکده ژنتیک و زیست فناوری کشاورزی طبرستان، دانشگاه علوم کشاورزی و منابع طبیعی ساری، ساری ایران

[2] گروه زراعت و اصلاح نباتات، دانشکده کشاورزی، دانشگاه بوعلی سینا، همدان، ایران

چکیده: پروتئین های شوک حرارتی (HSPs)، بعنوان چپرون‌های مولکولی با فعالیت های متنوع، برای رشد و نمو و پاسخ‌های به تنش‌ها ضروری هستند. به‌نژادگران گیاهی برای مقاوم ساختن گیاهان زراعی به شوری و خشک، استفاده از گیاهان هالوفیتی را مد نظر قرار داده‌اند. *Aeluropus littoralis*، بعنوان یک هالوفیت تک‌لپه علفی، یکی از گونه‌های مدل بالقوه برای کشف ژن‌های جدید پاسخ به تنش می‌باشد. در اینجا، ساختار اگزون/اینترون، موتیف‌ها/دامنه‌های حفاظت‌شده و الگوهای بیانی خانواده ژن *HSP100* در ژنوم *A. littoralis* شناسایی شد. در این مطالعه شش ژن منحصر به فرد *AlHSP100* غیر تکراری شناسایی شده که تغییرات ساختاری و فیزیکوشیمیایی قابل توجهی در بین زیرخانواده‌ها مشاهده شد. آنالیزهای فیلوژنتیک و موتیف نشان داد که پروتئین‌های یک زیرخانواده (AlHSP100.1-4) و پروتئین‌های سایر زیرخانواده‌ها (AlHSP100.5-6) دارای انواع، ترتیب و مقادیر مشابهی از موتیف هستند. در نهایت، بیان ژن *AlHSP100.3* با استفاده از RT-qPCR تحت تیمارهای دهیدراتاسیون، نمک، سرما و فیتوهورمون اسید آبسیزیک مورد تجزیه و تحلیل قرار گرفت و نشان داد که الگوهای بیان آنها در پاسخ به تنش‌های غیرزیستی متفاوت است. وجود تنظیم وابسته به تنش ژن *HSP100.3*، همانطور که توسط پاسخ اولیه به تیمار PEG و پاسخ دیرهنگام به تنش سرما مشهود است، احتمالاً با عناصر تنظیم‌کننده سیس واقع در بالادست این ژن مرتبط است. این مطالعه اطلاعات ارزشمندتری در خصوص درک پاسخ‌های تنش غیرزیستی توسط ژن‌های *HSP100* در *A. littoralis* فراهم می‌کند.

کلمات کلیدی: تنش غیر زنده، بیان ژن، هالوفیت، پروتئین‌های شوک حرارتی (HSPs)، تجزیه و تحلیل رونوشت.

ویراستار علمی
دکتر جونهوا پنگ،
مدیرتکنولوژی شرکت اگری‌ساینس اسپرینگ ولی، چین

تاریخ
دریافت: ۱۳ بهمن ۱۴۰۲
پذیرش: ۲۵ فروردین ۱۴۰۳
چاپ: ۱۷ اردیبهشت ۱۴۰۳

نویسنده مسئول
دکتر سیدحمیدرضا هاشمی‌پطرودی
shr.hashemi@sanru.ac.ir;
irahamidreza@yahoo.com

ارجاع به این مقاله
Hashemipetroudi, S.H., Mohammadi, S., Fatemi, F. (2023). Identification of *HSP100* gene family in *Aeluropus littoralis*. *J Plant Mol Breed* 11(2): 66-77.
doi: 10.22058/JPMB.2024.2023541.1294.

JPMB | Journal of Plant Molecular Breeding
Published by Genetics and Agricultural Biotechnology Institute of Tabarestan
2023 | Volume 11 | Issue 2

Association of SSR markers for primary branches in *Brassica juncea* L.

Manpreet Kour*, Lalita Kumari, Supriya Sharma

Sher-e-Kashmir University of Agricultural Sciences & Technology of Jammu, J&K (Jammu & Kashmir), India

Original paper

OPEN ACCESS

Edited by

Dr. Ali Dehestani,
Genetics and Agricultural Biotechnology Institute of Tabarestan (GABIT), Sari Agricultural Sciences and Natural Resources University (SANRU), Iran

Date

Received: 3 March 2024
Accepted: 8 April 2024
Published: 7 May 2024

Correspondence

Dr. Manpreet Kour
mkour5941@gmail.com

Citation

Kour, M., Kumari, L., and Sharma, S. (2023). Association of SSR Markers for primary branches in *Brassica Juncea* L. *J. Plant Mol. Breed* 11(2): 78-93.
doi: 10.22058/JPMB.2024.2024234.1296.

Abstract: The study utilized $F_{2:5}$ lines derived from a cross between Kafiav N Zagora and Pusa Karishma cultivars to tag genomic regions controlling primary branches in *Brassica juncea*. One hundred and thirty $F_{2:5}$ plants were used to characterize primary branch numbers, resulting in two pools of 12 genotypes for high (HPB) and low (LPB) branches. The average number of primary branches for HPB and LPB were 12.16 and 4.50, respectively. A set of 148 SSR (Simple Sequence Repeats) markers was used for parental polymorphism screening from which 14 polymorphic SSRs were used for molecular characterization of HPB and LPB bulks, tagging genomic regions. The allelic data scored for 14 polymorphic lines was tested using Student's *t*-test analysis to understand relationships for primary branches with SSR markers and amplified alleles. Based on this, two B-genome markers (Ni2-C12 and Ni2-A11) were discovered to be strongly linked to the number of primary branches. Bioinformatic analysis located these two markers within a 9 Mb region on chromosome B5 of *B. juncea*. Utilising $F_{2:5}$ lines of an inter-gene pool genetic cross, the current study was able to locate the loci regulating the number of primary branches on *B. juncea*'s sub-genome chromosome B5. Before proceeding with fine-mapping investigations to dissect the genomic region (between 55.9 and 64.9 Mb) of sub-genome chromosome B5, it is imperative to emphasize the necessity of verifying these results across diverse genetic backgrounds.

Keywords: *Brassica juncea*, primary branch number, BSA, SSR.

Introduction

Brassica juncea L. (Indian Mustard) is an annual herb belonging to an economically important plant family of angiosperms called *Brassicaceae* (formerly Cruciferae). This annual plant is an amphidiploid (AABB, 2n=4x=36) as it is the product of spontaneous hybridization between *Brassica nigra* (BB, 2n=16) and *Brassica rapa* (AA, 2n=20), (Axelsson et al., 2000). Two major gene pools of *B. juncea*, the Indian and the East European gene pool, contrast significantly for major agronomic traits such as oil content, branch number, yield, plant height, and pod size. Therefore, the main goal of *B. juncea* breeders is to transmit desired inheritable traits from one gene pool to another (Pradhan et al., 1993). *B. juncea* is mainly cultivated for its seed oil, which is widely consumed in South Asian countries like India, Bangladesh, Nepal, and Pakistan. India is the third largest producer of rapeseed mustard in the world, with 9.98% of the total area under cultivation coming from *B. juncea, B. rapa, and B. napus*. India makes up roughly 11.27% and 19.29% of the world's total mustard-producing area and yield, respectively (Kumar, 2016). Rapeseed-mustard, the second most significant edible oilseed crop in India, contributes 27.8% to the economy, with over 80% production from *B. juncea*, making it an essential industry element (Singh et al., 2013). The Jammu division of J&K state farmed 28000 ha of rapeseed-mustard, yielding over 800 kg ha^{-1} and producing 3188.32 quintals in 2021-2022 (Digest of Statistics 2020–21, J&K).

India's oilseed production increased by 43% between 2015-16 and 2020-21, but production hasn't kept up with demand as there's a shift towards processed foods, leading to increased vegetable oil imports. India's per capita vegetable oil consumption is projected to rise by 2.6% annually by 2030, necessitating a 3.4% annual import growth (Economic Survey, 2021-22). Per capita consumption of edible oil is predicted to rise from 13.4 kg to 23-43 kg by 2030 (Singh et al., 2017). Therefore, in order to meet the growing demands, seed output must be increased.

Oil yield can be raised by increasing the seed output (Chen and Heneen, 1992). Hence, it is necessary to accelerate *B. juncea*'s seed yield potential to meet the current oil yield requirements. The final seed yield is influenced by various factors such as the number of branches, siliques, seeds, and seed size (Snowdon, 2007). Branching in *B. napus* significantly influences seed output, with a positive correlation between grain yield and primary branches bearing siliqua. Factors like branch number, siliqua length, and phenotypic and genotypic levels are positively associated. The most important direct factors influencing seed yield are plant height, the number of siliquae per plant, and the number of primary and secondary branches per plant (Tiwari, 2019).

The seed output of the Indian mustard is closely associated with the number of primary branches on the main axis as primary and secondary branches on the main stalk, bear seed-bearing silique (Ramanujam and Rai, 1963; Singh and Singh, 1972). Thus, it is ideal to have more primary branches in order to produce more seeds. Therefore, it would be beneficial to be able to genetically modify branching in *Brassica* species to increase seed yield. For this, we must have a sufficient understanding of the genetic control of primary branches in *Brassica* species. Therefore, in order to use genotypes in breeding programmes in an efficient manner, a greater comprehension of this topic is required. The identification and mapping of QTLs in several *Brassica* species has been the focus of research efforts in recent years. Prior research on markers linked to branching, more precisely, the number of primary branches, has been reported for *B. juncea*, although not as much as for other *Brassica* species, such as *B. napus*. It is necessary to have markers that are closely linked to the target locus in order to apply MAS (Marker Assisted Selection) to a large number of samples and diverse crossings in various breeding programmes. Therefore, using a gene-tagging method known as bulk segregant analysis, the current work seeks to identify markers/genomic areas related to the number of primary branches in *B. juncea*.

Bulked Segregant Analysis (BSA) is a method for identifying markers associated with specific genes or genomic regions linked to phenotypic responses. It involves comparing DNA samples from segregating populations and assaying the bulks contrasting for a specific trait. Polymorphic markers are linked genetically to the locus associated with the trait used to create the bulk (Michelmore et al., 1991). Polymorphic molecular markers, closely

linked to major QTLs regulating a trait, co-segregate with the QTL, causing significant variation in the frequency of marker alleles within extreme groups. Chromosome location of these markers can be determined without genotyping every individual in the segregating population. The concept behind BSA is to capture representative genotypes at a specific locus while generating a random genetic background at unlinked loci (Michelmore et al., 1991). Selective genotyping offers a significant advantage over traditional QTL analysis by reducing the number of individuals analyzed, saving time and money by focusing on severe traits, and enabling the monitoring of gene behavior at specific gene loci through advancements in molecular marker techniques.

The goal of the current study was to find genomic areas or markers related to *B. juncea*'s primary branch number. A combination of BSA and molecular analysis using PCR-based molecular markers, or SSRs, was used to identify markers linked to the number of primary branches in *B. juncea*. The current study's findings will be applied to fine mapping and then MAS. Main research questions for this study:

- What is the utility of the segregating mapping population ($F_{2:5}$) in examining the genetics of the number of main branches?
- Is the segregating population diverse enough to support genomics and genetics research?
- To what extent would bulks (derived from morphological data) be pertinent to the desired trait?

Considering the aforementioned, the current study was carried out in *B. juncea* with the following goals:

1. Morphological characterisation of $F_{2:5}$ lines for primary branches to develop pools with extreme phenotypes for Bulk Segregant Analysis (BSA)
2. Molecular marker-based BSA of $F_{2:5}$ lines for primary branches.

Materials and Methods

Plant material

130 $F_{2:5}$ plants (representing 83 progenies) of a cross between Kafiav N Zagora (east European type from Bulgaria) and Pusa Karishma (Indian type, developed by IARI, New Delhi), which were significantly contrasting for major agronomic traits (Table 1), were assessed for this study. These two genotypes were used as parents for making genetic cross. Single seed descent method was used to establish the $F_{2:5}$ population, with plants chosen randomly for the following year, with no selection from F_2 onward.

Phenotyping and genotyping of the parents

Based on the previous years' data provided, it was found that the number of primary branches vary significantly for both the parents. Both Kafiav N Zagora and Pusa Karishma were having average primary branch count of 18.67 and 7.20, respectively. Genotyping of the parents of the mapping population was carried out by employing 148 arbitrarily selected SSR primers; out of which 73 belong to A genome (*B. rapa*) while 75 markers were from B genome (*B. nigra*).

Table 1. Table showing contrasting characters of the parents of the cross.

Trait	Kafiav N Zagora	Pusa Karishma
Plant height (cm)	262.77	156.62
Main shoot length (cm)	14.03	49.14
Siliqua number	26.50	35.20
Number of primary branches	18.67	7.20
Number of secondary branches	46.67	18.80
Siliqua length (cm)	2.57	4.00

Sowing of experimental material

$F_{2:5}$ lines from a genetic cross of Kafia N Zagora x Pusa Karishma were planted in a single 2-meter row, in the School of Biotechnology's experimental field at SKUAST-Jammu.

Morphological characterization and bulk formation

The number of primary branches on the main stalk of the $F_{2:5}$ segregating population, which was derived from a genetic cross between Kafia N Zagora and Pusa Karishma, was counted. First, 83 plant progenies with a high or low number of primary branches were chosen. Out of the 83 progenies, at least one plant was chosen for further analysis (selective genotyping) . Two bulks with extreme phenotype (number of primary branches), were formed by grouping together the lines with almost identical numbers of branches. Only plants with 10 or more primary branches were chosen for high primary branches. In a similar vein, plants with five primary branches or fewer were chosen for low primary branches. It was made sure that no two plants were chosen for bulk creation from the same offspring.

DNA extraction

Genomic DNA was isolated from young leaves by CTAB method of plant DNA extraction.

Molecular analysis

The initial marker polymorphism was identified by screening the parental genotypes. For further analysis of the $F_{2:5}$ lines, the markers that were polymorphic on the parents were utilised. SSR PCR profile used is given in Supplementary Table 1.

Results

Morphological analysis for primary branches

130 plants, representing 83 $F_{2:5}$ plant progenies, were used to score the primary branch numbers in the $F_{2:5}$ population. These 130 plants have varying numbers of primary branches, ranging from 2 (Block 1, line 22) to fifteen (Block 2, line 6), as depicted in Figure 1. Most plant progenies appear to have an approximately similar number of primary branches among different plants within each progeny based on visual observation. However, as these progenies comprised plants with both low and high numbers of main branches, a total of 5 (6.02%) plant progenies were discovered to be segregating based on primary branch count.

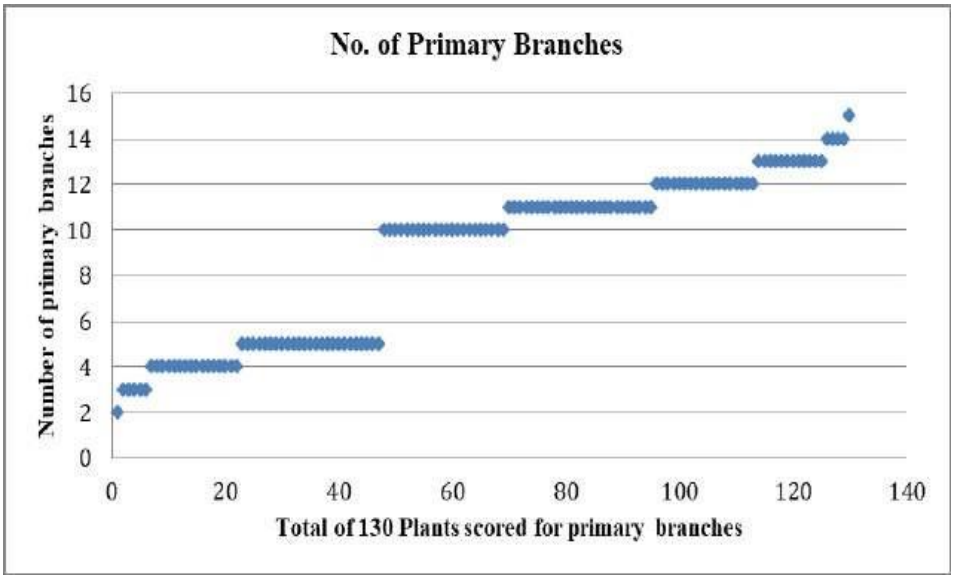

Figure 1. Scatter diagram showing distribution of primary branch number among 130 plants of F2:5 population.

Formation of bulks for primary branches

Plants with varying numbers of primary branches were selected to produce bulks for gene tagging using molecular markers (Table 2). Twelve plants each, were chosen from among the 130 plants for the higher primary branches (designated as "HPB") and lower primary branches (designated as "LPB"). There were 10 to 14 primary branches for HPB bulk, whereas there were about 4 to 5 primary branches for LPB bulk. For HPB and LPB bulks, the average number of primary branches was 12.16 and 4.50, respectively. Markers found to be polymorphic on parental genotypes were then utilised for gene tagging on these bulks.

Table 2. List of plants selected for bulk formation based on number of primary branches and molecular analysis.

Block no.	Line no.	Plant No.	No. of primary branches	Code of bulked individual plant
B1	L2	P5	10	HPB 1
B1	L15	P4	12	HPB 2
B1	L31	P4	14	HPB 4
B1	L33	P3	12	HPB 5
B2	L4	P1	12	HPB 6
B2	L13	P2	12	HPB 10
B2	L23	P1	13	HPB 12
B3	L32	P1	12	HPB 20
B3	L35	P3	13	HPB 21
B2	L20	P1	12	HPB 23
B2	L31	P2	12	HPB 24
B3	L18	P1	12	HPB 27
B2	L28	P1	12	HPB 14
B3	L10	P1	12	HPB 26
B1	L4	P4	4	LPB 2
B1	L12	P1	5	LPB 4
B1	L8	P1	4	LPB 5
B1	L30	P2	4	LPB 9
B1	L34	P1	5	LPB 10
B1	L37	P1	4	LPB 11
B1	L40	P3	4	LPB 13
B2	L32	P1	5	LPB 16
B3	L28	P1	4	LPB 19
B1	L28	P1	5	LPB 22
B1	L10	P2	5	LPB 23
B1	L23	P1	5	LPB 24

Identification of polymorphism between parents

To check for initial polymorphism among parental genotypes, 148 SSR markers (73 from A genome & 75 from B-genome) in total were used. 40 markers were identified as polymorphic, since they exhibited distinct and observable bands with distinct alleles between the two parental genotypes (Table 3 & 4; Figures 2, 3 & 4). Of these 40 polymorphic markers, twenty-six came from the B-genome and fourteen from the A-genome. Replicating the parental polymorphism screening results revealed that 38 markers were confirmed to be polymorphic, whereas 2 markers (A03_3174449 & Ni2-B01) were found to be monomorphic.

Table 3. List of A-genome markers polymorphic on the parents.

SSR marker	Sequence (5'-3')	Sequence (5'-3')
A01_2688930	CAATGTAATGGGAAGAAAATG	GTACCTCTCCTGGTCCTGTAT
A03_3174449	AAAGAAGAGCTTTGAAGAGGA	TTGATTCACAACACACATACC
A04_11549954	CATTTTCCTCCTTGAGATCTAT	CTGGTGGAAAACTTGATTTTA
A04_13468345	CATCACAAGCCAAGAAGAAT	AGAGTCTGTGGTTCATCTCCT
A04_7703506	CCCGTGATACGGACTTTATAC	TCTCATGTTAAAAGTTAGAGTGG
A05_25290881	ATAAAGATTTGATGGGAGGAG	GGTGGAGGAGGATAGTTGTAG
A06_12596970	CCAAGTGTAGTTATACCGAGTT	TTACTAACTCAGTCGAATTTGG
A06_20161352	GCATTACAGAGAGTGAGCAAT	TCCTCCTTGAAGTTTAGTGTG
A06_25201785	CAGGTCTAATTGCCATCACTA	CATATGACAGGTCCACCCTA
A06_7568964	TGGACACCTAAATTCAACGTA	GTTTTAGATGCCAATTAACGA
A07_12938471	CAAGCTTCTTCAGCTCATAAC	AGCCAAAAAGACGAAGATAGT
A08_2087658	CAGCAGAGTCCTTCTTGTTTA	GCAAATTAGTAAATTCCACTCAG
A08_8336436	AAAATTATGATACGGGTACGG	GTTAGCGCGAGAATATGTTAC
A09_27227566	GAAAGCGAGTAAGAAGAGAGC	ACTCATTGTCCGTAAACACAC

Table 4. List of B-genome markers polymorphic on the parents.

SSR marker	Sequence (5'-3')	Sequence (5'-3')
Ni1-A04	TCCTCCTACTTTGATACTTGC	ACGTCAAATACTTCACTGCC
Ni2-A11	AACAAACAAGAGTCGAATACGG	AATGCCCTCTAACTGAGCCC
Ni2-B01	AAGGAGATTGTTTTTGGGGC	AAGACTAATAAACACACGGCG
Ni2-B03	ACTTCTTGCCCTCCTCACC	AAATACTCACTGCAATACCCAGG
Ni2-C03	CGTAGAAGATGAACTCGGGG	CTCTTTCAGCTACTGCTGCG
Ni2-C09	ACGGAAGAAATCCAACCTCG	TATGCTTGGAAATGGTTTGG
Ni2-C12	ACATTCTTGGATCTTGATTCG	AAAGGTCAAGTCCTTCCTTCG
Ni2-F02	TGCAACGAAAAAGGATCAGC	TGCTAATTGAGCAATAGTGATTCC
Ni2-H03	TTTGAAGAAACAAAAATGGCG	TCATCTTCCCCTCTCATTCC
Ni2-H06	CATCAGATCCGACGAAATCC	TCCTTTGGACTGTGAAAAACG
Ni3-B07	GGAGAAGAGGAAGAAGAAGCC	CGACTTCTAGAGGAACCCCC
Ni3-C05	TTTCGTGCTTTGGTGTGAAG	TCCCCAAATCGAACCATAAG
Ni3-C08	CCCTAACACGGTGTCAACAG	GGCAGAATCATCGAGAGGTC
Ni3-G05	AGGAAGCATTTGCGCTAGTC	TCTACAACCACAACGTCCAAG
Ni4-A02	AGGACCACTGGGATACAAGC	ATTTGGAGCTGCGTACTTCG
Ni4-A09	AAAGGGCGAAGAAGCAGC	TTTCTTCCATTTGACCGACC
Ni4-B10	GTCCTTGAGAAACTCCACCG	CCGATCCCATTTCTAATCCC
Ni4-C06	CAGAGGCGAAAACGAGAGAG	TTTATAGACTTCCCGTGGGC
Ni4-D10	ACATGCGAAAGGGATTTGAC	TGCAAGTGAACTCAAAACAAAAG
Ni4-F09	CTGTTATGCAAGGTCATCGC	TGTTCCAGGTGAAGAAACCG
Ni4-F11	CGTAAGTTTCAATTGTCAACGG	TCGTACGAAACAATCAACGG
Ni4-G02	TTGGTGTCAGAAACAACG	ACACACGACGGATCTCTGC
Ni4-G06	TGACGGCTGAAGAAAATCAG	GTTTAACCTAAACCGAAAATC
Ni4-G08	ATTTGACGGACTCCTCTTGC	CACTTGGTAACTCTATGGATGCC
Ni4-G10	AGACTGAAATATTTTGGGACC	CGTTCTTCAACTTGTTCATCATC
Ni4-H03	GATGAACAGCAACAGCTTGG	CAAAATGTCGTTTGTTAGTCTTGG

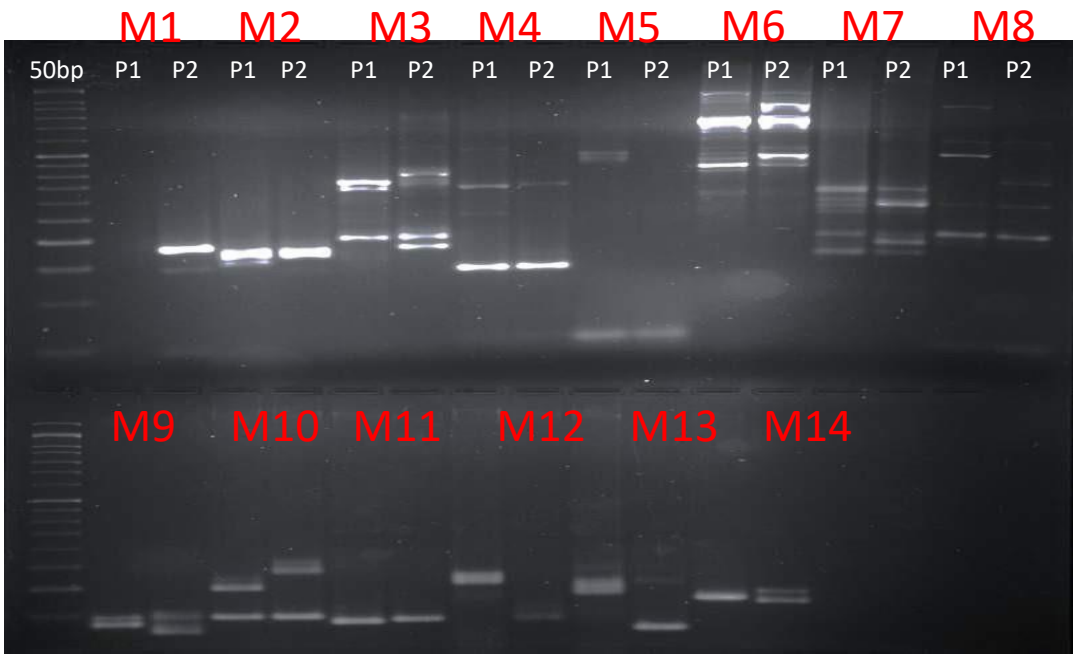

Figure 2. DNA polymorphism among two parental genotypes with SSR markers (markers labelled from M1 to M14; M1: A01_2688930, M2: A03_3174449, M3: A04_11549954, M4: A04_13468345, M5: A04_7703506, M6: A05_25290881, M7: A06_12596970, M8: A06_20161352, M9: A06_25201785, M10: A06_7568964, M11: A07_12938471, M12: A08_2087658, M13: A08_8336436, M14: A09_27227566). P1 and P2 refers to Parent 1 (Kafiav N Zagora) and Parent 2 (Pusa Karishma), respectively.

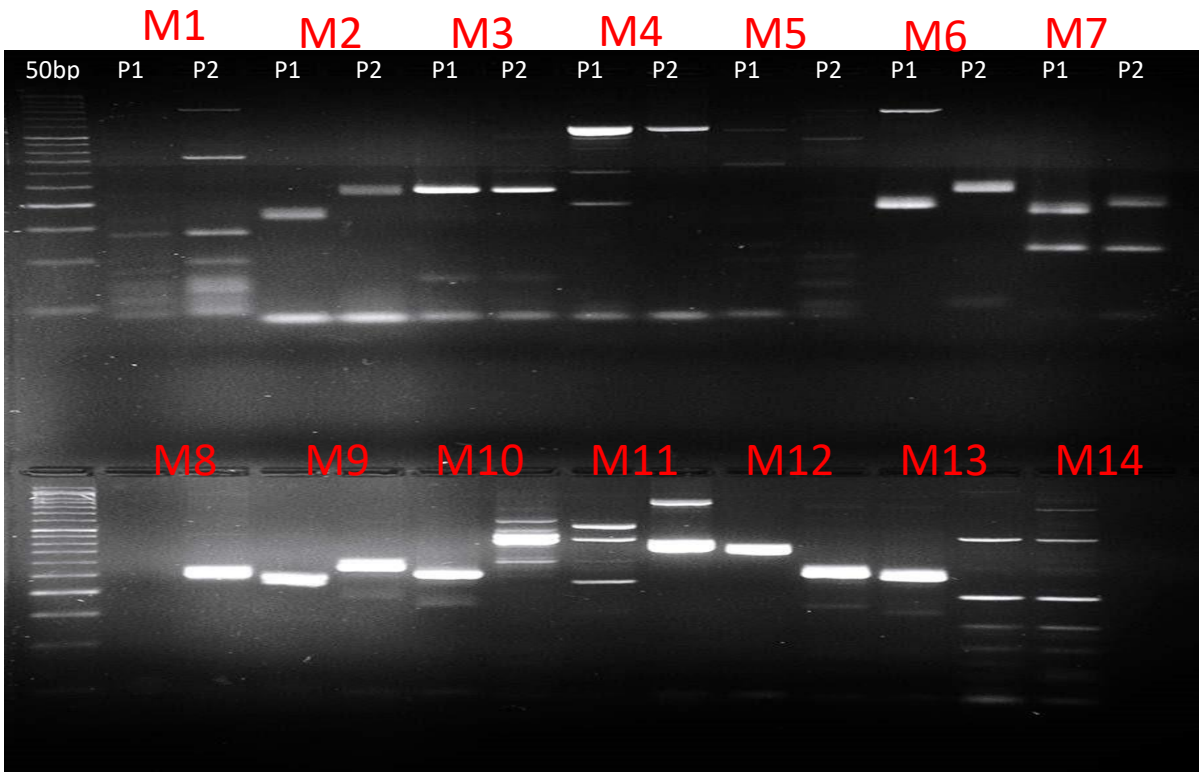

Figure 3. SSR Banding profile of the parents; M1: Ni1-A04, M2: Ni2-A11, M3: Ni2-B01, M4: Ni2-B03, M5: Ni2-C03, M6: Ni2-C09, M7: Ni2-C12, M8: Ni2-F02, M9: Ni2-H03, M10: Ni2-H06, M11: Ni3-B07, M12: Ni3-C08, M13: Ni3-G05, M14: Ni4-A02.

Molecular characterization of bulks using polymorphic markers

Twenty-six of the 38 polymorphic SSR markers were utilised to amplify the DNA of 24 lines, or two bulks. However, only 26 markers that were polymorphic on the parents could be tested for PCR amplification of the genotypes included in the two bulks. Moreover, no leaf samples were available at that time of the season for DNA isolation). Out of these 26 polymorphic markers tested on the bulks, 12 did not amplify any scorable polymorphism patterns on bulk genotypes, but 14 markers amplified segregating patterns for genotypes forming two bulks. Among the genotypes of two bulks, a total of 54 alleles were amplified by 14 polymorphic SSR markers (Table 6). Table 7 provides a comprehensive molecular profile of both bulk lines using 14 polymorphic primers.

Identification of markers associated with primary branches on B-genome

The relationship between the number of primary branches and genotypes that comprised two bulks was identified using both molecular and morphological data. To determine the relationship between marker alleles and primary branch number, the Student's *t*-test was utilised as none of the polymorphic markers produced distinct segregating patterns between the genotypes of two bulks. Based on the allele amplified in each genotype, the genotypes involved in the two bulks were divided into distinct classes, and each allele was assigned an alphabetic code for *t*-Test analysis.

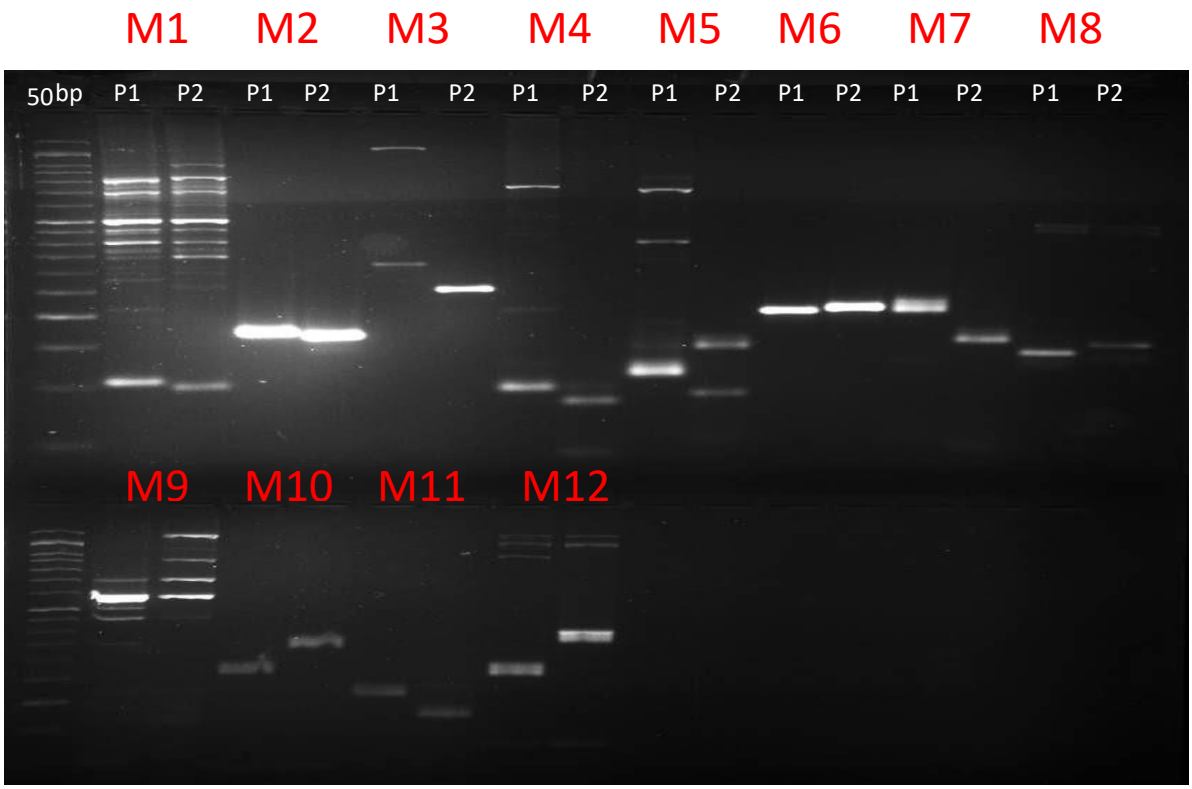

Figure 4. SSR Banding profile of the parents; M1: Ni4-A09, M2: Ni4-B10, M3: Ni3-C05, M4: Ni4-C06, M5: Ni4-D10, M6: Ni4-F09, M7: Ni4-F11, M8: Ni4-G02, M9: Ni4-G06, M10: Ni4-G08, M11: Ni4-G10, M12: Ni4-H03.

Table 6. List of SSR markers polymorphic on bulk lines and number of alleles amplified for each.

No	SSR Marker	No. of alleles amplified
1.	A04_13468345	3
2.	A06_12596970	5
3.	A08_8336436	2
4.	A06_7568964	5
5.	Ni2-H03	2
6.	Ni2-A11	3
7.	Ni2-B03	3
8.	Ni2-C09	8
9.	Ni2-C12	2
10.	Ni2-H06	3
11.	Ni3-C05	4
12.	Ni3-C08	3
13.	Ni4-G08	5
14.	Ni4-G10	6
	Grand Total	**54**

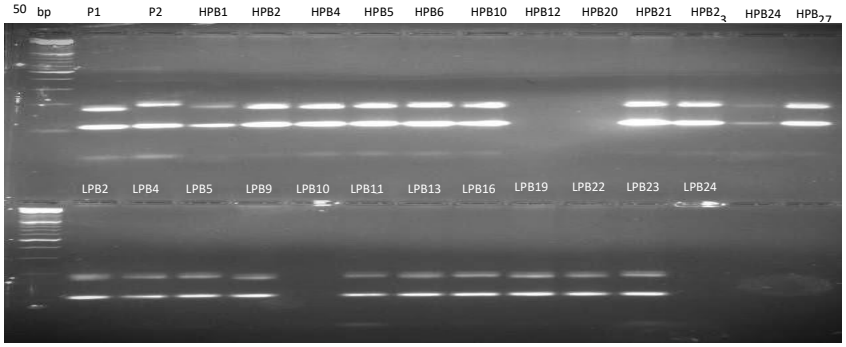

Figure 5. SSR banding profile of the bulk genotypes with the marker Ni2-C12. P1 as well as plants of the bulk 1 have common allele i.e., 190 bp whereas P2 and the plants of bulk 2, both have same (200 bp) allele amplified in them.

Two SSR markers, Ni2-C12 and Ni2-A11, were found to be significantly linked with the number of major branches based on *t*-test analysis. The estimation of association was based on the P-value for the *t*-test between alleles. The marker Ni2-C12 amplified two alleles of 190 bp and 200 bp among 20 genotypes out of the 24 genotypes of the two bulks. Scoreable bands were not amplified by the other four genotypes (Figure 5). The average number of primary branches for genotypes amplifying the 190 bp allele was 11.55, whereas the number for the 200 bp allele was 4.45 (Table 8). The *P*-value between the two alleles (i.e., 190 bp and 200 bp) was calculated using the data to be($P<0.001$) . Likewise, two alleles, 180 bp and 230 bp, were amplified by the Ni2-A11 alleles among the bulk genotypes. Four genotypes were heterozygous for Ni2-A11, as these four genotypes amplified these two alleles in heterozygous state. For alleles 180 bp, 7.75 was the average number of primary branches; for alleles 230 bp, it was 6.00; and for genotypes with heterozygous status, it was 12.67. For the *t*-Test, the *P*-value between the alleles 180 bp and 230 bp and 180 bp and the heterozygous condition (180 bp/230 bp) was 0.02. The heterozygous condition (180 bp/230 bp) and the 230 bp *P*-value for the *t*-test were found to be non-significant (Table 8).

Table 7. Results of molecular analysis of bulk lines.

Genotype	No. of primary branches	Ni2-A11	Ni2-C09	Ni2-H03	Ni2-H06	Ni2-C12	Ni2-B03	Ni3-C08	A0883364 36	A06_12596 970	A06_7568964	A04_13468 345	Ni4-G08	Ni4-G10	Ni3-C05
P1-Kafiav N Zagora	18.67	180	190	260	280	190	400	380	190	250	200	140	280	215	180
P2-Pusa Karish ma	7.20	230	230	250	250	200	null	360	130	300	240	140	360	180	150
HPB1	12	230	190/ 220	260	-	190	null		130/ 190	300	240	150	280	160	190
HPB2	12	180	218	250	250	190	400	380	130	300	240	140/ 150	220	215	180
HPB4	14	180	190/ 218	260	250	190	400	380	130/ 190	300	240	140/ 150	-	215	-
HPB5	12	230	230	250	250	190	390	380	130	250	220	140	280	200	160
HPB6	12	230	230	260	250	190	400	390	130	300	240	140/ 150	-	180	190
HPB10	12	180/ 230	190/ 220	260	250	190	400	380	130/ 190	300	245	150	280/ 360	215	180
HPB12	13	-	-	-	-	-									
HPB14	12						-	-	130	250	240	140	-	-	-
HPB20	12	-	190		-										
HPB21	13	230	190/ 220	260	250	190	400	360	130	300	240	140	-	-	180
HPB23	12	230	190	260	250	190	400	380	130		-	140/ 150	-	-	-
HPB24	12	-	190/ 230	260	-	190	null	380	-		null	140	-	-	-
HPB26	12						null	380	130	300	240	140/ 150	-	160/ 200	180
HPB27	12	180	190/ 230	260	250/ 280	190	400	380	130	300	-	150	-	-	180
LPB2	4	180/ 230	190/ 230	250	280	200	400	380	-	250	240	140/ 150	280/ 360	180	180
LPB4	5	230	218	260		200	400	380	130	300	-	150	360	180	180
LPB5	4	230	190	250	250	200	400	380	130/ 190	300	240	140	280/ 360	180	210
LPB9	4	180/ 230	190	260	250	190	-	380	130	300	245	140/ 150	-	215	180
LPB10	5	-	230	-	-	-	400	-	-	300	220	140	360	180	180
LPB11	4	230	190	260	250	200	null	380	130/ 190	250	240	140	360	180	190
LPB13	4	180/ 230	220	260	250/ 280	200	400	380	-	300	240	150	-	-	180
LPB16	5	230	190/ 220	260	250/ 280	200	400	380	130	300	200	150	260	180/ 215	180
LPB19	4	230	220/ 230	260	250/ 280	200	400	380	130	250	240	140	280		180
LPB22	5	230	190/ 220	250	250/ 280	200	400	380	-	300	240	140	-	-	180
LPB23	5	230	220	250	250	200	400	380	130	300	240	140/ 150	280	-	210
LPB24	5	-	190/ 220	250	250	-		380	130	300	240	150	280	215	180

Table 8. Details of polymorphic primers, alleles amplified and the significance among alleles for primary branches.

Marker name	Alleles	No. of genotypes allele amplified	Average number of primary branches/allele class	P-value (*t*-test)
A04_13468345	140	9	7.89	Non-significant
	150	7	7.86	
	140/150	8	9.34	
A06_12596970	200	1	15.00	Non-significant
	220	2	8.50	
	240	15	8.13	
	245	2	8.00	
A08_8336436	130	14	8.93	Non-significant
	130/190	5	9.20	
Ni2-A11	180	3	12.67	Significant 0.029 between 180bp and 230 bp, 0.02 between 180bp and heterozygous state
	230	12	7.75	
	180/230 (heterozygous)	4	6.00	
Ni2-B03	390	1	12.00	Non-significant
	400	16	8.00	
	Null allele	4	10.00	
Ni2-C09	190	5	7.20	Non-significant
	218	2	8.50	
	220	2	8.50	
	230	3	9.67	
	190/218	1	14.00	
	190/220	6	8.67	
	190/230	3	9.34	
	220/230	1	4.00	
Ni2-C12	190	11	11.55	Significant (P<0.001) (1.007 E-10
	200	9	4.45	
	250	12	9.08	
Ni2-H06	280	1	4.00	Non-significant
	250/280	6	6.00	
Ni3-C05	160	1	12.00	Non-significant
	180	14	7.29	
	190	3	9.34	
	210	2	4.50	
Ni3-C08	360	18	1.00	Non-significant
	380	1	7.50	
	390	1	1.00	
Ni4-G08	220	1	12.00	Non-significant
	260	1	5.00	
	280	5	7.60	
	360	3	4.67	
	280/360	3	6.67	
Ni4-G10	160	1	12.00	Non-significant
	180	7	5.58	
	200	1	12.00	
	215	5	9.40	
	160/200	1	12.00	
	180/215	1	5.00	
A06_7568964	200	1	5.00	Non-significant
	220	2	8.50	
	240	15	8.13	
	245	2	8.00	
Ni2-H03	Null	1	12.00	Non-significant
	250	7	6.71	
	260	14	8.92	

Tagging of 9 Mb region on chromosome B5 of B-genome for primary branches

The *B. nigra* genome assembly at http://brassicadb.cn/#/BLAST/ was utilised to do a sequence similarity search using the clone sequences of two highly linked markers, Ni2-C12 and Ni2-A11 (Supplementary Figure 1 and 2). Both markers' sequence similarity searches matched them to a 9 Mb range on *B. nigra*'s chromosome B5.

B5 was mapped to the markers Ni2-A11 and Ni2-C12 at 55.9 Mb and 64.9 Mb, respectively. The sequence similarity e-values for markers Ni2-A11 and Ni2-C12 were 4.19 x 10-121 and 6.28 x 10-80, respectively (Supplementary Figure 3 and 4).

Discussion

The present research focuses on identifying informative markers using BSA to identify markers related to primary branches in *B. juncea*. There have been some prior reports of markers associated with branching, specifically about the number of primary branches, in *B. juncea*, but not as much as in other *Brassica* species, such as *B. napus*.

A QTL analysis conducted on *B. juncea* (AABB) revealed 65 significant QTLs spread across 13 linkage groups, of which 8 were linked to branching habit, 4 to primary branch number, and 4 to secondary branch number (Ramchiary et al., 2007). Twelve genes that affect branch number, plant height, and seed output in *B. juncea* have been linked with yield, agronomic, and morphological features in the Brassica database (Yadava et al., 2012). The mustard gene for plant growth habit was mapped using molecular markers, with the Sdt1 gene found on the linkage group 15 of *B. juncea*. Ni4-A10 and SJ6842 primer pairs were found to be linked to the Sdt1 gene, with marker SB3140 (present Just above the marker Ni4-A10 in the linkage group) specifically targeting chromosome 5 of the B-genome, which corresponds to chromosome 15 of *B. juncea* (Kaur and Banga, 2015). Several markers for traits related to yield were found in *B. juncea* employing genome-wide association mapping. Chromosomes 2 and 3 of the B-genome displayed QTLs for grain yields. A QTL for secondary branch number was found on chromosome 7, which was also the site of a prior identification by Ramchiary et al. (2007)Ramchiary et al. (2007)Ramchiary et al. (2007)Ramchiary et al. (2007). Additionally, a QTL for seed size was discovered on chromosome A6 of the A-genome, confirming previous theories that a similar QTL existed on the corresponding chromosome of *B. juncea* (Ramchiary et al., 2007). The marker SB1822-1, which was found at 17.5 cM on chromosome B3, also had an effect on grain yield. On the other hand, SB3872-3, which was found at 60.9 cM on chromosome B5, had the most effect on seed size (Akhatar and Banga, 2015). The Pi gene, which creates pink leaves in ornamental kale (*B. oleracea*), was located between 0.6 and 2.4 cM on either side of the SSR marker Ni2-C12 and the co-dominant SCAR marker Boac04. Based on the *B. oleracea* reference genome sequence, Pi was located near the top of chromosome C3, syntenic to B5 of *B. nigra* (Zhu et al., 2016). A total of 57 MQTLs, of which 31 are located in sub-genome A and 26 in subgenome B, were determined by the scientists' consensus map, which effectively projected 798 QTLs linked to yield-related attributes, including primary branch number. The number of MQTLs found for traits associated to yield varied from one on chromosome B5 to a maximum of six on chromosomes A3 and B3 (Kumar et al., 2022).

Above findings provide a basis for additional genetic studies related to *B. juncea*'s branching process. Therefore, using BSA, an attempt was made in the current study to identify genetic markers linked to the number of primary branches. MAS for the target trait will eventually benefit from the current research problem's findings and fine mapping.

Morphological diversity for primary branches in $F_{2:5}$ population

Genetically fixed (almost) $F_{2:5}$ lines from a hybrid between East European and Indian genotypes were used in the current investigation. It was determined that there are differences between the two parents for a number of features, including the number of primary branches, based on the data from prior years for significant morphological traits. With no selection from F_2 onward, the $F_{2:5}$ population was created by a single seed descent approach, with plants being randomly picked for the following year. Based on this, morphological study of 130 plants was performed for the primary branches. Since primary branches in different plants ranged from 2 to 15, there was heterogeneity in the $F_{2:5}$ mapping population for primary branches. This suggested that there was sufficient variance in the population for genetic analysis to likely identify the gene or QTL causing the distribution of primary branches among F_5 plant progenies.

Use of F2:5 population for BSA

Common genetic variations governing a given trait are probably found by analysis of genotypes that

are comparable to each other for that trait. Morphological data of 130 plants was analysed. As a result, a total of 24 genotypes were found and divided into two pools (the HPB and LPB), each including 12 members. The primary number branch count in each pool varied significantly. The number of primary branches in the two bulk pools that were created differed significantly, with 12.16 primary branches in the HPB pool and 4.50 primary branches in the LPB pool. Similar primary branches (higher or lower) among genotypes would probably indicate that the alleles within each genotype pool are similar. Based on this, the significant marker allele-traits association was found using BSA and the Student's *t*-test.

Identification of 9 Mb genomic region for primary branches

According to sequence similarity e-values, both markers mapped to a high degree of certainty within a 9 Mb region of chromosome B5, suggesting that the genetic regulation of the primary branches in *B. juncea* is most likely located on chromosome B5. However, there are a lot of additional genomic areas or loci that could be involved in *B. juncea's* number of major branches.

Validation and fine mapping of 9 Mb region for primary branches

The number of primary branches was mapped to the 9 Mb region on chromosome B5 of B-genome of *Brassica juncea*. However, this finding needs to be confirmed using the same set of markers in genetically diverse populations**.** If verified, the 9 Mb region would be an excellent candidate for creating a detailed map of the area, which would enable the discovery of important genes and markers linked to the (number of) main branches. In the current study, the genomic region determining the number of primary branches in *B. juncea* was tagged using $F_{2:5}$ lines of a genetic hybrid between Kafiav N Zagora (east European type) and Pusa Karishma (Indian type). The following summarises the study's main findings:

- The primary branch numbers of the $F_{2:5}$ population were scored using a total of 130 plants, which came from 83 plant progenies.
- Of the plant progenies, 5 (6.02%) had plants with both low and high numbers of primary branches, indicating that these progenies were segregating based on primary branch count.
- Of the 130 plants, a total of 12 plants each were chosen to make HPB and lower primary branches LPB bulks.
- For HPB and LPB bulks, the average number of primary branches was 4.50 and 12.16, respectively.
- To check for initial polymorphism between parental genotypes, 148 SSR markers in total were employed.
- It was found that 38 SSR markers were polymorphic because they produced distinct and scoreable bands with distinct alleles between the two parental genotypes.
- Among the genotypes that make up two bulks, a total of 14 markers amplified 54 alleles.
- Two SSR markers, Ni2-A11 and Ni2-C12, were found to be significantly linked with the number of primary branches by Student's *t*-test analysis.
- On *B. nigra* chromosome B5, two highly associated markers (Ni2-A11 and Ni2-C12) were mapped to a 9 Mb genomic area spanning from 55.9 Mb to 64.9 Mb.

Conclusion

The study created two pools of genotypes with high and low numbers of primary branches from an $F_{2:5}$ population derived from a genetic cross between genotypes from the European and Indian gene pools. The molecular and morphological data of the parental genotypes and the pools was recorded. When the molecular and morphological data was subjected to bioinformatic (sequence similarity using BLAST) and statistical (Student's *t*-test) analysis, a 9 Mb genomic area between 55.9 Mb and 64.9 Mb on chromosome B5 of the B-genome of *B. juncea* was located.

Supplementary Materials

The supplementary material for this article can be found online at: https://www.jpmb-gabit.ir/article_712349.html.

Supplementary Table 1. Thermal Profile used for PCR.

Supplementary Figure 1. Screenshot of NCBI page showing clone sequence of Ni2-A11.

Supplementary Figure 2. Screenshot of NCBI page showing clone sequence of Ni2-C12.

Supplementary Figure 3. Blast hit of Ni2-C12 to chromosome B5 of *B. nigra* at 64.9 Mb.
Supplementary Figure 4. Blast hit of Ni2-A11 to chromosome B5 of *B. nigra* at 55.9 Mb.

Author Contributions

Conceptualization: M.K.; Methodology: M.K.; Software: S.S.; Validation: L.K. and S.S.; Formal analysis: M.K.; Investigation: M.K.; Data curation: M.K.; Original draft preparation: M.K.; Review and editing: L.K.; Visualization: M.K.; Supervision: M.K.; Project Administration: M.K.; and L.K,; All authors have read and agreed to the published version of the manuscript.

Funding

This research received no external funding.

Acknowledgments

Thankful to School of Biotechnology, SKUAST, Jammu, for providing research material and space.

Abbreviations

BSA, Bulked Segregant Analysis; SSR, Simple Sequence Repeats; HPB, Higher Primary Branches; LPB, Lower Primary Branches; Mb, Megabytes; QTL, Quantitative Trait Loci.

Conflicts of Interest Statements

The authors declare no conflict of interest.

References

Akhatar, J., and Banga, S.S. (2015). Genome-wide association mapping for grain yield components and root traits in *Brassica juncea* (L.) Czern & Coss. *Mol Breed* 35: 1-14.

Axelsson, T., Bowman, C., Sharpe, A., Lydiate, D., and Lagercrantz, U. (2000). Amphidiploid *Brassica juncea* contains conserved progenitor genomes. *Genome* 43(4): 679-688.

Chen, B., and Heneen, W. (1992). Inheritance of seed colour in *Brassica campestris* L. and breeding for yellow-seeded *B. napus* L. *Euphytica* 59: 157-163.

Kaur, H., and Banga, S. (2015). Discovery and mapping of *Brassica juncea Sdt1* gene associated with determinate plant growth habit. *Theor Appl Genet* 128: 235-245.

Kumar, A. (2016). Production barriers and technological options for sustainable production of rapeseed-mustard in India. *J Oilseed Brassica* 1(2): 67-77.

Kumar, R., Saini, D.K., Kumar, M., Priyanka, V., Akhatar, J., Kaushik, D., Sharma, A., Dhanda, P.S., and Kaushik, P. (2022). Revealing the genetic architecture of yield-related and quality traits in Indian mustard [*Brassica juncea* (L.) Czern. and Coss.] using Meta-QTL analysis. *Agronomy* 12(10): 2442.

Michelmore, R.W., Paran, I., and Kesseli, R. (1991). Identification of markers linked to disease-resistance genes by bulked segregant analysis: a rapid method to detect markers in specific genomic regions by using segregating populations. *Proc Natl Acad Sci USA* 88(21): 9828-9832.

Pradhan, A.K., Sodhi, Y.S., Mukhopadhyay, A., and Pental, D. (1993). Heterosis breeding in Indian mustard (*Brassica juncea* L. Czern & Coss): analysis of component characters contributing to heterosis for yield. *Euphytica* 69: 219-229.

Ramanujam, S., and Rai, B. (1963). Analysis of yield components in *Brassica campestris* var. yellow sarson.

Ramchiary, N., Padmaja, K., Sharma, S., Gupta, V., Sodhi, Y., Mukhopadhyay, A., Arumugam, N., Pental, D., and Pradhan, A. (2007). Mapping of yield influencing QTL in *Brassica juncea*: implications for breeding of a major oilseed crop of dryland areas. *Theor Appl Genet* 115: 807-817.

Singh, A.K., Singh, A.K., Choudhary, A.K., Aradhna Kumari, A.K., and Rakesh Kumar, R.K. (2017). Towards oilseeds sufficiency in India: present status and way forward. *J AgriSearch* 4(2): 80-84.

Singh, N., Vasudev, S., Kumar Yadava, D., Kumar, S., Naresh, S., Ramachandra Bhat, S., and Vinod Prabhu, K. (2013). Assessment of genetic diversity in *Brassica juncea Brassicaceae* genotypes using phenotypic differences and SSR markers. *Rev Biol Trop* 61(4): 1919-1934.

Singh, S.P., and Singh, D. (1972). Inheritance of yield and other agronomic characters in Indian mustard (*Brassica juncea*). *Can J Genet Cytol* 14(2): 227-233.

Snowdon, R.J. (2007). Cytogenetics and genome analysis in *Brassica* crops. *Chromosome Res* 15: 85-95.

Tiwari, V. (2019). Morphological parameters in breeding for higher seed yield in Indian mustard [*Brassica juncea* (L.) Czern. & Coss.]. *Electron J Plant Breed* 10(1): 187-195.

Yadava, S.K., Arumugam, N., Mukhopadhyay, A., Sodhi, Y.S., Gupta, V., Pental, D., and Pradhan, A.K. (2012). QTL mapping of yield-associated traits in *Brassica juncea*: meta-analysis and epistatic interactions using two different crosses between east European and Indian gene pool lines. *Theor Appl Genet* 125: 1553-1564.

Zhu, P., Cheng, M., Feng, X., Xiong, Y., Liu, C., and Kang, Y. (2016). Mapping of Pi, a gene conferring pink leaf in ornamental kale (*Brassica oleracea* L. var. acephala DC). *Euphytica* 207: 377-385.

JPMB
Journal of Plant Molecular Breeding
Published by Genetics and Agricultural Biotechnology Institute of Tabarestan
2023 | Volume 11 | Issue 2

مقاله پژوهشی

ارتباط نشانگرهای SSR با شاخه‌های اولیه در خردل هندی (*Brassica juncea* L.)

مانپریت کور*،لالیتا کوماری ،سوپریا شارما

دانشگاه علوم کشاورزی و منابع طبیعی جامو و کشمیر، هند

چکیده: در این مطالعه از لاین‌های F2:5 حاصل از تلاقی بین ارقام Kafiav N Zagora و Pusa Karishma برای نشان‌دار کردن مناطق ژنومی کنترل‌کننده شاخه‌های اولیه در *Brassica juncea* استفاده شد. ۱۳۰ گیاه F2:5 برای مشخص کردن تعداد شاخه‌های اولیه استفاده شد که منجر به دو خزانه از ۱۲ ژنوتیپ برای شاخه‌های زیاد (HPB) و کم (LPB) گردید. میانگین تعداد شاخه‌های اولیه برای HPB و LPB به‌ترتیب ۱۲.۱۶ و ۴.۵۰ بود. مجموعه‌ای از ۱۴۸ نشانگر SSR (توالی‌های تکراری ساده) برای غربالگری چندشکلی والدین استفاده شد که از آن ۱۴ نشانگر SSR چندشکل برای شناسایی مولکولی و نشان‌دار کردن مناطق ژنومی توده‌های HPB و LPB استفاده شد. داده‌های آللی امتیازدهی شده برای ۱۴ لاین چندشکل با استفاده از آزمون t– استیودنت (t-test) برای درک روابط شاخه‌های اولیه با نشانگرهای SSR و آلل‌های تقویت‌شده مورد آزمون قرار گرفتند. بر این اساس، دو نشانگر ژنوم B (Ni2-C12) و (Ni2-A11) شناسایی شدند که از همبستگی بالایی با تعداد شاخه‌های اولیه برخوردار بودند. تجزیه و تحلیل بیوانفورماتیک نشان داد این دو نشانگر در ناحیه ۹ Mb، بر روی کروموزوم B5 *B. juncea* قرار دارند. مطالعه حاضر با استفاده از لاین F2:5 حاصل از تلاقی خزانه بین ژنی، توانست مکان‌های تنظیم‌کننده تعداد شاخه‌های اولیه را در کروموزوم B5 زیر مجموعه ژنوم *B. juncea* شناسایی نماید. تایید این نتایج در زمینه‌های مختلف ژنتیکی پیش از مطالعات مکان‌یابی دقیق در ناحیه ژنومی کروموزوم B5 (بین ۵۵.۹ و ۶۴.۹ مگابایت) ضروری بنظر می‌رسد.

کلمات کلیدی: *Brassica juncea*، تعداد شاخه اولیه، BSA، SSR.

ویراستار علمی
دکتر علی دهستانی،
پژوهشکده ژنتیک و زیست‌فناوری کشاورزی طبرستان،
دانشگاه علوم کشاورزی و منابع طبیعی ساری

تاریخ
دریافت: ۱۳ اسفند ۱۴۰۲
پذیرش:۲۰ فروردین ۱۴۰۳
چاپ: ۱۸ اردیبهشت ۱۴۰۳

نویسنده مسئول
دکتر مانپریت کور
mkour5941@gmail.com

ارجاع به این مقاله
Kour, M., Kumari, L., and Sharma, S. (2023). Association of SSR Markers for primary branches in *Brassica Juncea* L. *J Plant Mol Breed.* 11(2): 77-93.
doi: 10.22058/JPMB.2024.2024234.1296.

JPMB | Journal of Plant Molecular Breeding
Published by Genetics and Agricultural Biotechnology Institute of Tabarestan
2023 | Volume 11 | Issue 2

Original paper

Genetic diversity and structure of Benin pineapple (*Ananas comosus* (L) Merr.) germplasm collection using Simple Sequence Repeat (SSR) markers

Chalotte Abike Oladjo Adjé[1,2*], Antoine Abel Missihoun[2], Paulin Sedah[2], Hubert Adoukonou Sagbadja[2], Enoch Gbenato Achigan-Dako[1], and Clément Agbangla[2]

1. Genetics, Biotechnology and Seed Science Unit (GBioS), Faculty of Agronomic Sciences, University of Abomey-Calavi, Abomey-Calavi, Republic of Benin
2. Faculty of Sciences and Techniques (FAST), University of Abomey-Calavi, 01 BP 526 Tri postal, Cotonou, Republic of Benin.

Abstract: Pineapple stands as a cornerstone among Benin's vital fruit crops, playing a pivotal role in enhancing both household food security and income. This delectable fruit is prominently featured among the key crops advocated for cultivation within the country. Despite the critical role this crop plays, our understanding of the diversity within genetic resources is remains limited. This study aimed to assess genetic variation and infer the population structure of 57 pineapple accessions collected from Benin's national core collection, using 10 simple sequences repeat (SSR) markers. The result showed a total of 23 alleles, ranging from 2 to 4, with a mean of 2.3 alleles per locus. The polymorphic information content was 0.34 whereas the mean expected heterozygosity was 0.43. The UPGMA dendrogram revealed two main clusters. The collection was determined to exhibit a structured composition comprising two distinct groups based on genetic analysis. This grouping was further validated by AMOVA, affirming its existence. Our work offers valuable insights into the genetic diversity within Beninese pineapple germplasm, thereby guiding strategic conservation efforts. Moreover, these findings open avenues for leveraging the genetic variation present in Benin's pineapple germplasm for future pineapple breeding programs, thereby enhancing pineapple cultivation and resilience.

Keywords: *Ananas comosus*, SSR, genetic variation, germplasm, molecular marker.

OPEN ACCESS

Edited by
Dr. Prasenjit Saha,
Meiogenix Inc, Ithaca, NY, USA

Date
Received: 9 March 2024
Accepted: 1 April 2024
Published: 11 May 2024

Correspondence
Dr. Chalotte Abike Oladjo Adjé
abikecharlotte@gmail.com

Citation
Adjé, O.A.C., Missihoun, A.A., Sedah, P., Sagbadja, H.A., Achigan-Dako, E. and Agbangla, C. (2023). Genetic diversity and structure of Benin pineapple (*Ananas comosus* (L.) Merr.) germplasm collection using Simple Sequence Repeat (SSR) markers. *J Plant Mol Breed*. 11(2): 94-106. doi:10.22058/JPMB.2024.2024521.1297.

Introduction

Pineapple (*Ananas comosus* (L) Merr.) is one of the most economically important tropical fruits, widely cultivated with the production estimated at 27.82 in 2020 (Shahbandeh, 2022). Dubbed the "queen of fruits" for its excellent flavour and taste, pineapple ranks as the third most significant tropical fruit globally, following Banana and Citrus (Hossain et al., 2015). Recently, pineapple consumption has surged due to its edible value and high nutritional and medicinal properties (*i.e.*, sugar, protein, digestive enzyme, bromelin, vitamins and acids). The fruit is highly perishable but adds value from its processing capacity (juice, wines, cakes, syrup, vinegar). Major producer countries are the Philippines, Costa Rica, Brazil, Indonesia, and China supplying more than 50% of the total output followed by India, Nigeria, Thailand, Mexico, and Colombia which provide most of the remaining. Other countries have contributed to pineapple production such as Benin.

In Benin, pineapple production has grown steadily from 215,000 tons in 2015 to 440,178 tons in 2020 in the past few years (DDAEP et al., 2021). Pineapple production is based on two leading cultivars Smooth Cayenne and Sugarloaf, or Perola recently included for exportation. The Benin Central Government has put effort into increasing the national production and increasing the export destination since 2016, but the export rate to Europe, the main international fresh pineapple market available, is still limited (less than 2% of the national production) (Fassinou Hotegni et al., 2012). Many constraints including fruit heterogeneity reduce the export potential. It was reported that the heterogeneity observed in fruit production can be caused by several factors such as planting material heterogeneity, and poor agronomic practices (Fassinou Hotegni et al., 2015). However, the confusion noted in pineapple cultivars due to variations in naming customs among researchers or farmers can also lead to this problem. Pineapple cultivars are often grouped according to their leaves and fruit characteristics. Cultivar groups including Cayenne, Spanish, Queen, Abacaxi, Perola, and Maipure have been documented (Noyer and Lanaud, 1997). Morphological characterization of Benin pineapple germplasm revealed five cultivars including Smooth Cayenne, Cayenne de Rothschild, Perola, Singapore Spanish, and Green Spanish. Those cultivars were grouped into three clusters: Cayenne, Spanish and Perola with some variations based on morphological variation (Adje et al., 2019). Morphological characterization of germplasm collections around the world triggered the establishment of cultivar groups based on morphological descriptors which are often influenced by the environmental, epistatic and pleiotropic effects (Leal and Antoni, 1981; Coppens d'Eeckenbrugge et al., 1997; Duval et al., 1997). Consequently, it is important to explore molecular markers to decipher the cultivar identification. More accurate

Several DNA markers have been applied to assess genetic diversity and relationship among pineapple accessions among them, the SSR markers. The SSR markers are most commonly used because they are ubiquitous, hypervariable, co-dominant, robust, specific chromosome and multi-allelic in nature (Rakshit et al., 2012). Microsatellite markers are widely used for the assessment of genetic diversity in several cultivated crop species such as sweet sorghum (Ali et al., 2008; Missihoun et al., 2015), onion (Mallor et al., 2014), rice (Ravi et al., 2003), and wheat (Salehi et al., 2018). Previous studies have reported the development of SSR markers capable of amplifying the entire genome of *A. comosus* and their use to look into a genetically diverse pineapple (Feng et al., 2013; Rodrígueza et al., 2013; Zhang et al., 2014). So far, few studies have explored the genetic diversity of pineapple germplasm in West Africa, despite the proliferation of cultivars produced over time. In this study, we employed SSR molecular markers for the first time to investigate the genetic diversity among fifty-seven pineapple accessions collected from various regions of Benin. We hypothesize that these accessions exhibit considerable variation and anticipate a robust correlation between pineapple morphological groups and the genetic groups.

Materials and Methods

Plant Materials

Fifty-seven (57) accessions were collected from the Benin pineapple core collection. The Benin pineapple core collection results in prospecting and

collection across different regions of the country. The samples used included 20 accessions of Perola group, 21 accessions of Cayenne group, 15 accessions of the Spanish group, and one of var. *bracteatus* (Table 1).

Genomic DNA extraction and SSR genotyping

Total genomic DNA was extracted from 200 mg of fresh leaves from each accession using the CTAB (Cetyl Trimethyl Ammonium Bromide) extraction protocol as previously described (Adjé et al., 2016). The quality of the extracted genomic DNA was checked by electrophoresis 1% agarose gel. All the accessions underwent genotyping using ten (10) SSR primers (listed in Table 2) distributed throughout the pineapple genome. These primers were developed by Kinsuat and Kumar (2007) and selected from the sequence information previously screened by Rodrígueza et al. (2013) for molecular diversity analysis in pineapple. The PCR reactions were performed in a total volume of 25 µl reaction solution containing 3 µl of 50 ng/µl the genomic DNA, 1.5 µl of 10 pmol of each primer, 1 µl of 1 mM of dNTPs mix, 0.2 µl 5U of Taq DNA polymerase, 5 µl of 5X PCR buffer, and 1.25 µl of 25 mM Magnesium Chloride (MgCl2). DNA amplification was performed in a Mastercycler nexus gradient (Eppendorf AG 22331 Hamburg), using the following program: 30s initial denaturation at 94 °C, followed by 35 cycles, each consisting of 94°C for 30s, primer annealing at 55 °C for 30 seconds; an extension at 72 °C for 1 min. The amplification is terminated by a final extension at 72 °C for 5 min. Amplification products were electrophoresed on a 3% agarose gel in 1x TBE solution at a constant power of 100V for 1 hour and viewed under UV light in E-Box gel documentation.

Data analysis

The markers' resolution and the discriminatory power were determined by calculating the Polymorphic Information Content (PIC), which offers an estimate of the discriminating power of each locus. The PIC value of a locus, which ranges from 0 (monomorphic) to 1 (highly informative), was calculated using PowerMarker software (Liu, 2005) according to the following formula:

$$PIC = 1 - \sum_{i=1}^{n} F_i^2$$

where: F_i is the frequency of the i^{th} allele in a locus. The dataset was analysed with MicroChecker v2.2.3 software (Van Oosterhout et al., 2004) to identify genotyping errors due to null alleles (nonamplified alleles), short allele dominance (large allele dropout), and the scoring of stutter peaks at each locus. The genetic diversity measure included percentage of polymorphic loci (P), number of alleles per locus (A), observed heterozygosity (Ho), expected heterozygosity (He), Shannon's diversity index (I), allele frequencies, were performed using GenAlEx software package vs. 6.5 (Peakall and Smouse, 2006). Nei genetic distances between pairs of accessions were calculated based on each dataset to investigate the genetic relationship between accessions. The clustering of accessions was performed based on the Nei genetic distance matrix using the unweighted pair group method with arithmetic averaging (UPGMA) with Power Maker software. For population genetic structure analysis, the Bayesian model-based clustering method of Structure V.2.3.3 software. Correlated allele frequencies were applied for the estimation of ancestry fractions of each cluster. The value of k (range 1–10) was performed. The Structure Harvester software version 0.6.92 was used to determine the optimum k value using the log probability of data, LnP(D) based on the rate of change in LnP(D) between successive K with burn of 100000 until 100000 iterations. Analysis of Molecular Variance (AMOVA) was performed to partition genetic variation among and within cultivars groups. Wright's F_{st} was used to estimate the cultivar's group differentiation and was calculated using the GenAlEx software package vs. 6.5 (Peakall and Smouse, 2006).

Results

SSR markers polymorphism and genetic diversity

All the ten markers used in this study generated a total of 23 alleles across the 57 accessions of pineapple with an average of 2.3 alleles per locus. Nine of the primers showed polymorphisms for all the accessions. The locus ACPCT124BM was monomorphic. The fragment sizes ranged from 105 pb (ANBR75) to 290 pb (ANBR73).

Table 1. Pineapple accessions used in this study. Cultivar names and groups identified by Adje, et al. (2019).

Accession code	Cultivar	Group	Accession code	Cultivar	Group
EAD1644	Smooth Cayenne	Cayenne	EAD1821	Perola	Perola
EAD1751	Baronne de Rothschild	Cayenne	EAD1678	Perola	Perola
EAD1784	Baronne de Rothschild	Cayenne	EAD1757	Perola	Perola
EAD1708	Smooth Cayenne	Cayenne	EAD1845	Perola	Perola
EAD1724	Smooth Cayenne	Cayenne	EAD1474	Perola	Perola
EAD1730	Smooth Cayenne	Cayenne	EAD1862	Perola	Perola
EAD1580	Smooth Cayenne	Cayenne	EAD1562	Perola	Perola
EAD1606	Smooth Cayenne	Cayenne	EAD1330	Perola	Perola
EAD1774	Smooth Cayenne	Cayenne	EAD1340	Perola	Perola
EAD1840	Smooth Cayenne	Cayenne	EAD1351	Perola	Perola
EAD1859	Smooth Cayenne	Cayenne	EAD1411	Perola	Perola
EAD1445	Smooth Cayenne	Cayenne	EAD1430	Perola	Perola
EAD1494	Smooth Cayenne	Cayenne	EAD1850	Singapore Spanish	Spanish
EAD1648	Smooth Cayenne	Cayenne	EAD1855	Green Spanish	Spanish
EAD1834	Smooth Cayenne	Cayenne	EAD1456	Green Spanish	Spanish
EAD1673	Smooth Cayenne	Cayenne	EAD1463	Singapore Spanish	Spanish
EAD1502	Smooth Cayenne	Cayenne	EAD1481	Green Spanish	Spanish
EAD1550	Smooth Cayenne	Cayenne	EAD1871	Green Spanish	Spanish
EAD1358	Smooth Cayenne	Cayenne	EAD1831	Green Spanish	Spanish
EAD1441	Smooth Cayenne	Cayenne	EAD1837	Singapore Spanish	Spanish
EAD2020	MD2	Cayenne	EAD1667	Green Spanish	Spanish
EAD1687	Perola	Perola	EAD1525	Green Spanish	Spanish
EAD1734	Perola	Perola	EAD1571	Singapore Spanish	Spanish
EAD1698	Perola	Perola	EAD1369	Singapore Spanish	Spanish
EAD1719	Perola	Perola	EAD1383	Green Spanish	Spanish
EAD1593	Perola	Perola	EAD1402	Singapore Spanish	Spanish
EAD1623	Perola	Perola	EAD1436	Green Spanish	Spanish
EAD176	Perola	Perola	EAD2222*	*bracteatus*	
EAD1679	Perola	Perola			

* The local name for this species code is unknown

The number of alleles detected per locus varied from 2 to 5. The marker ACLR179BMb amplified the high number of alleles whereas the minimum number was observed at ANBR81 (Supplementary Figure 1). The discriminative power of the markers was assessed by calculating the Polymorphism Information Content (PIC) provided the value of the nine polymorphic primers ranging from 0.033 to 0.658 with an average of 0.340. The lowest PIC value was observed for the locus ANBR81, in contrast the maximum was observed for the locus ACLR179BMb. According to the allelic frequencies, we considered 1 allele (4%) as rare (P<0.5), 4 (18%) as common alleles (0.05<P <0.2) and 18 (78%) as

most frequent alleles (P>0.2). The expected heterozygosity (*He*) values ranged from 0.095 (ANBR81) to 0.744 (ACLR179BMb) with a mean value of 0.413. The observed heterozygosity (H_0) varied from 0.1 (ANBR81) to 0.950 (ACPCT651BM) with the mean of 0.425 showing an excess of heterozygosity (Table 3). Analysis with MicroChecker software (at 95% of confidence level) highlighted the existence of null alleles at microsatellite marker ANBR81 (Table 2).

Phylogenetic analysis

The genetic relationship between pineapple accessions was assessed by computing the genetic distance within pairs of accessions. Nei's genetic distances between pineapple genotypes varied from 0 to 0.3, with a mean value of 0.15. The genetic distances within the pineapple cultivar group varied from 0 to 0.09, 0 to 0.12, and 0 to 0.16 respectively within the Spanish, Perola, and Cayenne groups. The UPGMA clustering analysis based on Nei's coefficient showed two main groups (Figure 1). There was no group made up exclusively of accessions from the same region. The first group (I) contained 31.57% of the accessions (14 accessions of Perola, 2 accessions of Cayenne, and 2 accessions of Spanish).

Table 2. Single Sequence Repeat (SSR) primers used for genetic diversity assessment of 57 pineapple accessions of Benin.

N°	Locus	Repeat Motif	Sequences	Fragments size	Na	Ne	I	H0	He	PIC
1	ACLR179BMa**	$(GTA)_4$	CCTTTGTTTTGTTACTTTTTAT CCAGTTATTTTTAGTAAAGTCC	227-243	2.000	1.471	0.56	0.400	0.320	0.269
2	ACLR179BMb**	$(TAA)_4$	GGACTTTACTAAAAATAACTGG ATACTAACAACACCTCTTTCAC	239-241	5.000	3.902	0.62	0.750	0.744	0.658
3	ACPCT124BM**	$(CCT)_8$	GTAGCAACAGCTATGAAAAC GATACAACGACAAGTACTACG	211-227	1.000	0.68	0.000	0.000	0	
4	ACPCT651BM**	$(GAA)_{13}$	GATACATAACAGTGTATTGGAG TAACTACTCTATGTTGTGACCA	210-220	3.000	2.266	0.69	0.950	0.559	0.518
5	ANBR58***	$(CT)_{21}$ $(CA)_{21}$	ATATGATAGGACTTACTTTTGG AAGGCTACAGATAGTTAAAGAG	147-268	2.000	1.835	0.65	0.300	0.455	0.388
6	ANBR72***	$(GA)_{27}$	TGCACCTTCTTACTTCTATAAT ACAACTAGCAAAACTTTGTATC	240-268	2.000	1.923	0.58	0.300	0.480	0.398
7	ANBR73***	$(CT)_{17}$	CATTAGATTAGTTCACAAACAA AGAATATTATGGAAAAATTGAG	280-288	2.000	2.000	1.52	0.700	0.500	0.379
8	ANBR75***	$(GA)_{30}$	ATGATCTCCTAAAAATCATAAG CTTAATTAGGGTTTTATTTGTC	109-110	2.000	1.995	1.10	0.750	0.499	0.397
9	ANBR80***	$(GA)_8$	GTTTAAGCAATAATTCCTAGAG TATAATCATGATGGAACATCTA	273-287	2.000	1.923	0.95	0.000	0.480	0.358
10	ANBR81***	(CT)21	TTAATCAAGTTCTTTAAAGGTT CTAGTAAAGTCTCTTTCCATTG	219-245	2.000	1.105	0.59	0.100	0.095	0.033
	Mean				2.3	1.94	0.806	0.425	0.413	0.340
	Standard Error				0.00	0.76	0.096	0.320	0.207	0.016

The following abbreviations represent Na: Mean value of alleles number; Ne: Number of effective alleles; I: Shannon information index; He: expected heterozygosity; Ho: observed heterozygosity; F: Fixation index and PIC: Polymorphic information content. The PIC values in bold represent the minimum, the maximum, and the mean values. **: Loci derived from *A. comosus* [modified from Kinsuat and Kumar (2007)]. ***: Loci derived from *Ananas bracteatus*. † Significant possibility of the presence of null alleles (95% confidence level) detected by Micro Checker (Van Oosterhout et al., 2004).

The second group (68.43%) was subdivided into 2 subgroups. The first subgroup IIa contained 14.28% of the accessions (8 accessions of Spanish) and the second subgroup contained 54.17% of the accessions (19 accessions of Cayenne, 6 accessions of Perola, and 5 accessions of Spanish). The accession Bracteatus EAD2222 diverged from the other accessions and constituted a separate branch on its own.

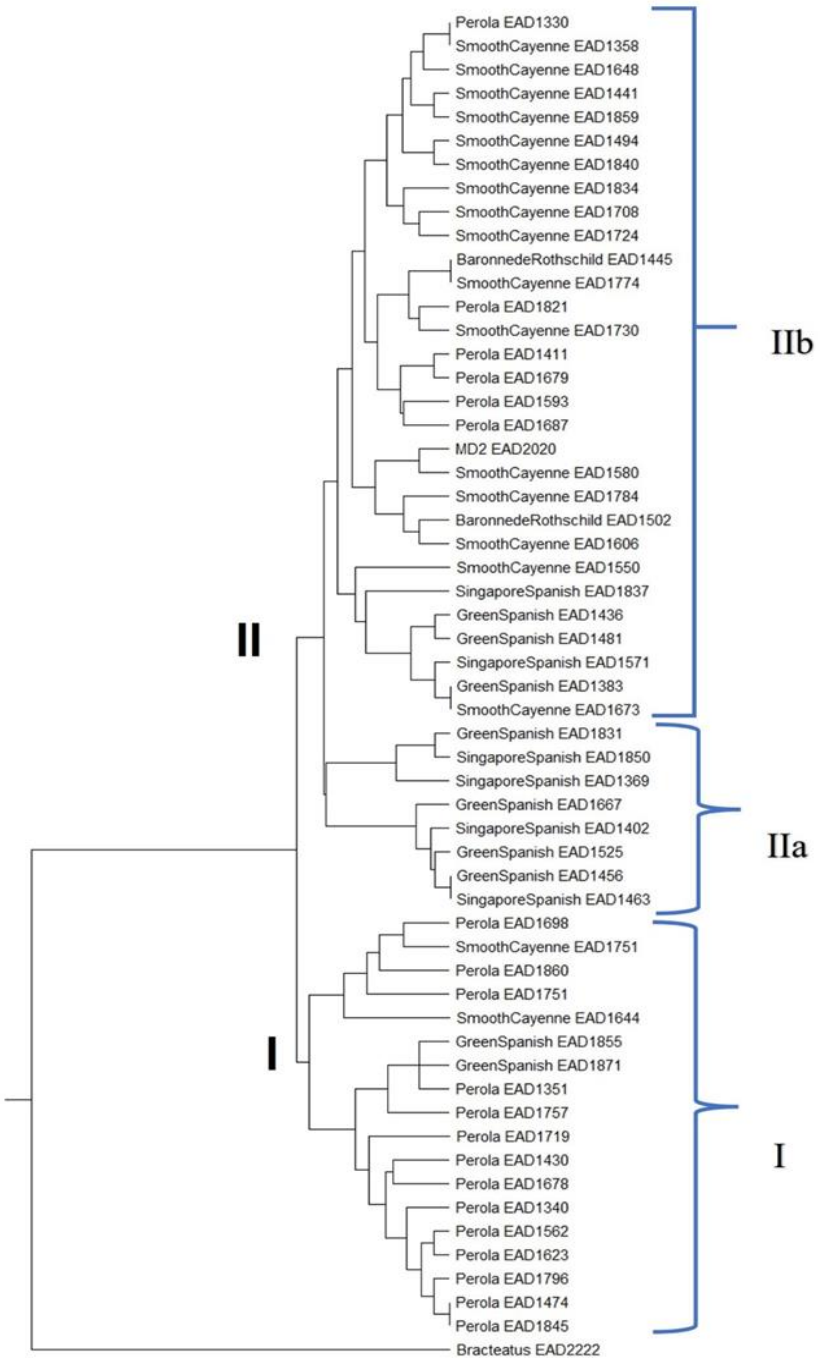

Figure 1. UPGMA cluster dendrogram (based on Nei genetic distance matrix) showing the relationships of 57 pineapple accessions based on 10 SSR markers.

Figure 2. Bar plot structure of K = 2 obtained by population STRUCTURE analysis software version 2.3.4 depicting the genetic relationships. The plot shows two major clusters separated by a straight line.

Population structure within pineapple collection

After conducting a total of 20 runs for every k value ranging from 1 to 10, the analysis showed that the optimal value of k was determined to be 2 (k=2). This suggests that accessions from the germplasm can be segregated into two major genetic clusters. The Evanno table presents values of Δk for every k from 1 to 10, where the optimal number of k (k=2) is shown by the highest yield of Δk (10.64) as given in Table 3 and Supplementary Figure 2. A scatter plot was computed based on the value and confirmed the optimal number of k as 2. The optimum model of k=2 suggested the existence of two mean sup. Membership of all accessions to a particular group was based on a likelihood threshold of 0.6 (Figure 2). Based on the threshold > 0.6, the study did not reveal any admixtures among the evaluated accessions. Group k1 had the largest membership with 58.93% of the accessions while the smallest was k2 which gathered 41.07% of the accessions. The two groups identified K1 (red color) and K2 (green color) were respectively composed of 33 accessions (most of Cayenne and Spanish) and 23 accessions (most of Perola). This structure confirmed the result of the dendrogram.

Table 3. Evanno table output generated by Structure Harvester.

K	Reps	Mean LnP(K)	Stdev LnP(K)	Ln'(K)	|Ln''(K)|	Delta K
1	20	-696.340000	0.294511	—	—	—
2	**20**	**-676.055000**	**5.209452**	**20.285000**	**55.435000**	**10.641234**
3	20	-711.205000	29.748516	-35.150000	23.425000	0.787434
4	20	-722.930000	138.020594	-11.725000	40.760000	0.295318
5	20	-693.895000	51.479147	29.035000	61.200000	1.188831
6	20	-726.060000	72.533255	-32.165000	3.485000	0.048047
7	20	-761.710000	60.080831	-35.650000	18.510000	0.308085
8	20	-815.870000	130.744138	-54.160000	61.660000	0.471608
9	20	-931.690000	211.083426	-115.820000	236.880000	1.122210
10	20	-810.630000	128.057923	121.060000	—	—

Table 4. Analysis of molecular variance (AMOVA) among and within pineapple accession groups of Benin. Groups include Spanish, Cayenne, Perola.

Source	df	SS	MS	Est. Var.	%
Among groups	1	4.151	4.151	0.046	2%
Among individual within groups	45	91.115	2.025	0.050	2%
Within individual groups	47	90.500	1.926	1.926	95%
Total	93	185.766		2.021	100%

Genetic differentiation of the identified pineapple populations

The analysis of molecular variance (AMOVA) followed by a principal coordinate analysis (PCoA) was performed to appreciate the degree of differentiation among the groups identified by Structure package. From the AMOVA, we noted that only 2% of the total genotypic variation was explained by the difference among the groups, and 2% was caused by the difference among individuals within the groups (Table 4).

The maximum of the variation had been observed within individuals within groups (96%). To support the result of the AMOVA, a low F_{ST} value (0.027) was observed in the two identified groups, and the haploid was high (Nm=14.80) suggesting the high gene exchange among the groups. These results suggested a low genetic differentiation among groups and very high within groups.

Discussion

This work based on the screening of 57 pineapple accessions, is the first detailed overview of genetic diversity and population structure in a representative collection of pineapple accessions in Benin using SSR markers. This study provides results highly useful for pineapple genetic resources conservation and management and exploitation in the breeding program in Benin.

Microsatellites (SSRs) have been considered as markers of choice for genetic and breeding applications (Sharma et al., 2021). They have been previously used to assess genetic diversity in pineapple cultivars and relatives (Gioia et al., 2019). Here, the genotyping of the Benin pineapple germplasm collection confirmed that the primers used were informative for diversity analysis. The average value of 2.3 alleles per locus is similar to those reported by Rodrígueza et al. (2013) but lower than the 3.9 reported by Ismail et al. (2020). The lower number of alleles observed compared to the previous could be attributed to a narrow diversity of the accessions used in the current study since the other authors used accessions already existing in their research institution in Malaysia. The polymorphism rate was 90%, while 100% was reported by Rodrígueza et al. (2013). The polymorphism rate was higher than the value of 40% reported by Kinsuat and Kumar (2007) who used 50 SSR markers and 53% by Rodrígueza et al. (2013) who tested 66 SSR markers. The low polymorphism rate reported by Kinsuat and Kumar (2007) and Feng et al. (2013) can be explained by the high number of SSR markers newly developed and tested for the first time by those authors to assess genetic diversity in *Ananas comosus var. comosus*. The mean PIC value of the primers was 0.340, less than 0.5 suggesting the lower discriminating nature of those markers as reported by Rodrígueza et al. (2013). The observed heterozygosity was higher than the expected heterozygosity for all cultivars showing the excess of heterozygotes, in contrast the deficit of heterozygosity was reported by Rodrígueza et al. (2013) and by Feng et al. (2013). The high value of the observed heterozygosity could indicate a variability in the alleles. The variability within the alleles can explain the high variations observed within the genotypes and confirm the somaclonal variations observed in pineapple. This can also explain the failure of the morphological or mass selection which is not successful and still showed other forms in the offspring.

Based on our molecular data, Spanish accessions share more alleles with Cayenne accessions than Pérola accessions. Thus, the Spanish could be closer

to Cayenne. This may also indicate an exchange of genetic information between those two cultivars. The two clusters revealed by the UPGMA dendrogram closely follow the botanical classification of the pineapple cultivars in Benin (Adje et al., 2019). Feng et al. (2013) reported four clusters including Cayenne, Queen, and Spanish accessions. Population structure occurrence of Benin pineapple accessions assessed using Bayesian cluster analysis with the STRUCTURE software corroborated the previous result and revealed the existence of two subpopulations K1 (mostly Cayenne accessions) and K2 (Perola accessions) within the pineapple collection in Benin. Ismail et al. (2020) also reported two subgroups in Malaysia germplasm without any morphological characteristics associated.

The AMOVA performed on the subpopulations obtained revealed high differentiation within individuals within the two groups (96%). This high variation matched with the several morphological variations reported by Tossou et al. (2015) in Cayenne and Perola cultivars. This observed variation can be also attributed to the nonexistence of a standard classification in pineapple and the nomenclatural confusion in pineapple taxonomy. Previous morphological characterization of the same samples from Benin showed three groups (Adje et al., 2019). The results showed observed a high consistency between the morphological and molecular classification confirming cultivar classification (Noyer and Lanaud, 1997). Incongruence between morphological and molecular clusters was reported by Zhao and Qin (2018), Feng et al. (2013) and Shoda et al. (2012). Previous genetic diversity studies using AFLP also showed the relationship between morphological and molecular clustering (Kato et al., 2004). In pineapple, morphological characterization is usually based on traits such as "presence or absence of spine on the leaf, leaf, fruit and flesh colour, fruit shape, etc." It was reported that the presence or absence of leaf-spine is controlled by one single gene whereas the fruit skin colour is controlled by the accumulation of anthocyanin, carotenoids and chlorophyll degradation (Collins, 1960; Brat et al., 2004). The phenotypic differentiation observed in those organs was not only due to the variation in levels of accumulation of the different pigments (Samouelian et al., 2009), it could also be justified by the genetic background behind it. During plant pigment biosynthesis, the disturbance of one or a few genes can greatly affect the plant morphology (Samouelian et al., 2009).

The narrowest Nei's genetic distance was noted between Perola and Cayenne cultivars (0.04). The same trend was reported by Rodrígueza et al. (2013). The relationship within cultivar groups of *A. comosus* var. *comosus* was not well documented. Feng et al. (2013) reported four clusters instead of three expected from conventional classification. The close relationship between Cayenne and Perola can be because, Cayenne cultivars are known to be derived from the ancestral pineapple plants originated from French Guiana (Collins, 1960). Through vegetative reproduction, these plants generate many phenotypic variant forms because of the high somaclonal variation rate for some morphological traits (Collins, 1960). Mutations are the major source of variation used in the selection of new cultivars. The diversity analysis highlighted a relatively average level of observed heterozygosity (Ho) within the identified groups of pineapple. This observation is in line with a vegetative reproduction regime of the species and a low allelic diversity is also generally within cultivars.

This research is a strong argument to the ongoing debate on pineapple production in Benin and in West Africa about the morphotype observed within the established morphological groups (Baafi et al., 2015; Tossou et al., 2015). According to Tossou et al. (2015), there are ten morphological types in Perola and four morphological types in Smooth Cayenne. However, according to farmers, there are four morphological types in Perola (conical sessile form, conical non-sessile form supported by the extension of the heart, cylindrical non-sessile form supported by the extension of the heart, cylindrical sessile form) and two morphological types in Smooth Cayenne (conical and cylindrical shape). These variations are related to fruit shapes, length, weight, and colour. Variations in shape may reflect the effect of cultivation practices (planting density, fertilization, flower induction) and abiotic factors (night temperature, sunburn, drought). Some authors demonstrated the effect of the environment on the colour and shape of the fruits (Py et al., 1987; Bartholomew and Sinclair, 1993). However, the

effect of environmental factors on the appearance of different forms of fruit has been less documented. Malézieux et al. (2003) noticed that after a long dryness, the leaves take on a pale green colour which turns pale yellow and finally red. During dry periods, leaf growth is slowed down, and leaves resume growth when water becomes available. Sunburn during inflorescence development can produce fruits that are severely distorted; these fruits being more abundant in cold periods. Our results showed evidence of genetic variation among existing germplasm and confirmed the high variability of the pineapple genome. The number of variations found in the Perola and Cayenne groups should be considered a red flag for the need for selection within breeding programs. We recommend that further studies using increased numbers of SSR markers for large-scale sampling in Perola and Cayenne can provide robust data to definitively answer the origin of morphological variation within these cultivars.

Conclusion

Exploring the genetic diversity and structure in pineapple germplasm holds significance for both conservation and improvement efforts. This work demonstrates that SSR markers can effectively differentiate between various groups, offering utility in the conservation of pineapple genetic resources. The findings reveal that Benin pineapple exhibits substantial diversity within distinct two groups. The insights generated in this study provide a valuable resource for breeders, enabling them to identify promising genotypes for enhancing the Benin pineapple production and meeting demands in the international market.

Supplementary Materials

The supplementary material for this article can be found online at: https://www.jpmb-gabit.ir/article_712245.html.

Supplementary Figure 1. Pictures of the agarose gel showing PCR amplification of marker ANBR81 (a) and marker ACLR179BMb (b).

Supplementary Figure 2. Scatter plot to determine true K value using log probability (ΔK) method.

Author Contributions

Conceptualization: C.O.A.A., E.G.A.D.; project administration: E.G.A.D., Supervision: H.A.S.. C.A., E.G.A.D.; Methodology: C.O.A.A., A.A.M.; E.G.A.D; data curation: C.O.A.A, P.S.; formal analysis, funding acquisition: C.O.A.A., validation, visualization: C.O.A.A., E.G.A.D; writing—original draft: C.O.A.A., writing review and editing: C.O.A.A., A.A.M., P.S., H.A.S., E.G.A.D, C.A.

Funding

The study was funded by the West Africa Agricultural Productivity Program (WAAPP/PPAAO) under contract No. 022/PPAAO/ProCAD.

Acknowledgments

The authors acknowledge the support of collaborators from the Genetics, Biotechnology and Seed Science (GBioS) Unit and the Molecular Genetics and Genome Analysis Laboratory.

Conflicts of Interest

The authors declare no conflict of interest.

References

Adjé, C., Achigan-Dako, E., and Agbangla, C. (2016). Optimizing genomic DNA isolation in pineapple (*Ananas comosus* L.) *J Plant Breed Genet* 4: 11-18.

Adje, C., Achigan-Dako, E., d'Eeckenbrugge, G., Hounnankpon, Y., and Agbangla, C. (2019). Morphological characterization of pineapple (*Ananas comosus*) genetic resources from Benin. *Fruits* 74(4): 167-179.

Ali, M., Rajewski, J., Baenziger, P., Gill, K., Eskridge, K., and Dweikat, I. (2008). Assessment of genetic diversity and relationship among a collection of US sweet sorghum germplasm by SSR markers. *Mol Breed* 21(4): 497-509.

Baafi, E., Osei, M.K., Agyeman, A., and Afriyie, J. (2015). Diversity studies on sugarloaf pineapple variety. *Int J Sci Knowl* 4(1): 14-25.

Bartholomew, D.P., and Sinclair, E. (1993). "Key to pest and disorders," in *Pineapple pests and disorders,* eds. R.H. Broadley, R.C.I. Wassman & E. Sinclair. (Brisbane: Department of Primary Industries), 1-7.

Brat, P., Hoang, L.N., Soler, A., Reynes, M., and Brillouet, J.M. (2004). Physicochemical characterization of a new pineapple hybrid (FLHORAN41 Cv.). *J Agric Food Chem* 52(20): 6170-6177. doi: 10.1021/jf0492621.

Collins, J.L. (1960). *The Pineapple: Botany, Cultivation and Utilization.* New York: Interscience Publishers Inc.

Coppens d'Eeckenbrugge, G., Leal, F., and Duval, M.-F. (1997). "Germplasm resources of pineapple," in *Horticultural Reviews,* ed. J. Janick. (New York: John Wiley & Sons, Inc.), 133-175.

DDAEP, ATL, and 7, A. (2021). Production d'ananas par commune campagne 2014-2015, 2020-2021. *Rapports d'activités*.

Duval, M.F., Coppens d'Eeckenbrugge, G., Ferreira, R.F., Cabral, J.R.S., and Bianchetti, B. (1997). First results from joint EMBRAPA-CIRAD *Ananas* germplasm collecting in Brazil and French Guyana. *Acta Hort* 425: 137-144.

Fassinou Hotegni, V., Lommen, W., Agbossou, E., and Struik, P. (2015). Selective plants pruning as a means to reduce heterogeneity in pineapple fruit quality. *SpringerPlus* 4(129): Doi 10.1186/s40064-40015-40907-40069.

Fassinou Hotegni, V., Lommen, W.J.M., Vorst, J.G.A.J.v.d., Agbossou, E.K., and Struik, P.C. (2012). Analysis of pineapple production systems in Benin. *Acta Hortic* 928: 47-58.

Feng, S., Tong, H., Chen, Y., Wang, J., Chen, Y., Sun, G., He, J., and Wu, Y. (2013). Development of pineapple microsatellite markers and germplasm genetic diversity analysis. *Biomed Res Int* 2013: 317912. doi: 10.1155/2013/317912.

Gioia, T., Logozzo, G., Marzario, S., Spagnoletti Zeuli, P., and Gepts, P.J.P.O. (2019). Evolution of SSR diversity from wild types to US advanced cultivars in the Andean and Mesoamerican domestications of common bean (*Phaseolus vulgaris*). *PLoS One* 14(1): e0211342.

Hossain, M.F., Akhtar, S., and Anwar, M. (2015). Nutritional value and medicinal benefits of pineapple. *Int J Food Sci Nutr* 4(1): 84-88.

Ismail, S.N., Ghani, N.S.A., Ab Razak, S.F., Abidin, R.A.Z., Mohd Yusof, M.F., Zubir, M.N., and Zainol, R. (2020). Genetic Diversity of Pineapple (*Ananas comosus*) Germplasm in Malaysia Using Simple Sequence Repeat (SSR) Markers. *Trop Life Sci Res* 31(3): 15-27. doi: 10.21315/tlsr2020.31.3.2.

Kato, C.Y., Nagai, C., Moore, P.H., Zee, F., Kim, M.S., Steiger, D.L., and Ming, R. (2004). Intra-specific DNA polymorphism in pineapple (*Ananas comosus* (L.) Merr.) assessed by AFLP markers. *Genet Resour Crop Evol* 51(8): 815-825.

Kinsuat, M., and Kumar, V. (2007). Polymorphic microsatellite and cryptic simple repeat sequence markers in pineapples (*Ananas comosus var. comosus*). *Mol Ecol Notes* 7: 1032–1035.

Leal, F., and Antoni, M.G. (1981). Description and key to the pineapple varieties in Venezuela. *Rev Facultad Agron, Univ Venezuela* 51-79.

Liu, K. (2005). PowerMarker: new genetic data analysis software. Version 3.0. *http://www.powermarker.net*.

Malézieux, E., Cote, F., and Bartholomew, D.P. (2003). "Crop environment, and vegetative physiology and growth " in *The Pineapple: Botany, Production and Uses,* eds. D.P. Bartholomew, R. Paull & K.G. Rohrbach. (Wallingford: CABI Publishing), 69-107.

Mallor, C., Arnedo-Andrés, M., and Garcés-Claver, A. (2014). Assessing the genetic diversity of Spanish *Allium cepa* landraces for onion breeding using microsatellite markers. *Sci Hortic* 170: 24-31.

Missihoun, A., Adoukonou-Sagbadja, H., Sedah, P., Agbangla, C., Ahanhanzo, C., and Dagba, R.A. (2015). Genetic diversity of *Sorghum bicolor* (L.) Moench landraces from Northwestern Benin as revealed by microsatellite markers. *Afr J Biotechnol* 14(16): 1342-1353.

Noyer, J.L., and Lanaud, C. (1997). RFLP analysis of rDNA variability in *Ananas* genus. *Acta Hortic* 425: 153-160.

Peakall, R., and Smouse, P.E. (2006). GENALEX 6: genetic analysis in Excel. Population genetic software for teaching and research. *Mol Ecol Notes* 6(1): 288-295.

Py, C., Lacoeuilhe, J.J., and Teisson, C. (1987). *The pineapple, cultivation and uses.* Paris: Editions G.-P. Maisonneuve.

Rakshit, S., Gomashe, S., Ganapathy, K., Elangovan, M., Ratnavathi, C., Seetharama, N., and Patil, J. (2012). Morphological and molecular diversity reveal wide variability among sorghum Maldandi landraces from India. *Plant Biotechnol J* 21: 145-156

Rodrígueza, D., Grajal-Martín, M.J., Isidrón, M., Petit, S., and Hormaza, J.I. (2013). Polymorphic microsatellite markers in pineapple (*Ananas comosus* (L.) Merrill). *Sci Hortic* 156: 127-130. doi: 10.1016/j.scienta.2013.03.026.

Salehi, M., A. , Arzani, M.T., and A., R. (2018). Genetic diversity of wheat wild relatives using SSR markers. *Genetika* 50: 131-141.

Samouelian, F., Gaudin, V., and Boccara, M. (2009). *Génétique moléculaire des plantes.* Editions Quae.

Shahbandeh, M. (2022). Global pineapple production by leading countries 2020. *Agriculture Farming* https://www.statista.com/statistics/298517: October, 04 2022.

Sharma, P., Mehta, G., Shefali, Muthusamy, S.K., Singh, S.K., and Singh, G.P. (2021). Development and validation of heat-responsive candidate gene and miRNA gene based SSR markers to analysis genetic diversity in wheat for heat tolerance breeding. *Mol Biol Rep* 48(1): 381-393. doi: 10.1007/s11033-020-06059-1.

Shoda, M., Urasaki, N., Sakiyama, S., Terakami, S., Hosaka, F., Shigeta, N., Nishitani, C., and Yamamoto, T. (2012). DNA profiling of pineapple cultivars in Japan discriminated by SSR markers. *Breed Sci* 62(4): 352-359. doi: 10.1270/jsbbs.62.352.

Tossou, C.C., Capo-Chichi, D.B.E., and Yedomonhan, H. (2015). Diversity and morphological characterization varieties of pineapple (*Ananas comosus* (L.) Merrill) grown in Benin. *J Appl Biosci* 87: 8113-8120.

Van Oosterhout, C., Hutchinson, W., Wills, D., and Shipley, P. (2004). MICRO-CHECKER: software for identifying and correcting genotyping errors in microsatellite data. *Mol Ecol Notes* 4: 535 - 538.

Zhang, J., Liu, J., and Ming, R. (2014). Genomic analyses of the CAM plant pineapple. *J Exp Bot* 65(13): 3395-3404. doi: 10.1093/jxb/eru101.

Zhao, H., and Qin, Y. (2018). "Genetic Diversity of Pineapple," in *Genetics and Genomics of Pineapple*. Springer), 51-59.

JPMB
Journal of Plant Molecular Breeding
Published by Genetics and Agricultural Biotechnology Institute of Tabarestan
2023 | Volume 11 | Issue 2

مقاله پژوهشی

بررسی ساختار و تنوع ژنتیکی ژرم‌پلاسم آناناس بنین (*Ananas comosus* (L.) Merr.) با استفاده از نشانگرهای SSR

شارلوت آبیک [۱و۲*]، آنتوان آبل میسیهون [۲]، پائولین سده [۲]، هوبرت آدوکونو ساگباجا [۲]، انوک گبناتو آچیگان-داکو [۱]، کلمان آگبانگلا [۲]

[۱] بخش ژنتیک، بیوتکنولوژی و علوم بذر (GBioS)،دانشکده علوم زراعی، دانشگاه آبومی کالاوی، آبومی کالاوی، جمهوری بنین
[۲] دانشکده علوم و فنون (FAST)، دانشگاه آبومی کالاوی،کوتونو، جمهوری بنین

چکیده: آناناس به عنوان محصولات مهم کشور بنین، نقشی اساسی در افزایش امنیت غذایی و درآمد خانوار برخوردار است. این محصول خوش طعم به دلیل مزه منحصر بفرد خود، در میان محصولات کلیدی مورد حمایت برای کشت در داخل کشور بنین قرار دارد. علیرغم اهمیت خاص این محصول، درک ما از میزان تنوع در منابع ژنتیکی آن محدود است. این مطالعه با هدف دسترسی به تنوع ژنتیکی و استنتاج ساختار جمعیت ۵۷ ژنوتیپ آناناس جمع‌آوری‌شده از کلکسیون ملی بنین، با استفاده از ۱۰ نشانگر (SSR) انجام گرفت. در مجموع ۲۳ آلل در این جمعیت شناسایی گردید. تعداد آلل‌ها در هر نشانگر بین ۲ الی ۴ متغیر بوده، که از میانگین ۲/۳ آلل در هر مکان نشانگری برخوردار بود. محتوای اطلاعات چندشکلی برابر با ۰/۳۴ بوده، در حالی که میانگین هتروزیگوسیتی مورد انتظار ۰/۴۳ بود. دندروگرام UPGMA دو خوشه اصلی را نشان داد. درکلکسیون آناناس مورد بررسی بر اساس تجزیه و تحلیل ژنتیکی، دو گروه مجزا با ترکیب ساختاری متمایز شناسایی شد. این گروه‌بندی توسط AMOVA نیز تأیید گردید. این مطالعه بینش ارزشمندی را در مورد میزان تنوع ژنتیکی در ژرم‌پلاسم آناناس بنین ارائه نموده که بواسطه آن فرایند حفاظت استراتژیک این گیاه را تسهیل می‌نماید. علاوه بر این، یافته‌های این تحقیق امکان استفاده از تنوع ژنتیکی موجود در ژرم پلاسم آناناس بنین را در برنامه‌های آتی به‌نژادی آناناس فراهم نموده که به نوبه خود موجبات افزایش کشت و سازگاری آناناس می‌شوند.

کلمات کلیدی: *Ananas comosus*، SSR، تنوع ژنتیکی، ژرم پلاسم، نشانگر مولکولی.

ویراستار علمی
دکتر پراسنجیت ساها،
مایوژنیکس، ایتاکا، ایالات متحده آمریکا

تاریخ
دریافت: ۱۹ اسفند ۱۴۰۲
پذیرش: ۱۳ فروردین ۱۴۰۳
چاپ: ۲۲ اردیبهشت ۱۴۰۳

نویسنده مسئول

Dr. Chalotte Abike Oladjo Adjé
abikecharlotte@gmail.com

ارجاع به این مقاله

Adjé, O.A.C., Missihoun, A.A., Sedah, P., Sagbadja, H.A., Achigan-Dako, E. and Agbangla, C. (2023). Genetic diversity and structure of Benin pineapple (Ananas comosus (L.) Merr.) germplasm collection using Simple Sequence Repeat (SSR) markers. *J Plant Mol Breed* 11(2): 94-106. doi:10.22058/JPMB.2024.2024521.1297.

JPMB | Journal of Plant Molecular Breeding
Published by Genetics and Agricultural Biotechnology Institute of Tabarestan
2023 | Volume 11 | Issue 2

Original paper

Assessment of the genetic diversity of onion cultivars (*Allium cepa*, Amaryllidaceae) collected in southern Benin

Relique Ignace Agbo[1*], Antoine Abel Missihoun[1], David Montcho[2], Lauriano Kpanou[3], Paulin Sédah[1], Germaine Avohou[1], Gustave Lambert Djèdatin[3], Clément Agbangla[1]

1. Faculty of Science and Technology, University of Abomey-Calavi, 01 BP 526 Cotonou, Republic of Benin
2. National University of Agriculture, BP 43 Kétou, Republic of Benin
3. National University of Science, Technologies Engineering and Mathematics, BP 14 Dassa-Zoumé, Republic of Benin

Abstract: Onion is one of the widely consumed vegetables in most food preparations. The present study aims to evaluate the genetic diversity of onion cultivars in southern Benin in 2023. DNA isolation of the fourteen (14) morphotypes collected was carried out using the CTAB protocol and amplified by PCR using five RAPD markers. The observed polymorphism rate was 100%. A total of 35 alleles were scored with an average of 7 per locus. The Polymorphism Information Content (PIC) of loci varies from 0.734 to 0.806 with an average of 0.784. The loci OPA08 (Na = 8 alleles, PIC = 0.806) was the most polymorphic and the most discriminating. OPB08 (Na = 6 alleles, PIC = 0.734) was the least polymorphic and the discriminating loci. The rate of rare alleles was Ra = 31.42%. The lowest genetic distance (D = 0.09) was observed between PVOV and PVAL but the highest (D = 0.94) was between FPAL and BQOV genotypes. The dendrogram classified the morphotypes into four genetic groups with a dissimilarity coefficient of 40% confirmed by the Principal Coordinate Analysis. These results are globally significant for the definition of strategies for the improvement, conservation and sustainable use of onion genetic resources in Benin.

Keywords: *Allium cepa*, Genetic differentiation, RAPD marker, Genetic group, Benin.

OPEN ACCESS

Edited by
Prof. Suresh Kumar,
Indian Agricultural Research Institute, India

Date
Received: 5 April 2024
Accepted: 2 May 2024
Published: 26 May 2024

Correspondence
Dr. Relique Ignace Agbo
agbosiram@gmail.com

Citation
Agbo, R.I., Missihoun, A.A., Montcho, D., Kpanou, L., Sedah, P., Avohou, G., Djedatin, G.L. and Agbangla, C. (2023). Assessment of the genetic diversity of onion cultivars (*Allium cepa*, Amaryllidaceae) collected in southern Benin. *J Plant Mol Breed* 11(2): 107-118. doi: 10.22058/JPMB.2024.2024966.1299.

Introduction

The onion (*Allium cepa* L.) is a herbaceous monocotyledon belonging to the family Amaryllidaceae and the genus Allium, one of the largest genera composed of 750 species including the shallot (*Allium cepa* L. var. *aggregatum* G. Don), multiplying onion (*Allium fistulosum* L.), garlic (*Allium sativum* L.) and leek (*Allium ampeloprasum* L. var. *porrum*.) (Fritsch and Friesen, 2002). Onion is a diploid bulb vegetable with a chromosome number of 2n = 2x = 16 with a largest genome size of 15290 Mbps/1C (King et al., 1998). It is a culture with asexual propagation and presenting a great morphological diversity in terms of weight, presence of scales, color and shape of bulbs and leaves, height of the plant, color of flowers, fertility and bulbil development (Pooler and Simon, 1993; Akter et al., 2015). The onion is a vegetable plant native to Central Asia, much appreciated by most populations around the world for its fresh, slightly spicy taste and its milder, more generous flavor which increases with cooking. It is widely consumed throughout the year in the majority of food preparations. Because of these curative properties, onion is used to relieve patients of certain illnesses such as: digestive disorders, hyperglycemia, heart disease, certain forms of cancer, rheumatism and cough (Birlouez, 2020). Sought after for its many uses, the domestication of the onion has been accompanied over time by a selection of cultivars with significant bulb development during the first year of cultivation. Known to the Egyptians, Romans and Greeks, this species was first exploited as a medicinal plant before becoming a condiment or vegetable (Doyle and Doyle, 1987).

Among the most cultivated vegetables in the world, the onion is ranked second, preceded by the tomato and is produced at different latitudes between 10°S and 65°N (Foury and Schweisguth, 1992; Ricciardi et al., 2020). Given its importance, the onion is cultivated in more than 140 countries for an annual global production estimated at 93,226,400 tons (Sakatai et al., 2019). In 2020, according to FAO statistics, the five main onion producing countries are India (26,738,000 tons), China (23,723,552 tons), the United States of America (3,821,044 tons), Egypt (3,155,649 tons) and Algeria (1,665,671 tons). In Sub-Saharan Africa, Nigeria and Niger are the two leading onion producing countries with annual production of 1,382,044 tons and 1,310,444 tons respectively (FAO, 2021).

In Benin, onion cultivation is mainly done in the north in the Alibori department but also in the south of the country in the Littoral, Atlantique, Mono and Couffo departments (Assogba-Komlan et al., 2006; Sikirou et al., 2011; Bello et al., 2012). Although the onion production sector is faced with numerous constraints including pressure from pests causing low levels of yield, this speculation contributes to the creation of more than 600,000 direct jobs and constitutes an important source of employment in urban, peri-urban environments and especially the banks of rivers and/or valleys in certain areas (Baco et al., 2005; Sikirou et al., 2011). Onion production in 2020 in Benin is 77,362 tons for a yield of 128,062 hg/ha (FAO, 2021). This production is very low to cover the consumption need for this vegetable in Benin. Thus, to satisfy its customers, the Beninese market is flooded with a multitude of local onion varieties coming from West African producing countries but mainly from Niger, which ranks 7th in the world as an onion producing country with a production of 1,310,444 tons after Nigeria with 1,382,044 tons of onion produced (Assogba-Komlan et al., 2006; FAO, 2021).

There is a variability and heterogeneity of shapes and colors of onion bulbs marketed in Benin which would be due to natural inter and intra specific crossings. Which creates the existence of homonymy and synonymy in onion cultivars in Benin. It is therefore urgent to carry out a genetic characterization study of onion cultivars consumed in Benin in order to remove not only this homonymy and synonymy but also to establish improvement strategies in order to boost the yield of this major crop. Thus, the National Institute of Agricultural Research of Benin (INRAB) carried out agro-morphological characterization studies which consisted of collecting onion cultivars and organizing them into collections based on agro-morphological descriptors or characters of the species. These studies made it possible to identify six (06) varieties of onion cultivated in Benin. These are: Amani Violet, Tana Red, Texas Grano 502, Galmi White, Ares and Malanville Violet (Mensah et al., 2019).

Given the influence of environmental factors on descriptors, it is essential to characterize onion cultivars at the molecular level using nucleic acid markers. Thanks to the advent of new molecular techniques which have followed one another, studies of the genetic diversity of onions based on several types of molecular markers giving greater polymorphism and numerous rare allelic forms have therefore made it possible to construct different intra-specific classifications. Nucleic acid markers (RAPD, RFLP, AFLP, SSR, etc.) have been widely used for the molecular genetic characterization of the species throughout the world (Baldwin et al., 2012), (Khosa et al., 2013), (Ricciardi et al., 2020). The use of RAPD (Random Amplified Polymorphic DNA) markers would allow the development of unique DNA profiles of onion genotypes due to a high level of polymorphism, its wide distribution in the genome and its ability to provide greater information genetics (Wilkie et al., 1993).

Unfortunately, studies on the evaluation of genetic diversity based on onion nucleic acid markers are rare and almost non-existent in Benin. It is therefore essential to know the genetic diversity of onion cultivars that the beninese market abounds with. The objective of this study is to evaluate the genetic diversity of onion cultivars (*Allium cepa*, Amaryllidaceae) in southern Benin.

Materials and Methods

Sampling plant material

The plant material consists of 14 onion morphotypes selected from a collection of 104 accessions sampled during a survey in several markets in the Atlantic and Littoral departments in southern Benin. These morphotypes were selected based on the shape and color of the bulb (Table 1, Figure 1).

Biological material

Young onion leaves represent the biological material used in this genetic characterization study. So, the onion bulbs were potted in a greenhouse in order to have young leaves from which the DNA is extracted. Polyethylene bags filled with potting soil were used to sow these bulbs. Each pot was labeled according to the morphotype it contained and watered twice a day as needed before and after germination. Around ten days after the germination of the onion bulbs, the young leaves were removed using sterile scissors, then wrapped in aluminum foil and labeled (write the morphotype code and the date of the sampling). Young leaves are used in because cell division (interphase and mitosis) is occurring and more intense at their level, which allows many more new cells to be obtained and therefore a high concentration of DNA extract. Once in the laboratory, the samples were stored in a refrigerator at a temperature of 4°C.

DNA isolation

The Laboratory of Molecular Genetics and Genome Analysis (LGMAG) of the Department of Genetics and Biotechnologies of the University of Abomey-Calavi (Benin) served as a framework for the molecular analyses. The protocol used for the extraction of genomic DNA from onion morphotypes is that using CTAB (Doyle and Doyle, 1987). Thus, 0.5 g of young leaf of each onion morphotype was weighed and then ground in a porcelain mortar with 1 ml of 2X CTAB solution. The ground material was then poured into a 2 ml Eppendorf tube then 50 µl of 20% sodium dodecyl sulfate (SDS) were added then the mixture was homogenized and incubated at 65°C for 1 hour. After 60 min, 800 µl of Chloroform Isoamyl Alcohol (CIA) in the proportions 24/1 were added to the cooled mixture then centrifuged at 10,000 rpm for 15 min. The upper aqueous phase containing the DNA is collected in a new 1.5 ml tube to which 800 µl of cold isopropanol was added and together was incubated at -20°C for 30 min. After incubation, the mixture was homogenized by inversion to precipitate the DNA. Centrifugation at 10,000 rpm for 10 min was done and the supernatant poured; 500 µl of 70% ethanol were added to the DNA pellet and centrifugation at 10,000 rpm for 5 min was done to purify the DNA. The DNA pellet is then dried and then taken up in 100 µl of Tris EDTA.

Verification of the DNA extract was carried out by electrophoresis on a 1% agarose gel. A mixture of 2 µl of DNA extract and 8 µl of 2X loading blue were deposited in the wells of the gel and migrated at 100V for 15 min with 1X TBE buffer. After migration, the gel was stained with ethidium bromide (0.1%BET) for 15 min then rinsed with

distilled water for a few minutes. Then the gel was visualized with a UV transilluminator.

RAPD markers

Five (05) RAPD markers (OPA02, OPA08, OPB05, OPN08 and OPB08) selected were used to evaluate the genetic diversity of the cultivars collected (Wilkie et al., 1993). The most polymorphic and discriminative markers (revealed in other research on the species) were selected to screen the collection of morphotypes using a thermal cycler. The reaction medium for the PCR is made to a final volume of 25 µL consisting of: 2.5 µL of PCR Buffer, 0.75 µL of MgCl2, 1 µL of dNTP, 7 µL of primer (primers), 0.25 µl of Taq polymerase, 10.5 µL of H2O and 3µl of DNA (Wilkie et al., 1993). The thermal cycler used for the amplification was the Peltier-Effect Cycling type (PTC 100TM) with an amplification program consisting of an initiation at 94°C for 5 min and 41 reaction cycles. Each cycle consists of denaturation at 94°C for 30 seconds, annealing of the primers at 37-44°C for 30 seconds and elongation carried out at 72°C for 1 min and was finished with a final extension at 72°C for 7 min (Wilkie et al., 1993).

The PCR products were separated by electrophoresis on a 3% agarose gel run at 80 V for 45 min to 1 h with 1X TBE buffer. The gel was stained with 0.1% BET for 15 min then rinsed with distilled water for 5 min. The bands were visualized on screen using a Trans UV illuminator (Figure 2).

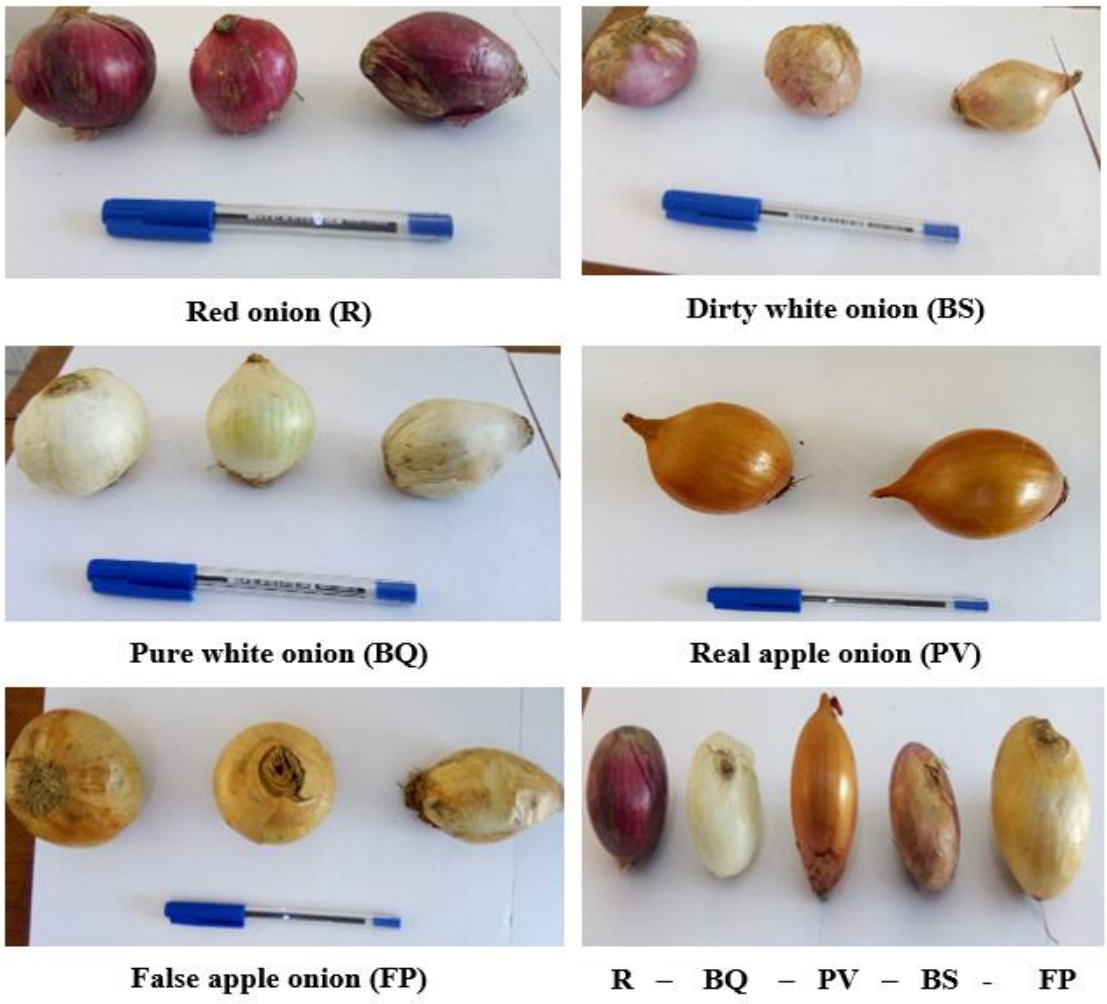

Figure 1. Onion morphotypes.

Table 1. Characteristics of selected onion morphotypes.

Cultivars names	Meaning of names	Shape of cultivars	Morphotypes code
Ayo massa vovo	Red onion	Elongated	RAL
		Flattened	RAP
		Ovoid	ROV
Ayo massa pomme	Real apple onion	Elongated	PVAL
		Ovoid	PVOV
Ayo massa pomme wégo	False apple onion	Elongated	FPAL
		Flattened	FPAP
		Ovoid	FPOV
Ayo massa wéwé tété	Pure white onion	Elongated	BQAL
		Flattened	BQAP
		Ovoid	BQOV
Ayo massa wéwé	Dirty white onion	Elongated	BSAL
		Flattened	BSAP
		Ovoid	BSOV

Data analysis

The bands obtained at each locus were recorded as allelic compositions. The absence and presence of bands are coded 0 and 1 respectively. The data obtained are recorded in an Excel sheet and constitute the analysis matrix. Genetic diversity parameters such as the polymorphism rate (P), allelic richness (Ra), the rate of rare alleles (Ar) and the Information Content of the polymorphism, PIC (Polymorphism Information Content) are estimated. The polymorphism rate is calculated by the number of polymorphic markers out of the total number of markers used. Allelic richness represents the number of alleles per locus. An allele is qualified as rare when its frequency (fi) is less than or equal to five (05) percent (fi ≤ 5%). The PIC values are calculated according to the formula: PIC = 1- Σ fi^2 with fi, the frequency of each allele (Agbo et al., 2021). The PIC value varies from 0 (monomorphic and non-discriminating locus) to 1 (highly discriminating loci, with several alleles each in low and equal frequency). Based on the binary matrix (0/1), genetic distances from (Nei, 1972) are calculated between pairs of morphotypes. To access the structure within the collection, a dendrogram is constructed according to the UPGMA method (Unweighted Pair-Group Method using the Arithmetic average) following the SAHN procedure (Sequential Agglomerative Hierarchical Nested method) of the NTSYS software version 2.11a (Rohlf 2000). In addition, to confirm the possible groupings of the cultivars analyzed, the DCENTER and EIGEN procedures of this software are used to carry out a Principal Coordinate Analysis (PCoA) based on the matrix of genetic coordinates in order to better appreciate the genetic differentiation between the groups obtained.

Table 2. Genetic parameters of the onion RAPD Primers used (Wilkie et al. 1993).

Primers	Primer sequence	PIC	Ra	Ar
OPA02	TGCCGAGCTG	0.795	7	2
OPA08	GTGACGTAGG	0.806	8	2
OPB05	TGCGCCCTTC	0.780	7	2
OPB08	GTCCACACGG	0.734	6	3
OPN08	ACCTCAGCTC	0.805	7	2
Mean	-	0.784	7	-

Results

Polymorphism and genetic variability

All of the RAPD markers used turned out to be polymorphic, i.e. a polymorphism rate of 100%. In total, 35 alleles were noted with an average of 7 per marker. The information content of the

polymorphism (PIC) ranges from 0.734 to 0.806 with an average of 0.784. The most polymorphic marker is the OPA08 marker with 8 alleles and the least polymorphic is the OPB08 marker with 6 alleles. The most discriminating marker is OPA08 with a PIC of 0.806 while the least discriminating is OPB08 with a PIC of 0.734. The rate of rare alleles is 31.42% (11 rare alleles out of 35) (Table 2).

Genetic structure of the collection

In order to evaluate the genetic structuring of onion morphotypes, a genetic distance matrix based on dissimilarity was constructed (Table 3). The lowest genetic distance (D = 0.09) is observed between the PVOV and PVAL morphotypes. On the other hand, the highest genetic distance (D = 0.94) is observed between the cultivars FPAL and BQOV on the one hand and between ROV and PVAL on the other hand. Dendrogram obtained from the cluster analysis of the 14 morphotypes, using the average distance algorithm (UPGMA SAHN method analysis), revealed four genetic groups with a dissimilarity coefficient proposed by the analysis procedure of 40% (Figure 3). The first group is made up of 2 morphotypes namely: PVAL and PVOV which are onion morphotypes qualified as true apples. The second group only includes quality white morphotypes such as BQAP, BQOV and BQAL.

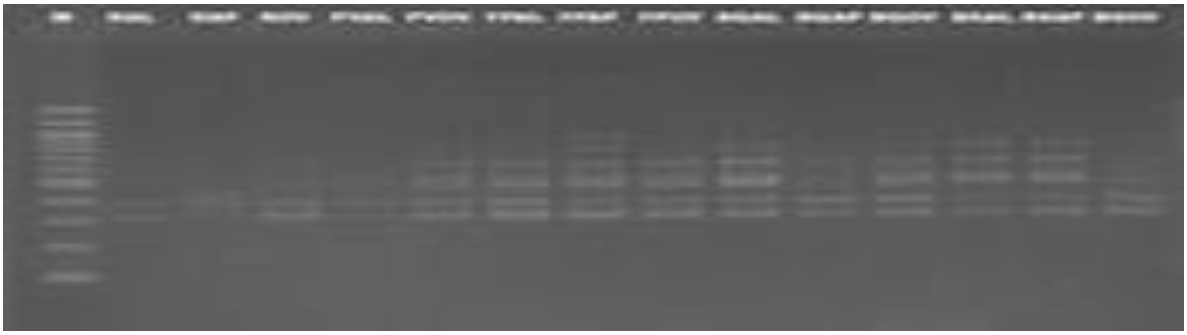

Figure 2. Polymorphic bands within the gel profile generated by the OPN08 marker used in the study. The codes correspond to the initials of the onion morphotypes and M: Size Marker.

Table 3. Genetic distance dissimilarity matrix of Nei (1972) estimated between different onion morphotypes.

	PVAL	ROV	BQAP	RAL	RAP	BQOV	BQAL	PVOV	BSAL	FPAP	FPAL	BSOV	FPOV	BSAP
PVAL	0.00													
ROV	0.94	0.00												
BQAP	0.40	0.52	0.00											
RAL	0.43	0.25	0.38	0.00										
RAP	0.35	0.42	0.48	0.22	0.00									
BQOV	0.43	0.69	0.20	0.42	0.51	0.00								
BQAL	0.37	0.59	0.24	0.29	0.37	0.37	0.00							
PVOV	0.09	0.82	0.53	0.46	0.46	0.37	0.50	0.00						
BSAL	0.41	0.51	0.59	0.32	0.58	0.51	0.54	0.27	0.00					
FPAP	0.50	0.51	0.72	0.25	0.49	0.63	0.54	0.53	0.21	0.00				
FPAL	0.64	0.66	0.91	0.52	0.52	0.94	0.69	0.66	0.41	0.32	0.00			
BSOV	0.27	0.54	0.50	0.28	0.28	0.54	0.37	0.38	0.24	0.24	0.35	0.00		
FPOV	0.35	0.58	0.65	0.36	0.43	0.69	0.52	0.37	0.25	0.18	0.35	0.21	0.00	
BSAP	0.71	0.62	0.73	0.34	0.54	0.77	0.40	0.90	0.43	0.23	0.36	0.36	0.41	0.00

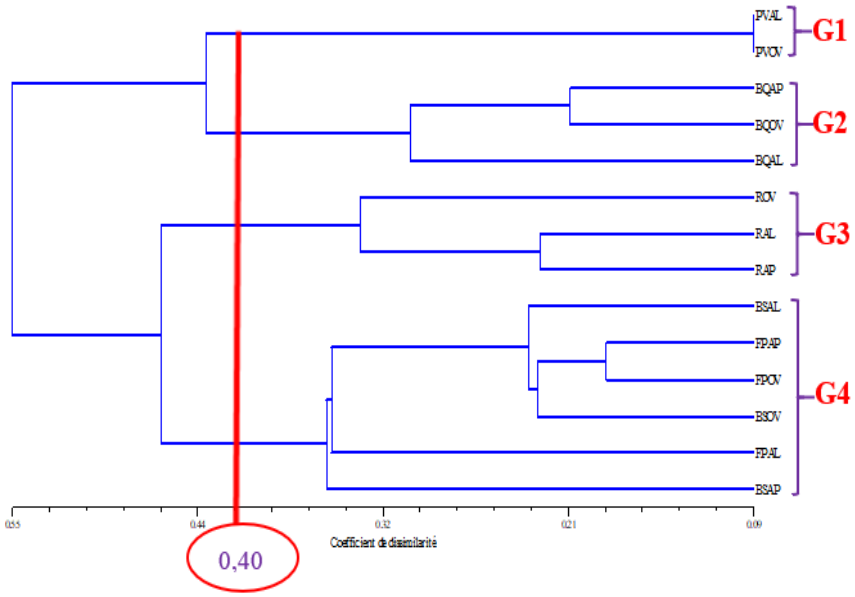

Figure 3. Dendrogram of onion morphotypes.

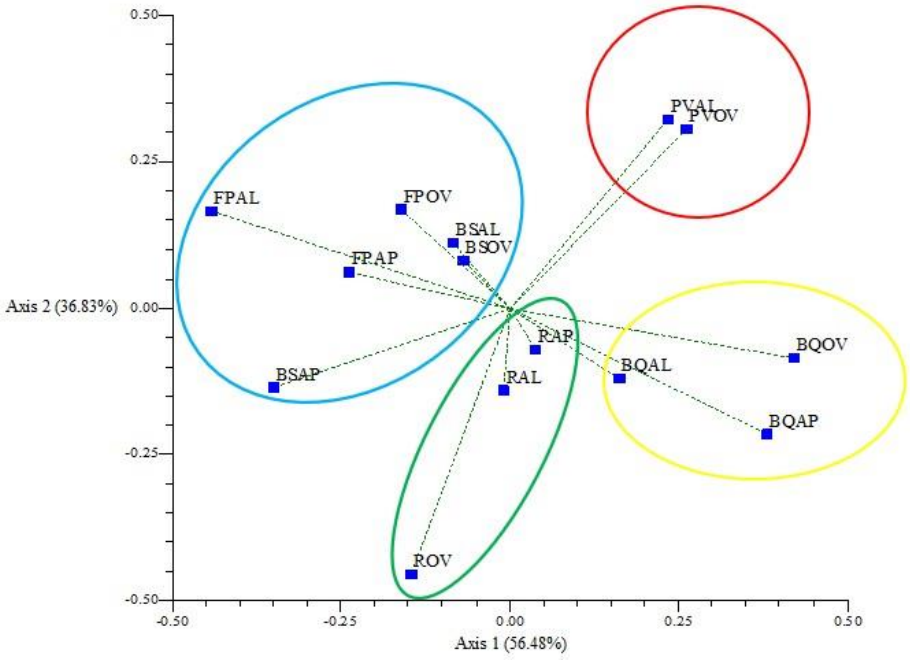

Figure 4. Principal Coordinate Analysis (PCoA) of onion morphotypes. The third group is made up only of Red morphotypes such as ROV, RAL and RAP. Finally, the fourth group is composed of a mixture of morphotypes of simple white onions and false apples such as BSAP, BSOV, BSAL, FPAP, FPAL, FPOV. This classification of the 14 morphotypes into four groups is confirmed by Principal Coordinate Analysis (PCoA). The first two axes express 93.31% of the total variation with 56.48% for axis 1 and 36.83% for axis 2.

Discussion

The onion is an agricultural crop of great importance in West Africa, the subject of intensive trade between countries. The onion sector constitutes for the majority of producers in this region a means of meeting daily needs. But several poorly performing local varieties are produced in these different countries, particularly in Benin. The varietal selection of a species involves its characterization with genetic markers which provide information on the genetic diversity of the species by referring to genome differences ranging from the rearrangement of a single base pair to an entire chromosome (Hamrick and Godt, 1996). Rouamba et al. (1994) report that the color and shape of onion bulbs are the main morphological descriptors that help differentiate African varieties. Variations in genome interactions with the environment reveal notable changes in plant diversity (Huang and Han, 2014). It should be noted that genetic diversity is a fundamental strategy in improving cultivars in terms of productivity and also for the conservation of agricultural crops (Sudha et al., 2019). Twenty-eight (28) morphological markers (descriptors) were identified from characters of onion bulbs, leaves, stems, flowers and seeds (Rabiou et al., 2015). Although these markers are easily observed by eye, they have the disadvantage of being dominant, influenced by the environment and often dependent on the stage of development of the plant (Cramer and Havey, 1999). However, nucleic acid markers (RAPD, RFLP, AFLP, SSR, etc.) directly resulting from existing polymorphism at the DNA level are very useful to differentiate the different varieties of onion, to distinguish the species from other cultivated species and spontaneous species of the genus *Allium* and to analyze the levels of introgression between the onion and other species of the genus (Rabiou et al., 2015). RAPD markers, although dominant, are widely used for the molecular genetic characterization of onion genetic resources (Sudha et al., 2019). This wide use is justified by the specificity, dominance, relatively high discriminating power, wide distribution (present along the genome) and multi-allelicism of RAPD markers. The results of the present study confirm this effectiveness of these markers by the high rate of polymorphism obtained (100%) and the high value of the average PIC (0.784).

The RAPD markers were able to group the collection of onions studied on the basis of molecular traits close to the color of the bulbs but not their shapes. Similar results were obtained by (McCallum et al., 2008)and (Khar et al., 2011)on the molecular characterization of onion with microsatellite markers. (Sudha et al., 2019)obtained 2 genotypic groups with 16 RAPD and SSR primers on a collection of nine (09) onion cultivars. This could mean that the shape of the onions (rounded, elongated or flattened) is not of genotypic origin but depends on environmental factors (climatic and edaphic). Indeed, the color of the onion bulb is mainly governed by a set of genes with Mendelian inheritance (Rieman, 1931). According to El-Shafie and Davis (1967), the white color of the bulb can be attributed either to an incompletely dominant color inhibitor gene (II), which suppresses all coloring, or to a recessive gene (rr) leading to the colorless mutants appearing in red varieties, yellow or brown. This could explain the predominance of white morphotypes. Kim et al. (2004) indicate the existence of another independent allele (P) which controls the purple color of the bulbs. According to Fossen et al. (1996), the presence of flavonoid compounds from the anthocyanin family produces colors in the bulb varying from red to purple. It should be noted that the genetic groups obtained in this study include cultivars belonging to different local varieties. These morphotypes would be synonyms.

The literature has documented the existence of six (06) varieties of onion cultivated in Benin (Mensah et al., 2019). These varieties found in southern Benin come from local crops and also imports. The four (04) genetic groups obtained in the present work corroborate these different varieties, apart from the cultivars qualified as true apple. In fact, this group of morphotypes is a genetically modified variety imported by traders. The genetic group of red onion morphotypes corresponds to the varieties Rouge de Tana, Violet d'Amani, Violet de Malanville and Ares; the white quality group represents onions of the Blanc de Galmi variety; the heterogeneous group consisting of simple white morphotypes and false apples corresponds to the Texas Grano 502 varieties. These cultivars bearing different local

names but which belong to the same genotypic class could be synonyms. Indeed, according to the work of (Boukary et al., 2012) and those conducted by Rabiou et al. (2015) in Niger, certain synonyms of onion names designate different ecotypes, but these ecotype names vary depending on the language of the producer; the same ecotype can have different vernacular names from one site to another. This synonymy is therefore lifted by this marker.

Also, we note the massive use of improved onion varieties in Africa and in particular in Benin which could lead to the loss of the genetic diversity of this very important crop. The presence in Benin of numerous imported varieties resulted in the relatively high rate of rare alleles (31.42%) obtained in the present study of the characterization of the onion collection which is explained by gene flow during exchanges. onion seed companies and the strong heterogeneity of onion cultivars present in southern Benin.

To avoid this decline in genetic structure, it is essential to take measures to conserve the germplasm of the species (Rouamba et al., 2001). It is in this sense that FAO through RADHORT (African Horticulture Development Network) and IPGRI (International Plant Genetic Resources Institute), now Bioversity International, had set up networks to coordinate the collection, conservation and use of wild species, improved varieties, farmer varieties and ecotypes of onion in Africa (Currah, 2002).

Conclusion

This summary study has highlighted a significant level of diversity of onion cultivars in southern Benin. The molecular genetic characterization of onion cultivars with RAPD markers made it possible to determine the genetic structure of the 14 onion morphotypes in four (04) genotypic groups. These results show that the local variety names given by traders and producers do not reflect perfect identity of the genotype of the cultivars. These results are generally significant for the definition of strategies for the improvement, conservation and sustainable use of onion genetic resources in Benin.

Supplementary Materials

No supplementary material is available for this article.

Author Contributions

Conceptualization, methodology, formal analysis, writing—original draft preparation, R.I.A.; read the protocol and improved the manuscript drafted, A.A.M. and D.M.; collection and sampling, R.I.A. and L.K.; molecular analysis, R.I.A., P.S. and GA; validation, writing—review and editing, R.I.A., G.L.D. and C.A. All authors have read and approved the final manuscript.

Funding

The authors declare that no funds, grants, or other support were received during the preparation of this manuscript.

Acknowledgments

The authors thank the onion producers and traders.

Conflicts of Interest Statements

The authors declare that they have no conflict of interest.

References

Agbo, R.I., Missihoun, A., Montcho, D., Dagba, R., Sédah, P., and Agbangla, C. (2021). Spatial scale patterns of genetic diversity and gene flow in populations of sweet detar (*Detarium microcarpum* Guill. & Perr.; Fabaceae). *Annu Res Rev Biol* 37(5).

Akter, M., Biswas, A., Siddique, S., Hossain, S., and Ivy, N. (2015). Estimation of genetic diversity in onion (*Allium cepa* L.). *The Agriculturists* 13(1): 26-34.

Assogba-Komlan, F., Sikirou, R., Singbo, A., and Azagba, J. (2006). *Mieux conduire la culture de l'oignon sous regime pluvial au Sud du Bénin. Référentiel technico-économique (RTE).* Bénin.

Baco, M., Bello, S., and Assogba-Komlan, F. (2005). Etude socio-économique de la production et de la commercialisation de l'oignon dans l'Alibori. *Bull de la Recherche Agron du Bénin* 47: 26-37.

Baldwin, S., Pither-Joyce, M., Wright, K., Chen, L., and McCallum, J. (2012). Development of robust genomic simple sequence repeat markers for estimation of genetic diversity within and among bulb onion (*Allium cepa* L.) populations. *Mol Breed* 30: 1401-1411.

Bello, S., Amadji, G., Gbehounou, G., Aho, N., and Ahanchede, A. (2012). Influence de la densité de repiquage sur l'enherbement et la production d'oignon au Nord-est du Bénin. *J Animal Plant Sci* 15(1): 2074-2082.

Birlouez, É. (2020). Petite et grande histoire des légumes. *Petite et grande histoire des légumes*: 1-176.

Boukary, H., Roumba, A., Adam, T., Barage, M., and Saadou, M. (2012). Interaction between onion ecotypes variability and agroclimatics factors in Niger. *Tropicultura* 30(4): 209-215.

Cramer, C.S., and Havey, M.J. (1999). Morphological, biochemical, and molecular markers in onion. *HortScience* 34(4): 589-593.

Currah, L. (2002). 16 Onions in the tropics: cultivars and country reports. *Allium crop science: Rec Adv* 2(17): 379.

Doyle, J.J., and Doyle, J.L. (1987). A rapid DNA isolation procedure for small quantities of fresh leaf tissue. *Phytochem Bull* 19: 11-15.

El-Shafie, M., and Davis, G.N. (1967). Inheritance of bulb color in the onion (*Allium cepa* L.). *Vegetable Crops of Russia*.

FAO, F. (2021). Agriculture Organization of the United Nations. FAOSTAT–food and agriculture data: http://www. FAO. org/faostat/en/# data/FBS, Rome (Headquarters). *Accessed online*.

Fossen, T., Andersen, Ø.M., Øvstedal, D.O., Pedersen, A.T., and Raknes, Å. (1996). Characteristic anthocyanin pattern from onions and other *Allium* spp. *J Food Sci* 61(4): 703-706.

Foury, C., and Schweisguth, B. (1992). Onion. *Amélioration des espèces végétales cultivées: Objectifs et Critères de Sélection.*: 406-473.

Fritsch, R., and Friesen, N. (2002). Evolution, domestication and taxonomy. *Allium crop science: Rec Adv*: 5-30.

Hamrick, J., and Godt, M.W. (1996). Effects of life history traits on genetic diversity in plant species. *Philosophical Transactions of the Royal Society of London. Series B: Biological Sciences* 351(1345): 1291-1298.

Huang, X., and Han, B. (2014). Natural variations and genome-wide association studies in crop plants. *Annu Rev Plant Biol* 65: 531-551.

Khar, A., Lawande, K., and Negi, K. (2011). Microsatellite marker based analysis of genetic diversity in short day tropical Indian onion and cross amplification in related *Allium* spp. *Genet Resour Crop Evol* 58: 741-752.

Khosa, J., Dhatt, A., Negi, K., and Singh, K. (2013). Characterization of Allium germplasm using bulb onion derived SSR markers. *Crop Improv* 40(1): 69-73.

Kim, S., Binzel, M.L., Yoo, K.S., Park, S., and Pike, L.M. (2004). Pink (P), a new locus responsible for a pink trait in onions (*Allium cepa*) resulting from natural mutations of anthocyanidin synthase. *Mol Genet Genomics* 272(1): 18-27.

King, J., Bradeen, J., Bark, O., McCallum, J., and Havey, M. (1998). A low-density genetic map of onion reveals a role for tandem duplication in the evolution of an extremely large diploid genome. *Theor Appl Genet* 96: 52-62.

McCallum, J., Thomson, S., Pither-Joyce, M., Kenel, F., Clarke, A., and Havey, M.J. (2008). Genetic diversity analysis and single-nucleotide polymorphism marker development in cultivated bulb onion based on expressed sequence tag–simple sequence repeat markers. *J Am Soc Hort Sci* 133(6): 810-818.

Mensah, A.C.G., Sikirou, R., Assogba-Komlan, F., Yarou, B.B., Midingoyi, S.K., Honfoga, J., Dossoumou, M.E., Kpéra, G.N., and Djinadou, A.K.A. (2019). *Mieux produire l'oignon au Bénin. Référentiel technico-economique (RTE). MAEP/INRAB/FIDA/ProCar/PADMAR/World Vegetable Center/Bénin.* Bénin.

Nei, M. (1972). Genetic distance between populations. *Midl. Nat.* 106(949): 283-292.

Pooler, M., and Simon, P. (1993). Characterization and classification of isozyme and morphological variation in a diverse collection of garlic clones. *Euphytica* 68: 121-130.

Rabiou, A., Bakasso, Y., Adam, T., Saadou, M., and Baudoin, J.-P. (2015). Biologie, diversité et outils pour l'analyse de la diversité génétique de l'oignon, *Allium cepa* L.(synthèse bibliographique). *Biotech, Agro, Société et Envir* 19(2).

Ricciardi, L., Mazzeo, R., Marcotrigiano, A.R., Rainaldi, G., Iovieno, P., Zonno, V., Pavan, S., and Lotti, C. (2020). Assessment of genetic diversity of the "acquaviva red onion"(*Allium cepa* L.) apulian landrace. *Plants* 9(2): 260.

Rieman, G.H. (1931). Genetic Factors for Pigmentation in the Onion and their Relation to Disease Resistance.

Rohlf , F. (2000). NTSYS-pc: numerical taxonomy and multivariate analysis system, version 2.1. *New York: Exeter Software*.

Rouamba, A., Sandmeier, M., Sarr, A., and Ricroch, A. (2001). Allozyme variation within and among populations of onion (*Allium cepa* L.) from West Africa. *Theor Appl Genet* 103: 855-861.

Rouamba, A., Sarr, A., and Ricroch, A. (1994). Dynamic management of genetic resources of *Allium cepa* L.(onion) in West Africa. *Acta Hortic* 443: 185-190.

Sakatai, D.P., Chendjou, R., Bassala, J.-P.O., Sobda, G., Kamga, R., and Hamidou, A. (2019). Caractérisation de cinq variétés d'oignons (*Allium cepa* L.) à partir des paramètres physiques de la maturation des bulbes en vue d'optimiser leur production à l'Extrême-Nord Cameroun. *Afr Sci* 15(1): 314-331.

Sikirou, R., Hoteigni, J., Godonou, I., James, B., Grehounou, G., and Assogba-Komlan, F. (2011). Performance of varieties of Gboma (*Solanum macrocarpon*) under disease pressure with organic amendment in Southern Benin. *Annal Des Sci Agro* 15(2): 205-216.

Sudha, G.S., Ramesh, P., Sekhar, A.C., Krishna, T.S., Bramhachari, P., and Riazunnisa, K. (2019). Genetic diversity analysis of selected onion (*Allium cepa* L.) germplasm using specific RAPD and ISSR polymorphism markers. *Biocatal Agric Biotechnol* 17: 110-118.

Wilkie, S.E., Isaac, P.G., and Slater, R.J. (1993). Random amplified polymorphic DNA (RAPD) markers for genetic analysis in Allium. *Theor Appl Genet* 86: 497-504.

JPMB
Journal of Plant Molecular Breeding
Published by Genetics and Agricultural Biotechnology Institute of Tabarestan
2023 | Volume 11 | Issue 2

مقاله پژوهشی

ارزیابی تنوع ژنتیکی ارقام پیاز (*Allium cepa*، Amaryllidaceae) جمع‌آوری شده در جنوب بنین

رلیک ایگنس اگبو*[۱]، آنتوان ابل میسهون[۱]، دیوید مونچو[۲]، لوریانو کپانو[۳]، پائولین سده [۱]، ژرمن آوهو[۱]، گوستاو لمبرت جداتین[۳]، کلمنت آگبانگلا [۱]

[۱] دانشکده علوم و فناوری، دانشگاه آبومی-کالاوی، کوتونو، جمهوری بنین
[۲] دانشگاه ملی کشاورزی، کتو، جمهوری بنین
[۳] دانشگاه ملی علوم، مهندسی فناوری و ریاضیات، داسه-زوم، جمهوری بنین

چکیده: پیاز یکی از سبزیجات پرمصرف در مواد غذایی بشمار می‌رود. مطالعه حاضر با هدف بررسی تنوع ژنتیکی ارقام پیاز در جنوب بنین در سال ۲۰۲۳ انجام شد. استخراج DNA ۱۴ مورفوتیپ جمع‌آوری‌شده با استفاده از پروتکل CTAB انجام شد و با استفاده از پنج آغازگر RAPD در PCR تکثیر شد. میزان پلی‌مورفیسم مشاهده شده ۱۰۰٪ بود. در مجموع ۳۵ آلل با میانگین ۷ در هر جایگاه امتیازدهی گردید. محتوای اطلاعات چندشکلی(PIC) جایگاه‌ها از ۰،۷۳۴ تا ۰.۸۰۶ با میانگین ۰.۷۸۴ متغیر بود. آغازگر OPA08 (Na = PIC = 8 0.80)، بیشترین چندشکلی و تمایز را نشان داد. آغازگر OPB08 (Na = 6 آلل، PIC = 0.734) دارای کمترین چندشکلی و جایگاه متمایزکننده بود. میزان آلل‌های نادر Ra = 31.42 درصد بود. کمترین فاصله ژنتیکی (D = 0.09) بین ژنوتیپ‌های PVOV و PVAL مشاهده شده، در حالی‌که بیشترین فاصله (D = 0.94) بین ژنوتیپ‌های FPAL و BQOV بود. دندروگرام مورفوتیپ‌ها را به چهار گروه ژنتیکی با ضریب عدم تشابه ۴۰٪ خوشه‌بندی نمود که نتایج توسط تجزیه و تحلیل مختصات اصلی نیز تایید گردید. بطورکلی نتایج این تحقیق می‌تواند برای تعریف استراتژی‌هایی به منظور بهبود، حفاظت و استفاده پایدار از منابع ژنتیکی پیاز در کشور بنین مورد استفاده قرار گیرد.

کلمات کلیدی: *Allium cepa*، تمایز ژنتیکی، نشانگر RAPD، گروه ژنتیکی، بنین.

ویراستار علمی
دکتر سروش کومار،
موسسه تحقیقات کشاورزی هندوستان، هند

تاریخ
دریافت: ۱۷ فروردین ۱۴۰۳
پذیرش: ۱۳ اردیبهشت ۱۴۰۳
چاپ: ۶ خرداد ۱۴۰۳

نویسنده مسئول
دکتر رلیک ایگنس آگبو
agbosiram@gmail.com

ارجاع به این مقاله
Agbo, R.I., Missihoun, A.A., Montcho, D., Kpanou, L., Sedah, P., Avohou, G., Djedatin, G.L., and Agbangla, C. (2023). Assessment of the genetic diversity of onion cultivars (*Allium cepa*, Amaryllidaceae) collected in southern Benin. *J Plant Mol Breed.* 11(2): 107-118. doi:10.22058/JPMB.2024.2024966.1299.

JPMB | Journal of Plant Molecular Breeding
Published by Genetics and Agricultural Biotechnology Institute of Tabarestan
2023 | Volume 11 | Issue 2

Genome-wide analysis of the *HSP90* gene family and their roles in soybean growth and development

Original paper

Samira Mohammadi*, Firouzeh Sohrevardi, Ghorbanali Nematzadeh

Genetics and Agricultural Biotechnology Institute of Tabarestan (GABIT), Sari Agricultural Sciences and Natural Resources University (SANRU). Sari. Iran.

Abstract: Heat shock protein of 90 kDa or HSP90 plays an important dynamic role in regulating biotic and abiotic stresses through multiple functional mechanisms. The present study aimed to perform a comprehensive analysis of the *HSP90* gene family in soybean. In total, 20 *HSP90* genes from soybean were identified and showed unequal distribution on the 13 chromosomes. The evolutionary tree divided these genes into three main groups based on their subcellular localization. In Group I, nearly all of the *HSP90* genes are distributed in the nucleus or cytoplasm. In Group II, the *HSP90s* were mostly classified in the endoplasmic reticulum. *HSP90* genes were exclusively found in the mitochondria or chloroplast in Group III. Phylogenetic relationships have shown that genes in similar subgroups have the same exon-intron structure and number of introns. Glyma14g219700, Glyma17g258700, and Glyma07G207600 were identified as hub proteins based on their high degrees of interaction. In addition, *Glyma02g302500*, *Glyma08g332900*, *Glyma14g219700*, *Glyma17g258700*, and *Glyma18g074100* genes displayed high expression levels in all of the tissues at different developmental stages. These findings provide a complete overview of the *GmHSP90* gene family classification and evolution, which can help to identify the functional properties of the *HSP90* genes in soybean growth and development.

Keywords: Gene expression profiling, gene structure, heat shock protein, phylogenetic analysis, protein-protein interaction network, subcellular localization.

OPEN ACCESS

Edited by

Dr. Parviz Heidari,
Shahrood University of Technology,
Iran

Date

Received date: 06 June 2022
Accepted date: 16 May 2024
Published: 26 May 2024

Correspondence

Dr. Samira Mohammadi
s.mohamadi@stu.sanru.ac.ir

Citation

Mohammadi, S., Sohrevardi, F. and Nematzadeh, G.A. (2023). Genome-wide analysis of the *HSP90* gene family and their roles in soybean growth and development . *J Plant Mol Breed*. *11* (2): 119-132.
doi: 10.22058/JPMB.2024.555256.1256.

Introduction

Plants encounter inevitable environmental challenges such as heat shock, cold, salt, submergence, drought, nutrient deficiency, and chemical pollution, which severely limit their normal growth and development (Vaughan et al., 2018). When plants are faced with these stresses, specific defense responses or mechanisms activate at both molecular and physiological levels. One of these responses is the induction of heat shock proteins (HSPs) for the survival of stressed cells (Sangster and Queitsch, 2005). HSPs are divided into five main categories based on their molecular weight, namely, HSP100, HSP90, HSP70, HSP60, and small HSP (sHSP, HSP20) (Wang et al., 2004).

HSP90s are molecular chaperones and highly conserved in prokaryotes to eukaryotes, which helps to regulate and maintain the compatibility of various proteins and also protects normal cells against stress stimuli. In eukaryotes, HSP90s play a wide variety of roles in stress signaling, including stabilizing and, or correctly folding their client proteins, and assisting in protein degradation (Hoter et al., 2018).

HSP90 chaperones are involved in transcription factors and protein kinase folding, along with activating a substrate for initiating stress signaling (Song et al., 2019). The *HSP90* gene family under normal or stressful conditions is responsible for preventing protein aggregation and facilitating denatured proteins refolding, which helps protein folding with the participation of other chaperones and the formation of a mechanism (Picard, 2002; Wang et al., 2004).

HSP90 protein includes an ATP-binding domain at the N-terminal, an intermediate domain, and a dimerization domain at the C-terminal (Pearl and Prodromou, 2006). The expression patterns of the *HSP90* gene family have been broadly studied in various plant tissues and organs, and it has been found that HSP90s affect the plant's tolerance to biotic and abiotic stresses (Chen et al., 2018; di Donato and Geisler, 2019; Song et al., 2019; Bettaieb et al., 2020).

The *HSP90* genes were examined in *Aeluropus littoralis* (Hashemipetroudi et al., 2019), *Cucumis sativus* L. (Zhang et al., 2021), pepper (Jing et al., 2020), barley (Chaudhary et al., 2019), *Nicotiana tabacum* (Song et al., 2019), and a variety of lower plants to higher plants (Li et al., 2020). Cucumber *HSP90* genes were differentially expressed under gibberellin, photoperiod, and temperature, powdery, and downy mildew stimuli (Zhang et al., 2021). *HSP90* genes of *Brassica napus* played crucial roles in seed germination and development (Reddy et al., 1998). It has been found that the *HSP90* family is involved in the differentiation and development of cotton fiber through the homeostasis maintenance of cellular (Sable et al., 2018).

Soybean (*Glycine max* L.) is a nutritionally and economically important crop, the world's most important edible oilseed crop due to its oil content, vegetable protein, and nutritional value. This plant also provides essential amino acids for animals and humans. In addition, it is used as a food supplement and pharmaceutical source (Shelke et al., 2023). However, the risk of damage from abiotic and biotic stresses threatens soybean production)Zhang et al., 2015(.

In rice, *OsHsp90-2* and *OsHsp90-4* genes were upregulated to heat, cold, salt, and drought stresses (Hu et al., 2009). It has been shown that in Arabidopsis, expression of *HSP90* genes increased by salt and heat stresses (Prasad et al., 2010; Mishra and Grover, 2016). According to the available information about the functional diversity of *HSP90* genes in plants, HSP90 proteins can be considered ideal targets for improving the development of soybean cultivars tolerant to a wide range of stresses. Thus, we investigated *HSP90* genes and estimated their evolutionary relationships, functional protein domains analysis, physicochemical features, gene structure, conserved motifs analysis, subcellular and chromosomal localization, and expression analysis during soybean growth and development. The findings of this study have revealed a better comprehension of *GmHSP90* genes in soybean, while providing a basis for the complete investigation of candidate genes in the future.

Materials and Methods

Identification of soybean HSP90 proteins

The *G. max* genome sequences were downloaded from the Phytozome v13 database. To collect GmHSP90 protein sequences, profile hidden

Markov models (HMMs) of the HSP90 domain (Pfam: PF00183) were retrieved from the Pfam database and sent as a query for the search of BLASTP in the whole *G. max* genome sequence (Finn et al., 2015). Then, identified sequences were checked for the existence of the HSP90 domain using the InterProScan (Jones et al., 2014) and the SMART program (Letunic et al., 2014).

Protein properties analysis

Information of the GmHSP90 proteins, including amino acid number, molecular weight, instability index, aliphatic index, isoelectric point, and grand average of hydropathicity index (GRAVY), were calculated using compute pI/Mw tool from ExPASy (Gasteiger et al., 2005).

Subcellular and chromosomal localization

The online program WoLF PSORT server was used to predict the subcellular locations of the GmHSP90 proteins (Horton et al., 2007). The chromosomal distribution of *GmHSP60* genes was determined using the MapChart program (Voorrips, 2002).

Phylogenetic analysis

In this study, we construct two phylogenetic trees so that we could first classify the HSP90 protein sequences in soybean and then compare them with the HSP90 proteins of other plants including Arabidopsis, maize, and rice. MEGA 7.0 software was used to align the HSP90 sequences and then constructed phylogenetic trees using the Neighbor-Joining algorithm with 1000 bootstrapping tests to ensure clustering accuracy (Kumar et al., 2016).

Conserved motif and gene structure analysis

The Gene Structure Display Server GSDS 2.0 tool was used to identify the exon-intron structure of GmHSP90 members (Hu et al., 2014). The conserved motifs in the GmHSP90 proteins were identified with the MEME tool using the following parameters: maximum number of motifs, 20; minimum motif width, 6; and maximum motif width, 100 (Bailey et al., 2009). Then, conserved motifs of GmHSP90s were annotated using the InterProScan tool.

Proteins interaction network prediction

Functional and physical interactions between soybean HSP90 proteins were predicted using the STRING database (http://string-db.org/) (Szklarczyk et al., 2019) and visualized by the Cytoscape v3.10.1 software (http://cytoscape.org/) (Shannon et al., 2003).

RNA-Seq analysis

To determine *HSP90* gene family expression during soybean growth and development, RNA-seq data from 14 tissues, including flower, nodule, young leaf, root, one cm pod, pod shell 10 DAF, pod shell 14 DAF, seed 10 DAF, seed 14 DAF, seed 21 DAF, seed 25 DAF, seed 28 DAF, seed 35 DAF, and seed 42 DAF, were downloaded from SoyBase (Brown et al., 2021). The normalized expression data were transformed by log10, and the heat map was drawn using the CIMminer program (Scherf et al., 2000).

Results

Identification of the HSP90 proteins in Soybean

In total, 20 *HSP90* genes were identified in the soybean genome (Table 1). Domain analysis revealed the presence of HSP90 (Pfam: PF00183) and Histidine kinase-like ATPase (HATPase_c) (Pfam: PF02518) domains. Although all GmHSP90 proteins have at least one conserved HSP90 domain, the HATPase_c domain is present in 13 GmHSP90s. Noteworthy, Glyma10G098300, and Glyma07G207600 have two HSP90 domains. The number of amino acids of the GmHSP90 proteins ranged from 281 (Glyma10G098300) to 847 (Glyma14G219700) and had a molecular weight of 33.10 – 97.38 kDa. The aliphatic indexes varied from 77.09 (Glyma14G007700) to 94.93 (Glyma07G207600). The values of the isoelectric point were between 4.86 (Glyma17G258700) and 9.60 (Glyma19G098200), which indicates the change of protein nature from acidic to basic. Investigating the protein instability index showed that only 13 GmHSP90 proteins have indexes below 40, which can be considered stable proteins. The GRAVY values of GmHSP90 proteins were negative, which can be concluded that all of them are hydrophilic (Table 1).

Subcellular localization

Subcellular localization of the 20 GmHSP90s revealed that 11 GmHSP90 proteins are active in the cytoplasm, 5 proteins in the chloroplast, 2 proteins in the nucleus, and 2 proteins in the endoplasmic reticulum (Table 1).

Table 1. The physicochemical characteristics and subcellular location of the GmHSP90 proteins.

Proposed name	Animo acids	Molecular weight (kDa)	pI	GRAVY	Instability index	Aliphatic index	Subcellular localization
Glyma10G098300	281	33.10	5.37	-0.741	40.63	83.20	Cytoplasm
Glyma17G182500	360	42.92	5.70	-0.750	39.07	79.03	Cytoplasm
Glyma17G220000	323	37.71	6.04	-0.627	40.44	74.24	Nucleus
Glyma17G258700	814	93.29	4.86	-0.717	31.37	79.64	Endoplasmic reticulum
Glyma09G131500	699	80.39	4.95	-0.646	40.01	82.56	Cytoplasm
Glyma07G207600	304	34.44	5.88	-0.356	25.93	94.93	Cytoplasm
Glyma02G305600	791	89.72	5.25	-0.550	37.42	79.86	Chloroplast
Glyma02G302500	702	80.33	4.96	-0.584	35.98	82.51	Cytoplasm
Glyma02G124500	794	90.09	4.91	-0.560	50.01	80.31	Chloroplast
Glyma19G098200	311	36.89	9.60	-0.511	47.69	85.24	Nucleus
Glyma03G114400	740	85.55	8.73	-0.354	30.98	88.96	Cytoplasm
Glyma11G227000	406	46.37	5.53	-0.225	44.23	87.36	Cytoplasm
Glyma14G011600	700	80.19	4.98	-0.590	36.29	82.60	Cytoplasm
Glyma14G219700	847	97.38	4.91	-0.693	31.38	80.57	Endoplasmic reticulum
Glyma14G007700	797	90.50	5.13	-0.575	36.20	77.09	Chloroplast
Glyma08G332900	699	80.18	4.97	-0.594	36.49	83.96	Cytoplasm
Glyma08G032900	655	75.88	6.28	-0.530	38.60	82.90	Chloroplast
Glyma01G068000	793	90.11	4.94	-0.567	52.70	79.81	Chloroplast
Glyma18G074100	702	80.38	4.94	-0.579	35.53	84.30	Cytoplasm
Glyma16G178800	699	80.29	4.97	-0.637	39.62	82.98	Cytoplasm

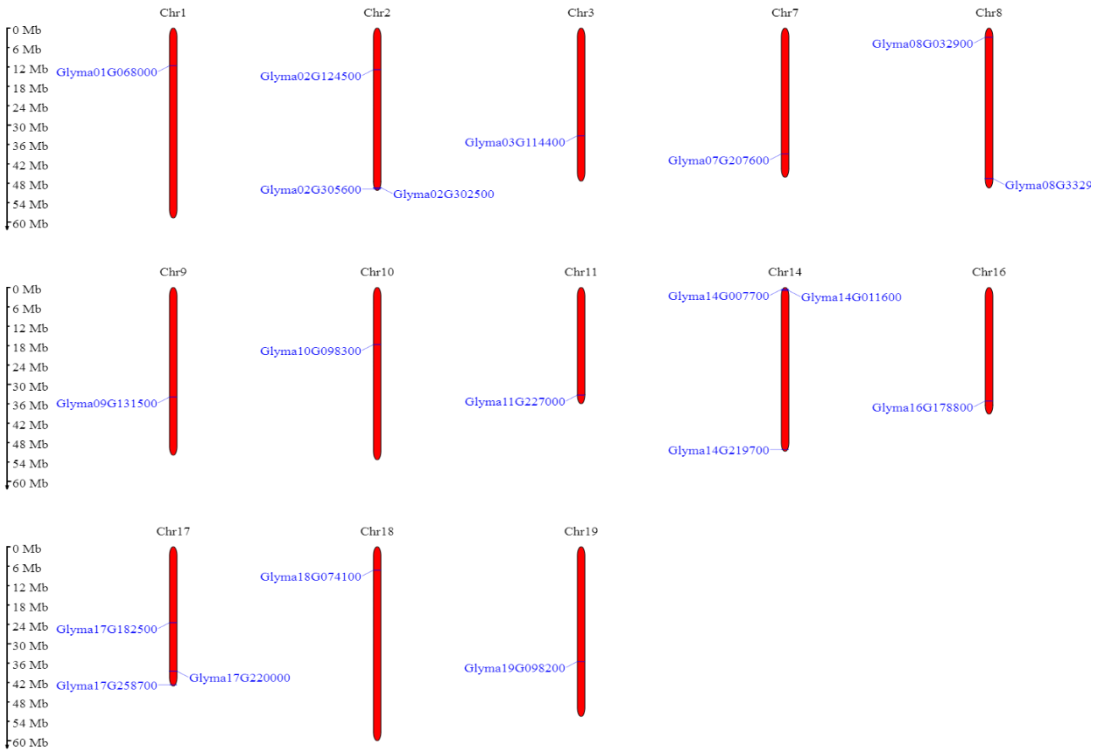

Figure 1. Chromosomal location of *GmHSP90* genes. The scale bar represents gene position (Mb) in soybean chromosomes.

Chromosomal location of GmHSP90 genes

The 20 soybean *HSP90* genes were distributed among 13 chromosomes, excluding chromosomes 4, 5, 6, 12, 13, 15 and 20 (Figure 1). The number of *GmHSP90* genes in each chromosome was significantly different. Chromosomes 2, 14, and 17 carried 3 *GmHSP90* genes; two genes were found in chromosome 8; only one gene was found in other chromosomes.

Motif analysis and gene structure of the GmHSP90s

Analysis of exon-intron structure showed that the number of introns in the soybean *HSP90* genes varied from 0 to 18 (Figure 2). However, no intron was observed in the Glyma19G098200, whereas 18 introns were observed in the Glyma02G305600, Glyma14G007700, Glyma02G124500, and Glyma01G068000 genes. The motif analysis identified 20 conserved motifs, and 13 motifs were detected as the domains associated with the HSP90 protein family (Figure 3 and Table 2). The results showed that related proteins shared the conserved motifs. Furthermore, the number and composition of motifs in the same subgroups were similar but were different from the proteins in other subgroups (Figure 3).

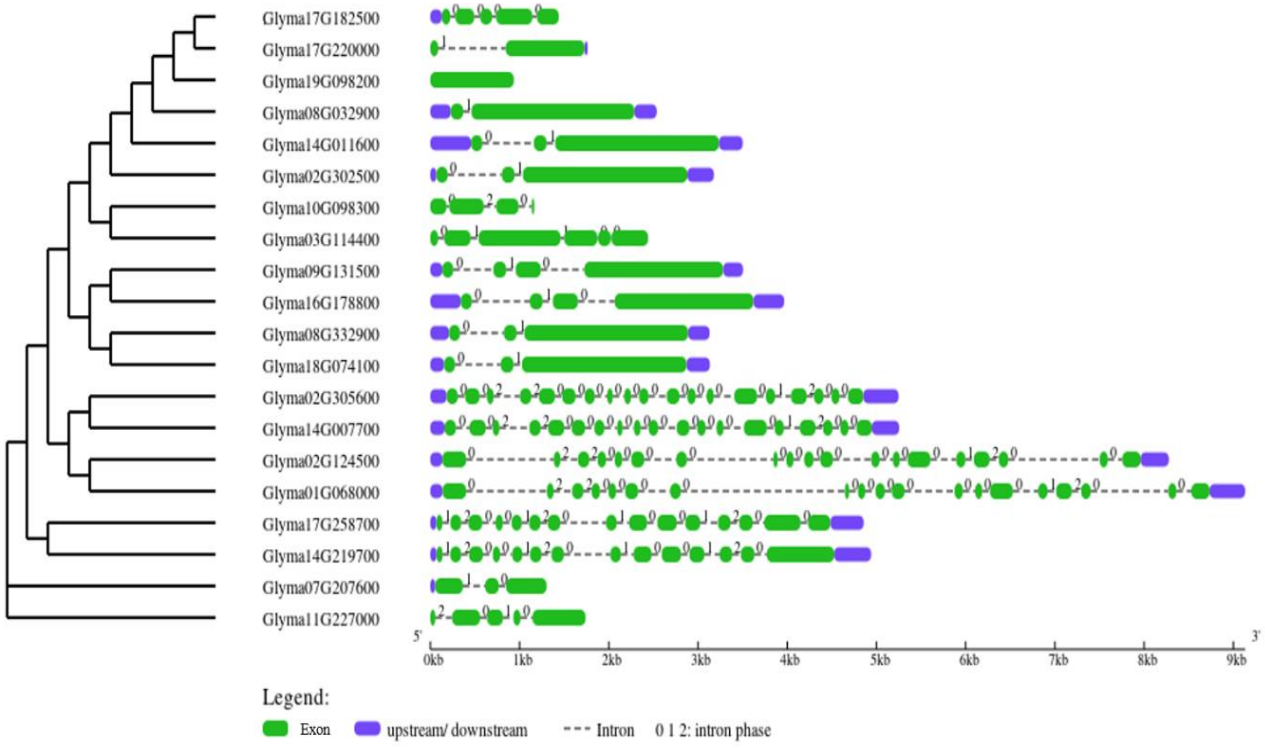

Figure 2. Phylogenetic tree and exon-intron distribution in the HSP90 genes in G. max. Phylogenetic tree was mapped using MEGA7.0 based on the Neighbor-Joining distance algorithm with 1000-replicates bootstrap. Blue and green boxes indicate the upstream/downstream UTR regions and exons, respectively, while dashed lines indicate introns. The splicing phases are indicated by 0, 1, and 2. Using the size at the bottom, it is possible to estimate the length of introns and exons.

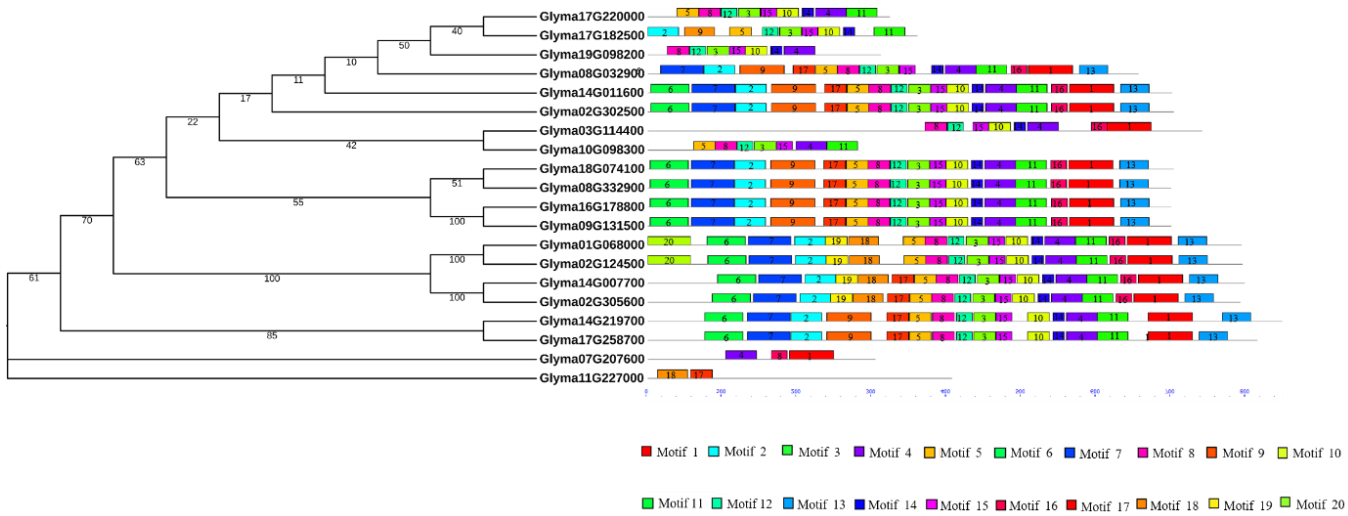

Figure 3. Phylogenetic tree and motif analysis of GmHSP90 proteins. The colored boxes illustrate motifs and gray lines show the non-conserved sequences.

Table 2. List of the putative motifs and annotation in GmHSP90s**.** Numbers in the first column indicate the motifs represented in Figure 3.

Motif	Width	Best possible match	E-value	Annotation
1	59	LVDSPCCLVTGEYGWSANMERIMKAQALRDSSMAGYMSSKKTMEINPDNPIMEELRKRA	4.5e-549	HSP90 domain
2	41	MIGQFGVGFYSAYLVADKVIVTTKHNDDEQYVWESQAGGSF	2.2e-326	HSP90 domain
3	29	LMPEYLSFVKGIVDSEDLPLNISREMLQQ	2.5e-320	HSP90 domain
4	41	YVTRMKEGQKDIYYITGESKKAVENSPFLEKLKKKGYEVLY	9.1e-419	HSP90 domain
5	29	PIWMRKPEEITKEEYAAFYKSLTNDWEEH	2.7e-252	HSP90 domain
6	51	AETFEFQAEINRLLDLIINSLYSNKEIFLRELISNASDALDKJRFESLTDK	2.9e-355	HSP90 domain
7	57	AQPELFIHIKPDKDNNTLSIIDSGIGMTKADLVBNLGTIARSGTKEFMEALAAGADV	1.5e-337	HSP90 domain
8	29	LAVKHFSVEGQLEFKAILFVPKRAPFDLF	1.4e-273	HSP90 domain
9	59	GENLGRGTKITLFLKEDQLEYLEERRLKDLIKKHSEFISYPISLWIEKTTEKEISDDED	4.6e-256	HSP90 domain
10	29	AENKEDYNKFYEAFSKNLKLGIHEDSQNK	4.7e-238	HSP90 domain
11	41	MVDAIDEYAVGQLKEYEGKKLVSATKEGLKLDESEEEKKKK	3.4e-256	HSP90 domain
12	21	TRKKPNNIKLYVRRVFIMDNC	6.4e-218	HSP90 domain
13	38	KDLVLLLFETALLTSGFSLDDPNTFGNRIHRMLKLGLS	3.4e-217	HSP90 domain
14	15	LLRYHSTKSGDEMTS	3.3e-112	-
15	21	KILKVIRKNLVKKCIEMFFEI	4.2e-150	-
16	21	FDGLCKVIKDVLGDKVEKVVV	1.6e-109	-
17	29	DVDEDKEKEEKKKKTIKEVSHEWELVNKQ	4.7e-101	-
18	40	FSEPERIEGLVKNYSQFVSFPIYTWQEKSTTKEVEEDEDP	2.0e-061	HSP90 domain
19	29	SYVIKEETDPEKLJPRGTRJTLYLKEDDK	1.6e-024	-
20	57	MAPVPSRTMATASLASLPPSSPFARASLLRSAFLPPQIGRGRKCFSPAAGLRWTQRR	3.1e-020	

Evolutionary classification of HSP90 genes

To investigate the phylogenetic relationships of *HSP90* genes in soybean, Arabidopsis, maize, and rice species, the phylogenetic classification of the amino acid sequences of 47 identified proteins was constructed based on the Neighbor-Joining distance algorithm (Figure 4). The evolutionary tree divided these genes into three main groups based on their subcellular localization. The distribution of *HSP90* genes in different species showed unique patterns

and slight differences in each group. In Group I, nearly all of the *HSP90* genes are distributed in the nucleus or cytoplasm. In Group II, the *HSP90*s were mostly classified in the endoplasmic reticulum. *HSP90* genes were exclusively found in the mitochondria or chloroplast in Group III. Among the three groups, group I was the largest, with 28 members. After that, there was group II with 13 members, and group III with six members.

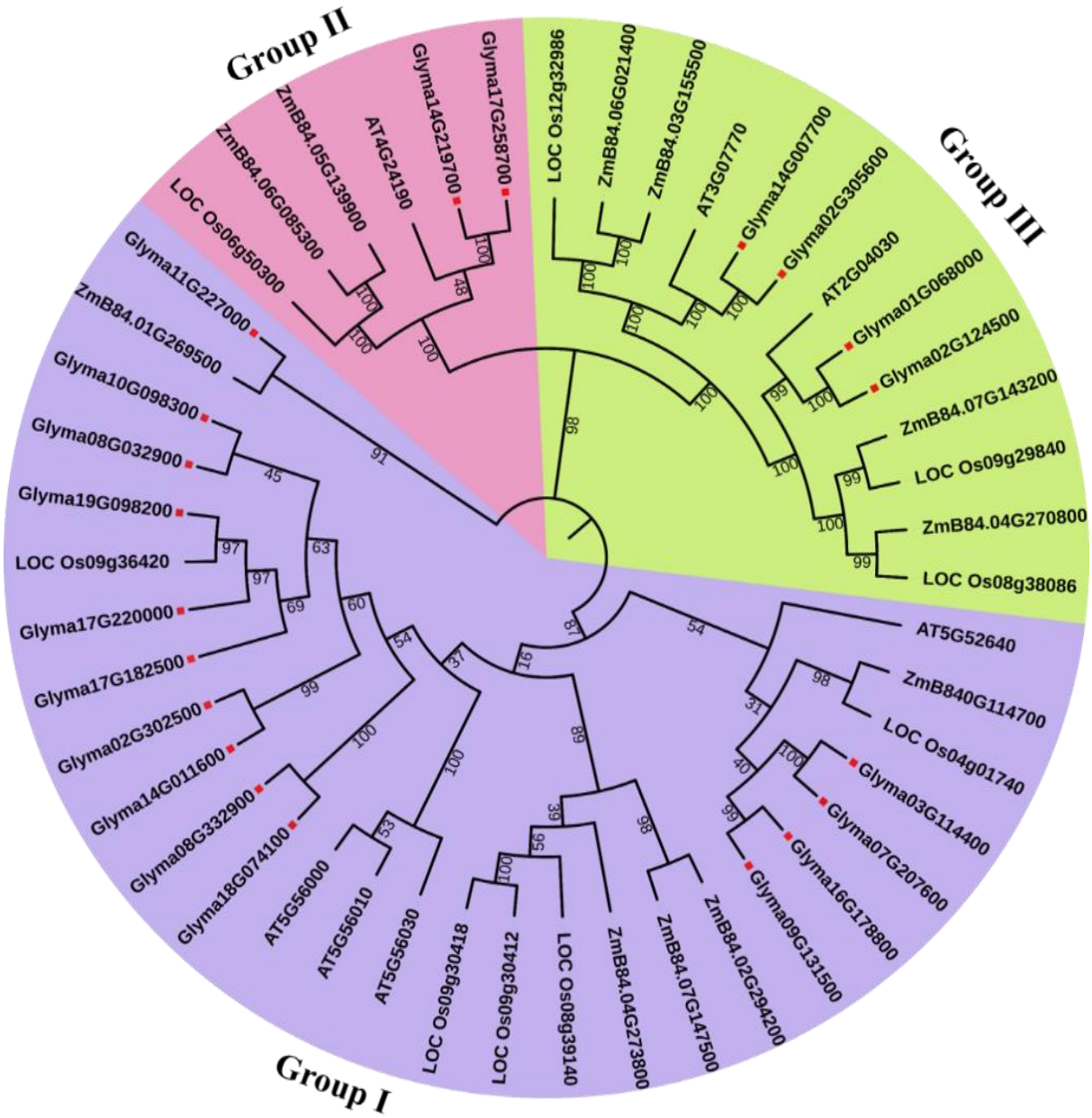

Figure 4. Phylogenetic tree of HSP90 family members from *Glycine max*, *Arabidopsis thaliana*, *Oryza sativa*, and *Zea mays* species. The HSP90s were divided into three groups (groups I–III) based on the clustering of the protein sequence which were showed by different colors. GmHSP90 proteins are marked with red shapes Bootstrap values are indicated on each branch.

Protein-protein interaction network of GmHSP90 proteins

The protein interaction network for GmHSP90 proteins was predicted using the STRING database and plotted by the Cytoscape software. Clustering of the network using MCODE algorithm showed that this protein network has three clusters, the first, second, and third clusters are composed of 8, 8, and 4 proteins (nodes), respectively (Figure 5A). We identified three key hub proteins, Glyma14g219700, Glyma17g258700, and Glyma07G207600, based on their high degrees of interactions, which are shown in red color (Figure 5B). This indicates the importance of these proteins in signaling responses to various environmental conditions.

Soybean HSP90 family gene expression patterns

Due to the lack of the expression patterns of two *GmHSP90* genes (*Glyma07g207600* and *Glyma03g114400*) in the soybean RNA-seq database, the expression profiles of 18/20 *GmHSP90* members were analyzed. A heat map showed that the majority of the *GmHSP90s* revealed preferential expression patterns, and only four *GmHSP90* genes (*Glyma10g098300*, *Glyma17g182500*, *Glyma17g220000*, and *Glyma19g098200*) had no expression in any tissues (Figure 6). The expression data analysis demonstrated that 14 genes were expressed in 14 tissues and organs at different developmental stages. *Glyma02g302500*, *Glyma08g332900*, *Glyma14g219700*, *Glyma17g258700*, and *Glyma18g074100* genes displayed high expression levels in all of the tissues. Therefore, it can be concluded that the *GmHSP90* genes played vital roles in different processes during soybean growth and development.

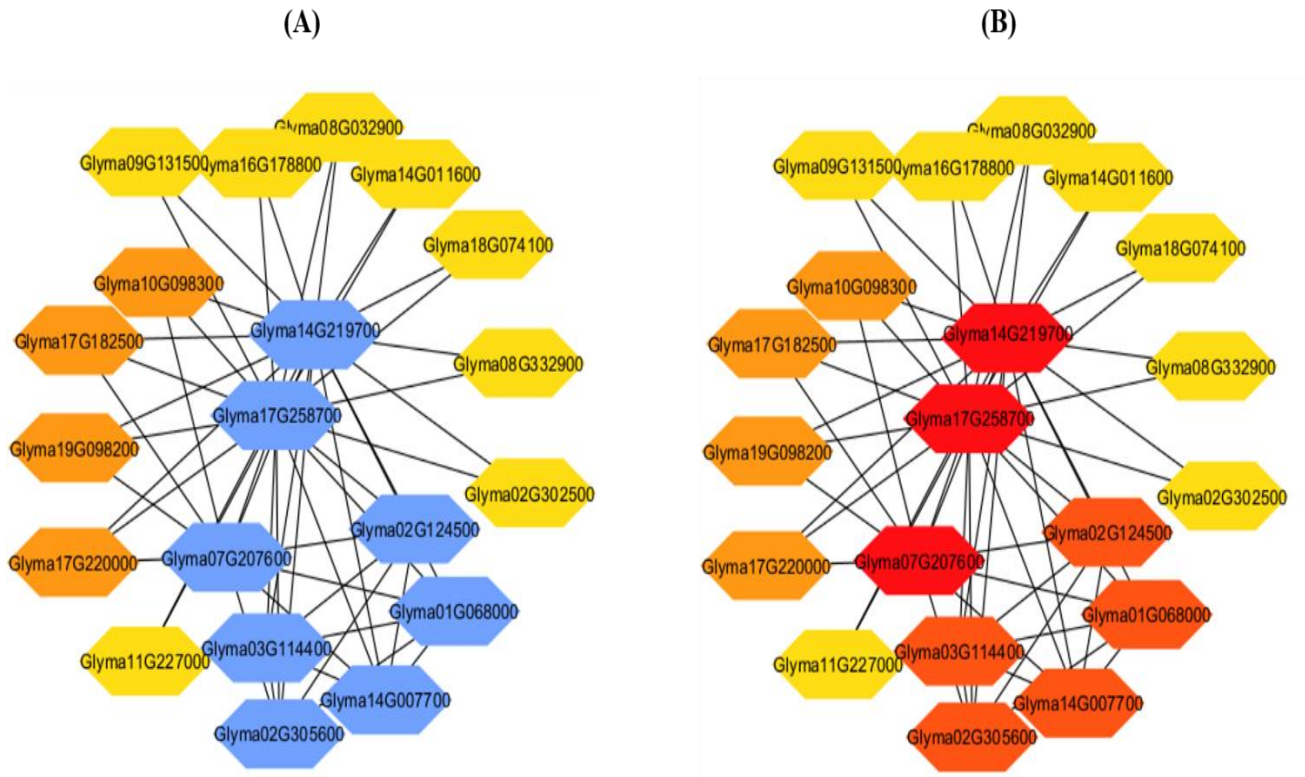

Figure 5. Protein-protein interaction network of GmHSP60 proteins. The protein-protein interaction network for GmHSP60 proteins was extracted using the STRING database and visualized by the Cytoscape software. Colored hexagons and lines represent nodes and edges, respectively. A) Network clustering: blue, yellow, and orange hexagons show the proteins located in the first, second, and third clusters, respectively. B) Network analysis: proteins located in red hexagons were identified as hubs.

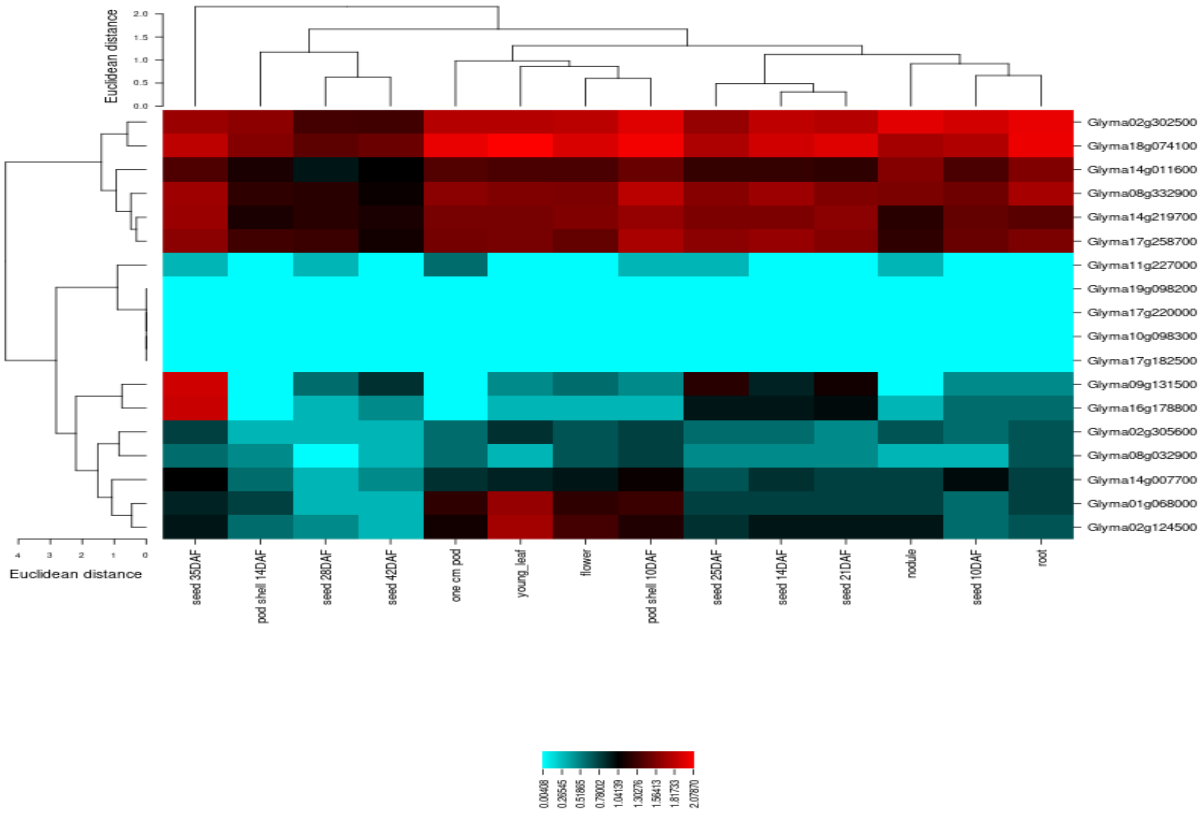

Figure 6. Heat map showing the levels of *GmHSP90* genes expression in multiple tissues, organs, and developmental stages. Blue and red colors respectively indicate low and high expressions.

Discussion

HSP90 proteins, which can be found in prokaryotes and eukaryotes, are highly conserved molecular chaperones. These proteins play a major role in the cell cycle, transduction of signals, and more essential biological processes (Pearl and Prodromou, 2006). A comprehensive analysis of the soybean *HSP90* gene family has been conducted in this study to assess evolutionary relationships, subcellular and chromosomal localization, conserved motifs, gene structure, and expression profiles.

The *GmHSP90* genes were mainly distributed at two ends of the chromosomes, similar to the *HSP90* genes distribution of *Malus sieversii*, rice, and *Nicotiana tabacum* (Hu et al., 2009; Song et al., 2019; Haxim et al., 2021). Most of the GmHSP90 proteins are located in the cytoplasm. This feature is shared with *Brachypodium distachyon* (Zhang et al., 2021) and Arabidopsis (Sarkar et al., 2009), and suggests that HSP90 proteins may have their primary site of action in the cytoplasm, where protein assembly occurs (Vabulas et al., 2010). Some proteins are active in the chloroplast, nucleus, and endoplasmic reticulum. The existence of spatial variation for GmHSP90 proteins probably indicates the diverse functional roles of these genes in different cellular processes.

To describe and understand the existing functional characteristics of examined genes, it may be important to consider these evolutional relationships. To determine the species' evolutional relationships and to estimate paralogs and orthologs, within and between species, phylogenetic analysis is frequently used (Bettaieb et al., 2020). High bootstrapping values have supported the phylogenetic tree, and have shown that *GmHSP90* genes have been classified into three main subgroups. This is consistent with the findings of prior studies (Zhang et al., 2013; Zhang et al., 2017). The results indicated that exon-intron structures and the number of introns were similar

within each subgroup, while genes from various subgroups have differing gene structures. Also, the distribution of conserved motifs in the same group shows a similar pattern. These analyses suggested that the evolutionary classification of *GmHSP90* genes is reliable. In addition, these findings revealed that the genes located in each group are highly conserved, which probably indicates the similar functions of the members of each group.

Analysis of subcellular location indicated that in Group I, nearly all of the *HSP90* genes are distributed in the nucleus or cytoplasm. In Group II, the HSP90s were mostly classified in the endoplasmic reticulum. *HSP90* genes were almost exclusively found in the mitochondria or chloroplasts in Group III.

The number of introns was similar on some sister pairs within the branches of a phylogenetic tree. However, some sister pairs continued to show changes in gene structure, as well as numbers. The results demonstrated intron loss/gain in *HSP90* encoding genes during the structural evolution. It is known that the protein structure determines its function (Bai et al., 2002). This study indicated that there was a different gene structure for GmHSP90 protein sequences. The number of introns mainly depends upon gene transcription regulation sensitivity, and it is more likely that plants can respond to various developmental and environmental stimuli with lower numbers of introns (Appiah et al., 2021).

Using the protein-protein interaction network, Glyma14g219700, Glyma17g258700, and Glyma07G207600 were identified as hub proteins. It has been found that hub genes play significant roles in various biological processes (Mishra et al., 2023). The heat map data shows that the majority of *GmHSP90* genes are expressed in a variety of soybean organs and tissues. So, it can be concluded that they may be involved in growth and development. Heat map revealed expression profiles of paralogous pairs from various subfamilies, and it was found that most paralogous pairs at the high level of sequence homology have identical expression profiles in the number of different tissues. In particular, the *Glyma02g302500* and *Glyma18g074100* pairs were strongly expressed in all types of tissues. However, in all seed stages, *Glyma08g032900* and *Glyma02g305600* genes showed very low expression.

Conclusion

Soybean has 20 genes encoding *HSP90*, and they are located on 13 chromosomes. The organization of conserved motifs and gene structure confirmed the phylogenetic classification. *GmHSP90* gene family expression profiles in various tissues indicate that these genes play essential roles in soybean growth and development. According to the general information about these genes and their possible participation in plant growth and development, further study of the *HSP90* gene family will be facilitated, especially about their biological functions and evolutionary history.

Author Contributions

Conceptualization, S. M. and F. S.; methodology, S. M.; software, S. M.; validation, S. M., F. S. and G. A.N.; formal analysis, S. M.; investigation, S. M.; resources, S. M.; data curation, S. M.; writing—original draft preparation, S. M.; writing—review and editing, S. M.; visualization, S. M.; supervision, S. M.; project administration, S. M.. All authors have read and agreed to the published version of the manuscript.

Funding

This research received no external funding.

Acknowledgments

Conflict of Interest Statement

The authors declare no conflict of interest

References

Appiah, C., Yang, Z.-F., He, J., Wang, Y., Zhou, J., Xu, W.-Z., Nie, G., and Zhu, Y.-Q. (2021). Genome-Wide identification of *Hsp90* gene family in *Perennial Ryegrass* and expression analysis under various abiotic stresses. *Plants* 10(11): 2509.

Bai, J., Pennill, L.A., Ning, J., Lee, S.W., Ramalingam, J., Webb, C.A., Zhao, B., Sun, Q., Nelson, J.C., and Leach, J.E. (2002). Diversity in nucleotide binding site–leucine-rich repeat genes in cereals. *Genome Res* 12(12): 1871-1884.

Bailey, T.L., Boden, M., Buske, F.A., Frith, M., Grant, C.E., Clementi, L., Ren, J., Li, W.W., and Noble, W.S. (2009). MEME SUITE: tools for motif discovery and searching. *Nucleic Acids Res* 37: 202-208.

Bettaieb, I., Hamdi, J., and Bouktila, D. (2020). Genome-wide analysis of *HSP90* gene family in the Mediterranean olive (*Olea europaea* subsp. *europaea*) provides insight into structural patterns, evolution and functional diversity. *Physiol Mol Biol Plants* 26(11): 2301-2318.

Brown, A.V., Conners, S.I., Huang, W., Wilkey, A.P., Grant, D., Weeks, N.T., Cannon, S.B., Graham, M.A., and Nelson, R.T. (2021). A new decade and new data at SoyBase, the USDA-ARS soybean genetics and genomics database. *Nucleic Acids Res* 49(D1): D1496-D1501.

Chaudhary, R., Baranwal, V.K., Kumar, R., Sircar, D., and Chauhan, H. (2019). Genome-wide identification and expression analysis of *Hsp70*, *Hsp90*, and *Hsp100* heat shock protein genes in barley under stress conditions and reproductive development. *Funct Integr Genomics* 19(6): 1007-1022.

Chen, J., Gao, T., Wan, S., Zhang, Y., Yang, J., Yu, Y., and Wang, W. (2018). Genome-wide identification, classification and expression analysis of the *HSP* gene superfamily in tea plant (*Camellia sinensis*). *Int J Mol Sci* 19(9): 2633.

di Donato, M., and Geisler, M. (2019). *HSP 90* and co‐chaperones: a multitaskers' view on plant hormone biology. *FEBS letters* 593(13): 1415-1430.

Finn, R.D., Coggill, P., Eberhardt, R.Y., Eddy, S.R., Mistry, J., Mitchell, A.L., Potter, S.C., Punta, M., Qureshi, M., and Sangrador-Vegas, A. (2015). The Pfam protein families database: towards a more sustainable future. *Nucleic Acids Res* 44: 279-285.

Gasteiger, E., Hoogland, C., Gattiker, A., Wilkins, M.R., Appel, R.D., and Bairoch, A. (2005). "Protein identification and analysis tools on the ExPASy server," in *The proteomics protocols handbook,* ed. J.M. Walker. (New York City, New York, United States: Humana Press), 571-607.

Hashemipetroudi, S.H., Mohammadi, S., and Kuhlmann, M. (2019). Analysis of expression pattern of genome and analysis of *HSP90* gene family in *Aeluropus littoralis* under salinity stress. *Crop Breed J* 11(31): 134-143.

Haxim, Y., Si, Y., Liu, X., Wen, X., Kahar, G., Ding, Y., Li, X., and Zhang, D. (2021). Genome-wide characterization of *HSP90* gene family in *Malus sieversii* and their potential roles in response to Valsa mali infection. *Forests* 12(9): 1232.

Horton, P., Park, K.J., Obayashi, T., Fujita, N., Harada, H., Adams-Collier, C., and Nakai, K. (2007). WoLF PSORT: protein localization predictor. *Nucleic Acids Res* 35: 585-587.

Hoter, A., El-Sabban, M.E., and Naim, H.Y. (2018). The HSP90 family: structure, regulation, function, and implications in health and disease. *Int J Mol Sci* 19(9): 2560.

Hu, B., Jin, J., Guo, A.-Y., Zhang, H., Luo, J., and Gao, G. (2014). GSDS 2.0: an upgraded gene feature visualization server. *Bioinformatics* 31(8): 1296-1297.

Hu, W., Hu, G., and Han, B. (2009). Genome-wide survey and expression profiling of heat shock proteins and heat shock factors revealed overlapped and stress specific response under abiotic stresses in rice. *Plant Sci* 176(4): 583-590.

Jing, W., Fangjun, T., Chengliang, L., Xilu, Z., Lijun, O., Juntawong, N., Fei, W., Chunhai, J., Xuexiao, Z., and Wenchao, C. (2020). Genome-wide identification and analysis of *HSP90* gene family in pepper. *Acta Horticulturae Sinica* 47(4): 665.

Jones, P., Binns, D., Chang, H.-Y., Fraser, M., Li, W., McAnulla, C., McWilliam, H., Maslen, J., Mitchell, A., and Nuka, G. (2014). InterProScan 5: genome-scale protein function classification. *Bioinformatics* 30(9): 1236-1240.

Kumar, S., Stecher, G., and Tamura, K. (2016). MEGA7: molecular evolutionary genetics analysis version 7.0 for bigger datasets. *Mol Biol Evol* 33(7): 1870-1874.

Letunic, I., Doerks, T., and Bork, P. (2014). SMART: recent updates, new developments and status in 2015. *Nucleic acids res* 43(D1): D257-D260.

Li, W., Chen, Y., Ye, M., Wang, D., and Chen, Q. (2020). Evolutionary history of the heat shock protein 90 (*Hsp90*) family of 43 plants and characterization of Hsp90s in *Solanum tuberosum*. *Mol Biol Rep* 47(9): 6679-6691.

Mishra, R.C., and Grover, A. (2016). Constitutive over-expression of rice ClpD1 protein enhances tolerance to salt and desiccation stresses in transgenic *Arabidopsis* plants. *Plant Sci* 250: 69-78.

Mishra, S., Chaudhary, R., Pandey, B., Singh, G., and Sharma, P. (2023). Genome-wide identification and expression analysis of the GRAS gene family under abiotic stresses in wheat (*Triticum aestivum* L.). *Sci Rep* 13(1): 18705.

Pearl, L.H., and Prodromou, C. (2006). Structure and mechanism of the Hsp90 molecular chaperone machinery. *Annu Rev Biochem* 75(1): 271-294.

Picard, D. (2002). Heat-shock protein 90, a chaperone for folding and regulation. *Cell Mol Life* 59(10): 1640-1648.

Prasad, B.D., Goel, S., and Krishna, P. (2010). In silico identification of carboxylate clamp type tetratricopeptide repeat proteins in *Arabidopsis* and rice as putative co-chaperones of Hsp90/Hsp70. *Plos One* 5(9): e12761.

Reddy, R.K., Chaudhary, S., Patil, P., and Krishna, P. (1998). The 90 kDa heat shock protein (hsp90) is expressed throughout *Brassica napus* seed development and germination. *Plant Sci* 131(2): 131-137.

Sable, A., Rai, K.M., Choudhary, A., Yadav, V.K., Agarwal, S.K., and Sawant, S.V. (2018). Inhibition of heat shock proteins HSP90 and HSP70 induce oxidative stress, suppressing cotton fiber development. *Sci Rep* 8(1): 1-17.

Sangster, T.A., and Queitsch, C. (2005). The HSP90 chaperone complex, an emerging force in plant development and phenotypic plasticity. *Curr Opin Plant Biol* 8(1): 86-92.

Sarkar, N.K., Kim, Y.-K., and Grover, A. (2009). Rice sHsp genes: genomic organization and expression profiling under stress and development. *BMC Genom* 10(1): 1-18.

Scherf, U., Ross, D.T., Waltham, M., Smith, L.H., Lee, J.K., Tanabe, L., Kohn, K.W., Reinhold, W.C., Myers, T.G., and Andrews, D.T. (2000). A gene expression database for the molecular pharmacology of cancer. *Nat Genet* 24(3): 236-244.

Shannon, P., Markiel, A., Ozier, O., Baliga, N.S., Wang, J.T., Ramage, D., Amin, N., Schwikowski, B., and Ideker, T. (2003). Cytoscape: a software environment for integrated models of biomolecular interaction networks. *Genome Res* 13(11): 2498-2504.

Shelke, D.B., Chambhare, M.R., Nikalje, G.C., and Nikam, T. (2023). Improvement of soybean crop for yield, stress tolerance, and value-added products using a transgenic approach. *Adv Agric* 2023. doi: 10.1155/2023/8166928.

Song, Z., Pan, F., Yang, C., Jia, H., Jiang, H., He, F., Li, N., Lu, X., and Zhang, H. (2019). Genome-wide identification and expression analysis of *HSP90* gene family in *Nicotiana tabacum*. *BMC Genet* 20(1): 1-12.

Szklarczyk, D., Gable, A.L., Lyon, D., Junge, A., Wyder, S., Huerta-Cepas, J., Simonovic, M., Doncheva, N.T., Morris, J.H., and Bork, P. (2019). STRING v11: protein–protein association networks with increased coverage, supporting functional discovery in genome-wide experimental datasets. *Nucleic Acids Res* 47(D1): D607-D613.

Vabulas, R.M., Raychaudhuri, S., Hayer-Hartl, M., and Hartl, F.U. (2010). Protein folding in the cytoplasm and the heat shock response. *Cold Spring Harb Perspect Biol* 2(12): a004390.

Vaughan, M.M., Block, A., Christensen, S.A., Allen, L.H., and Schmelz, E.A. (2018). The effects of climate change associated abiotic stresses on maize phytochemical defenses. *Phytochem Rev* 17: 37-49.

Voorrips, R. (2002). MapChart: software for the graphical presentation of linkage maps and QTLs. *J Hered* 93(1): 77-78.

Wang, W., Vinocur, B., Shoseyov, O., and Altman, A. (2004). Role of plant heat-shock proteins and molecular chaperones in the abiotic stress response. *Trends Plant Sci* 9(5): 244-252.

Zhang, J., Li, J., Liu, B., Zhang, L., Chen, J., and Lu, M. (2013). Genome-wide analysis of the Populus *Hsp90* gene family reveals differential expression patterns, localization, and heat stress responses. *BMC Genom* 14(1): 532.

Zhang, K., He, S., Sui, Y., Gao, Q., Jia, S., Lu, X., and Jia, L. (2021). Genome-wide characterization of *HSP90* gene family in cucumber and their potential roles in response to abiotic and biotic stresses. *Front Genet* 12: 584886.

Zhang, L., Zhao, H.-K., Dong, Q.-l., Zhang, Y.-Y., Wang, Y.-M., Li, H.-Y., Xing, G.-J., Li, Q.-Y., and Dong, Y.-S. (2015). Genome-wide analysis and expression profiling under heat and drought treatments of *HSP70* gene family in soybean (*Glycine max* L.). *Front Plant Sci* 6: 773.

Zhang, M., Shen, Z., Meng, G., Lu, Y., and Wang, Y. (2017). Genome-wide analysis of the *Brachypodium distachyon* (L.) P. Beauv. *Hsp90* gene family reveals molecular evolution and expression profiling under drought and salt stresses. *PloS One* 12(12): e0189187.

JPMB
Journal of Plant Molecular Breeding
Published by Genetics and Agricultural Biotechnology Institute of Tabarestan
2023 | Volume 11 | Issue 2

مقاله پژوهشی

تجزیه و تحلیل گسترده ژنومی خانواده ژنی *HSP90* و نقش آن‌ها در رشد و نمو سویا

سمیرا محمدی*، فیروزه سهروردی، قربانعلی نعمت‌زاده

پژوهشکده ژنتیک و زیست‌فناوری کشاورزی طبرستان، دانشگاه علوم کشاورزی و منابع طبیعی ساری، ساری، ایران

چکیده: پروتئین شوک حرارتی ۹۰ کیلو دالتونی یا HSP90 از طریق چندین مکانیسم عملکردی، نقش مهمی در تنظیم تنش‌های زیستی و غیرزیستی بر عهده دارد. مطالعه حاضر با هدف انجام تجزیه و تحلیل جامعی از خانواده ژنی *HSP90* در سویا انجام شد. در مجموع، ۲۰ ژن *HSP90* در سویا شناسایی شدند و توزیع غیر یکنواختی روی ۱۳ کروموزوم نشان دادند. روابط فیلوژنتیکی نشان داد که ژن‌های واقع در زیرگروه‌های یکسان دارای ساختار اگزون – اینترون و تعداد اینترون‌های مشابه هستند. تجزیه و تحلیل مکان‌یابی سلولی نشان داد که تقریباً تمام ژن‌های *HSP90* واقع در گروه اول، در هسته یا سیتوپلاسم توزیع شده‌اند. ژن‌ها در گروه دوم، بیشتر در شبکه آندوپلاسمی واقع شده‌اند. ژن‌های *HSP90* واقع در گروه سوم نیز تقریباً در میتوکندری یا کلروپلاست یافت شده‌اند. Glyma14g219700، Glyma17g258700 و Glyma07G207600 بر اساس بیشترین ارتباط با سایر پروتئین‌ها، به‌عنوان پروتئین‌های هاب شناسایی شدند. علاوه بر این، ژن‌های *Glyma02g302500*، *Glyma08g332900*، *Glyma14g219700*، *Glyma17g258700* و *Glyma18g074100* سطوح بیان بالایی را در تمام بافت‌ها و در مراحل نموی مختلف نشان دادند. این یافته‌ها با ارائه اطلاعات کلی از طبقه‌بندی و تکامل خانواده ژنی *GmHSP90*، می‌تواند به شناسایی خصوصیات کارکردی ژن‌های *HSP90* در رشد و نمو سویا کمک نماید.

کلمات کلیدی: پروتئین شوک حرارتی، پروفایل بیان ژن، ساختار ژنی، شبکه برهم‌کنش پروتئین – پروتئین، روابط فیلوژنتیکی، مکان‌یابی سلولی.

ویراستار علمی
دکتر پرویز حیدری،
دانشگاه صنعتی شاهرود، ایران

تاریخ
دریافت: ۱۶ خرداد ۱۴۰۱
پذیرش: ۲۷ اردیبهشت ۱۴۰۳
چاپ: ۶ خرداد ۱۴۰۳

نویسنده مسئول
دکتر سمیرا محمدی
s.mohamadi@stu.sanru.ac.ir

ارجاع به این مقاله
Mohammadi, S., Sohrevardi, F. and Nematzadeh, G.A. (2023). Genome-wide analysis of the *HSP90* gene family and their roles in soybean growth and development . *J Plant Mol Breed. 11* (2): 119-132.
doi: 10.22058/JPMB.2024.555256.1256.

Contents:

Address:

Genetics and Agricultural Biotechnology Institute of Tabarestan (GABIT)
Sari Agricultural Sciences & Natural Resources University (SANRU)
Khazar Abad road, Sari, Mazandaran, Iran P.O.Box: 578
www.jpmb-gabit.ir Tel : +981133687744